UNIVERSITY OF
LIVERPOOL

The role of ion channels in chondrocytes

Thesis submitted in accordance with the requirements of the University of Liverpool for the degree of Doctor in Philosophy

By

Rebecca Lewis

July 2011

ABSTRACT

Chondrocytes are the cells of articular cartilage responsible for the production and maintenance of their extracellular matrix (ECM). They exist in a unique environment of low partial pressures of oxygen, low pH and avascularity (Urban, 1994). The chondrocyte environment is also challenged by constant osmotic fluxes during osmolarity changes induced by joint loading. This thesis investigates the ion channels expressed by chondrocytes and examines the possible functions for these channels.

Whole cell and single channel electrophysiological experiments identified chloride, sodium, potassium and non-selective cation conductances in isolated canine chondrocytes. Whole-cell current clamp measurements of membrane potential (*Vm)* showed that chondrocytes have very depolarised *Vm* compared to other cell types (in the range of -8 to -14mV, measured from bovine, ovine, equine and canine chondrocytes).

Permeability experiments carried out in whole-cell voltage clamp mode determined that the non-selective cation current was selective for calcium over sodium and potassium at a level similar to that of the transient receptor potential vanilloid type five and six channels (TRPV5 and 6). RT-PCR detected mRNA for TRPV4 and TRPV5 channels. The effect of these channels on chondrocyte membrane potential (*Vm*) was determined using whole-cell current-clamp electrophysiology. Experiments with the selective TPRV5 inhibitor econazole suggest that TRPV5 is constitutively active and important for setting the depolarised *Vm*. Conversely, TRPV4 appeared to be inactive at rest and when activated by the selective agonist 4 α-phorbol 12,13-

didecanoate indirectly caused an increase in potassium conductance and thus membrane hyperpolarisation.

A low conductance sodium channel was also identified. Sensitivity to low concentrations of amiloride and benzamil indicate that this channel is the epithelial sodium channel (ENaC). Whole-cell current-clamp showed that this ENaC had a small but significant contribution to the *Vm*.

A mixed population of chloride channels was found in the chondrocyte using single channel and whole-cell current and voltage clamp recordings. This population consisted of a maxi-chloride channel and a calcium-activated chloride channel.

A model of chondrocyte *Vm* was then developed combining the approach of Hodgkin and Huxley (1952b) with parameters measured in the patch clamp experiments. This model was able to simulate many of the effects of inhibition of channel conductances on the resting membrane potential. Whole-cell current clamp experiments using inhibitors of the ion conductances discovered previously, verified the models predictions.

This thesis then tested the hypothesis that the depolarised *Vm* of chondrocytes facilitates volume regulation. Cell volume experiments discovered that at more negative *Vm* chondrocytes were unable to regulate their volume upon hypotonic challenge. At more positive potentials, cell volume recovery was significantly greater. This is likely to be due to the greater driving force for potassium efflux and suggests that the depolarised *Vm* is an adaptation which allows the chondrocyte to effectively regulate its volume.

ACKNOWLEDGEMENTS

There are numerous people I owe my thanks to, too many to personally mention here, but I would sincerely like to thank everyone who has helped and supported me over the course of my studies.

I am indebted to my supervisor, Dr. Richard Barrett-Jolley for his invaluable support, encouragement and expertise over the years. He has been a fantastic mentor.

I am also incredibly grateful to Prof. John Innes, Dr. Caroline Dart and Dr. Gregor Purves for their guidance, assistance in the lab and use of their facilities. I would like to thank Dr. Anne Vaughan-Thomas for teaching me the dissection techniques used in this work. I would also like to thank the Biotechnology and Biological Sciences Research Council; these studies would never have taken place without the funding they have provided.

Thanks go to all the lab members I have worked with over the years, in particular Claire Feetham, Dr. Carol Hercock and Dr. Iain Young, who took it upon themselves to ensure I always stayed well caffeinated.

Finally, although I am unable to name them all personally, I am hugely grateful to all my family and friends. Especially Mum, Richard, Sim and Joe, thank you so much for all your love and support over the years, it means so much.

CONTENTS

LIST OF FIGURES

LIST OF TABLES

LIST OF ABBREVIATIONS

This section lists the abbreviations used in this thesis. SI units and chemical element symbols are omitted from this list.

AQP	aquaporin channel
ATP	adenosine triphosphate
BK	calcium-activated potassium channel
CaCC	calcium-activated chloride channel
cDNA	complementary deoxyribonucleic acid
CFTR	cystic fibrosis transmembrane regulator
DEG	degenerin
DMEM	dulbeccos modified eagles medium
DMSO	dimethyl sulfoxide
ECM	extracellular matrix
ENaC	epithelial sodium channel
GAG	glycosaminoglycan
GAPDH	glyceraldehyde 3-phosphate dehydrogenase
GHK	Goldman-Hodgkin-Katz
KATP	ATP-sensitive K^+ channel
MIP	major intrinsic protein
mRNA	messenger ribonucleic acid
NaMS	sodium methanesulfonate
NFA	niflumic acid

NKCC	$Na^+/K^+/Cl^-$ cotransporter
PDD	4 α-phorbol 12,13-didecanoate
P_o	open probability
RMP	resting membrane potential
RT-PCR	reverse-transcription polymerase chain reaction
RVD	regulatory volume decrease
RVI	regulatory volume increase
siRNA	short-interference ribonucleic acid
SITS	4-Acetamido-4-isothiocyanato-2,2-stilbenedisulfonic acid disodium salt hydrate
TEA	tetraethylammonium chloride
TRP	transient receptor potential
TRPC	transient receptor potential canonical
TRPM	transient receptor potential melastatin
TRPV	transient receptor potential vanilloid
TRPA	transient receptor potential ankyrin
TRPP	transient receptor potential polycystin
TRPML	transient receptor potential mucolipin
VAHC	voltage-activated hydrogen channels
VGCC	voltage-gated calcium channels
VGSC	voltage-gated sodium channels
VRAC	volume-regulated chloride channel

1

INTRODUCTION

1.1 Joints, cartilage and chondrocytes

Synovial joints connect long bones of the skeleton, allowing free movement. They form a cavity between bones which contains synovial fluid; this acts as a lubricant to decrease friction between the bones meeting at the synovial joint and absorbs shock (Lee & Urban, 1997). Articular cartilage is a type of hyaline cartilage that covers the surface of bones which meet at a synovial joint (Mankin, 1982). As a joint moves, cartilage is vital for smooth articulation, reducing friction and shock absorption (Tatari, 2007).

Cartilage can be separated into distinct regions according to the depth of the tissue. The superficial zone is the furthest away from the bone, accounting for 10-20% of the tissue. The medial zone accounts for up to 60% of the tissue, whilst the deep zone accounts for up to 30% (Brighton *et al.*, 1973). The morphology of chondrocytes, the cells of cartilage, varies according to the region of cartilage in which they lie. Superficially, they are small and flattened (Archer & Francis-West, 2003), becoming more ovoid in shape when situated in the medial zone. In the deep zone they may form short columns of large, round cells (Brighton *et al.*, 1973). A fourth layer of cartilage is present at the interface between cartilage and bone, known as the calcified zone. Very few chondrocytes are found in this region (Martel-Pelletier *et al.*, 2008). Throughout cartilage, chondrocytes occur singularly within spaces called lacunae in the extracellular matrix (ECM) (Stockwell, 1975).

A chondrocytes primary function is to synthesise and secrete proteoglycans, collagen and non-collagenous proteins to maintain the ECM (Fassbender, 1987). The ECM is made up of a collagen fibre meshwork and negatively charged proteoglycans, which attract positive cations (Broom & Marra, 1985). Proteoglycans contribute to cartilage rigidity, stability and durability during compression (Redini, 2001) and bind water, which can make up 65-80% of cartilage (Martel-Pelletier *et al.*, 2008). They consist of a core protein attached to glycosaminoglycan (GAG) molecules, and water binds to the carboxyl and sulphate groups in these molecules. Despite being linked by the core protein, because these GAGs are negatively charged they repel each other, creating a mesh network, within which water molecules become immobilised (figure 1.1) (Maroudas & Evans, 1972).

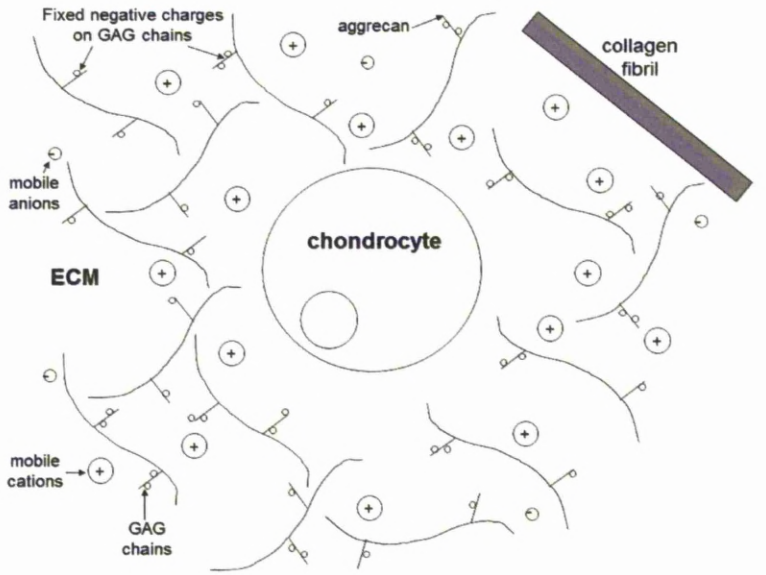

Figure 1.1 Schematic showing the location of a chondrocyte embedded in cartilage and the structure of its extracellular matrix.

Types II, IX and XI collagen form a tensile fibril network within cartilage, supporting the proteoglycans. Type VI collagens form adjacent to chondrocytes and may be

involved in attachment of the chondrocyte to the extracellular matrix (Bruckner & Van der Rest, 1994). In the superficial zone of cartilage collagen can account for up to 65% of tissue content. Non-collagenous proteins, such as Anchorin CII, are also involved in chondrocyte anchorage (Fernandez *et al.*, 1990). Chondrocytes maintain cartilage by establishing a balance between replacing degraded macromolecules and increasing synthesis in response to injury (Martin & Buckwalter, 2000). In return, the cartilage matrix protects chondrocytes from mechanical stress placed on the joint (Buckwalter & Mankin, 1998; Martin & Buckwalter, 2000). There is a relatively high matrix to cell volume ratio, particularly in mammalian articular cartilage where chondrocytes occupy no more than 10% of the total tissue volume (Stockwell, 1971). Arguably, the most important requirement of the ECM synthesised by articular chondrocytes is that it is able to withstand physical deformation as a joint articulates. Chondrocyte metabolic activity is directly correlated with the weight of mechanical stress placed on the cartilage; increased activity when the cartilage is heavily loaded provides maximum proteoglycan content (Urban, 1994). The ability of articular cartilage to withstand and respond to pressure and shearing forces is vital for it to fulfil its function.

Articular cartilage provides a challenging environment for the chondrocyte for three main reasons. Firstly, articular cartilage is avascular. Many nutrients, therefore, face steep concentration gradients and large travel distances; indeed, most nutrient/waste exchange occurs through diffusion from the synovial fluid (Lee & Urban, 1997; Allan, 1998). This avascularity also results in very low partial pressures of oxygen at the chondrocyte level (Wilkins *et al.*, 2000; Gibson *et al.*, 2008). Secondly, the ECM has a lower pH and higher osmolarity than most other cellular

environments (Browning *et al.*, 1999). The network of negatively charged proteoglycans surrounding each chondrocyte attracts positive cations resulting in a lowered extra-cellular pH. The hypoxic environment caused by the tissues avascularity (oxygen concentrations within cartilage reduce near to the cartilage-bone margin to almost zero (Otte, 1991)) adds to the low pH as the chondrocytes undergo mainly anaerobic glycolysis, thus creating excess lactic acid. In turn, this build-up of excess acid is difficult to remove due to the avascularity of the cell environment. Finally, the ECM surrounding the cells is constantly changing. As any joint moves it is thought that chondrocytes react to the increased mechanical stress with cell deformation by changing intracellular ion concentrations to try and maintain homeostasis of the ECM. It is also thought that with differing mechanical loads, chondrocyte secretions are altered, with proteoglycans and enzymes being secreted. This could be in response to intracellular calcium waves, as seen in other tissues (Sudhof, 2004). These intracellular changes may be caused by altered ion channel activity, which in turn will affect the current across the cell membrane as ions enter the cell. Once the mechanical loading ceases the chondrocyte can return to its resting state. However, it has been shown that with maintained mechanical loading the chondrocyte will react and change more slowly (Guilak *et al.*, 1999a). This could enable the cartilage to alter its composition to respond to the demands of the body. Alternatively, it appears that with repeated loading cycles the articular cartilage may be unable to recover fully from mechanical stresses (Urban, 1994). The processes which lead from these stresses and mechanical loads to changes in chondrocyte function are not understood. It is believed that the signals transduced by ion channels within a chondrocyte membrane enable these cells to regulate the

ECM (Erickson *et al.*, 2001; Yellowley *et al.*, 2002; Sanchez & Wilkins, 2004; Sanchez *et al.*, 2006). It is also believed that these channels may change (in number, composition etc.) in order to cope with the maintenance of the changing ECM (Buckwalter & Mankin, 1998). If we can understand how these processes interact, and can be pharmacologically controlled, we can potentially modulate their function with the intention of preventing or controlling cartilage degeneration. An emerging potential target for control of cartilage deterioration is the chondrocyte resting membrane potential (RMP).

1.2 Chondrocyte resting membrane potential

Until quite recently, the concept of the RMP being important for the control of chondrocyte function had not been widely discussed; however there are a number of clues emerging that this may be as important for chondrocytes as it is for other cells. Studies on the RMP of chondrocytes have found values varying between -12mV (Wright *et al.*, 1992) and -43mV (Ponce, 2006), which are generally considered relatively depolarised potentials, but similar to other non-excitable cells (Freedman, 1998).

The RMP has been shown to be central to the secretion and synthesis of substances in a variety of other cell types (Breittmayer *et al.*, 1996; McCarty, 1999; Penyige *et al.*, 2002). In general terms, the RMP of cells is central to the control of its function and its signalling with the local cellular environment. When the cell is at its RMP, ion movement into and out of the cell is at equilibrium. When a cell membrane is depolarised away from the RMP the cell generally becomes active, and this frequently leads to increases in cytosolic calcium ions and secretion (Sudhof, 2004;

Berridge, 2005). A similar scheme has been hypothesised for the chondrocyte (Hall *et al.*, 1996b). The suggestion is that as mechanical stress is placed on the chondrocyte this ionic equilibrium is disrupted, ion movements occur and cell signalling is altered. It seems likely, therefore, that if the RMP of chondrocytes is changed by ion channel manipulation, their ability to produce ECM will be compromised. This conjecture is indeed supported by experiments where RMP modifying ion channel blockers reduced the production of matrix mRNAs (Wu & Chen, 2000b), proteins and sulphated glycosaminoglycans (Mouw et al., 2007). Chondrocyte proliferation is also inhibited by blockers of ion channels (Wu & Chen, 2000b; Wohlrab *et al.*, 2002) and apoptosis increased (Grishko et al., 2010) As with other cells, the chondrocyte RMP is determined by the balance of positive and negative ion permeabilities in the cell membrane. These permeabilities are, in turn, established by the chondrocyte channelome (the complement of expressed ion channels and porins).

Ultimately, the RMP of any cell is determined by the behaviour of its compliment of ion channels. Ion channels are the essential components that control ion movement in and out of the cell (Hodgkin & Huxley, 1952a). They are embedded within the plasma membrane and usually consist of one or more subunits with a central aqueous pore, which opens by conformational change (reviewed by Catterall, 1995). The stimulus for opening (gating) is specific to each ion channel, and may be voltage, chemically or mechanically induced (Sachs, 1991; Unwin, 1993).

The Goldman-Hodgkin-Katz (GHK) voltage equation can be used to calculate a value for the RMP, when the cell is in equilibrium (Goldman, 1943; Hodgkin & Katz, 1949b).

$$\text{RMP} = \frac{RT}{F} ln\left(\frac{P_{Na^+}[Na^+]_{out} + P_{K^+}[K^+]_{out} + P_{Cl^-}[Cl^-]_{in} + P_{X^+}[X^+]_{out}}{P_{Na^+}[Na^+]_{in} + P_{K^+}[K^+]_{in} + P_{Cl^-}[Cl^-]_{out} + P_{X^+}[X^+]_{in}}\right)$$

Where, P_{Na^+}, $P_{K^+}$and P_{Cl^-} are the relative permeabilities of the combined sodium channels, potassium channels, and the chloride channels. The GHK equation describes how a change of relative permeability of the membrane to individual ions affects the RMP. The GHK equation was developed by Hodgkin and Huxley to calculate changes in membrane potential from individual ionic currents. This is discussed more in Chapter 7.

In neurones and striated muscle, there is the general principle that voltage-gated sodium channels (NaV_x) are largely responsible for the upstroke of an action potential and delayed rectifier potassium channels (Kv_x) are responsible for the repolarisation of the cell following the action potential. In the example of a neurone, there are additional voltage-gated calcium channels (CaV_x), which facilitate secretion of neurotransmitter. There are also a plethora of other ion channels which control the RMP, the ease with which a cell can be stimulated to fire an action potential (excitability) and the speed at which an action potential conducts. A chondrocyte does not conduct action potentials however, and so a fundamental question was "does the chondrocyte express ion channels?" The most basic answer to that question ("yes") has been known for some time. However the

next two questions would be, which ion channels does it express and what do they do?

1.3 Which ion channels are expressed in chondrocytes?

The process of identifying which ion channels and transporters are expressed in chondrocytes is the first aim of this thesis, but work has already begun in this area by my own and in other groups. It has been discovered that chondrocytes possess aquaporins (Mobasheri *et al.*, 2004b), and several members of the potassium channel family (Grandolfo *et al.*, 1990; Wilson *et al.*, 2004; Mobasheri *et al.*, 2007b). Voltage-gated channels including calcium, hydrogen, chloride and sodium channels (Sugimoto *et al.*, 1996a; Zuscik *et al.*, 1997) have been shown to be present, along with several different transporters, for example, the Na^+/H^+ antiporter, the $Na^+/K^+/Cl^-$ cotransporter and the Na^+/K^+-ATPase (Wilkins & Hall, 1992). Groups thus far have concentrated mainly on the potassium channel family or voltage-gated channels. This thesis aims to investigate the contributions of these and other, as yet unidentified, ion channels to chondrocyte function.

1.3.1 Potassium channels

1.3.1.1 Voltage-gated potassium channels

One of the first discovered ion conductances in biology was the potassium delayed rectifier (Katz, 1949). The ion channels underlying this are now known to be Kv channels, members of the Kv potassium channel family. This family is one of the largest ion channel families with at least 40 members of six transmembrane domains (Grissmer *et al.*, 1994). Interestingly, these were also one of the earliest

ion channels discovered in chondrocytes (Walsh *et al.*, 1992). Kv channels have now been reported in chondrocytes by a number of authors and have been shown to be archetypal slowly inactivating ion channels (Wilson *et al.*, 2004; Mobasheri *et al.*, 2005a; Ponce, 2006).

Relatively few studies have attempted to establish the molecular identity of the delayed rectifier in chondrocytes. However, reports suggest that these channels are similar between species (chicken, canine, equine, and elephant) in terms of their steady-state half-activation voltage and slope (Wilson *et al.*, 2004; Mobasheri *et al.*, 2005a; Ponce, 2006). Half activation parameters and activation time constant data taken from a number of studies suggest that the potassium channel of chondrocytes is likely to be a member of the Kv 1.x (Mobasheri *et al.*, 2005a). Pharmacological data are discussed in Mobasheri *et al* (2005a) and are not entirely consistent for Kv 1.x channels or one particular Kv channel. Immunohistochemical and RT-PCR data from the same study, have unequivocally revealed the presence of Kv 1.4 subunits in equine chondrocytes. Kv 1.6 has been revealed in murine chondrocytes (Clark *et al.*, 2010). Since Kv channels are known to exist as functional heteromultimers (Villalonga *et al.*, 2010) it is suggested that articular chondrocytes may express Kv 1.x, probably as a heteromultimer including the Kv 1.4 or Kv 1.6 subunits and probably some other, as yet unidentified, Kv subunit(s) (Barrett-Jolley *et al.*, 2010).

1.3.1.2 Inwardly rectifying potassium channels

K_{ATP} channels are a subfamily of inwardly rectifying potassium channels and are the only member of this group to have been shown in articular chondrocytes

(Mobasheri *et al.*, 2007b). These channels are closed by intracellular ATP and thus serve to couple metabolism to membrane excitability (Quayle *et al.*, 1997; Ashcroft & Gribble, 1998; Minami *et al.*, 2004). Structurally these channels exist as heteromultimers. Each functioning protein consists of four ATP binding cassette proteins (SUR) surrounding four inwardly rectifying potassium channel subunits (Kir 6.x) (Babenko *et al.*, 1998). In addition to being opened by decreasing intracellular ATP, K_{ATP} channels are also frequently observed to be opened by low oxygen tension and hypoxia (Dart & Standen, 1994). This suggests that these channels are important in hypoxia-mediated cell signalling (Phillis, 2004). As the chondrocyte exists at such low partial pressures of oxygen, it is suggested that the K_{ATP} channel seen in chondrocytes may be important for regulation of cartilage metabolism and sensing ATP levels within the cell (Mobasheri *et al.*, 2005b).

1.3.1.3 Calcium-activated potassium channels

Several studies have identified calcium-activated potassium channels in chondrocytes (Grandolfo *et al.*, 1992; Long & Walsh, 1994; Martina *et al.*, 1997; Mozrzymas *et al.*, 1997). These channels are reported to be opened by stretch and there are two theories as to the exact mode of activation. These can be termed either calcium dependent or calcium independent mechanisms. The calcium dependent hypothesis would require that stretch led to an increase in intracellular Ca^{2+} and that this activated the BK channel. Indeed a number of studies show changes in intracellular Ca^{2+} with osmotic or other mechanical challenge (Grandolfo *et al.*, 1998; Guilak *et al.*, 1999b; Yellowley *et al.*, 2002; Sanchez *et al.*, 2003; Sanchez & Wilkins, 2004). The source of such Ca^{2+} is controversial, but potentially,

dogma states that it must come from either influx (e.g., a channel or other transporter protein (Sanchez *et al.*, 2003; Sanchez & Wilkins, 2004; Phan *et al.*, 2009)) or from intracellular stores (Grandolfo *et al.*, 1998). The calcium independent hypothesis would involve either direct sensing of stretch by the channel itself, or coupling of the channel to other mechanoreceptors such as integrins (Mobasheri, 2002). The function of BK activation by stretch is still unknown, but there are a few clear possibilities. Firstly, the BK channel could be acting as an "osmolyte" channel (Hall *et al.*, 1996b; Kerrigan & Hall, 2008), since activation of potassium conductances will allow potassium ions to leave, decrease intracellular osmotic potential and facilitate regulatory volume decrease. Secondly, it is possible that it is the influence of the BK channel on the membrane potential which is critical, as it is in vascular tissue (Ledoux *et al.*, 2006). In addition to the body of work showing the presence of BK channels, there have also been a few reports of SK activity in chondrocytes, although no functional explanation for its presence (Wright *et al.*, 1996; Lee *et al.*, 2000; Ramage *et al.*, 2008; Funabashi *et al.*, 2010).

1.3.2 Sodium channels

The epithelial sodium channel (ENaC) is known to be responsible for sodium control in the kidney and colon, and has been shown to be important for the cellular control of volume in hepatocytes (Rossier *et al.*, 2002). It is also found in lung tissue (Mall *et al.*, 1998), and the taste buds (Lindemann, 2001). It is a member of the degenerin (DEG) and ENaC superfamily (Mano & Driscoll, 1999). ENaC is a heteromeric channel, formed of up to four subunits; α, β, δ, and γ (Canessa *et al.*, 1994) and is closely related to the acid sensing ion channels.

This channel is thought to be one of the most selective sodium ion channels and is significantly more permeable to sodium than potassium (Eaton *et al.*, 1995). Immunohistochemistry studies have shown that this channel is expressed in the chondrocyte (Trujillo *et al.*, 1999b), however, to date there has been no functional evidence shown.

Voltage-gated sodium channels (VGSC) are integral membrane proteins that are activated in response to voltage-changes across the plasma membrane (Catterall, 1995). The presence of tetrodotoxin sensitive VGSC has been reported in rabbit chondrocytes and in chondrocytes from osteoarthritic cartilage (Sugimoto *et al.*, 1996a; Ramage *et al.*, 2008).

1.3.3 Calcium channels

Voltage-gated calcium channels (VGCC) are a group of calcium permeable voltage-gated ion channels found in excitable cells (e.g., glial cells, neurones, etc. (Catterall, 1991)). The presence of L-type VGCCs in chondrocytes was suggested by Wright *et al* (1996) on the basis of pharmacological inhibition of calcium-dependent hyperpolarization by somatostatin and cadmium. This was supported by evidence of VGCC activity in growth plate chondrocytes, which was inhibited by cadmium (Zuscik *et al.*, 1997). It should be noted that whilst this is a plausible hypothesis, both somatostatin and cadmium affect a range of other ion channels including transient receptor potential channels (Carlton *et al.*, 2004), which may be present in chondrocytes. Ultrastructural studies have confirmed the presence of L-type VGCCs in mouse limb bud chondrocytes (Shakibaei & Mobasheri, 2003). These channels appear to be organized around β-1 integrin receptors with kinases and cytoskeletal

complexes in close proximity. The presence of L-type (and T-type) calcium channels in chondrocytes was recently supported by Mancilla *et al* (2007), however, Sanchez and Wilkins (2004) found that osmotically induced changes in intracellular calcium ions were not influenced by more selective L-type calcium channel blockers (including verapamil). In contrast aggrecan and collagen synthesis induced by electrical stimulation of cartilage is dependent upon the activity of VGCCs (Xu *et al.*, 2009). Clearly, further evidence for the presence of this channel is needed to clarify these data.

1.3.4 Transient receptor potential channels

Transient receptor potential channels (TRPs) are a super-family of related ion channels that are relatively non-selectively permeable to cations[1]. TRPs are found in many cell types, from yeast to mammals and several have been proposed to exist in chondrocytes (Gavenis *et al.*, 2009; Phan *et al.*, 2009). There are 6 sub-families: canonical (TRPC), melastatin (TRPM), vanilloid (TRPV), ankyrin (TRPA), polycystin (TRPP), mucolipin (TRPML) and TRPN (no-mechanoreceptor potential C) (Alexander *et al.*, 2008). The TRPC and TRPM subfamilies have seven and eight channel members, respectively. The TRPV and TRPP subfamilies have six and two channel members, whilst TRPA and TRPML each have one channel member (Kang *et al.*, 2007). All functional TRP channels have the same basic structure of six

---

[1] Transient Receptor Potential Channels. Authors: David E. Clapham, Bernd Nilius, Grzegorz Owsianik. Last modified on 2010-04-07. Accessed on 2010-06-24. IUPHAR database (IUPHAR-DB), http://www.iuphar-db.org/DATABASE/FamilyMenuForward?familyId=78.

transmembrane units with cytosolic N and C termini (Owsianik *et al.*, 2006). Whilst TRP channels can be modulated by a number of stimuli, none of the channels show substantial voltage sensitivity. The TRPC group mainly function as calcium store-dependent channels, activated by a decrease in intracellular calcium (Clapham *et al.*, 2001). They have a selectivity for Ca^{2+} over Na^{+} of between 1 and 6 (Kang *et al.*, 2007). The TRPV subfamily is also thought of as the mechano-sensitive group, as its members can be modulated by a number of physical stimuli. The subfamily can be further divided into two groups based on cation selectivity; TRPV1-4 have a rather low selectivity between mono and di-valent cations and are only slightly more permeable to calcium (P_{Ca}/P_{Na} of less than 10) whereas TRPV5 and 6 are highly permeable to calcium (P_{Ca}/P_{Na} can be greater than 100). TRPV1-4 stimuli include temperature (and capsaicin), phorbol-diesters and possibly mechanical stimuli such as stress. These channels are often thought of as the pain receptor channels, due to the nature of the stimuli they are sensitive to (reviewed by Patapoutian *et al.*, 2009).

TRPV4 is the only TRP channel to have been identified in non-diseased cultured chondrocyte (Phan *et al.*, 2009). A study on osteoarthritic chondrocytes found several TRP channel types; TRPC1, 3 and 6, TRPM1, 5 and 7, and TRPV1 and V6 (Gavenis *et al.*, 2009).

1.3.5 Chloride channels

Chloride channels are found in almost every animal cell (Nilius *et al.*, 1997) and have been shown to be involved in the regulation of cell volume, regulation of pH, control of cell membrane potential and also involved in the transport of amino acids

(Gronemeier et al., 1994). The largest sub-family within the chloride channel group is the ClC family, which contains nine members (ClC 1-9). Of these nine, only four are thought to be membrane bound proteins (ClC-1, 2 Ka and Kb), the others all have intracellular localisations (Estévez *et al.*, 2004). There are four other members of the chloride channel family, all functionally distinct from one another. These are the maxi-chloride channel, the volume-regulated chloride channel (VRAC), the calcium-activated channel and the cystic fibrosis transmembrane regulator (CFTR).

Voltage-dependent chloride channels and the maxi-chloride channel have been demonstrated functionally in chondrocytes (Sugimoto *et al.*, 1996a; Tsuga *et al.*, 2002), although there has been no molecular identification of the exact subtype. It has been shown that this large-conductance chloride channel contributes to the RMP of chondrocytes, as pharmacological inhibition of the channel significantly depolarised the membrane (Tsuga *et al.*, 2002). In addition to this, inhibition of this channel appears to have necrotic effects on the chondrocyte, suggesting that the activity of this channel plays an important part in chondrocyte survival (Wohlrab *et al.*, 2004). Of course, these necrotic effects could occur due to the effect that inhibition of this channel has on the membrane potential, rather than as a result of direct action on the chloride channel.

Another chloride channel family member found in chondrocytes is the CFTR (Liang *et al.*, 2010). Whilst the function of this channel in chondrocytes remains unknown, in other tissues the CFTR can function as a regulator of other ion channels, such as ENaC and VGCCs, both of which are known to be expressed in chondrocytes (Mall *et al.*, 1998; Nilius & Droogmans, 2003; Arniges *et al.*, 2004).

1.3.6 Hydrogen channels

The expression of voltage-activated hydrogen channels (VAHC) in chondrocytes has been demonstrated electrophysiologically (Sanchez *et al.*, 2006). In other cell types VAHCs are known to have roles in pH homeostasis, being able to rapidly induce an increase in intracellular pH through efflux of hydrogen ions (DeCoursey, 1991). In microglia, VAHCs have been shown to influence cell response to osmotic challenges, this has also been demonstrated in chondrocytes by use of fluorescence experiments (Morihata *et al.*, 2000; Sanchez *et al.*, 2003).

1.3.7 Acid-sensing ion channels

Two further ion channels recently identified in chondrocytes are the acid sensing channel, ASIC1a and ASIC3 (Kolker *et al.*, 2010; Yuan *et al.*, 2010) and the connexin43 hemichannel (Knight *et al.*, 2009). ASIC are very small cation selective channels closely related to ENaC (reviewed by Wemmie *et al.*, 2006). As their name implies, they are opened by extracellular protons. This is particularly relevant to chondrocyte biology since chondrocytes are routinely exposed to relatively acidic conditions, as low as pH 6.6 for example (Wilkins *et al.*, 2000). In vitro studies show that these channels mediate an increase in intracellular calcium upon exposure of chondrocytes to acidic conditions. This intracellular Ca^{2+} is likely to be a signal for production of enzymes and for proliferation. Potentially, inappropriate increases in calcium could result in cell death from either necrosis or apoptosis (Kolker *et al.*, 2010; Yuan *et al.*, 2010). The role of the connexin 43 is possibly more complex. Knight *et al* (2009) found it to be constitutively active in about 40% of chondrocytes, and as such it might be expected to profoundly depolarize the membrane. In

summary, the suggested scheme of connexin43 involvement was that mechanical stimulation of chondrocyte cilia activates the hemichannel which then acts as a conduit for ATP release. This released ATP then acts on chondrocyte membranes (via P2 purinoceptors) to increase intracellular Ca2+ (Knight *et al.*, 2009).

1.3.8 Aquaporin channels

Aquaporins (AQP) are a family of small integral membrane proteins related to the major intrinsic protein (MIP), sometimes called AQP0 (Agre *et al.*, 1993). The first AQP discovered, AQP1, was identified during experiments investigating the identity of the rhesus blood group antigens (Denker *et al.*, 1988). Oocytes from Xenopus laevis microinjected with in vitro-transcribed mRNA of AQP1 (previously known as CHIP28) exhibited increased osmotic water permeability compared to uninjected controls. This observation, combined with the reversible inhibition induced by mercuric chloride, provided the first molecular evidence for water channels (Preston *et al.*, 1992). Since the identification of AQP1 the field has expanded to now include study of AQP in all types of organisms. Over a dozen AQP have been identified in mammals. The classical AQP transport water exclusively. However, a second class of AQP has now been identified (Rojek *et al.*, 2008), these so-called aquaglyceroporins also transport small, uncharged molecules such as glycerol and urea; examples include AQP3, AQP7, and AQP9 (Carbrey *et al.*, 2003). Many models of chondrocyte function involve changes in volume (Hall *et al.*, 1996b). For this to occur there must be pathways for the movement of water into and out of the cell. The discovery of AQP channels in chondrocytes would appear to provide an appropriate mechanism (Mobasheri & Marples, 2004; Mobasheri *et al.*, 2004a;

Mobasheri *et al.*, 2004b; May *et al.*, 2007). Studies have shown a loss of volume regulation with inhibition of AQP channels (May *et al.*, 2007) and reductions in migration and adhesion of chondrocytes (Liang *et al.*, 2008).

1.3.9 Ion pumps and co-transporters

Three ion pumps have been identified in chondrocytes; the Na^+/H^+ antiporter, the $Na^+/K^+/Cl^-$ cotransporter (NKCC) and the Na^+/K^+-ATPase (Wilkins & Hall, 1992; Trujillo *et al.*, 1999a). These are membrane-bound proteins responsible for maintaining the intracellular concentrations of the appropriate ions. The Na^+/K^+-ATPase has a high number of copies per chondrocyte (~$1.5x10^5$ Mobasheri *et al.*, 1998)) and will upregulate its numbers following a sustained increase in intracellular sodium. The intracellular sodium concentration will, of course, be dependent on extracellular factors. Therefore it is likely that this pump is able to play a role in the adaptation of a chondrocyte to its extracellular environment (Trujillo *et al.*, 1999b). Increasing amount of evidence is showing that ion pumps may also be important in the control of chondrocyte volume and this is discussed further below.

1.4 What do chondrocyte ion channels do?

To fully understand the function of chondrocyte ion channels it is necessary to know exactly how each channel contributes to the RMP. One way to do this is to measure the RMP and apply agonists and antagonists of the particular ion channel of interest. This has some major disadvantages however. The first of these is that one would need rather selective activators and inhibitors for each ion channel. For many ion channels these simply do not exist. The second disadvantage is that the behaviour of ion channels will differ in different ionic and thermal conditions and

with different levels of dissolved oxygen and carbon dioxide. It is difficult to be confident of the level of each of these variables *in vivo* and to complicate matters further the variables are likely to also change in disease states. To set-up totally physiological (and pathophysiological) conditions covering each of the possible combinations is unrealistic. Furthermore, the *in vivo* chondrocyte is likely to be exposed to various hormones, autacoids and mediators. One would need to study ion channels with and without each of these in each of the possible combinations of physiological variables. A final disadvantage is that as the cell RMP is dynamically linked to the function of several different ion channels, one could determine that a particular ion channel blocker initiated a change in RMP, but this change may have involved other ion channels too, which were themselves affected by the change of RMP. One approach to tackling these problems is to follow the procedures used to study the function of neurones and muscle (Hodgkin *et al.*, 1949; Ling & Gerard, 1949; Weidmann, 1951; Hodgkin & Huxley, 1952b). One can attempt to identify each of the major ion channels expressed in the chondrocyte membrane and build a computer simulation of their activities. Variables for parameters such as temperature and ionic composition can be included and estimates made of how these would change with variations of cellular environment. Having built such a model one can investigate the predicted effects on RMP of any one of the known ion channels. When one has clear "results" one can then check back in various *in vitro* models to see if specific challenges do result in the predicted outputs. If the model matches the data then it strengthens the validity of the model, if there is a mismatch the model must be refined and modified. This is an iterative process. This model can be loosely based on the work of Hodgkin and Huxley (Hodgkin & Huxley,

1952b), which describes how changes in ionic current density affect the RMP. Further refinement of this basic model will then introduce changes of membrane potential with time using linear differential equations.

1.5 Volume regulation

Chondrocytes location, embedded in cartilage, means that these cells are subjected to significant dynamic loads during physical activity (Eckstein *et al.*, 1999). The limb joints in a galloping horse, for example, will routinely experience compressive forces of 7,500 Newtons (Setterbo *et al.*, 2009). Contact pressures have been directly measured in human hip joints and are reported to be as high as 18MPa (Hodge *et al.*, 1986). Under pressure, cartilage exudes fluid (McCutchen, 1962) and thus decreases in volume. This involves changes in water content of the interstitial component of cartilage and consequent changes in extracellular osmotic potential (Mow *et al.*, 1992; Mow *et al.*, 1999; Sivan *et al.*, 2006). Typical osmolarities for many mammalian cells are in the region of 300mOsm. However, under load, the osmolarity of the extracellular matrix of cartilage is believed to be approximately 480mOsm (Urban, 1994). More recently, osmolarities as high as 550mOsm have been used to model the three dimensional microenvironment of chondrocytes under load (Xu *et al.*, 2010). Changes in osmotic pressure are reversible upon relaxation (Mow *et al.*, 1992; Urban, 1994) and so during normal usage chondrocytes will be cyclically exposed to both increasing and decreasing osmotic forces. Healthy chondrocytes are able to regulate their volume with remarkable resilience throughout these osmotic pressure cycles (Bush & Hall, 2001a). However,

chondrocytes swell during the decreasing phases of the osmotic pressure cycle (Bush & Hall, 2001b) and are vulnerable to damage (Bush *et al.*, 2005).

When subjected to osmotic challenge any cell has to react to overcome the changes in osmolarity, and maintain its volume. Exactly how the chondrocyte maintains its volume is unknown, although it is thought that the cell uses ion channels to manipulate its intracellular osmolarity to oppose any passive water uptake or loss. There are two methods of cell volume control; regulatory volume increase (RVI) and regulatory volume decrease (RVD).

1.5.1 RVD

When a cell is submitted to a hypotonic challenge it swells due to the passive uptake of water via osmosis. As the cell takes up an increasing volume of water the cells will oppose this by effluxing ions, thus decreasing the intracellular osmolarity until it is once more in equilibrium with the extracellular environment. The exact mechanisms of ion channel involvement are not currently known, although there have been various hypotheses. It is likely that the passive water movement which occurs in both RVI and RVD is facilitated by aquaporin channels. How the cell moves ions to oppose water flux is less clear, however.

The open probability of stretch-activated ion channels generally increases in response to mechanical deformation of the plasma membrane (Sachs, 1991). Although very little is known about chondrocyte stretch-activated ion channels and the macromolecular complexes in which they function, it is thought that they may be linked to the cytoskeleton via b1- integrins (Mobasheri *et al.*, 2002). This may be responsible for their gating by transmitting extracellular physical forces of stretch or

pressure to the channels, causing them to undergo a conformational change. Activation of these ion channels may lead to changes in cell activity via alteration of the resting membrane potential (Mobasheri *et al.*, 2002). This is supported by studies using ion channel blockers that disrupt the process of mechanotransduction (Wu & Chen, 2000a; Mouw *et al.*, 2007). Other studies have suggested that there are "osmo-sensing" channels in the cell membrane which somehow react to the change in osmolarity and thus increase the intracellular ionic concentration allowing an efflux of sufficient ions to drive a decrease in cell volume (regulatory volume decrease) (Hall *et al.*, 1996b). The identity of these channels has, however, remained unknown.

It is possible that the channel responsible for ion efflux is a potassium channel (Hoffmann & Dunham, 1995; Hoffmann *et al.*, 2009). As the cell volume increases it seems likely that the membrane stretches in response. It has been suggested that the BK channel may be activated by membrane stretch and therefore an efflux of potassium is responsible for returning the cell back to its original volume, however the exact mechanism for this is unknown (Long & Walsh, 1994; Mobasheri *et al.*, 2010). One would also expect there to be a matching anion efflux (chloride, for example) to maintain electroneutrality and reduce the total loss of potassium ions. A maxi-chloride channel could potentially provide this efflux and possibly explain why it is thought to be a volume-sensing channel (Tsuga *et al.*, 2002).

1.5.2 RVI

RVI is the process by which a cell recovers its volume following a hypertonic challenge. When exposed to a hypertonic solution a cell will shrink in volume, as

water passively leaves the cell via aquaporins in the membrane. To oppose this shrink, a cell will try to influx ions so that water will follow back into the cell. Numerous mechanisms have been proposed for this, with the most popular being that RVI is controlled by various Na^+ pumps. As the cell shrinks these pumps can operate in reverse-mode and return ions to the cell, increasing intracellular osmolarity and drawing water back in. One of the pumps implicated in this is the NKCC co-transporter. This has been shown to be involved in cell volume increase in smooth muscle and kidney cells (Lytle, 1997; Russell, 2000). However, a recent study found that although the NKCC is present in growth-plate chondrocytes significant inhibition of this channel did not block the RVI process in chondrocytes (Bush *et al.*, 2010). All the channels and transporters involved in this process are yet to be identified.

1.6 Volume control and cartilage degeneration?

Osteoarthritis is the most prevalent connective tissue disease of both humans and other animals, including cats and dogs, where the incidence of disease in larger breeds can approach 75%. In humans the incidence is at 60% in men and 70% in women over the age of 65 (Goldring & Goldring, 2007). This degenerative disease is usually only detected once the patient has experienced significant pain in a joint, by which time damage to the tissue is irreversible. The processes leading to this condition are not well understood, although it is believed it may result from trauma, joint abnormalities and/or ageing. It is believed that these changes may be a result of, or cause, changes in chondrocyte function. For example, ageing results in

structural and compositional changes within cartilage, causing a loss of strength and volume of the tissue (Simon & Green, 1971; Creamer & Hochberg, 1997).

Chondrocytes are responsible for the secretion of proteoglycans to maintain the strength of cartilage, which, in turn, determines its water content. It is thought that as the ageing/degenerative process happens, proteoglycan production decreases and as a result less water is bound within the network. This leads to a softening of the cartilage, commonly known as chondromalacia, and an increase in water in the joint (Stockwell, 1991). This instability within the joint eventually leads to cartilage erosion and, ultimately, loss of function as the cartilage is no longer able to protect the bones from the mechanical stresses placed upon it. As water is no longer bound within the tissue these stresses result in greater variations in hydrostatic pressure. These greater osmotic pressures are thought to further exacerbate the degeneration process, leading to further joint instability as tissue volume increases (Bush & Hall, 2003; Wilson *et al.*, 2004). Decrease in osmotic potential (increased water content) has been linked to the early onset of osteoarthritis (Stockwell, 1991) and loss of volume control has been specifically linked to chondrocyte death and the progression of osteoarthritis (Bush & Hall, 2003; Bush *et al.*, 2005). The exact processes leading to this point, however, remain unknown. Apoptosis of chondrocytes, the mechanism of controlled cell death, has been linked to the pathogenesis of osteoarthritis, however, little is known about the processes involved. Indeed, chondrocyte apoptosis could be a result of the disease, rather than a causative factor. (Kerr et al., 1972; Mobasheri, 2002; Kim & Blanco, 2007).

It has been reported that chondrocytes from osteoarthritic tissue appear distended, having swollen to fill the space available in the lacunae (Stockwell, 1991). One explanation for this is that as the proteoglycan content decreases and water content increases, the cells counteract this by uptake of water through osmosis, leading to cell swelling greater than that seen in healthy cartilage as the cells try to maintain an iso-osmotic environment (Bush & Hall, 2005). In many tissues, failure or malfunction of ion channels may cause the pathways that allow the cells to self-regulate to become blocked or imbalanced. In addition to this, changes in function of ion channels will affect the RMP of the cell, which may, in turn, affect cell function. It has been shown that certain chondrocyte secretions (various matrix mRNAs) can be affected by alteration of the RMP using ion channel inhibitors but the mechanisms underlying this are unknown (Wu & Chen, 2000b).

1.7 Aims

This work has two main aims. The first aim is to determine the types and functions of ion channels expressed in articular chondrocytes, in a number of species, using electrophysiology and polymerase chain reaction. Once channels have been identified, measuring the chondrocyte RMP and examining the effect of each of these ion channels on the RMP will lead into the second aim, which is to produce a mathematical model of membrane potential. Iterative testing and refining of this model will be performed, using *in vitro* experiments on chondrocytes. The function of identified channels will be investigated, with particular emphasis on the control of cellular volume. A model of chondrocyte volume will be built which can again be tested and refined based on the results from the *in vivo* experiments.

2

METHODS

2.1 Tissue dissection and cell culture

Canine cartilage was removed from stifle and elbow condyles of large, skeletally mature, bull terrier types euthanatized for unrelated clinical reasons (body mass 12-16kg; age <4 years). Bovine, ovine and equine joints were sourced from a local abattoir. All tissue was less than 36 hours post mortem when dissected.

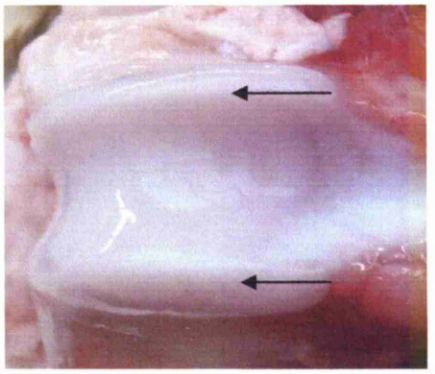

Figure 2.1 Canine stifle joint showing areas where cartilage is removed from. The joint has been opened up by removal of the joint capsule. Arrows show area on condyle from which cartilage scrapings were taken. Strips of cartilage were peeled from the condyles and transferred immediately to Dulbecco's Modified Eagles Medium supplemented with penicillin-streptomycin and fungizone as described in the text.

For canine articular cartilage, stifle and elbow joints were dissected and scrapings removed from the condyles (figure 1). Equine, ovine and bovine cartilage scrapings were removed from the metacarpophalangeal joint. The cartilage pieces were then washed in Dulbeccos Modified Eagles Medium (DMEM) supplemented with 1000mg/L glucose, 4mM L-glutamine and 110 mg/L sodium pyruvate, 2%

Penicillin/Streptomycin solution (10000:10000ug) and 1% Fungizone-antimyotic solution (250ug/ml). The shavings were placed in sterile filtered DMEM with 0.1% collagenase type II and incubated overnight for 14-16 hours at 37°C with shaking.

Isolated cells were then filtered, centrifuged at 3000*g* and resuspended in DMEM. This was repeated three times to wash the cells before cells were suspended in DMEM, as above, plus 10% Foetal Calf Serum. The cell solution was then put into culture flasks and incubated for two days before being washed, centrifuged and resuspended in fresh medium with serum. Cells were then left to culture until confluent. Cells were considered ready for patch clamping when they reached 70-100% confluence.

Smooth muscle cells were isolated from rat aorta for membrane potential measurements. Aortic tissue was placed into chilled zero calcium buffer containing (in mM): 137 NaCl, 5.4 KCl, 0.44 NaH_2PO_4, 0.42 Na_2HPO_4, 1 $MgCl_2$, 10 HEPES and 10 glucose, pH 7.4 with NaOH. All connective tissue was cleaned off and the aorta was cut transversely to form rings of smooth muscle. These rings were then incubated for 55 minutes at 35°C in a 0.1mM calcium buffer and enzyme mix containing 1.4 mg ml^{-1} papain, 0.9 mg ml^{-1} dithioerythritol and 0.9 mg ml^{-1} bovine serum albumin (BSA). The 0.1mM calcium buffer had the same composition as the zero calcium buffer with the addition of 0.1mM $CaCl_2$. After enzyme treatment the aortic tissue was removed from the mixture and washed twice in 0.1mM calcium buffer with 0.9 mg ml^{-1} BSA. The tissue was then transferred into 0.1mM calcium buffer (with no BSA) and triturated with a Pasteur pipette until single cells were dispersed. The cell

suspension was then transferred to glass-bottomed dishes ready for electrophysiology.

All cell isolation and culture reagents were from Invitrogen, UK.

2.2 Electrophysiology

Cells were passaged with 1x trypsin and resuspended in DMEM, before being plated out and left to lightly adhere to glass-bottomed electrophysiological recording chambers ready for patch clamping. Cells were used when freshly isolated, at first expansion and then up to and including the 3rd passage, Previous studies have shown that chondrocytes in culture begin to lose their differentiated phenotype in later passages (Kang *et al.*, 2007). The differentiated chondrocytes of cartilage *in vivo* express type II collagen, which is endogenous to this tissue, and this has been found to be true for first, second and third passage chondrocytes. However, as the passage number increases the chondrocytes become de-differentiated, lose their phenotype and start producing type I collagen, endogenous to skin, tendon and bone tissue, in place of type II. Thus experiments on chondrocytes of passage number 4 and above were not carried out as these chondrocytes appear to lose their phenotype.

Patch pipettes were fabricated using fire-polished 1.5mm o.d. borosilicate glass capillary tubes (Sutter Instrument, Novato CA, USA supplied by INTRACEL, UK). They were pulled using a two-step electrode puller (Narishige, Japan) and when filled with the various pipette solutions had a resistance in the range of 3-8MOhm depending on their usage. Pipettes used for single-channel recordings had higher resistances than those used for whole-cell experiments in order to reduce noise on

the recordings. All solutions used in electrophysiological experiments are detailed in Table 1 (extracellular solutions) or Table 2 (intracellular solutions). Junction potentials are shown in Table 3 for the relevant extracellular and intracellular solution pairings and were calculated using JpCalc (Barry & Lynch, 1991).

All reagents used in electrophysiology were from Sigma-Aldrich, UK, unless stated otherwise.

2.2.1 Inside-out patch clamp

To achieve an inside-out patch, a cell-attached patch was first formed by moving the pipette into contact with the cell surface. Applying negative pressure to the cell membrane achieved a giga-seal, and patches of the cell membrane were excised by moving the pipette away. This exposed the cytosolic surface of the membrane to the intracellular bath solution. Single channel activity was measured in voltage clamp and recorded with an Axopatch 200a amplifier (Axon Instruments, USA). Data were typically filtered at 2kHz and sampled at 10kHz with a DigiData 1200B interface attached to a PC typically running the WinEDR software (Dr. John Dempster, University of Strathclyde).

All single channel experiments were performed under "potassium-free" conditions, see Tables 1 and 2 for solutions. Previously, large conductance potassium channels have been identified in chondrocytes by my group, and others (Grandolfo *et al.*, 1992; Mobasheri *et al.*, 2010), so this thesis initially set out to investigate what other conductances may be present. Eliminating potassium from the experimental solutions would allow smaller conductances to be seen.

Single-channel all-points amplitude histograms were created in WinEDR. Amplitudes taken at various holding potentials were used to create current-voltage (*IV*) curves and from the equation of the fitted line channel reversal potentials (*Vrev*) and slope conductances (*g*) could be calculated. Raw channel recordings were fitted using QuB software (Qin et al, SUNY, Buffalo, NY) to calculate open probabilities.

2.2.1.1. Equilibrium Potentials

The Nernst equation is a formula which allows the calculation of the equilibrium potential (E_I) that occurs due to the separation of charged ions by a selectively permeable membrane. Due to the differential distribution of ions in the intracellular and extracellular solutions it is not known where the equilibrium potentials for each ion lies. Using the Nernst equation (Equation 1) it is possible to calculate the E_I for each ion within the solutions.

$$E_I = -58 * z * log\left(\frac{[I]_{in}}{[I]_{out}}\right) \qquad \text{Equation 1}$$

where; E_I is the equilibrium potential of the ion, z is the valency of the ion and $[I]_{in}$ and $[I]_{out}$ are, respectively, the intracellular and extracellular concentrations of the ion. For a pure selective ion channel the E_I equates to the reversal potential (V_{rev}) of the channel at which the channel current is zero. This calculated V_{rev} can then be compared to the experimentally measured value taken from the *IV* curves.

2.2.2 Whole-cell voltage clamp

For whole-cell clamp a giga-seal was achieved as described above for inside-out patch clamp. Applying additional negative pressure ruptured the cell membrane to

form a whole-cell seal. All voltage-clamp experiments were performed using the same equipment set-up as the single-channel experiments.

Tail currents were used to measure non-selective cation currents. Tail currents consisted of a 1s voltage step at 0mV followed by a step at 80mV for 3s before stepping to -80mV. This protocol was repeated 14 times, on each iteration the pulse potential increased by +10mv, to a maximum holding voltage of +50mV.

Voltage ramps were used to record whole-cell benzamil- and gadolinium-sensitive currents. Voltage ramp protocols consisted of a 50ms voltage step at 0mV followed by a 4.5s linear ramp from -60mV to +80mV. This was repeated every 50s. Difference currents were obtained by subtraction of a ramp in the presence of benzamil and/or gadolinium from that run in vehicle control. Full details are given in the relevant chapters.

To study the relative whole-cell permeability of monovalent cations and calcium ions, solutions containing the appropriate ion to be tested were used (see Table 1 and Chapter 3) Permeability ratios were calculated using the equations of Voets *et al.* (2002), using the reversal potentials (V_{rev}) of the gadolinium-sensitive current-voltage ramps.

For monovalent cations:

$$P_x/P_{Na} = exp(\Delta V_{rev} * F/RT) \qquad \text{Equation 2}$$

Where, P_x/P_{Na} is the ratio of the permeability of ion *x* relative to sodium, ΔV_{rev} is the difference in reversal potential between the conductance of ion *x* and that of sodium, F is Faradays constant (value of 96,485.3415 C mol^{-1} used here), R is the gas

constant (taken to be 8.314472 J K^{-1} mol^{-1}) and T is temperature (293K in these experiments).

For calcium ions:

$$P_{Ca}/P_{Na} = \left(1 + exp(V_{rev} * F/RT)\right) * \frac{([Na]_i + \alpha[Cs]_i)exp(V_{rev} * F/RT) - [Na]_e - \alpha[Cs]_e}{4[Ca]_e}$$

Equation 3

Where, $[Na]_i$ and $[Na]_e$ are the intracellular and extracellular sodium concentrations, respectively, $[Cs]_i$ and $[Cs]_e$ are the intracellular and extracellular caesium concentrations, respectively, V_{rev} is the reversal potential of the calcium conductance, F, R and T have the same definitions as above and α is defined as the permeability ratio of sodium to caesium:

$$\alpha = P_{Cs}/P_{Na}$$ Equation 4

2.2.3 Whole-cell current clamp

RMP were measured in current clamp mode by three different amplifiers (Axon Axopatch 200a, 200b, Cairns Optoclamp) and by sharp electrode recordings. For RMP recordings using sharp electrodes (NPI SEC-05LX amplifier), electrodes were filled with 1 or 2M KCl and had resistance of approximately 100mOhm. The extracellular solution was physiological saline (Table 1).

The effect of temperature on the RMP was measured using the same set up as above (Axopatch 200b amplifier) and the bath solution was monitored by a temperature control unit (TC-10npi).

2.2.4 Video imaging and Switch Clamp

Switch-clamp voltage clamp methods involve a rapid switching between current injections and voltage measurements as a cell is clamped. The voltage measured from the membrane is compared to a holding voltage and the difference between the two is then used in the next round to inject the appropriate current to bring the membrane to the desired voltage.

Cells were voltage clamped with single sharp electrodes filled with 1 or 2M KCl, under switch clamp mode (SEC 05LX, NPI amplifier). When filled electrodes had a resistance of approximately 100mOhm. Input voltage pulses were viewed on an oscilloscope (Tektronix 2225 50MHz) and switching frequency was 35kHz.

Cells were videoed whilst under switch clamp with a Hitachi (KP-M3E/K CCD) camera attached to a Nikon Eclipse microscope magnification ~1000x.

2.2.5 Voltage-sensitive dye membrane potential measurements

To measure the membrane potential with optical dyes oxonol VI was used (Apell & Bersch, 1987; Wohlrab *et al.*, 2001). Oxonol VI (100-300nM) was added to the perfusion solution, for at least 15 minutes prior to commencement of recording. Perforated patch methods were used, where 200nM amphotericin B (stock concentration 30mg/ml in DMSO) was added to the pipette solution (physiological saline, table 2) to puncture the membrane held by the pipette. The optical system (Hitachi KP-M3E/K CCD camera attached to a Nikon Eclipse microscope, G-2A filter set, magnification ~1000x) was calibrated by measuring the average intensity in a chondrocyte, under perforated patch clamp at a range of membrane potentials. The intensity versus voltage calibration curve was then used to extrapolate membrane potentials of surrounding un-clamped chondrocytes.

2.3 Cell volume measurements

Cells were visualised under a Philips Toucam Hi-resolution webcam attached to the eyepiece of the microscope (NIKON, 400x magnification). YAWCAM software (www.yawcam.com) was used to capture and file images every 10 seconds. Cells were bathed in physiological saline for at least 20 minutes prior to recording starting. A hypertonic solution was created by addition of 180mM sucrose to physiological saline to create a solution of 489mOsm. For experiments which required cells to experience a hypotonic shock, the bathing solution at the start of the experiment was the 489mOsm physiological saline and the cells were subjected to the usual physiological saline (309) to provide the hypotonic challenge.

Extracellular (mM)	Na	K	Ca	Cl	Mg	Cs	SO_4	Li	Glucose	Hepes	pH adjustment
ENaC – Single channel	155	0	4	158	0	0	0	0	0	10	NaOH
ENaC – LiCl	0	9	2	151	1	0	0	140	0	10	KOH
RMP – Physiological saline	145	5	2	151	1	0	0	0	0	10	NaOH
Whole-cell voltage ramps – Sodium methanesulfonate	155	0	2	4	0	0	0	0	0	10	NaOH
TRP- Ca permeability	105	0	30	169	2	0	0	0	0	10	NaOH
TRP – Na permeability	154	0	0	154	2	0	0	0	0	10	NaOH
TRP – Cs permeability	2	0	0	139	2	135	0	0	0	10	NaOH
TRP – K permeability	0	154	0	154	2	0	0	0	0	10	KOH
BK – Stretch	0	115	2	115.6	1.6	0	0	0	10	10	KOH

Table 1 Extracellular solutions used during electrophysiology and cell volume measurements. All extracellular solutions were pH 7.4

Intracellular (mM)	Na	K	Ca	Cl	Mg	Cs	SO_4	Gluconate	EGTA	BAPTA	TEA	Hepes	pH adjustment
ENaC – Single channel	188	0	0	10	0	0	90	0	5	0	10	10	NaOH
RMP – Physiological saline	0	150	0	28	1	0	0	115	5	0	10	10	KOH
Whole-cell voltage ramps – Sodium methanesulfonate	150	0	0	0	0	0	0	0	0	5	0	10	NaOH
TRP – Permeability	2	0	0	137	1	135	0	0	5	0	0	10	NaOH
BK – Stretch	0	152	0	150	1	0	0	0	0.5	0	0	10	KOH

Table 2 Intracellular solutions used during electrophysiology. All intracellular solutions were pH 7.2

Extracellular solution	Intracellular solution	V_j (mV)
ENaC – Single channel	ENaC – Single channel	-5.9
RMP – Physiological saline	RMP – Physiological saline	-14.4
RMP – Physiological saline	1M KCl (Sharp electrode)	-3.7
BK - Stretch	BK - Stretch	-7

Table 3 Junction potentials (Vj) calculated for the combinations of extracellular and intracellular solutions shown. Calculation was performed with JpCalc (Barry & Lynch, 1991).

2.4 RT-PCR

2.4.1 Primer Design

Nucleotide sequences of the channels were sourced from the NCBI nucleotide database[2]. To identify areas of homology between sequences, FASTA sequences were input into ClustalW (Chenna *et al.*, 2003) for alignment. Once an area of homology had been found, the sequence was input into Primer3 (Rozen & Skaletsky, 2000). Primer picking conditions were left on standard settings. Primer pairs produced by Primer3 were then analysed by NetPrimer (PREMIER Biosoft International, Palo Alto, CA). Primer pairs with none or few hairpins, dimers and repeat and runs were selected for use in PCR.

2.4.2 RNA extraction and preparation of cDNA from chondrocytes

Total RNA was extracted from first expansion canine chondrocytes by use of an RNeasy Mini Kit (Qiagen, UK) according to manufacturer's instructions. Briefly, cells were lysed by addition of a lysis buffer then centrifuged. The supernatant was used in all subsequent stages and the pellet discarded. The sample was cleaned by addition of ethanol before being transferred to an RNeasy mini column (from kit) and centrifuged. The spin column now containing the total RNA was washed before elution of the total RNA by addition of RNase-free water. Total RNA was then purified by elimination of genomic DNA using deoxyribonuclease I, Amplification Grade (Invitrogen, UK). Isolated total RNA was then used as a template to create

---

[2] http://www.ncbi.nlm.nih.gov/nuccore/

first-strand cDNA by Superscript II Reverse Transcriptase (Invitrogen, UK). 1µl of this cDNA was used as a template for PCR using the primer sets in Table 3. A negative control ("-RT") was created for every tissue by the substitution of reverse transcriptase for RNase-free water in the mix. This "–RT" was then used alongside the prepared cDNA in every PCR reaction. Substituting RNase-free water for the reverse transcriptase prevents synthesisation of first strand cDNA from the total RNA therefore there will be no product produced during the subsequent PCR reaction. The PCR reaction mix (BIOTAQ DNA Polymerase kit; BIOLINE, UK) consisted of: 5µl 10xNH_4 buffer, 1µl 100mM dNTP mix, 1.5µl 50mM $MgCl_2$ solution, 1µl BIOTAQ DNA polymerase, 2µl of forward primer and 2µl of reverse primer made up to 50µl with double-distilled water. PCR was performed with 40 cycles in total on a Techgene FTGene2D thermocycler (Techne, UK). PCR consisted of an initial denaturation step at 92°C for 30s, an annealing step at the appropriate temperature for 30s and an extension step of 72°C for 60s. Individual annealing temperatures for each of the primer sets are shown in Table 3. If running the PCR at the appropriate annealing temperature failed to produce a product then touchdown PCR was run. Touchdown PCR consisted of an initial denaturation step at 92°C for 30s, an annealing step at 65°C for 30s and an extension step of 72°C for 60s. The annealing step was decreased by 1°C with each cycle to a final temp of 56°C. PCR products (10µl) were separated by electrophoresis on a 1.5% agarose gel (2 hours at 80mV) and the bands were visualised by Gel Red (Biotium, Cambridge, UK) staining using a UV transilluminator (BioRad, UK). Sequencing was performed by Beckman Coulter Genomics (Essex, UK).

2.4.3 RNA extraction and preparation of cDNA from animal tissue

Rat mesenteric artery, tracheal smooth muscle and cardiac muscle and canine mesenteric artery were dissected out and placed in appropriate volumes of RNAlater (Sigma, UK) to stabilise and protect cellular RNA. For extraction of total RNA, tissue samples were removed from RNAlater and weighed. 30mg of tissue was placed in a lysis buffer before being homogenised then centrifuged, the supernatant was removed and total RNA then extracted as above. The PCR cycles were as described above in *2.4.2*. These tissue samples were used to identify positive controls from the primer pairs.

Channel	Source (Accession number or citation)	Species mRNA	Primer pair sequences (5' – 3'; Top = Forward, Bottom = Reverse)	Size (bp)	Annealing Tm (°)
TRPC3	FJ205711	Canine	GCATTCTCAATCAGCCAACA	176	62
			GTTGCTTGGCTCTTGTCCTC		
	(Walker *et al.*, 2001)	Canine	ATTATGGTCTGGTTCTTGG	331	59
			GAGAAGCTGAGCACAACAGC		
	(Gavenis *et al.*, 2009)	Human	CTGCAAATGAGAGCTTTGGC	388	57
			AACTTCCATTCTACATCACTGTC		
	(Rose *et al.*, 2007)	Rat	TCAGGCGGGCAGTCCACATGAT	601	70
			GCCCGTGTCTCTCCAGGGGTTC		
	(Rose *et al.*, 2007)	Rat	TGGAACCCCTGGAGAGACACGG	801	70
			CGTTTGCAGGGAGAATGTACGCGA		
TRPC6	(Walker *et al.*, 2001)	Canine	TTCCTGTTCCCTTCAACCTG	372	62
			GTTCCCCTTCATTCACCTCA		
	(Gavenis *et al.*, 2009)	Human	AAGACATCTTCAAGTTCATGGTC	322	60
			TCAGCGTCATCCTCAATTTCC		
TRPV4	EF561643	Canine	AGCGAGACATTCAGCACCTT	621	62
			AGCATCGTCAGTCCTCCACT		
TRPV5	BC110554	Murine	GCCCCTAACATCTTCCCTCT	165	61
			TGTCCATATTTCTTCCACTT		
	AY762624	Rat	CACAGTGATGCTGGAGAGGA	~300-	62
			GTGGCTATTGCTGCTTAGGG	350	
	AY206695	Human	CCATGCTACTCAGGGACGAT		62
			CATGCCAAGCACTCTTTCAA	178	
	(Li *et al.*, 2010)	Rat	TTGGTGCCTCTCGCTACTTT		62
			CAGAGTTCGTCCCTCTCCTG	265	
	(Kunert-Keil *et al.*, 2006)	Murine	CGTTGGTTCTTACGGGTTGAA		63
			GTTTGGAGAACCACAGAGCCTCTA	172	
TRPV6	NM_022413	Murine	TGTCCTTTGCTCTGGTGTTG	244	62
			TCAAAGGTGCTGAACAGTGC		
	NM_053686	Rat	AGATGATTTTTGGCGACCTG	205	61
			GGCAGGTCCACGTTGTAGTT		

	DQ013292 AY225461 (Wilkens *et al.*, 2009) (Teerapornpuntakit *et al.*, 2009)	Rabbit Human Bovine Rat	GCACCTTTGAGCTGTTCCTC GATGAGCAGGTTGAGCATGA CTCAAGCCCAGGACCAATAA AGAGCAAGGGGAGAAATGGT GCCCTGCGAACTATAGCGTGGATCT -GCCCT TGGAAGGCCTGTGCGTAGCG ATCCGCCGCTATGCAC AGTTTTTCTGGTCACTGTTTTT	131 169 328 80	62 62 68 62
TREK-1	AF171068	Human	AGGTGGGAGAGTTCAGAGCA CAGCAATCTCTTCACCAGCA	300	62
TRAAK	AF302842	Rat	ATCACTACCATCGGCTACGG GCACATGCCACTTCAAGAAA	187	62
ClC-1	NM_001003124.1	Canine	AATGGATTTCCCCTTTGACC TCCGCAGGGTATAGGCATAG GAGGCTGGACTTGTGTGTCA GGAAGCCCTGTGGAGTATCA GGAGCCTGCAGATCAAAGAC GATTGGTCGATGCAGCAGTA	433 181 192	62 62 62
GAPDH	AB038240.1	Canine	CATCAACGGGAAGTCCATCT GTGGAAGCAGGGATGATGTT	429	62

Table 4. Primer sequences for each of the channel proteins investigated. Primers were purchased from Sigma-Aldrich (Cambridge, UK).

2.5 Analysis

Electrophysiological data were digitised and analysed using the WinEDR and WinWCP programs (John Dempster, University of Strathclyde). All membrane potentials are corrected for liquid junction potentials estimated using JPCalc (Barry & Lynch, 1991). Unless otherwise stated, statistical significance was assessed by t-test or ANOVA, as appropriate, in Minitab (Minitab Ltd, UK) with statistical significance defined as $P<0.05$. Figures were prepared using SigmaPlot (Systat Software, Inc. [SSI], San Jose, CA). All values are quoted as mean±SEM, with sample size = *n*.

3

TRANSIENT RECEPTOR POTENTIAL CHANNELS

3.1 Introduction

The transient receptor potential (TRP) channel family is one of the largest ion channel families. It contains more than 20 individual ion channels, divided into seven subgroups. They are generally thought of as non-selective cation channels, due to the majority of the groups having no or little selectivity for one cation over another, or even for mono- and di-valents. However, the physiological properties of these channels, in particular their mode of activation, can differ significantly.

TRPV4 is the only TRP channel to have been identified in non-diseased isolated chondrocytes (Phan *et al.*, 2009). In most tissues TRPV4 is non-selective for mono- and di-valents, however, under chondrocyte physiological conditions its selectivity for calcium increases, and calcium becomes the primary conducted ion. TRPV4 is known to be activated by a number of factors including heat (>27°C), phorbol esters, arachidonic acid and hypo-osmotic cell swelling (Liedtke *et al.*, 2000; Voets *et al.*, 2002). It has also been shown to promote chondrogenesis by inducing SOX9 transcription through the Ca^{2+}/calmodulin pathway (Muramatsu *et al.*, 2007). In chondrocytes TRPV4 has been shown to respond to hypo-osmotic stress whereby it becomes activated and influxes calcium into the cell. The hypothesis behind this is that this calcium influx activates a calcium-activated potassium channel, allowing efflux of potassium which in turn will drive water out of the cell, reducing cell volume (Phan *et al.*, 2009).

Several TRP channels have been identified in human osteoarthritic patients (Gavenis *et al.*, 2009). The expression of these in culture throughout two different passages was determined. TRP channels identified were the TRPC1, 3 and 6, TRPM1, 5 and 7, and TRPV1 and V6. No functional hypotheses for these channels have been provided and none of these channels have been described in healthy chondrocytes, so far.

This chapter investigates a non-selective cation conductance seen in potassium-free solutions, characterises this conductance using single channel and whole-cell electrophysiology and investigates the expression of several TRP channels in chondrocytes using RT-PCR. Then the effect of the identified TRP channels on membrane potential is determined, using a variety of pharmacological agents and temperature.

3.2 Methods

As described in Chapter 2, inside-out patch clamp with potassium-free conditions was used for all single channel data shown and for whole-cell voltage clamp tail currents. In separate experiments whole-cell voltage ramps were run in sodium methanesulfonate (NaMS) solutions (Tables 1 and 2). Permeability was measured from the reversal potential of difference currents run with 100μM gadolinium III (Gd^{3+}). Gd^{3+} was prepared as a stock solution in distilled water before being diluted to the appropriate concentration in the electrophysiological bath solution. Econazole and 4 α-phorbol 12,13-didecanoate (PDD) stocks were prepared using dimethylsulfoxide (DMSO) and diluted to the desired concentration in

electrophysiological bath solutions. Final DMSO concentration was no more than 1 in 10,000, which was not found to have any effect on membrane currents. Experiments were performed at room temperature (22-25°).

3.3 Results

3.3.1 Single channel electrophysiology

In potassium-free solutions (see Tables 1 and 2 for extracellular and intracellular solutions, respectively), the clearest conductance was a large, relatively non-selective cation channel (figure 3.1a), seen in 53% of patches (32/61). Slope conductance was 67±5pS (n = 5) and current reversed at a reversal potential (V_{rev}) of 21±4mV (n = 5; figure 3.1c). Mean open probability of the channel was 0.6±0.1 at -40mV (n = 5). Gadolinium III (Gd) is a well-known inhibitor of non-selective cation channels so the effect of this was tested during single channel recordings. Application of 100μM Gd reduced channel open probability by 75±9% (n = 5; figure 3.1d).

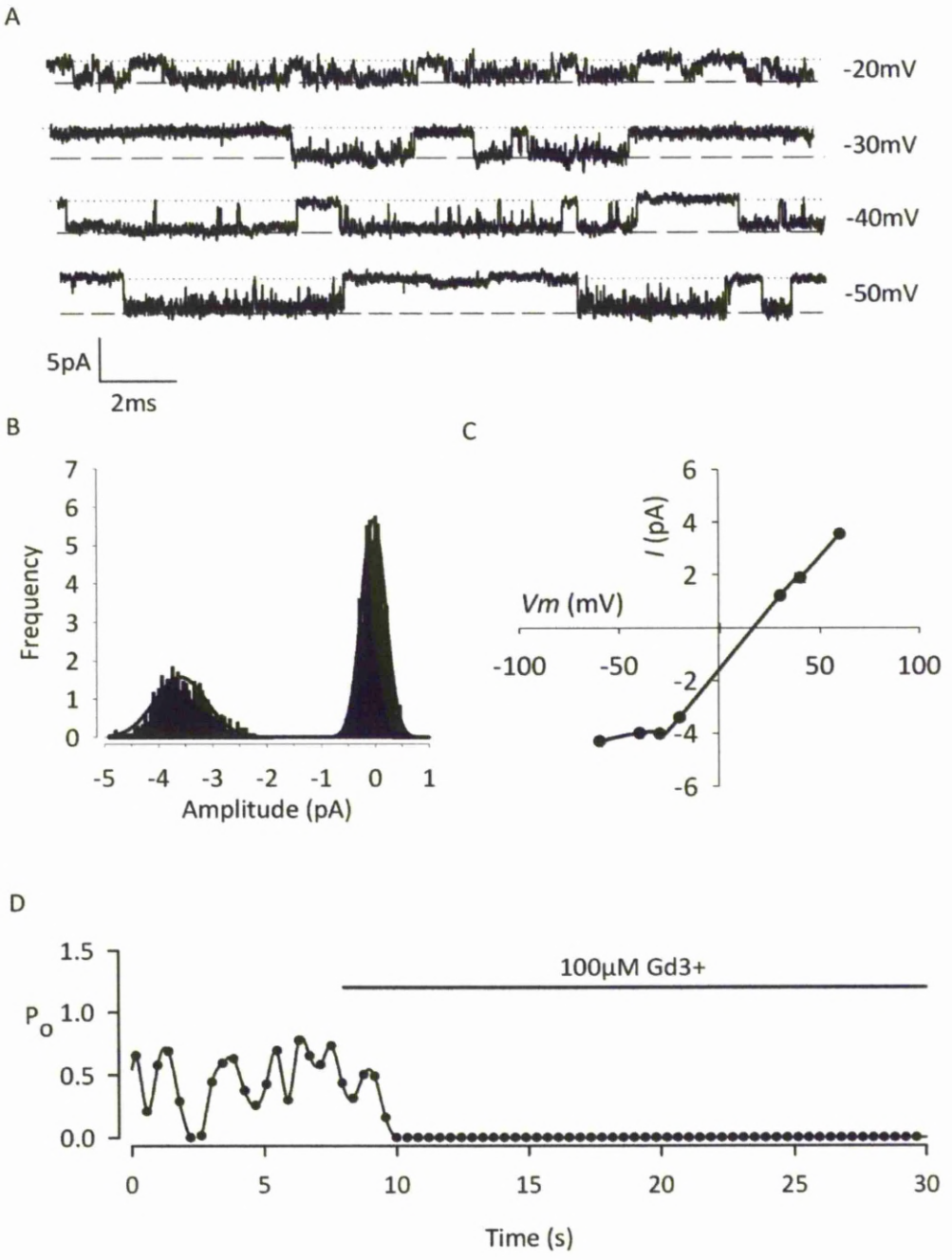

Figure 3.1 Patch clamp electrophysiology demonstrates the presence of gadolinium-sensitive ion channels. All of these experiments were performed in the potassium-free solutions (see Tables 1 and 2)A) Traces of inside-out high conductance single channel activity at -20, - 30, -40 and -50mV. B) All-points amplitude histogram for the high conductance channel at -50mV. C) Current-voltage curve for single-channel recordings. Error bars for data are smaller than the symbols. A solid line is drawn through the points. D) Open probability (P_o) versus time, calculated over successive 0.4s windows before and during the addition of 100µM gadolinium III (Gd3+).

3.3.2 Whole-cell voltage clamp

Whole-cell tail currents recorded in the same solutions as the single-channel data revealed little rectification and reversed at 1±5mV (n = 5; figure 3.2a and b). 100μM Gd^{3+} inhibited this whole-cell current by 85 ± 7% ($p \leq 0.001$). The whole-cell current exhibited weak voltage sensitivity with Boltzmann parameters for slope and half maximal activation of k = 83mV and $V_{1/2}$ = -38mV. Subtraction of tail-current data in the presence of 100μM Gd^{3+} from control data produced a difference current curve with reversal potential of approximately 20mV (figure 3.2c).

In order to isolate the TRP conductance further whole-cell voltage ramps were run in sodium methanesulfonate solutions. Sodium and calcium were the only permeable ions in these solutions, as methanesulfonate will not permeate ion channels. The sodium methanesulfonate solutions were used to produce difference currents by addition of 100μM Gd^{3+} (figure3.3a; see Tables 1 and 2 for extracellular and intracellular solutions, respectively). To create difference currents, voltage ramps were run in control methanesulfonate solutions and then 100μM Gd^{3+} added and ramps repeated. The ramps run in the presence of Gd^{3+} were then subtracted from the control ramps and the result, the difference current, was used to determine reversal potential of the Na^{+} current. Mean inhibition of whole-cell current was 80±9% with 100μM Gd^{3+}, (n = 5, $p \leq 0.001$). The measured reversal potential of the difference current under these conditions was -1±3mV (n = 5; figure 3.3b).

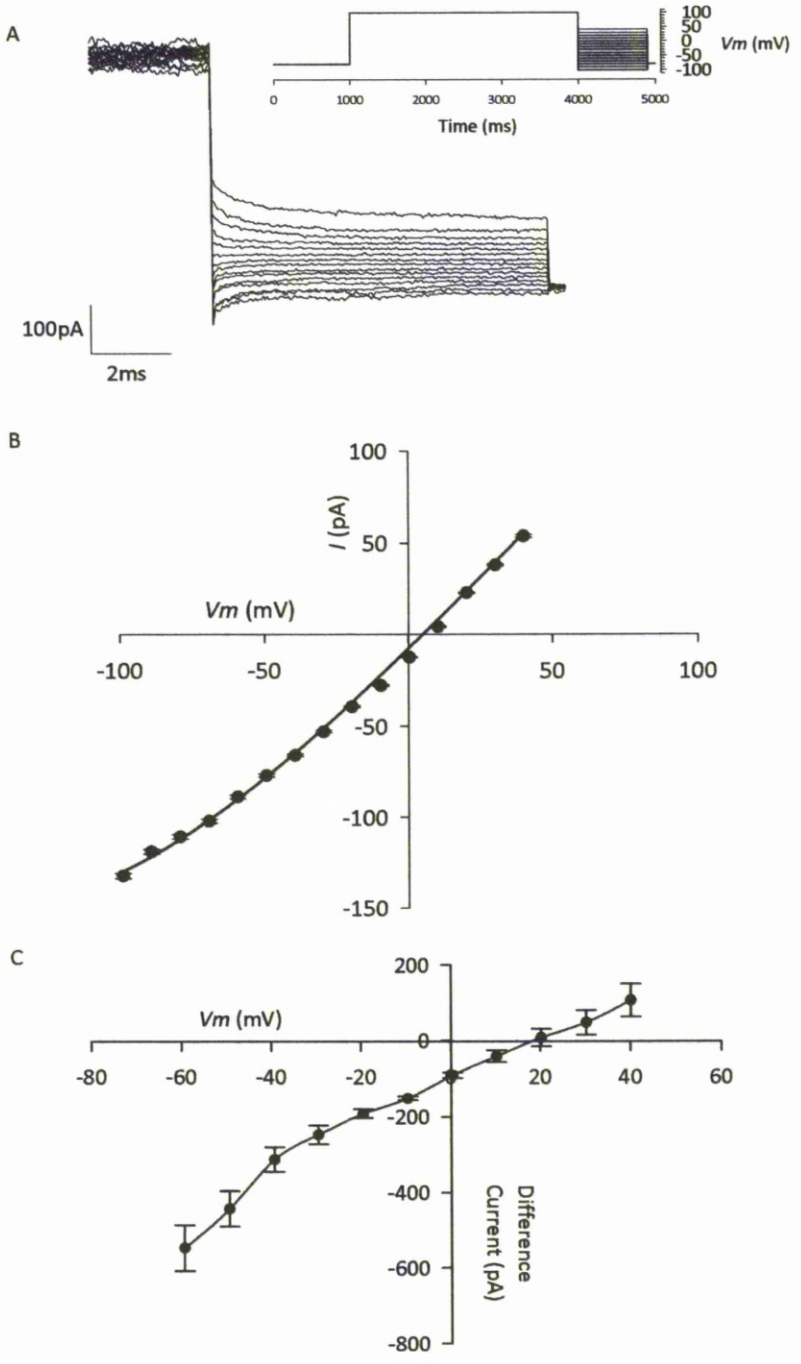

Figure 3.2 Whole-cell gadolinium-sensitive tail currents in potassium-free solutions. A) Whole-cell tail currents elicited by the step protocol illustrated in the inset. B) Current-voltage curve from whole-cell tail currents. Error bars for data are smaller than the symbols. Fitted with the standard Boltzmann curve; $G = G_0 + \frac{G_{max}}{\left\{1+exp\left[-\frac{(V_c - V_{0.5})}{k}\right]\right\}}$ where G_0 and G_{max} are the minimum and maximum conductance densities, respectively, $V_{0.5}$ is the midpoint parameter, and k is the slope. C) Difference current for the gadolinium sensitive component of whole-cell tail currents.

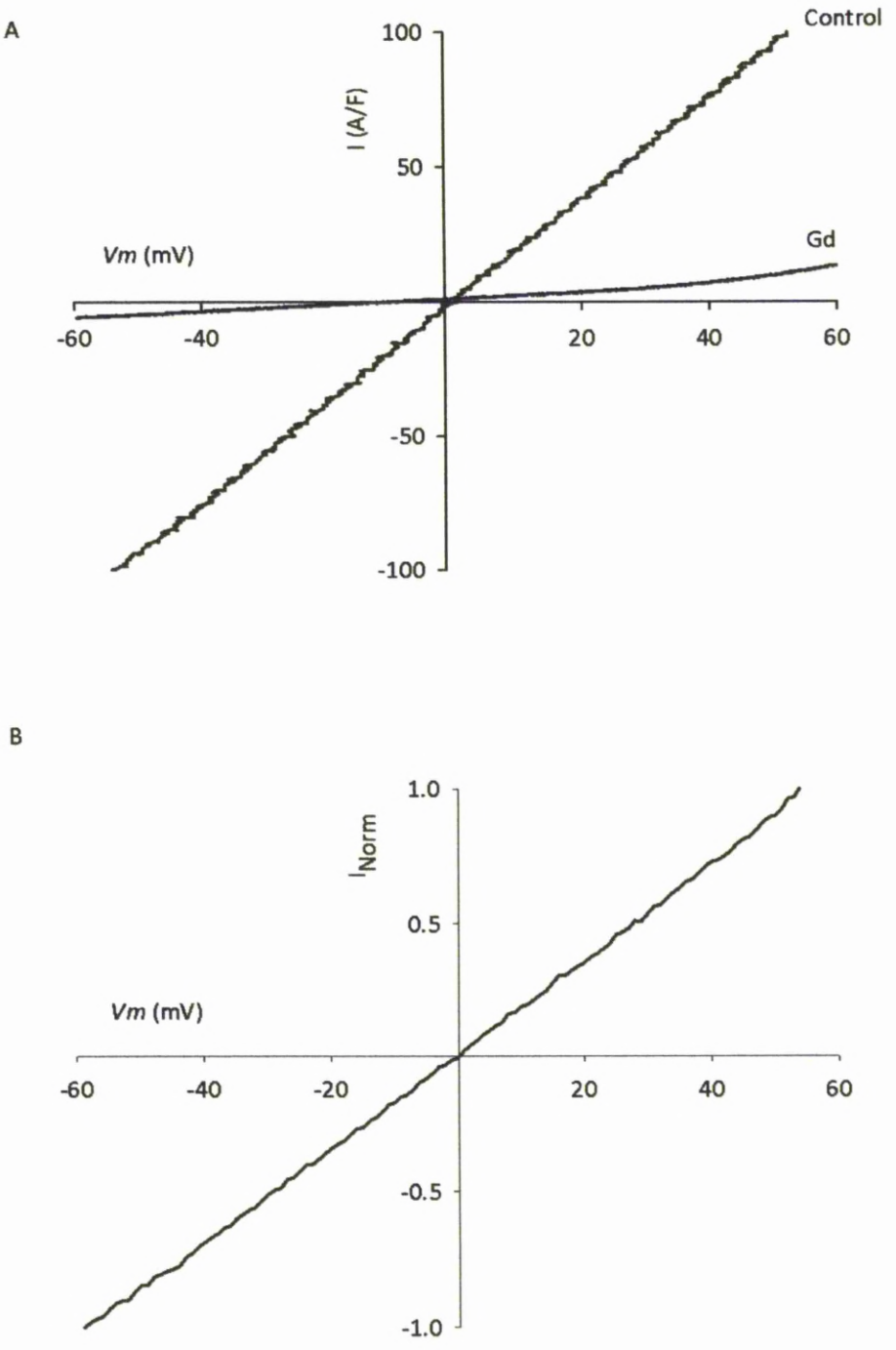

Figure 3.3 Whole-cell voltage-ramps demonstrate the presence of gadolinium-sensitive whole-cell conductances. A) Whole-cell current ramps in "methanesulfonate solutions" (see Tables 1 and 2). Command potential (*Vm*) on the x axis, current on the y axis (normalised for cell size). Control (vehicle) or in the presence of gadolinium III (Gd). B) The Gd^{3+} difference current, normalised to that at -60mV. Difference currents were calculated by subtracting ramps run in the presence of 100μM Gd^{3+} from those run in control solutions.

3.3.3 Identity of the gadolinium-sensitive cation channel(s)

Reverse transciption-PCR (RT-PCR) and permeability electrophysiology experiments were performed, as described in Chapter 2, to identify the channel, or channels, responsible for this non-selective current.

Firstly, a number of channels which could possibly be this Gd^{3+}-sensitive channel were identified (Table 4). PCR primers were designed, as described, to target these proteins and RT-PCR was run to identify if the mRNA of these channels was present. Canine first expansion chondrocytes were found to contain both TRPV4 and TRPV5 mRNA (figure 3.5a and b). The other primer pairs listed in table 4 (TRPC3, TRPC6, TRPV6, TREK-1 and TRAAK) failed to detect any mRNA in canine chondrocytes. However, it was not possible to identify positive controls for these primer groups. These primers were also run with touchdown and conventional PCR against canine mesenteric artery and rat mesenteric artery, tracheal smooth muscle and cardiac muscle and failed to produce any mRNA product. TRPV4 and TRPV5 PCR products were sequenced (Beckman Coultier Genomics, Essex, UK) (figure 3.6a and b). Canine TRPV4 had 97% homology to the human TRPV4 sequence and canine TRPV5 had 98% homology to the murine TRPV5 sequence.

Then, using whole-cell voltage ramps in the presence and absence of gadolinium, the permeabilities of Na^+, Cs^+, K^+ and Ca^{2+} were measured. Full details of each of the solutions used can be found in Table 1. To determine Na permeability, for example, "TRP – Na permeability" was used as the extracellular (bath) solution to run control ramps and then 100μM Gd^{3+} added and ramps repeated. The ramps run in the presence of Gd^{3+} were then subtracted from the control ramps and the result, the

difference current, was used to determine reversal potential of the Na^+ current. The experiments were then repeated but with the Cs^+ and K^+ solutions. The reversal potential of the difference current from each of these ions was subtracted from the sodium reversal potential and this change in reversal potential (ΔV_{rev}) was then substituted into Equation 2 to give the relative permeability of each of these ions to sodium. This was then repeated using the Ca^{2+} extracellular solutions and the exact reversal potential of the difference current from these experiments was substituted into Equation 3. The intracellular (pipette) solution remained the same throughout all mono-and di-valent permeability experiments. P_K/P_{Na} was 1.02±0.06 (n = 10) whilst P_{Cs}/P_{Na} was 1.2±0.1 (n = 9). Cs^+ and K^+ permeability's were not significantly different to that of Na^+ (p>0.05). Ca^{2+} permeability was significantly greater than that of Cs^+ and K^+ (p≤0.0001) and the calculated P_{Ca}/P_{Na} was 78±9 (n = 5).

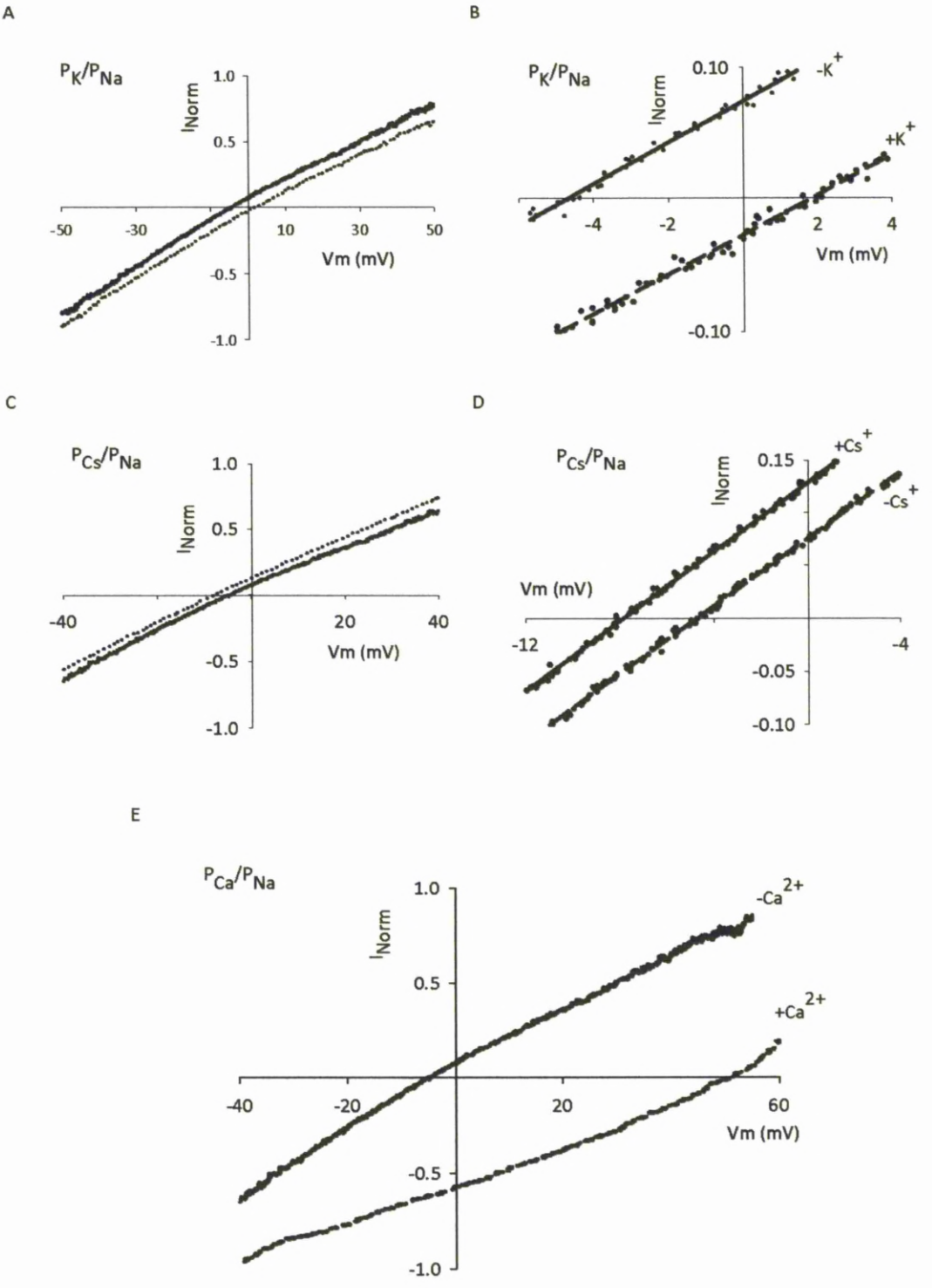
A
P_K/P_{Na}
I_{Norm}
1.0
0.5
-0.5
-1.0
-50
-30
10
30
50
Vm (mV)
B
P_K/P_{Na}
I_{Norm}
0.10
-0.10
$-K^+$
$+K^+$
-4
-2
2
4
Vm (mV)
C
P_{Cs}/P_{Na}
I_{Norm}
1.0
0.5
-0.5
-1.0
-40
20
40
Vm (mV)
D
P_{Cs}/P_{Na}
I_{Norm}
0.15
-0.05
-0.10
$+Cs^+$
$-Cs^+$
Vm (mV)
-12
-4
E
P_{Ca}/P_{Na}
I_{Norm}
1.0
0.5
-0.5
-1.0
$-Ca^{2+}$
$+Ca^{2+}$
-40
-20
20
60
Vm (mV)

Figure 3.4 Gadolinium difference current has high permeability to calcium ions. A, and B) Gadolinium-sensitive (Gd) current-voltage ramp with 150mM external NaCl (solid line) or 150mM external KCl (broken line). B shows the same data as A, but magnified to show ΔV_{rev} more clearly. The permeability ratio was then calculated from Equation 2. C and D) Gd-sensitive current-voltage ramp with 150mM external NaCl (solid line) or 150mM external CsCl (broken line). D) Shows the same data as C, but magnified to show ΔV_{rev} more clearly. The permeability ratio was then calculated from Equation 2. E) Current-voltage ramp with 150mM external NaCl (solid line) or 30mM $CaCl_2$ and 105mM NaCl (broken line). The permeability ratio was then calculated from Equation 3. The full solutions for A to E are described in the methods (Tables 1 and 2).

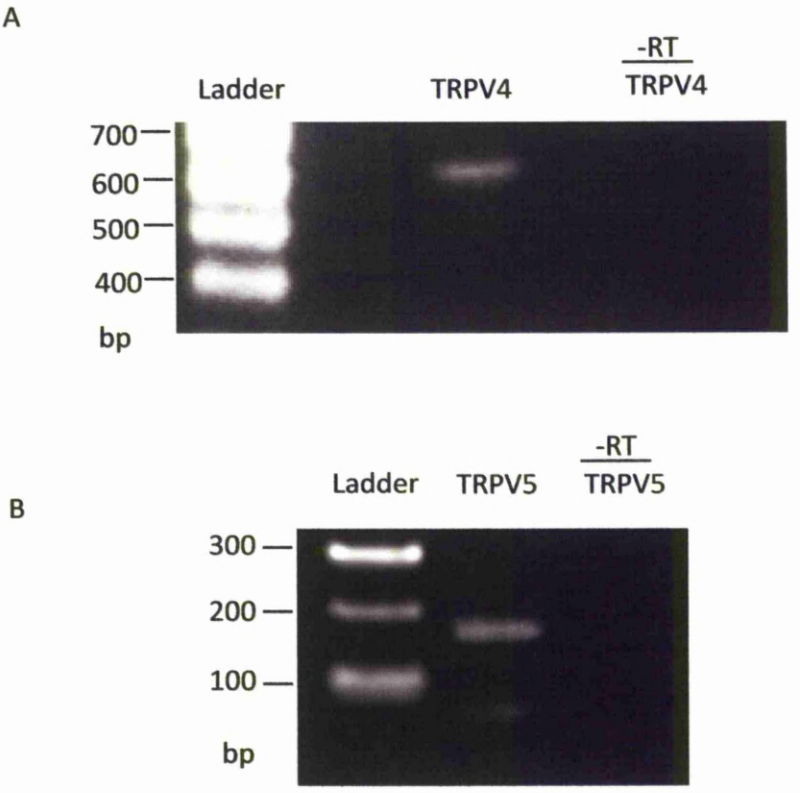

Figure 3.5 RT-PCR expression of TRPV4 and TRPV5. Specific primers for TRPV4 and TRPV5 were used. mRNA (629bp) product encoding TRPV4 (A) and mRNA (164bp) product encoding TRPV5 (B) was detected in extracts of first expansion chondrocytes. GAPDH was used to determine cDNA viability (not shown). Omission of reverse transcriptase served as a negative control.

A

Canine TRPV4

```
CCGNNTTTAGNNGNNGANNTCTNGCTGGGGTTCCCCATGTTGTCCAGAGGCACCACCACCT 61
CGTCCGGGTTCGAGTTCTTGTTCAGCTCCACCACGCGCGGAACCACCGAGGACCAGCGATC 122
CCTCCGGAGGCGGCCCACGGTGTGTGAGAAGCCATAGTACTGGTAGTTCTCGCTCTTGCCT 183
GGGTCCTCATTAATGATGCCCAAGTTCTGGTTCCAGTGAGACCAGTTCACCTCGTCCACCC 244
TGAAGCACCACCTGCGGTCTGGAGTGCCGTCCGAGCTCTTTCCCACAGTCACCATCTCGCC 305
AGAGCGGAAGGCCTTCCTCAGGAACACGGGGAAGGACCGCTCGATGTCCAGGATGGTGGTG 366
GCCCACTGCAGCTTCCAGATATGCTTGCTCTCCTTGGAGACCTGGCCCACTGTCTCCCCCA 427
TGAGGGCGATGAGCATGTTGAGGAGCAGCACGAAGGTGAGGATGATGTAGGTGACGAGCAG 488
GATGATGAAGACCACGGGGTACTTGGTGCTGCTCAGCATCTCCAGGTCACCCATGCCGATG 549
GTCAGCTTGAAGAGGTCCAGGAGGAAGGTGCTGAATGTCTTCGCTA                 597
```

B

Canine TRPV5

```
CAGCNTANTGGCCAGAATATGGNACTGTCCTTTCTGGAGCTTGTGGTTTCCTCCAAGNAGA 61
NAGAGGCTCGNCAGATTCTAGAACAGACCCCAGTGAAGGAGCTGGTGAGCCTGAAGTGGAA 122
GAAATATGGACAANNNNNTNNTN                                         144
```

Figure 3.6 cDNA sequences of canine TRPV4 and TRPV5. Sequences detected by rt-PCR in canine chondrocytes. A) TRPV4 primers detected product around 629bp (some bp not detected in sequencing and not shown above). B) TRPV5 primers detected product around 164bp (again, some of these bp not detected in the sequencing and not shown). Sequencing performed by Beckman Coultier Genomics (Essex, UK).

3.3.4 Membrane potential

It was expected that TRPV4 activation would cause a depolarisation in the membrane potential (*Vm*) due to the cationic influx that would occur from the opening of the channel. However, this was not seen. TRPV4 activation by 4alpha-PDD caused a significant hyperpolarisation in *Vm* of 55±4mV (n = 3; $p<0.001$; figure 3.7c). It was hypothesised that the influx of calcium from TRPV4 activation was activating a calcium-activated potassium channel. When caesium, a non-permeant ion of potassium channels, was added to the intracellular (pipette) solution the *Vm* did not change significantly (-1±1mV; n = 5; $p>0.05$), supporting this hypothesis. TRPV4 is a heat-sensitive channel that is activated by temperatures >27°C. The effect of heat (bath solution was heated to 30°C) on *Vm* caused a change of -13±1mV (n = 3; figure 3.7).

As well as being inhibited by gadolinium III TRPV5 is also known to be blocked by econazole (Nilius *et al.*, 2001). Use of these pharmacological agents on the *Vm* caused hyperpolarisation of the membrane. Gadolinium caused a decrease of 30±4mV (n = 8, $p\leq0.0005$) and econazole a decrease of 18±3mV (n = 5, $p\leq0.005$) (figure 3.7a and b).

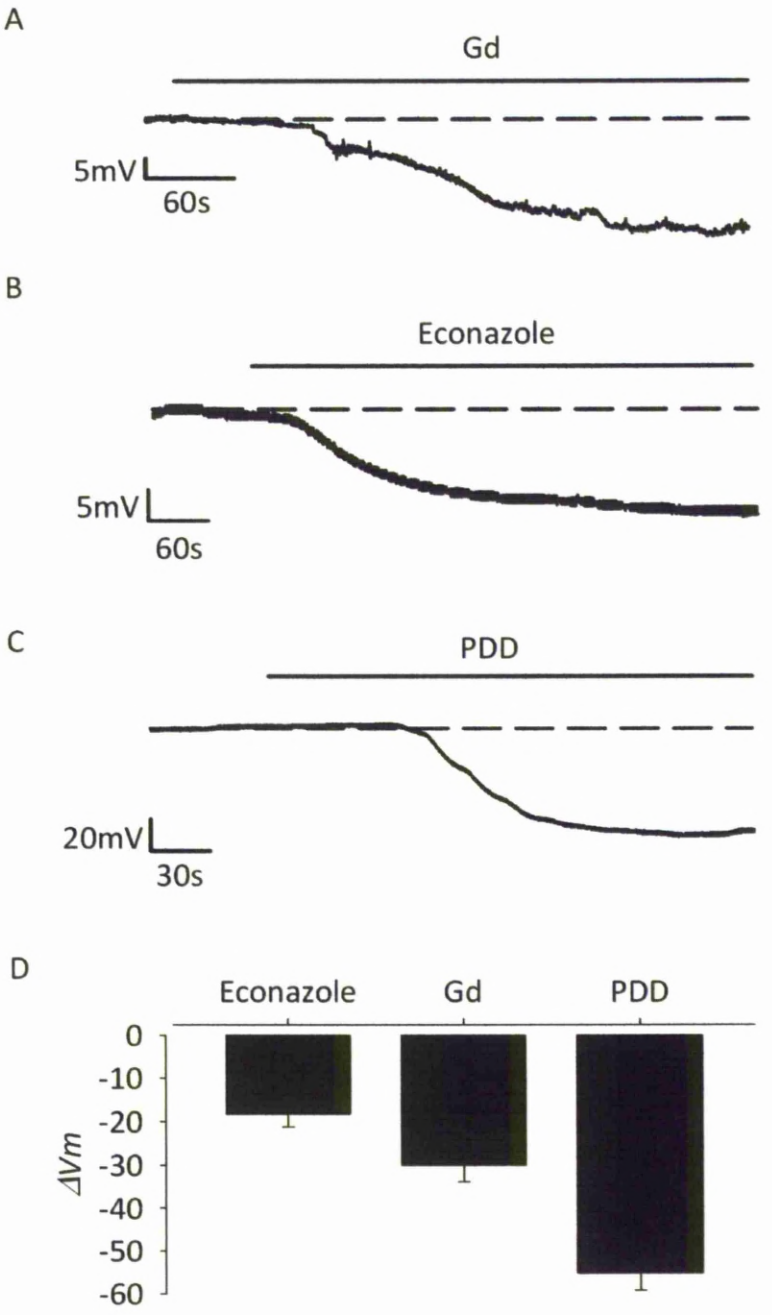

Figure 3.7 4alphaPDD, gadolinium and econazole sensitive ion channels contribute to the RMP. Block of channels by gadolinium (Gd; A and D) or econazole (B and D) drive the membrane potential in a negative direction. Activation of TRPV4 channels by PDD (C and D) also drives the membrane potential in a negative direction. Membrane potential records during the application of A) 100μM Gd, B) 10μM Econazole and C) 1μM PDD. D) Summary data for; 100μM Gd (n = 8), 10μM econazole (n = 5) and 1μM PDD (n = 3). Each of these conditions significantly shifted the membrane potential.

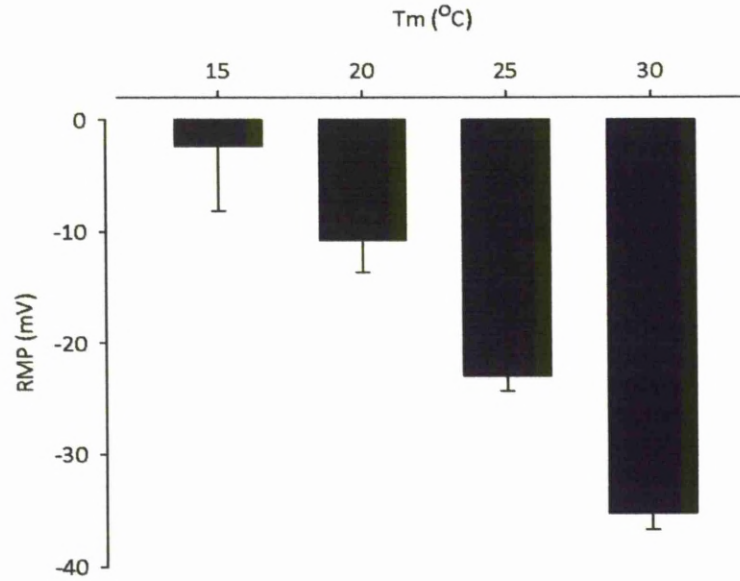

Figure 3.8 Effect of temperature on membrane potential. Membrane potentials were recorded in in physiological solutions (see Tables 1 and 2) using current-clamp mode at four different temperatures. Bath temperatures of 15°C, 20°C, 25°C and 30°C produced membrane potentials of -2, -11, -23 and -35mV, respectively.

3.4 Discussion

Potassium-free solutions were initially used in this chapter to characterise a non-selective cation conductance. Previously, large conductance potassium channels have been identified in chondrocytes by my group and others (Grandolfo *et al.*, 1992; Mobasheri *et al.*, 2010) so this chapter set out to investigate what other, smaller, conductances may be present by eliminating potassium conductances.

The whole-cell voltage ramp protocols clearly demonstrate that the majority of the total resting (non-potassium) current is generated by a Gd^{3+}-sensitive conductance. It is likely that the Gd^{3+}-sensitive conductance is comprised of more than one type of channel, however, the permeability data suggest that TRPV5 dominates. TRPV5 is one of the few ion channel conductances with little selectivity between Cs^{+}, Na^{+} and K^{+} ions, but high permeability to Ca^{2+} ions (Vennekens *et al.*, 2000; Owsianik *et al.*, 2006; Alexander *et al.*, 2008). The presence of TRPV5 mRNA by RT-PCR serves to further support the notion that these cells express TRPV5. This is the first time that TRPV5 has been shown in chondrocytes.

In this chapter it was found that 100μM Gd^{3+} caused a significant deflection in the membrane potential of around -30mV ($p \leq 0.01$). This showed that the Gd^{3+} inhibition of the non-specific cation channels significantly affected the RMP of the cell. In addition econazole, a relatively selective inhibitor of TRPV5 (Nilius *et al.*, 2001), hyperpolarised the membrane in a similar manner to Gd itself. That Gd^{3+} hyperpolarises the chondrocyte by more than the econazole implies that Gd^{3+} may additionally inhibit other conductances in the cell, possibly a TRPV4 conductance.

TRPV4 has been identified in both pig and canine chondrocytes by PCR (Phan *et al.*, 2009; Lewis *et al.*, 2010). The electrophysiological signature has also been revealed; that of a high conductance, non-selective cation channel. TRPV4 is frequently characterised as a stretch activated channel (Nilius *et al.*, 2004) and is regarded to be a conduit for stretch activated entry of calcium ions. It may be that this channel is, in chondrocytes, key to linking membrane stretch to calcium mobilisation, activation of calcium activated potassium channels and hyperpolarisation. Interestingly, TRPV4 protein is expressed in bone (in both osteoblasts and osteoclasts) and its deficiency in knockout mice suppresses unloading-induced bone loss (Mizoguchi *et al.*, 2008). Mechanotransduction is a crucial component of bone matrix turnover and these recent knockout studies indicate that TRPV4 plays a critical role in unloading induced bone loss. Disruption of TRPV4 in the inner ear has been shown to cause delayed-onset hearing loss, making the cochlea vulnerable to acoustic injury (Tabuchi *et al.*, 2005). Therefore, TRPV4 may have important functions in cartilage turnover as well (Mizoguchi *et al.*, 2008).

On activating TRPV4 one would intuitively expect a depolarisation of the membrane, due to this channels selectivity for Ca^{2+} and other cations. However, as shown here, activation of this channel by both heat and the phorbol ester, PDD, induced a hyperpolarisation of the chondrocyte membrane potential. One explanation for this is that this sudden influx of calcium activates a calcium-activated channel, whose ion conductance will hyperpolarise the membrane, such as the BK/SK channels or the CaCC. This theory appears to be supported by the data from membrane potential experiments where caesium was added to the intracellular solution, abolishing any change in membrane potential upon addition

of PDD. Caesium does not permeate through any of the K^+ ion channel family, therefore when it is present, no change in membrane potential on the addition of PDD would suggest that the calcium-activated potassium channels are blocked. This suggests that the TRPV4 channel is not contributing to *Vm* but is instead acting as a calcium-influx pathway enabling activation of calcium-activated potassium channels, the expression of which is investigated later in this thesis. This, along with the membrane hyperpolarisation that happens upon both TRPV4 activation and membrane stretch may suggest some sort of localisation of calcium-activated potassium channels and TRPV4. Calcium imaging and fluorescence experiments could be used to show possible local increases in Ca^{2+}. It should be noted, however, that the temperature and PDD experiments provided significantly different degrees of hyperpolarisation. PDD hyperpolarised the membrane four times as much as temperature did. This could be due to 30°C not being warm enough to fully activate all the TRPV4 channels or it could be due to PDD having an effect on other TRP channels.

The PCR primer sets used in this study were successful at producing TRPV4 and TRPV5 mRNA from canine chondrocytes. However, all the other primer sets failed to produce any mRNA, even in tissues where they have previously been found. This would suggest that these primer sets are unusable.

As well as providing additional evidence for the activation of calcium-activated potassium channels by TRPV4, the changes in RMP with temperature offer additional insight into possible cold-sensitive channels present in chondrocytes. At 15°C the membrane potential increased slightly. TRPA1 and TRPM8 are cold-

activated channels (temperatures below 17°C and 22°C, respectively) and upon activation will influx cations into the cell. Both are non-selective for mono- over di-valent cations. An influx of cations into the cell will cause the membrane potential to become more positive, as was seen with the decrease in temperature.

The existence of these cation-selective channels in chondrocytes may seem surprising; however the data shown in this Chapter would suggest that they have a significant contribution to the membrane potential. Previous studies have shown the dependence of the chondrocyte membrane potential on potassium and chloride-selective channels (Tsuga *et al.*, 2002). The dependence of membrane potential on the activity of these TRP channels will be investigated later in this thesis.

4

EPITHELIAL SODIUM CHANNELS

4.1 Introduction

Amiloride-sensitive epithelial Na+ channels (ENaC) play a key role in Na^+ transport and fluid homeostasis across the epithelia of the kidney, lung, and colon (Kellenberger & Schild, 2002). ENaC has been shown to be present in articular cartilage although functional evidence for ENaC in cartilage is still lacking (Trujillo *et al.*, 1999b).

ENaCs are made up of 4 transmembrane subunits (2αβγ), forming a pore in the membrane which allows the passage of Na^+ ions (figure 4.1). ENaCs are significantly more permeable to sodium and lithium than potassium with P_{Li}/P_{Na} ~1.3 and P_K/P_{Na} ~0.1 (Eaton *et al.*, 1995; Garty & Palmer, 1997). These channels are sensitive to micromolar concentrations of amiloride and benzamil (IC_{50} 100-200nM and 10-50nM respectively; Smith & Benos, 1991).

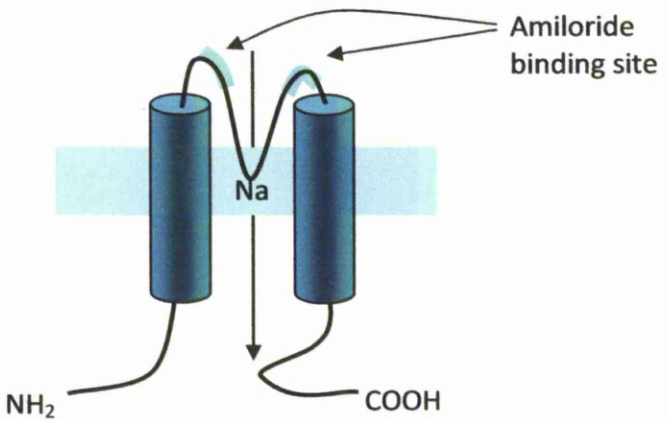

Figure 4.1 Diagrammatic representation of one ENaC subunit. The transmembrane span has two extracellular amiloride binding sites. Functional ENaCs are formed from four of these transmembrane subunits.

The ENaCs main function in the kidney, bladder, and colon is control of sodium reabsorption (Rossier *et al.*, 2002). They are found in lung tissue (Mall *et al.*, 1998) and the taste buds (Lindemann, 2001) and are known to regulate blood volume and pressure through sodium balance in the arterial system (Canessa *et al.*, 1994).

In chondrocytes the role of ENaC is less clear; however, it is thought to be one of mechanotransduction, possibly where the channel contributes to the maintenance of the RMP (Shakibaei & Mobasheri, 2003). This, in turn, may regulate signalling pathways that allow chondrocytes to maintain their ECM and prevent chondrocyte apoptosis (Wright *et al.*, 1996; Shakibaei *et al.*, 2001; Shakibaei & Mobasheri, 2003). It is thought that the mechanotransduction pathways involving ENaC become progressively defective during osteoarthritis, leading to a loss of chondroprotective mechanisms (Salter *et al.*, 2004). It is possible that ENaC subunits are differentially expressed in chondrocytes, potentially to cope with different mechanical stresses throughout the zones of articular cartilage, and changes in chondrocytic properties during disease (Trujillo *et al.*, 1999b; Shakibaei *et al.*, 2001).

Sodium transport is thought to be heavily involved in cell volume regulation (Hall *et al.*, 1996b). Several reports have suggested that this sodium balance is created by ion pumps or co-transporters (Kerrigan *et al.*, 2006; Bush *et al.*, 2010), such as the NKCC transporter. However, these studies have failed to show that it is ultimately these ion pumps responsible for cell volume recovery after hyperosmotic challenge. These studies find that there is another, unknown, conductance contributing to chondrocyte RVI as inhibition of the NKCC ion pump does not fully inhibit cell volume recovery (Kerrigan *et al.*, 2006). This suggests that another ion conductance

is contributing to the regulation of cell volume. The ENaC could be responsible for an influx of sodium ions during RVI which would allow the chondrocyte to regain its volume.

This chapter aims to characterise the ENaC in chondrocytes using single channel and whole-cell electrophysiology. Cells will then be submitted to hypertonic challenges and changes in their volume will be measured. These experiments will be repeated in the presence of the ENaC inhibitor benzamil to determine the role of this channel in cell volume regulation.

4.2 Methods

As described in Chapter 2, inside-out patch clamp with potassium-free conditions was used for all single channel data shown. In separate experiments whole-cell voltage ramps were run in sodium methanesulfonate (NaMS) solutions (see Tables 1 and 2). Amiloride and benzamil stocks were prepared using dimethylsulfoxide (DMSO) and diluted to the desired concentration in electrophysiological bath solutions. Final DMSO concentration was no more than 1 in 10,000, which was not found to have any effect on membrane currents. Experiments were performed at room temperature (22-25^{o}C).

To determine the effect of ENaC on RVI physiological solutions were used (see Table 1). The control solution had an osmolarity of 309mOsm. This osmolarity was increased by the addition of 180mM sucrose to create a hypertonic solution which would initiate RVI.

4.3 Results

4.3.1 Inside-out patch clamp

Under potassium-free conditions (see Table 1 and 2 for extracellular and intracellular solutions) the most frequently seen channel activity was a low amplitude channel (figure 4.2a). It was seen in 60% of patches (12/20) and appeared to be constitutively active. Single-channel activity reversed at a membrane potential of -1±5mV (n = 5) and mean conductance was 9±0.4pS (n = 5; figure 4.2c). The calculated E_{Na} under these conditions was -6mV, which coupled to the very small conductance would be consistent with this channel being an ENaC.

The ENaC is known to be highly sensitive to amiloride so the effect of this channel inhibitor was investigated. Open probabilities (P_o) were calculated for the channel before and after application of an ENaC channel inhibitor, amiloride. Channel P_o in control conditions was 0.3±0.06 and decreased by 97±2% after application of 10μM amiloride (n = 3; figure 4.2d).

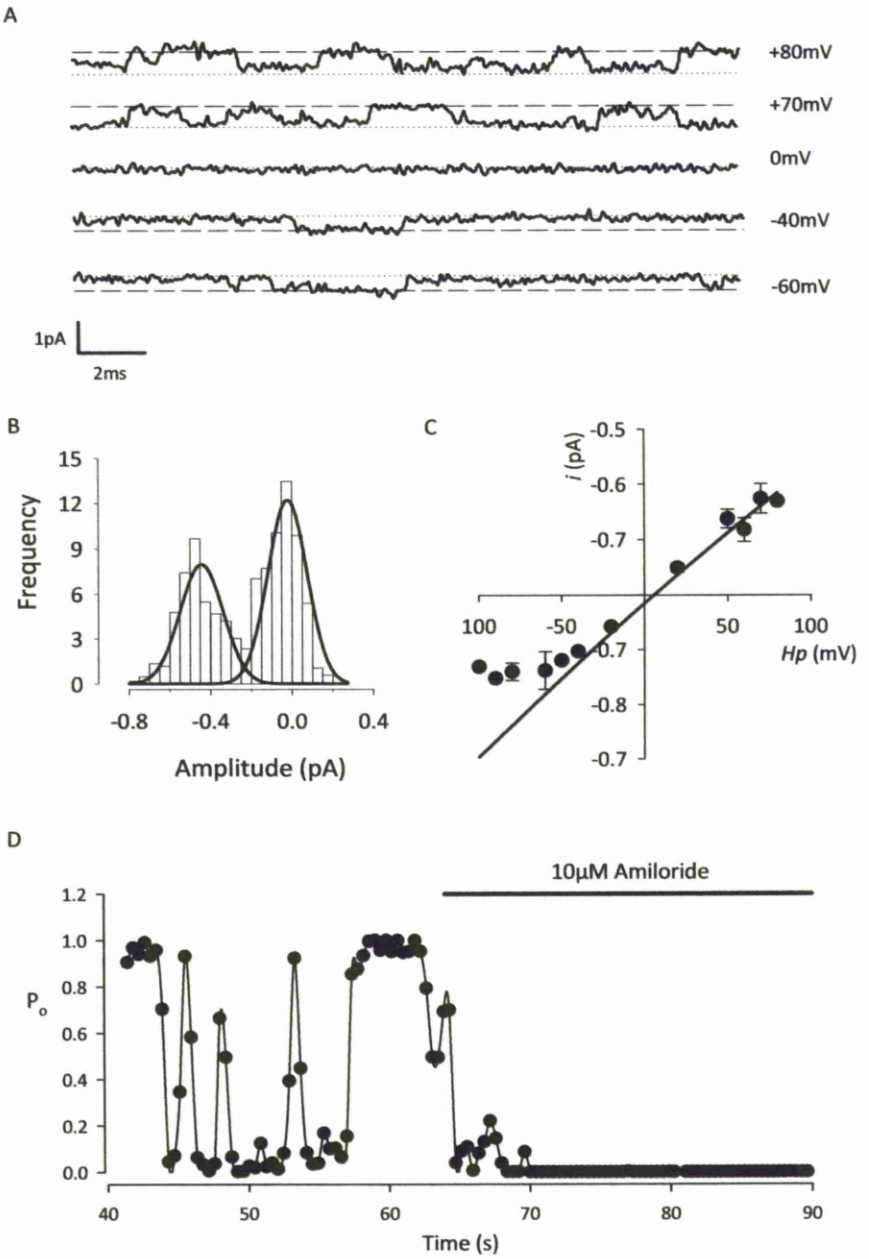

Figure 4.2 Patch-clamp recording reveals the presence of amiloride-sensitive low conductance ion channels. A) Traces of inside-out low conductance single channel activity at +80, +70, 0, -40, and -60mV. B) All-points amplitude histogram at -40mV. C) Single channel current-voltage curve. D) Open probability (P_o) versus time, calculated over successive 0.4s windows before and during the addition of amiloride (10μM).

4.3.2. Whole-cell electrophysiology

After identifying a low-conductance amiloride-sensitive sodium channel, electrophysiological experiments were performed on the whole-cell to determine the contribution of this channel to whole-cell current. As discussed in Chapter 3, whole-cell voltage ramps were run in sodium methanesulfonate solutions (see Tables 1 and 2) so that the principal permeant ion was sodium. Whole-cell voltage ramps were used to produce difference currents by subtracting the ramps run with 100nM benzamil from those run in the control solution, as described in Chapter 3 (figure 4.3a). Mean inhibition of whole-cell current with 100nM benzamil was 22±7%, (n = 3, $p \leq 0.001$). The measured reversal potential of the difference current under these conditions was 5±3mV, (n = 3; figure 4.3b).

The effect of this low conductance sodium channel upon membrane potential was then investigated using whole-cell current clamp methods. Once cell *Vm* had stabilised, amiloride was added and the change in membrane potential recorded (figure 4.4a). Upon inhibiting ENaC with 10μM amiloride there was a change in the membrane potential (*Vm*) of -9.5±0.8mV (n = 5, $p<0.01$; figure 4.4a and c). Similar experiments were performed using 100nM benzamil, which caused a change in membrane potential of -7.5±1.7mV (n =5, $p<0.01$; figure 4.4b and c).

4.3.3 Cell volume measurements

Cells were exposed to a hypertonic (489mOsm) physiological saline and their size was measured throughout. On exposure to the hypertonic solution cell size decreased significantly by 35±3% (n = 5, $p<0.001$; figure 4.5a). Within 20 minutes of reaching their smallest size, cells under control conditions had returned to 92±4% of

their original volume, not significantly different to starting volume (p=0.07). When 100nM benzamil was added to the hypertonic solution cells shrank by 41±3% (n = 5; figure 4.5a), not significantly different to the cells in control solution (p=0.3). However, in this solution they were unable to return to their original volume, reaching only 63±3% of their starting volume 20 minutes after maximum shrink, significantly less than the cells in control solution (p<0.005).

ENaC is also highly permeable to lithium ions so this experiment was repeated with the same physiological saline except the sodium ions had been replaced by lithium. The cells exhibited slightly less, but still significant, shrink upon exposure to a hypertonic solution (26±3%, n = 5, p<0.001; figure 4.5b) and within 20 minutes of reaching maximum shrink had returned their volume to (98±2%; n = 5) of the original size (not significantly different to starting volume; p=0.35).

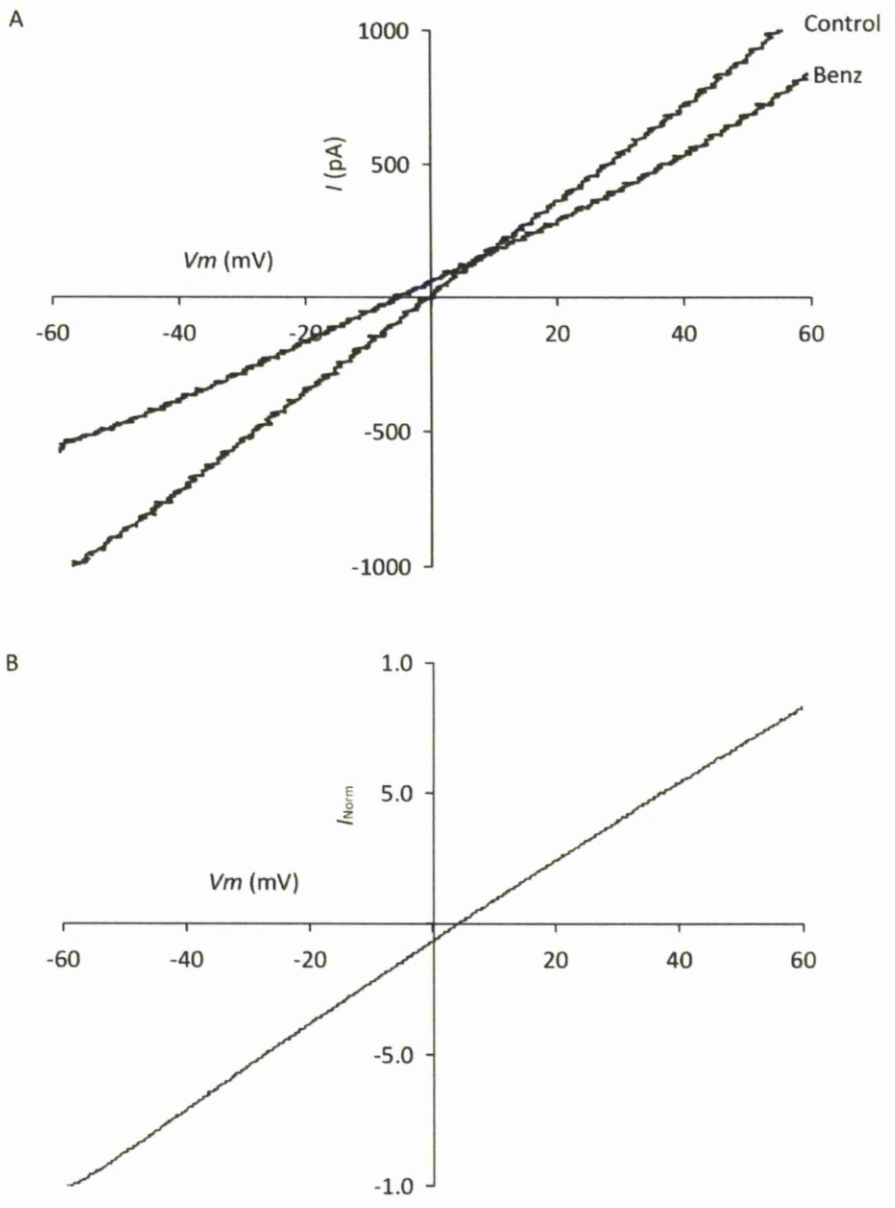

Figure 4.3 Whole-cell voltage-ramps demonstrate the benzamil-sensitivity of whole-cell current. A) Whole-cell voltage ramps in "methanesulfonate solutions" (see Tables 1 and 2). Command potential (*Vm*) on the x axis, current on the y axis (normalised for cell size). Control (vehicle) or in the presence of benzamil ("benz"). B) The benzamil difference current, normalised to that at -60mV. Difference currents were calculated by subtracting ramps run in the presence of 100nM benzamil from those run in control solutions.

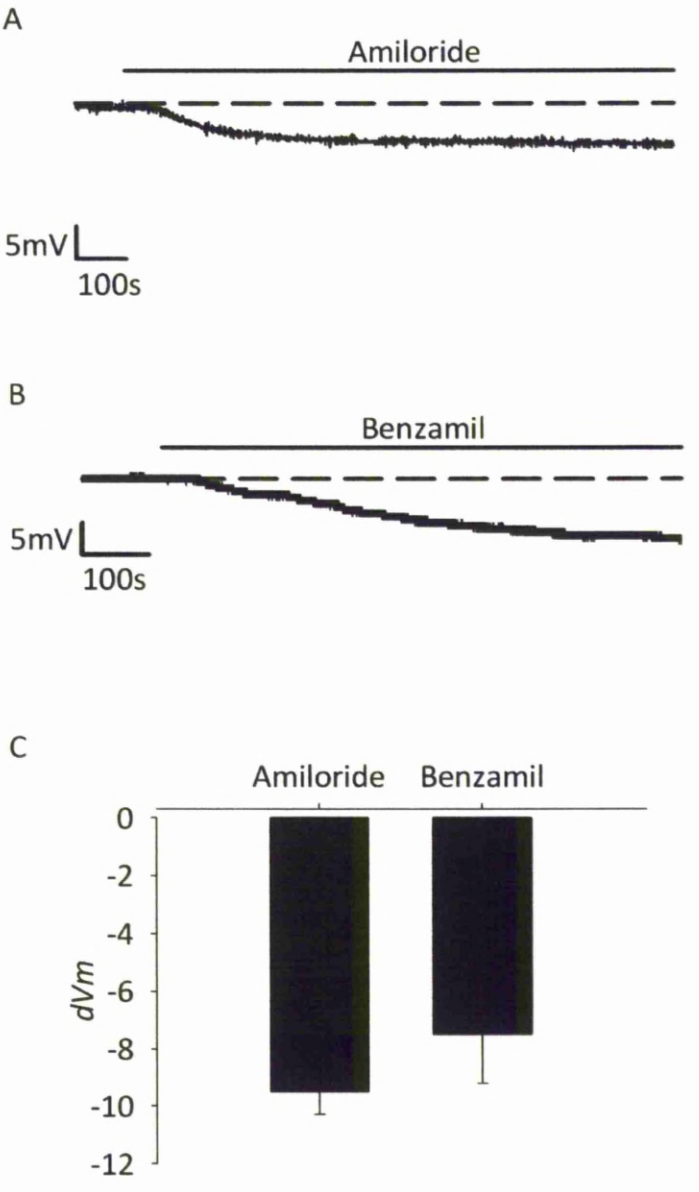

Figure 4.4 Amiloride and benzamil-sensitive ion channels contribute to the membrane potential. Block of channels by amiloride (*A* and *C*) or benzamil (*B* and *C*) drives the membrane potential in a negative direction. Membrane potential record during the application of *A*, 10μM amiloride and *B*, 100nM benzamil.

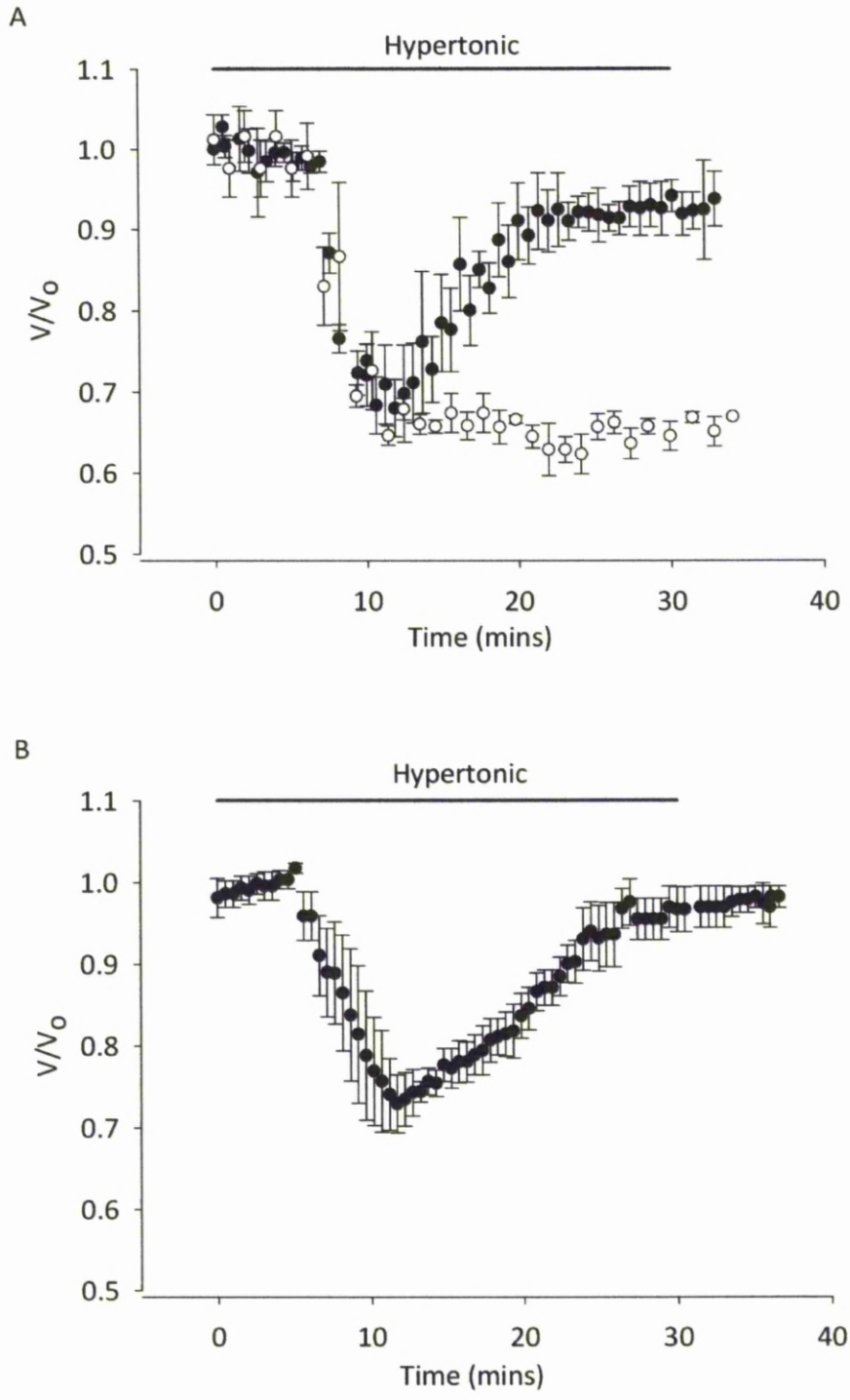

Figure 4.5 ENaC contribution to maintenance of cell volume. A hypertonic (489mOsm) physiological solution (see Table 1 and Chapter 2) was applied to chondrocytes whilst filming cells. Cell surface area was then measured and converted to volume. Lines on both graphs indicate the duration of the hypertonic challenge. A) Under physiological saline control conditions (filled circles) and with the addition of 100nM Benzamil (empty circles). B) The same physiological saline as in A but with NaCl substituted for LiCl.

4.4 Discussion

Epithelial sodium channels (ENaC) have previously been identified in chondrocytes immunohistochemically (Trujillo *et al.*, 1999b) where the presence of α, β and γ subunits was shown.

The values found here provide strong functional evidence for an amiloride sensitive ENaC in canine articular cartilage. This study provides the first single channel electrophysiological evidence of functional ENaC expression in canine articular chondrocytes and supports previously published molecular evidence for the presence of ENaC in chondrocytes (Trujillo *et al.*, 1999b).

The amiloride-sensitive epithelial sodium channels (ENaC) were blocked using 10μM amiloride. The ENaC channel is said to have a high affinity ligand binding site to which the amiloride binds (Canessa *et al.*, 1994). At higher concentrations amiloride has been shown to activate certain channels, such as non-selective cation transporters in frog skin therefore to avoid the possibility of this happening in the present experiments a concentration in the μM range was used (Cox, 1997). The average deflection of the membrane potential was around -8mV. This was close to the value found for benzamil inhibition of the membrane potential, suggesting that the majority of this change is due to ENaC.

Little is known about the RVI mechanism in chondrocytes, although it has been shown in other tissues that ENaC plays a role in control of sodium ion transport during this process (Rossier *et al.*, 2002). In this chapter the RVI experiments suggest that a significant component of the RVI response is due to ENaC. Benzamil significantly inhibited cell volume recovery following a hypertonic challenge. It has

previously been suggested that the NKCC co-transporter is important for cell RVI (Bush *et al.*, 2010). To investigate this, the RVI experiments were repeated using lithium instead of sodium chloride solutions. ENaC is highly permeable to lithium, whereas the NKCC will be unable to transport lithium ions. RVI was not affected in the lithium solutions, reinforcing the benzamil experiment results that ENaC does contribute to control of cell volume. It is possible that the contribution of both ENaC and the NKCC pump (Bush *et al.*, 2010) maintains the chondrocytes ability to regulate its volume so effectively.

Experiments by others have indicated differential ENaC subunit expression throughout the zone of articular cartilage (Ali Mobasheri, personal communication). It is known that different stages of lung development, for example, express different ENaC subunits. As the chondrocyte faces a constantly changing environment it is possible that different subunits are also expressed here to cope with the different mechanical stresses.

5

CHLORIDE CHANNELS

5.1 Introduction

Chloride channels are found in almost every animal cell (Nilius *et al.*, 1997) and have been shown to be involved in the regulation of cell volume, regulation of pH, control of cell membrane potential and also involved in the transport of amino acids (Nilius, 1998). The chloride ion channel family contains five subgroups, including voltage-gated, calcium-activated, volume-regulated and maxi (large conductance) channels, which are present in many cells. Voltage-gated and maxi-chloride channels have been shown in rabbit articular chondrocytes (Sugimoto *et al.*, 1996b).

A number of studies have suggested that chloride channels are important for control of the RMP and control of cell-volume (reviewed by Barrett-Jolley *et al.*, 2010). It is hypothesised that during regulatory volume decrease (RVD) a cell effluxes potassium ions (Lewis *et al.*, 2011). One would also expect there to be a matching anion efflux (chloride, for example) to maintain electroneutrality of the membrane and reduce the total loss of potassium ions. A maxi-chloride channel could provide this efflux and possibly explain why it is thought to be a volume-sensing channel (Tsuga *et al.*, 2002).

Previous studies on chondrocytes have failed to convincingly identify the exact chloride channel family member present. It is distinctly possible that chondrocytes express more than one type of chloride channel (Sugimoto *et al.*, 1996b).

In this chapter the functional expression of chloride channels in chondrocytes was investigated, using both inside-out patch clamp and whole-cell electrophysiology. Pharmacological blockers of several of the chloride ion channel family were used to determine contribution of different chloride channels to the whole-cell current. RT-PCR was used to investigate the expression of a member of the ClC family in canine chondrocytes. Cell volume experiments were performed using a specific chloride channel inhibitor to determine the effect of inhibition of these channels on RVD.

5.2 Methods

As described in Chapter 2, inside-out patch clamp with potassium-free conditions was used for all single channel data shown. Physiological solutions ("RMP-physiological", Table 1 and 2) were used for whole-cell voltage ramps and current clamp experiments measuring RMP. 4-Acetamido-4-isothiocyanato-2,2-stilbenedisulfonic acid disodium salt hydrate (SITS) and niflumic acid (NFA) stocks were prepared using dimethylsulfoxide (DMSO) and diluted to the desired concentration in electrophysiological bath solutions. Final DMSO concentration was no more than 1 in 10,000. Room temperature for these experiments was 22-25°.

To determine the effect of chloride channels on RVD, physiological solutions were used (see Table 1). Cells were incubated for up to an hour in a solution with an osmolarity of 489mOsm, created by adding 180mM sucrose to the physiological solution in table 1. RVD was initiated by perfusing the cells with the standard physiological solution of 309mOsm.

5.3 Results

5.3.1 Inside-out patch clamp

Single channel inside-out patch clamp in potassium-free solutions (see Tables 1 and 2) identified a population of ion channels with a mean slope unitary conductance of 183±3pS (n = 5; figure 5.1a). These channels reversed at a holding potential of 34±6mV (n = 5; figure 5.1c), indicative of a chloride current (calculated equilibrium potential, E_{Cl} ~ -35mV). This channel activity was seen in approximately 30% of patches with a mean open probability (P_o) of 0.7±0.1 (n = 3) and was inhibited by the chloride-channel blocker SITS at a concentration of 100μM. Application of 100μM SITS decreased channel P_o by 83±6% (n = 3; $p<0.05$).

5.3.2 Whole-cell electrophysiology

In whole-cell voltage clamp mode, 100μM SITS significantly inhibited voltage ramps by 52±6% (n = 4; $p<0.05$) at 20mV (figure 5.2b). SITS is a relatively non-selective inhibitor of anionic currents so to further characterise this chloride current, a more specific channel inhibitor was used; niflumic acid (NFA). NFA inhibits the calcium-activated chloride channel (CaCC), which is also believed to be a volume-sensitive chloride channel. 100μM NFA significantly inhibited whole-cell current by 18±2% at 20mV (n = 15, $p<0.01$; figure 5.2a). A combined application of 100μM SITS and 100μM NFA was investigated using the same whole-cell voltage ramp protocol. The application of these drugs significantly inhibited whole-cell current by 46±6% at 20mV (n = 4, $p<0.05$; figure 5.2c). The effect of NFA on whole-cell current at 15mV is shown as a dose-response curve (figure 5.3b). An IC_{50} value of 90±16μM was calculated from the equation shown (n = 3; figure 5.3).

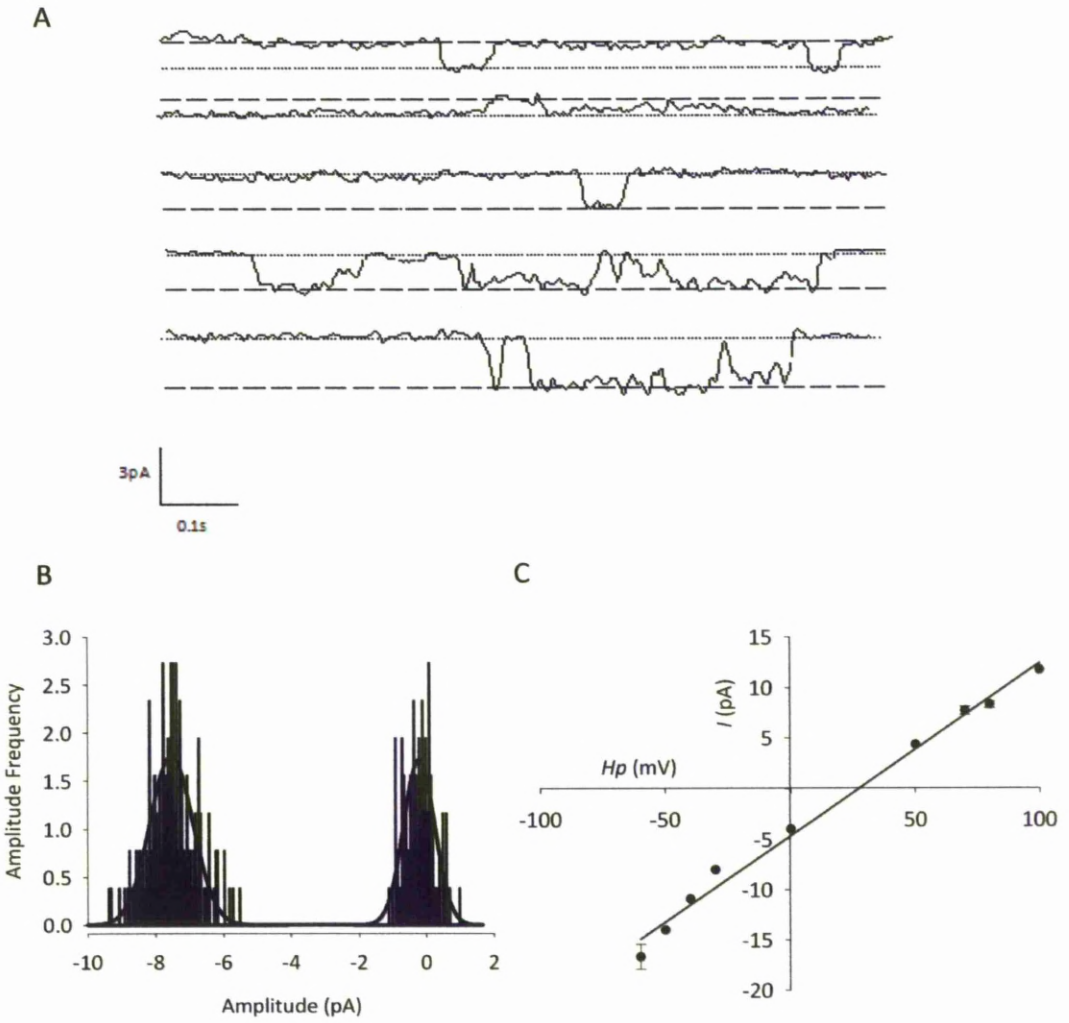

Figure 5.1 Patch-clamp electrophysiology reveals the presence of SITS-sensitive ion channels A) Traces of inside-out single channel activity (from top to bottom) 50mV, 40mV, -10mV, -50mV and -70mV. The dotted line indicates the closed state whilst the dashed line indicates the open state. B) All-points amplitude histogram at -70mV. C) Current-voltage curve for single-channel recordings. Some error bars for data are smaller than the symbols. A straight line is fitted to the points.

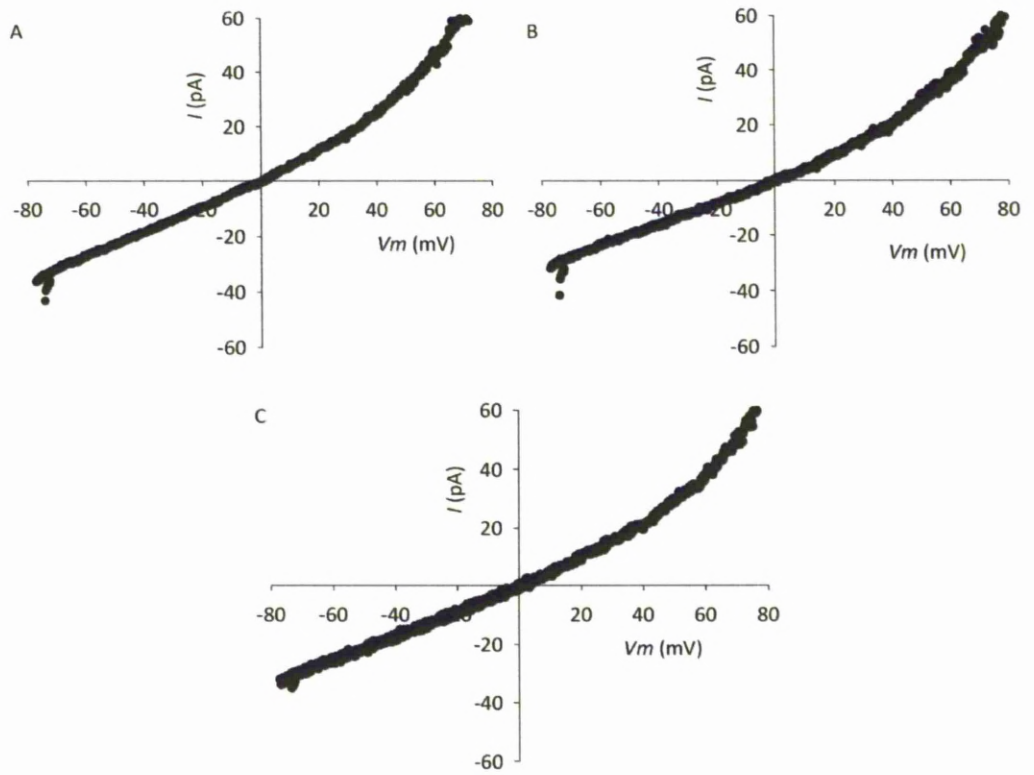

Figure 5.2 Patch clamp electrophysiology demonstrates the presence of SITS-sensitive whole-cell conductances. Whole-cell voltage ramps were run in the presence and absence of varying concentrations of niflumic acid (NFA) and 4-Acetamido-4-isothiocyanato-2,2-stilbenedisulfonic acid disodium salt hydrate (SITS). The curves in the presence of the drugs were then subtracted from the control curves to produce the difference curves. These are shown in A-C. A) Difference curve of current sensitive to 100μM NFA. Current was significantly inhibited by 18±2% at 20mV (n = 15; $p<0.01$). B) Difference curve of current sensitive to 100μM SITS. Current was significantly inhibited by 52±6% at 20mV (n = 4; $p<0.05$). C) Difference curve of current sensitive to a combined application of 100μM NFA and 100μM SITS. Current was inhibited by 46±6% at 20mV (n = 4; $p<0.05$).

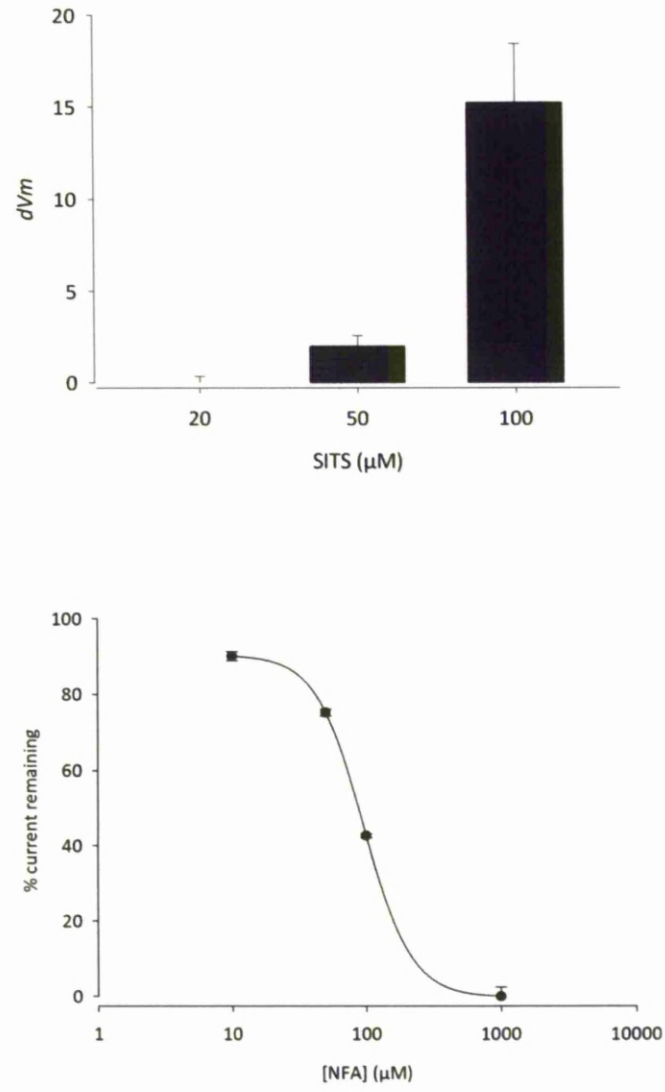

Figure 5.3. Application of different concentrations of SITS and NFA on membrane potential and whole-cell current. A) Histogram of change in membrane potential (δVm) measured in current-clamp mode upon application of 20, 50 and 100µM of 4-Acetamido-4-isothiocyanato-2,2-stilbenedisulfonic acid disodium salt hydrate (SITS). B) Dose response curve for whole-cell current change in presence of niflumic acid (NFA) at 15mV. Whole-cell voltage ramps were run in the presence and absence of NFA then subtracted from one another to determine the current remaining after NFA application. Curve is fitted with $f = max - 100 * \frac{[NFA]^n}{([NFA]^n + (EC_{50})^n)}$ where max is the maximum effect of NFA on current, [NFA] is the concentration of NFA (µM), EC50 is the midpoint parameter (µM) and n the slope of the curve (no units).

5.3.3 Membrane potential measurements

As previous studies have described chloride channels sensitive to 1mM SITS contributing to the membrane potential (*Vm*) in chondrocytes (Tsuga *et al.*, 2002), this effect was also investigated here using different SITS concentrations. Whole cell current-clamp experiments were performed which showed that 100μM SITS induced a significant change of +12±3mV (n = 5, $p<0.01$; figure 5.3a). Neither 50μM nor 20μM SITS concentrations had a significant effect on the *Vm* (n = 6, $P>0.05$).

5.3.4 RT-PCR

RT-PCR was performed on first expansion canine chondrocytes using primers targeted to the canine ClC-1 channel (Table 4), as described in Chapter 2. After PCR thermocycling the PCR products were separated on a 1.5% agarose gel and visualised with ultra-violet light. GAPDH primers were run before the ClC-1 primers to test for viable chondrocyte cDNA (figure 5.4a). Although cDNA was found to be viable, the primers used did not detect any mRNA product (figure 5.4b).

5.3.5 Cell volume measurements

NFA, a calcium-activated chloride channel blocker, showed a significant inhibition of whole-cell current (figures 5.2 and 5.3; $p<0.5$). The effect of this inhibition on cell volume control was investigated. After incubation in a 489mOsm solution cells were exposed to a relatively hypotonic (309mOsm) physiological saline and their size was measured throughout. On exposure to the hypotonic solution cell size increased significantly by 64±4% (n = 5, $p<0.001$; figure 5.5). Within 15 minutes of reaching

their largest size, cells under control conditions had returned to within 24±10% of their original volume. When 100μM NFA was added to the hypotonic solution cells swelled significantly by 50±9% (n = 5, p<0.005; figure 5.5), not significantly different to the cells in control solution (p=0.9). 15 minutes after reaching their largest size, cells had returned to within 25±6% of their original volume, similar to the control cells (p=0.8). There is the possibility, however, that if the solutions had been left on for longer than 30 minutes the control cells would have been able to regulate their volume effectively. Within the last 5-10minutes of hypertonic treatment it appears that the control cells may be starting to return to their original volume.

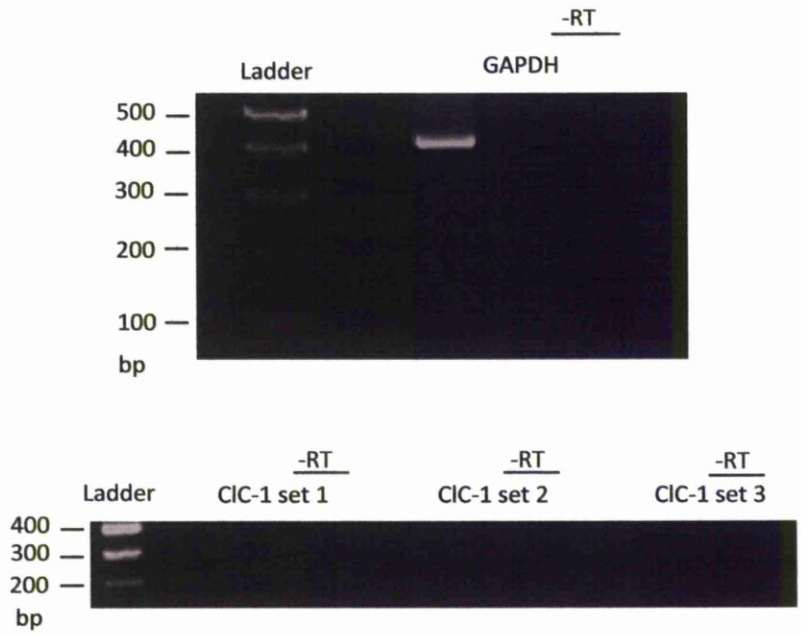

Figure 5.4 RT-PCR with GAPDH and ClC-1 primer sets. RT-PCR was run on first expansion canine chondrocytes using the three CLC-1 primer sets (Table 4). PCR products were run on a 1.5% agarose gel at 80mV for two hours and visualised and photographed under UV light. For a negative control A) GAPDH was detected showing viable cDNA (PCR product at 429bp). B) No mRNA for ClC-1 was detected by any of the primer sets in these cells. Products were expected between 100 and 300bp.

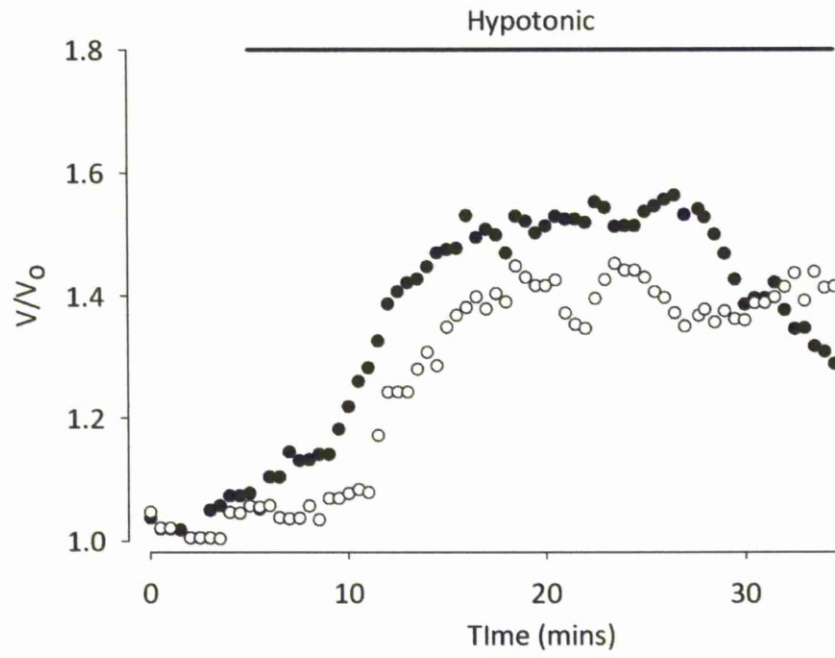

Figure 5.5 Chloride channel contribution to cell volume regulation. Chondrocytes were subjected to a hypotonic physiological solution, duration indicated by the solid line on the graph above (moving from physiological saline with 180mM of sucrose added (osmolarity of 489mOsm) to physiological saline, see Table 1 and text for description). This was done in the absence of NFA (control; filled circles) and in the presence of 100μM NFA (empty circles). NFA had no effect on chondrocyte ability to decrease volume after 15 mins.

5.4 Discussion

The data here have identified a channel with a reversal potential near to the chloride Nernst potential, with an amplitude similar to that expected for a chloride channel and shown this to be sensitive to the chloride channel blocker SITS. The existence of SITS susceptible chloride channels in chondrocytes has previously been reported by Tsuga *et al* (Tsuga *et al.*, 2002) for cultured rabbit articular chondrocytes. However this is the first demonstration of chloride channels in canine articular chondrocytes. A conductance of around 180pS is within expected parameters for a maxi-chloride channel, and similar to conductance levels determined in other studies (Sugimoto *et al.*, 1996a; Tsuga *et al.*, 2002).

A significant inhibition of whole-cell current was found to occur with 100μM SITS. The effect of SITS was shown to correspond to a 40% inhibition of whole-cell conductance. As SITS is relatively non-selective for members of the chloride family, it is thought that the concentration used here is inhibiting most chloride conductance within the cell. The more selective calcium-activated chloride channel (CaCC) inhibitor, NFA, was found to account for nearly 20% of the whole-cell current. This value is possibly slightly higher than would be expected, given that the CaCC is a relatively low conductance channel, so it may be possible that the NFA is inhibiting other conductances (Gögelein *et al.*, 1990).

The RT-PCR experiments searched for ClC-1, a member of the ClC subfamily of chloride channels. The primer sets used here were unable to detect any mRNA for this channel, however positive controls for the primers were not run so it may be that the primers do not work, rather than the channel is not present.

Since it was demonstrated that NFA has an effect on whole cell conductance and that CaCC are responsible for a large component of chloride current, it was investigated whether the inhibition of CaCC would have any effect upon cell volume regulation. It is known that RVD involves an efflux of potassium as well as the hypothesised efflux of chloride (Lewis *et al.*, 2011). Here, no difference was seen in RVD in the presence of NFA. Cells in the presence of NFA actually appeared to swell less than those without NFA, although there was not shown to be a significant difference. A possible explanation for this could be that although the CaCC is not directly involved in an efflux of chloride during volume regulation, inhibition of this current causes a depolarisation of the membrane potential (*Vm*), similar to that reported in this chapter with SITS. Lewis *et al* (2011) shows that a more positive *Vm* enables cells to respond to hypotonic challenges more effectively. If NFA is depolarising the membrane potential then this would mean that the cell is able to efflux potassium more effectively and thus control its volume. The results from the volume analysis experiments could be explained if NFA can be demonstrated to increase membrane potential.

6

POTASSIUM CHANNELS

6.1 Introduction

Channels of the potassium family have been some of the most studied ion channels in chondrocytes (Grandolfo *et al.*, 1990; Wilson *et al.*, 2004; Mobasheri *et al.*, 2007b). The potassium ion channel family is one of the largest ion channels families with over 40 members (Alexander *et al.*, 2008). The Kv, K_{ATP} and calcium-activated sub groups have been reported in chondrocytes (Grandolfo *et al.*, 1992; Walsh *et al.*, 1992; Mobasheri *et al.*, 2007a). This chapter will look at the Kv and calcium-activated channels.

The Kv channel was one of the first ion channels discovered in chondrocytes and has now been reported by a number of authors in a range of species (Wilson *et al.*, 2004; Mobasheri *et al.*, 2005a; Ponce, 2006; Clark *et al.*, 2010). There is controversy over the exact subunits of the channel that are expressed in chondrocytes. However, the majority of the functional data agrees that there is likely to be a Kv1.X subtype, with possibly a Kv4.X subtype also present (Mobasheri *et al.*, 2005a; Clark *et al.*, 2010). Immunohistochemical and RT-PCR data have revealed the presence of Kv1.4 subunits in equine chondrocytes (Mobasheri *et al.*, 2005a) and Kv1.6 in the mouse (Clark *et al.*, 2010). The calculation of Kv current is described by Equation 5 taken from Hodgkin and Huxley (Hodgkin & Huxley, 1952b).

$$g_K = \left\{(g_{K\infty})^{\frac{1}{4}} - \left[(g_{K\infty})^{\frac{1}{4}} - (g_{K0})^{\frac{1}{4}}\right] exp(-t/\tau_n)\right\}^4 \qquad \text{Equation 5}$$

Where, g_{K_∞} is the value the conductance will eventually reach and g_{K_0} is the value at time = 0.

Calcium-activated potassium channels have been identified in chondrocytes by a large number of studies (Grandolfo *et al.*, 1992; Long & Walsh, 1994; Martina *et al.*, 1997; Mozrzymas *et al.*, 1997). A member of this sub-family of ion channels, the large calcium-activated potassium channel (BK), is reported to be opened by stretch (Grandolfo *et al.*, 1992). The deformation of the membrane is thought to be one of several modes of mechanotransduction pathways involved in sensing and responding to membrane load (Guilak *et al.*, 1995; Knight *et al.*, 1998). The open probability of stretch-activated ion channels generally increases in response to mechanical deformation of the plasma membrane (Sachs, 1991). Thus, load-induced changes in the chondrocyte membrane, including membrane stretch, are likely to play a key role in the signal-transduction cascades associated with chondrocyte ion channel signalling.

This chapter investigates the stretch-sensitivity of the calcium-activated potassium channel in equine chondrocytes using cell-attached patch. Whole-cell patch-clamp electrophysiology is used to functionally identify the principal stretch-activated ion channel in equine articular chondrocytes. Further analysis is also performed on Kv channel data obtained by my group on equine chondrocytes (Mobasheri *et al.*, 2005a).

6.2 Results

6.2.1 BK activation by stretch

Stretch was applied to cell-attached patches by use of a SAM12 medical suction pump (MG Electrical Ltd, UK) attached to the patch pipette. Pipettes were filled with "BK-stretch" extracellular solution (see Table 1). A stretch-activated channel was identified when 200mmHg of pressure was applied to the cell membrane. This channel had an amplitude of 9±1pA at a membrane potential of 38mV (n = 3). The slope conductance of these channels was calculated to be 118±9pS (figure 6.1). Other data collected at the same time by my group (Mobasheri *et al.*, 2010) shows that the pharmacology of this channel is also consistent with it being a large calcium-activated potassium channel. When 3mM tetraethylammonium chloride (TEA) or 1µM iberiotoxin were added to the pipette solution (i.e. the extra-cellular solution in cell-attached patch) channel activity was significantly inhibited. Application of TEA reduced channel activity by approximately 70%, iberiotoxin application reduced channel activity by approximately 90%.

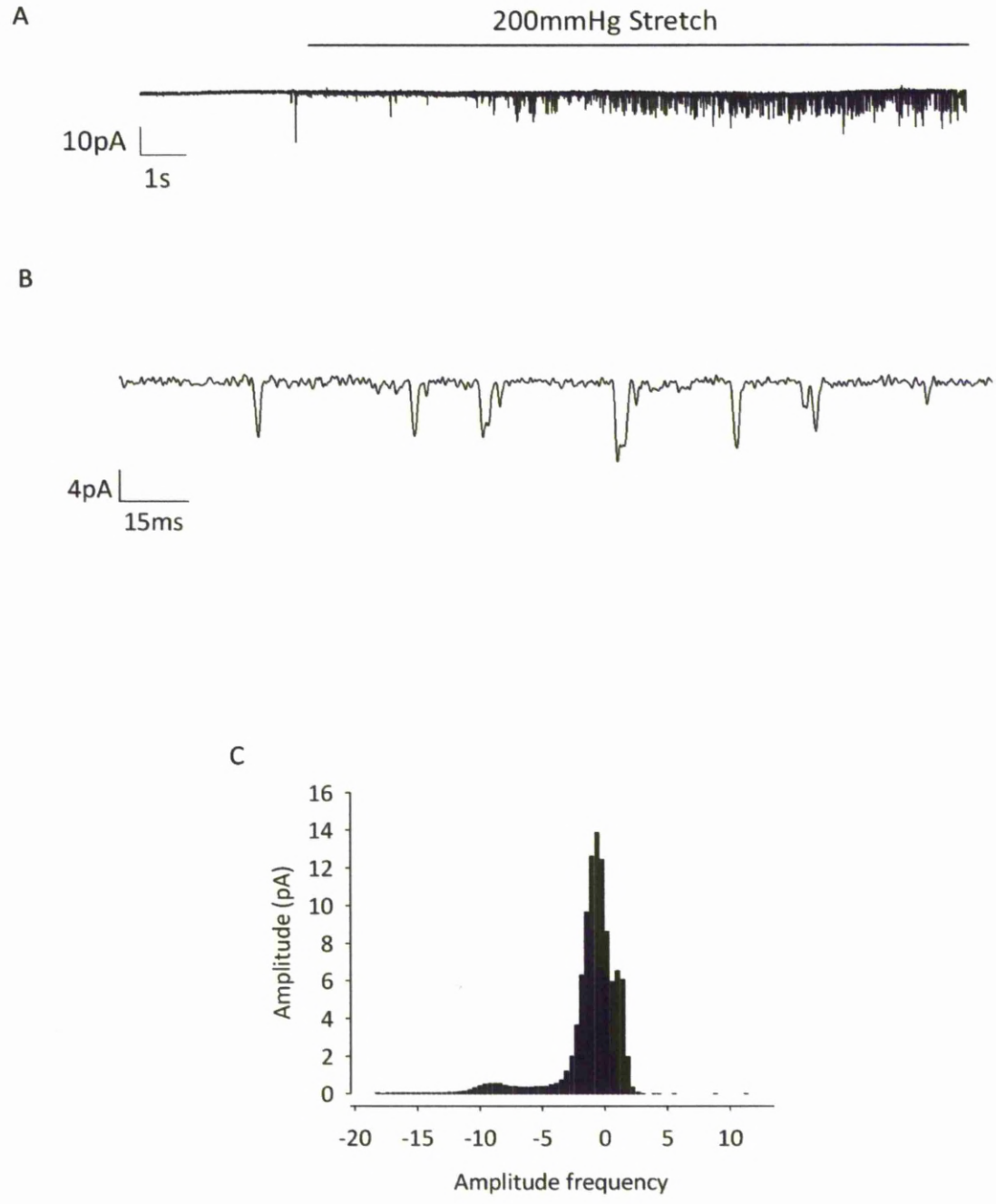

Figure 6.1 Activation of ion channels by membrane stretch. A) Raw trace showing application of suction (as indicated by the solid bar) to the patch pipette of chondrocytes under cell-attached mode of recording increases membrane current with 115mM K^+ in the pipette. *Vm* = 38 mV. B) Raw trace showing single channels in the "tail" of the suction response from 'A'. C) All-points amplitude histogram at 38mV measured from channel activity shown in A and B.

6.2.2 Kv analysis

To provide a mathematical description of the Kv data previously published by my group (Mobasheri *et al.*, 2005a) the Hodgkin and Huxley model of potassium conductance (Equation 6) was adapted to account for any inactivation of current with time, similar to the Hodgkin and Huxley sodium conductance expression.

$$g_K = \left\{(g_{K\infty})^{\frac{1}{4}} - \left[(g_{K\infty})^{\frac{1}{4}} - (g_{K_0})^{\frac{1}{4}}\right] exp(-t/\tau_n)\right\}^4 \left[h_\infty - (h_\infty - h_0)\exp\left(-\frac{t}{\tau_h}\right)\right]$$

Equation 6

Where, $g_{K\infty}$ is the value the conductance will eventually reach, assumed here to be the peak (maximum) conductance. g_{K_0} is the conductance at time = 0, assumed here to be zero. $h_\infty$is the value the inactivating current will reach (this was assumed to be 0 as in Hodgkin and Huxley (Hodgkin & Huxley, 1952b)) and h_0 is the initial fraction of inactivation.

WinEDR was used to produce values for τ_n, $\tau_h$and g_K by fitting whole-cell currents recorded from a voltage-clamp protocol of depolarising steps, from a holding potential of -80mV and increasing in 10mV increments to a maximum of +60mV (figure 6.2a).

τ_n and g_K values were then used to obtain values for α_n and b_n from Equation 7 and 8.

$$n_\infty = \frac{\alpha_n}{\alpha_n + \beta_n}$$ Equation 7

$$\tau_n = \frac{1}{\alpha_n + \beta_n}$$ Equation 8

It was assumed that:

$$n_{\infty} = \left(\frac{G_K}{G_{K\infty}}\right)^{\frac{1}{4}} \qquad \text{Equation 9}$$

τ_h values were calculated from:

$$\tau_h = \frac{1}{\alpha_h + \beta_h} \qquad \text{Equation 10}$$

In order to model the Kv current at any given membrane potential (Vm) (see Chapter 7) it was necessary to calculate $\alpha_n(Vm)$, $\beta_n(Vm)$ and $\alpha_h(Vm)$ (β_h was assumed to be zero in the normal physiological range (Hodgkin & Huxley, 1952b)). To do this, $\alpha_n(Vm)$, $b_n(Vm)$ and $\alpha_h(Vm)$were fitted to the experimental data using Equations 11, 12 and 13, respectively (fits shown in figure 6.2).

$$\alpha_n(Vm) = \frac{a(b-Vm)}{e^{\frac{-Vm+a}{a}} - 1} \qquad \text{Equation 11}$$

$$\beta_n(Vm) = ce^{\frac{-Vm}{d}} \qquad \text{Equation 12}$$

$$\alpha_h(Vm) = e * \left[1 - \exp\left(\frac{-Vm}{f}\right)\right] + g \qquad \text{Equation 13}$$

Where, Vm is membrane potential and a to g are constants. Mean best-fit parameters for a to g are summarised in Table 5. These values will be used in Chapter 7 to calculate the Kv current contribution to the chondrocyte membrane potential.

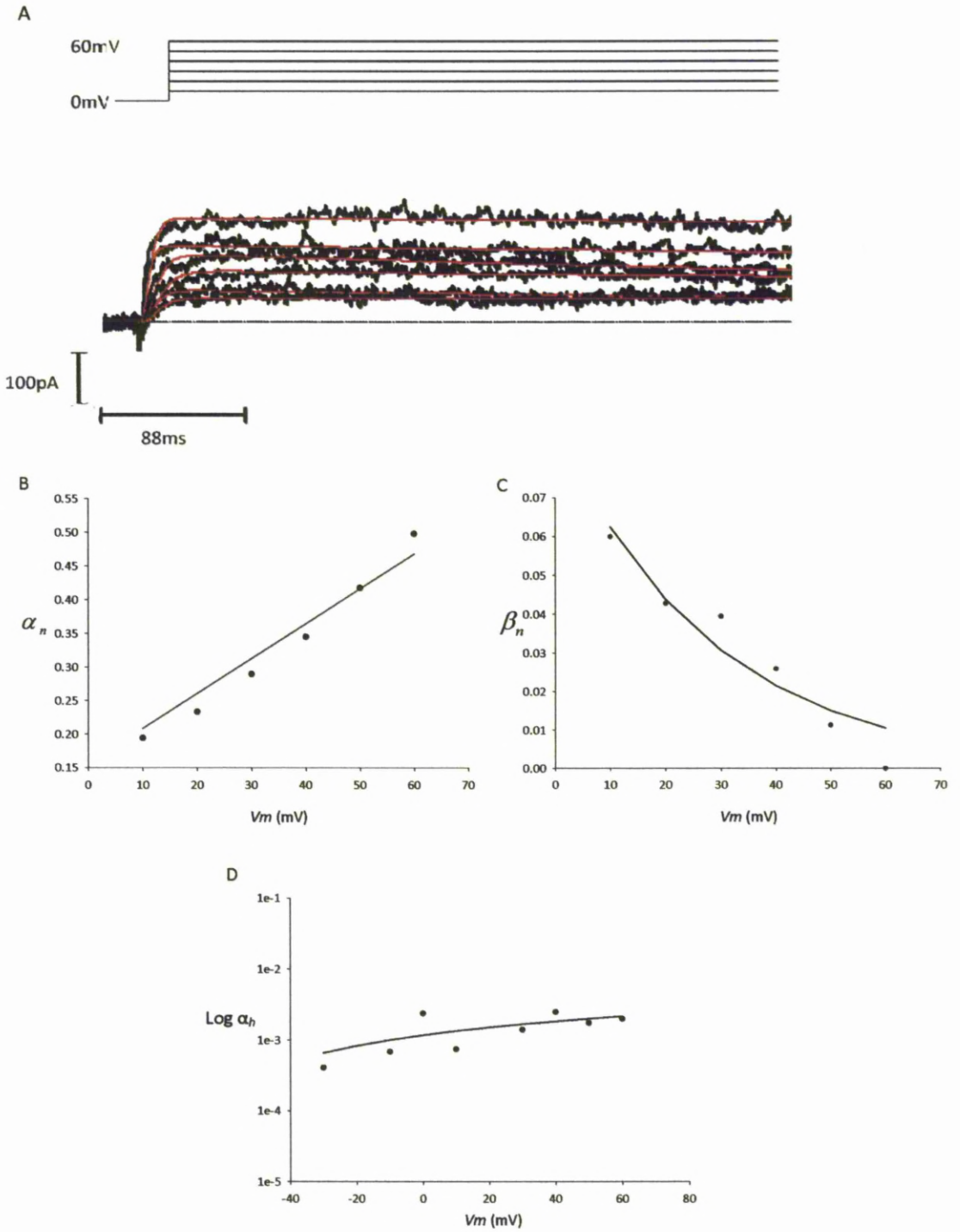

Figure 6.2 Kv current analysis. A) Representative trace of Kv current data fitted in this chapter. Red line shows fit to data as described in the text. B) Line fitted to the data is from $\alpha_n(Vm) = \frac{a(b - Vm)}{exp^{\frac{-Vm+a}{a}} - 1}$ C) Curve fitted to the data is from $\beta_n(Vm) = c * exp^{\frac{-Vm}{d}}$. D) Curve fitted to the data is from $\alpha_h(Vm) = e * \left[1 - exp\left(\frac{-Vm}{f}\right)\right] + g$. The filled circles show values for Kv current and the curve is a fit to that data by minimising chi-^{2}. The fitting process is described in the text.

Constant	Mean	SEM
a	0.02	8.7
b	28.2	0.01
c	0.04	0.01
d	0.01	0.004
e	0.0002	0.0001
f	0.3	0.02
g	0.0009	0.0003

Table 5 Values for Kv constants to be used to calculate the Kv current in Chapter 7. Summary of the best fit parameters for a, b, c and d obtained as described in this section and used to allow calculation of Kv conductance for inclusion in a model of membrane potential.

6.3 Discussion

The stretch-activated channel identified in this chapter had a size (slope conductance) and reversal potential consistent with it being a large calcium-activated potassium channel (BK) (Latorre *et al.*, 1989; Cui *et al.*, 2009). Other data collected at the same time by my group (Mobasheri *et al.*, 2010) shows that the pharmacology of this channel is also consistent with it being a large calcium-activated channel. When 3mM tetraethylammonium chloride (TEA) or 1μM iberiotoxin were added to the pipette solution (i.e. the extra-cellular solution in cell-attached patch) channel activity was significantly inhibited. Application of TEA reduced channel activity by approximately 70%, iberiotoxin application reduced channel activity by approximately 90%.

Membrane stretch is a realistic physiological challenge for the chondrocyte and directly linked to changes in matrix production (Urban *et al.*, 1993). Stretch will occur in two contexts. Firstly, when the chondrocyte is deformed by compressive force, the cell passes from a virtually spherical conformation to an approximate ellipsoid (Guilak, 1994; Urban, 1994). For a given volume, an ellipsoid has a greater surface area than a sphere and so membrane stretch is the result. Secondly hypo-osmotic conditions cause cell swelling increase cell radius, and consequently increase its surface area (Urban *et al.*, 1993). These increases in membrane surface area are likely to be met by stretch rather than the production of a new membrane. This membrane stretch will be limited to a theoretical maximum of approximately 3% at which point it may be expected to rupture (Morris & Homann, 2001). In the experiments shown in this chapter, only stretch using negative pressure was

investigated. However, my group also showed that the two different membrane stretch paradigms produced results consistent with the opening of potassium channels in response. Both of these approaches have their strengths and weaknesses. The direct membrane stretch (cell-attached patch) experiments allowed the investigation of the situation when neither intracellular nor extracellular environments were altered, but this did not allow effects on the whole cell to be seen. The osmotic challenge experiments presented in Mobasheri *et al* (2010), required, by definition, alterations of extracellular environment and changes in the cytosol by the patch pipette solution. The results from the osmotic challenge, however, still showed that a hypotonic solution will cause a hyperpolarisation of the membrane potential which can be inhibited with TEA, again indicative of a BK channel.

The change in membrane potential with a hypertonic challenge shown in Mobasheri *et al* (2010) is interesting as there have been various hypotheses about the function of BK in chondrocytes. A hypotonic challenge will cause a cell to swell as it passively uptakes water. As described in Chapter 1, cells use regulatory volume decrease (RVD) to oppose this water uptake by effluxing ions. The hyperpolarisation of membrane potential described in Mobasheri et al (2010) is likely to be due to activation of a calcium-activated potassium channel. In Chapter 3 the effect of activation of the TRPV4 channel on membrane potential was described. Surprisingly TRPV4 activation caused a hyperpolarisation in the membrane potential. This could be explained by the influx of calcium from the opening of TRPV4 activating the BK channel, rather than the BK channel being activated directly by membrane stretch, i.e. BK is activated by the calcium-dependent hypothesis described in Chapter 1.

The hyperpolarisation caused by TRPV4 activation was greater than that seen by simply stretching the membrane with a hypotonic solution (-13mV compared to -55mV; Chapter 3). There could be a number of reasons for this. It is probably most likely that the hypotonic challenge was only activating a small percentage of the TRPV4 channels, thus not all the BK channels were activated. The hypotonic situation used in Mobasheri *et al* (2010) is not particularly physiologically accurate. *In vivo* chondrocytes are thought to experience osmolarities ranging from between 300-500mOsm (Urban, 1994). Changing from approximately 300mOsm to 130mOsm, as in Mobasheri *et al* (2010), is a hypotonic challenge that is physiologically irrelevant to the chondrocyte. In RVD experiments described later in this thesis (see Chapter 7) a hypotonic challenge was applied by changing from a solution of 489mOsm to 309mOsm, likely to be more physiologically relevant for the chondrocyte. It would be interesting to repeat the experiments in Mobasheri *et al* (2010) with these physiological conditions to see whether a greater degree of hyperpolarisation is seen.

The voltage-activated potassium channel (Kv) analysis described here is a well-known method of determining Kv activation parameters. The Kv channel data fitted here were taken from elephant and equine chondrocytes (Mobasheri *et al.*, 2005a). The immunohistochemistry data presented in this study showed the presence of Kv1.4 subunits, which possibly create a heteromultimeric Kv channel with other Kv subunits in chondrocytes. The constant values calculated here will be input into a model of membrane potential in Chapter 7 to enable calculation of the contribution of total potassium current to membrane potential in the chondrocyte.

7

MODELLING CHONDROCYTE FUNCTION

7.1 Introduction

Initial theories on ion transport across a cell membrane did not include the concept of ion channels. Instead it was believed that ions would independently move across a homogenous membrane in the same manner they would in free solution and that a linear electrical gradient existed across the whole membrane (Goldman, 1943). This theory is known as the 'constant field theory'.

This theory was later adopted by Hodgkin and Katz (Hodgkin & Katz, 1949a) whilst analysing the membrane properties of squid axons. However, in examining the sodium permeability of the membrane they had difficulty in understanding the selective permeability of the membrane to sodium. They continued with the assumption that the resting membrane was permeable to potassium and chloride ions but only sparingly permeable to sodium ions. Hodgkin and Katz suggested that as the membrane became "active" (depolarised) the membrane became selectively more permeable to sodium but this didn't fit with the idea of a linear electrical gradient. They hypothesised that instead of crossing the membrane in ionic form, sodium ions became bound to a lipid soluble molecule, which became able to cross the membrane when it was depolarised. This meant that they assumed that the resting membrane was more permeable to potassium than sodium but during an action potential this situation reversed and the membrane became more permeable

to sodium than potassium. Combining their observations with those of Goldman gave rise to the *GHK* equation:

$$E = \frac{RT}{F} ln\left(\frac{P_{Na^+}[Na^+]_{out} + P_{K^+}[K^+]_{out} + P_{Cl^-}[Cl^-]_{in}}{P_{Na^+}[Na^+]_{in} + P_{K^+}[K^+]_{in} + P_{Cl^-}[Cl^-]_{out}}\right) \quad \text{Equation 14}$$

Where $[X]_{out}$ and $[X]_{in}$ are the extracellular and intracellular concentrations of the relevant ions, P_X are the permeability coefficients of the relevant ions and *R*, *T* and *F* have the standard definitions. This equation can be expanded to take into account other ions in a solution, for example, calcium. However, this equation is only relevant to a membrane at equilibrium. As the permeabilities of the ions change so does the membrane potential. A model was needed whereby the membrane potential could be determined at any stage.

Following on from these observations, Hodgkin and Huxley (Hodgkin & Huxley, 1952b) showed that current through the membrane was carried by charging the membrane capacity or by the movement of ions through resistances in parallel with the capacity. They divided the ionic current into that carried by potassium ions, sodium ions or other ions, such as chloride, which they called the "leakage current". The value of each ionic current (I_X) was determined by the conductance of the ion (G_X), and the difference between the membrane potential and the equilibrium potential (E_X) for that ion. This was represented as

$$I_X = G_X[E - E_X] \quad \text{Equation 15}$$

Where E is the membrane potential.

Hodgkin and Huxley (1952b) determined that the equilibrium potential was a constant but that conductance and membrane potential were functions of time. They were now able to calculate ionic currents for the permeant ions; the next step was to show how these could affect the total membrane current.

Total membrane current was initially defined as:

$$I = Cm\frac{dV}{dt} + I_i \qquad \text{Equation 16}$$

Where, I is the total membrane current, I_i is the total ionic current density (i.e. I_K + I_{Na} + I_{other}) Cm the membrane capacitance, V the change in membrane potential and t is time. The measurement of individual ionic currents is described in more detail below. Chondrocytes are essentially small spherical cells, in which it can be anticipated that there will be no "space-clamp" effects, i.e., potential will always be evenly distributed across the surface of the membrane. This means that a fully propagating action-potential model, as developed by Hodgkin and Huxley (1952b), is unnecessary to describe the membrane potential of these cells.

In this chapter this approach is used to calculate *Vm* from data presented in previous chapters. This calculated *Vm* is then compared to experimentally measured values. There have been varying reports of the value of the chondrocyte resting membrane potential (RMP). The first measurements stated RMPs of -10.6mV and -12mV in ovine and human chondrocytes respectively (Wright *et al.*, 1992), whereas later reports claimed to find more negative values. These more negative RMPs include -46mV on mouse chondrocytes (Clark *et al.*, 2010), -41mV on rabbit chondrocytes (Sugimoto *et al.*, 1996a) and -20mV on a human cell line,

OUMS-27 (Funabashi *et al.*, 2010). Thus, the first half of this chapter uses a number of methods to measure RMP in chondrocytes from several species and under several different conditions. A model of chondrocyte membrane potential is constructed in Microsoft® Visual Basic which follows the principles of the Hodgkin and Huxley equation described above. The model is tested by experiment as various pharmacological inhibitors of ion channels previously identified are used to change the membrane potential. The second half of this chapter sets out to uncover the function of the chondrocyte RMP and describes a model developed to show the influence of RMP on control of cell volume. The predictions from this model are then tested against cells from diseased tissue.

7.2 Results

7.2.1 Initial measurements of chondrocyte resting membrane potential

The RMP of canine chondrocytes was measured using both whole-cell patch clamp and sharp electrode recording. At temperatures of 24-25°C in physiological saline solution (see Tables 1 and 2), values of -6.1±0.5mV (n = 53) were recorded with whole-cell patch clamp and -7.3±1.8 (n = 19) with sharp electrodes (Figure 7.1a). The value measured by patch clamp was consistent across a range of large animal species (Figure 7.1b). Studies have shown that these cells retain a substantially native chondrocyte phenotype for the first few passages in culture, (see Chapter 1 and Benya & Shaffer (1982)). Therefore, RMP measured from chondrocytes in slices of cartilage (sharp electrodes -7.5±0.7mV, n = 10), freshly dissociated (-6±2; n = 5), first expansion (-9±1; n = 5) and first passage chondrocytes (-6±1; n = 18; all in patch

clamp) were compared. These were not significantly different to each other ($p>0.05$; Figure 7.1b). As a control, RMP from aortic smooth muscle cells were recorded on the same equipment in the same physiological saline; these had RMP in the conventional significantly negative range (-47.9±3.7mV; $n = 5$) (Figure 7.1d[3]). To measure membrane potential from intact cells which had neither been impaled by a sharp electrode, or patch clamped, an optical dye study of the membrane potential was performed (Figure 7.1e and f). This gave a membrane potential value of -8.6±8mV (n=14).

[3] *Note this figure is from Lewis et al., 2011, and the values shown for DRG and hypothalamic neurones were kindly provided by Dr Gareth Bruce and Dr Richard Barrett-Jolley.*

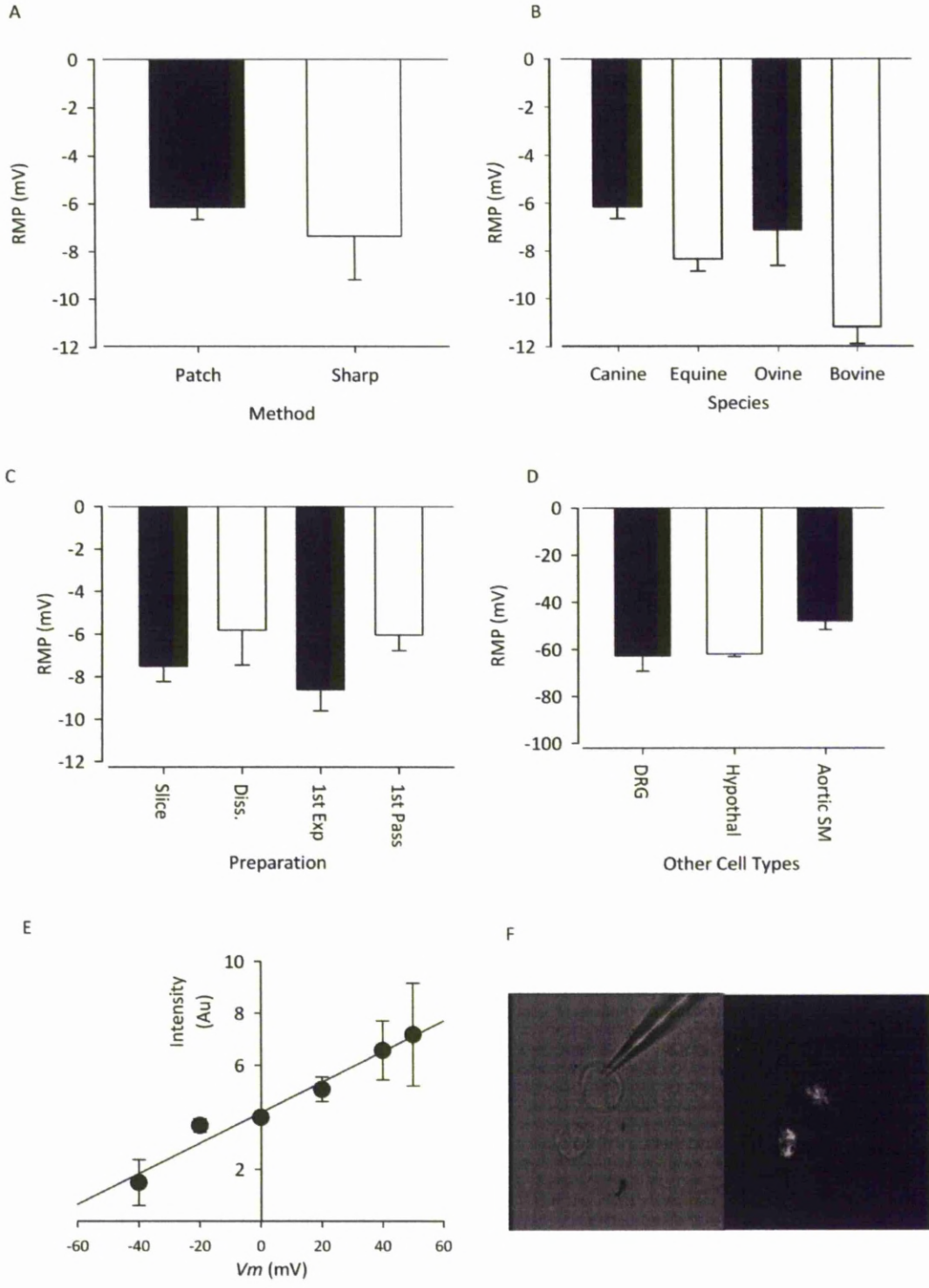
A
0
-2
-4
-6
-8
-10
-12
RMP (mV)
Patch
Sharp
Method
B
RMP (mV)
Canine
Equine
Ovine
Bovine
Species
C
RMP (mV)
Slice
Diss.
1st Exp
1st Pass
Preparation
D
0
-20
-40
-60
-80
-100
RMP (mV)
DRG
Hypothal
Aortic SM
Other Cell Types
E
Intensity (Au)
10
8
6
2
-60
-40
-20
0
20
40
60
Vm (mV)
F

Figure 7.1 Freshly dissociated and primary cultured chondrocytes from a range of species exhibit relatively positive resting membrane potentials. A) RMPs measured in canine chondrocytes by patch clamp and sharp electrodes (n = 50, 19). B) RMPs measured by the whole-cell patch-clamp technique in canine (n = 50, as *A*), equine (n = 9), ovine (n = 8) and bovine (n = 5) chondrocytes. C) RMPs measured by sharp electrodes in cartilage slices ("slice", n = 10) and whole-cell patch clamp from freshly dissociated canine chondrocytes ("diss.", n = 5), from first expansion chondrocytes ("1st Exp", n = 5) and canine chondrocytes following the first passage ("1st Pass", n = 22). D) Control cell type demonstrating conventionally negative RMP recorded in the same solutions and on the same equipment as the chondrocyte RMPs. Values for DRG and Hypothalamic neurones kindly provided for this thesis by Dr R. Barrett-Jolley and Dr G. Bruce; DRG, dissociated rat dorsal root ganglion neurones; Hypothalamic, paraventricular nucleus pre-autonomic neurones; Aortic SM, isolated smooth muscle cells from rat aorta. All patch clamp experiments in this figure were performed with standard physiological intracellular and extracellular solutions, except the sharp electrode recording experiment in *A* where the extracellular solution was the same standard physiological saline, but the electrode was filled with 1M KCl. E) Calibration curve for the voltage sensitive dye measurements, *AU* is arbitrary units of relative intensity. F) Two chondrocytes, one patched, one not patched under visible light (left panel) and epifluorescence (right panel) with 100nM oxonol VI dye in physiological solutions (see Tables 1 and 2).

7.2.2 Model of chondrocyte resting membrane potential

A simple model that can account for the relatively depolarised RMP was constructed as follows. Since the chondrocyte is essentially a small spherical cell and assuming that the principal ion channel conductances have now been identified RMP was calculated as the equilibrium membrane potential (*Vm*) obtained by solving:

$$Cm\frac{dV_m}{dt} = -(I_{BK} + I_{Kv} + I_{KATP} + I_{ENaC} + I_{Cl} + I_{TRPV5}) \quad \text{Equation 17}$$

Where Cm is the average membrane capacitance (12 pF) and I_x is the membrane current (see below) passing through the channel x. Table 6 contains the parameter values assumed and additional to those given in the text.

For the K_V channel:

$$I_{Kv} = G_{Kv}(Vm - E_k) \quad \text{Equation 18}$$

Where G_{Kv} is the conductance of the K_V channel and E_k the equilibrium potential for K^+ ions. The K_V channel is treated as a "Hodgkin-Huxley" channel as described in Chapter 6 (Hodgkin & Huxley, 1952b).

$$I_{Kv} = n^4\bar{G}_{Kv}(Vm - E_k) \quad \text{Equation 19}$$

Where $\bar{G}_{Kv}$ is the maximum Kv conductance and n^4 the gating variable determined from:

$$\frac{dn}{dt} = \alpha_n(1 - n) - \beta_n n \quad \text{Equation 20}$$

α_n and β_n were calculated from Equations 21 and 22 as described in Chapter 6.

$$\alpha_n(Vm) = \frac{a(b-Vm)}{e^{\frac{-Vm+a}{a}}-1} \quad \text{Equation 21}$$

$$b_n(Vm) = ce^{\frac{-Vm}{d}} \quad \text{Equation 22}$$

The best fit parameters a, b, c and d are given in Chapter 6, Table 4.

The other channels are approximated to time-independent linear conductances at membrane potentials relevant to the chondrocyte.

For the BK channel:

$$I_{BK} = G_{BK}(Vm - E_k) \quad \text{Equation 23}$$

$$G_{BK} = \bar{G}_{BK}\frac{[Ca^{2+}]}{[Ca^{2+}]+BKEC_{50}} \quad \text{Equation 24}$$

Maximum conductance of the BK channel ($\bar{G}_{BK}$) is 1.147nS/patch, estimated from the average maximum cell-attached patch current. Some data for this channel is shown in Chapter 6 but this value comes from the data shown in (Mobasheri *et al.*, 2010). However, the low cytoplasmic Ca^{2+} value in the whole-cell patch clamped cell means that I_{BK} is vanishingly small under these conditions. For example, the calculated intracellular calcium concentration with 5mM BAPTA was less than 1nM (calculated with maxchelator http://www.stanford.edu/~cpatton/maxc.html). In the switch-clamp (sharp-electrode) volume experiments, calcium levels will be controlled by the cells native calcium buffering systems, therefore I_{BK} will have very little contribution to the RMP (Iannotti & Brighton, 1989).

For the K_{ATP} channel:

$$I_{KATP} = G_{KATP}(Vm - E_k) \quad \text{Equation 25}$$

Where;

$$G_{KATP} = \bar{G}_{KATP}\left(1 - \frac{[ATP]}{[ATP]+K_{ATP}IC_{50}}\right) \qquad \text{Equation 26}$$

$\bar{G}_{KATP}$, $[ATP]$ and corresponding IC_{50} are estimated from (Mobasheri *et al.*, 2007b).

For the epithelial sodium channel and the chloride channel, respectively:

$$I_{ENaC} = G_{ENaC}(Vm - E_{Na}) \qquad \text{Equation 27}$$

$$I_{Cl} = G_{Cl}(Vm - E_{Cl}) \qquad \text{Equation 28}$$

Where G_{ENaC} is the ENaC conductance shown in Chapter 4 and G_{Cl} is the chloride conductance shown in Chapter 5, scaled for the whole-cell by calculating $n*i*P_o$ (Values given in Table 6).

For the TRP channel current:

$$I_{TRPV5} = G_{TRPV5}(Vm - V_{TRPV5}) \qquad \text{Equation 29}$$

Where G_{TRPV5} is calculated from the whole-cell data shown in Chapter 3 (value given in Table 6). The tail current voltage clamp experiments showed only weak voltage sensitivity (Boltzmann parameters for slope (k) and half maximal activation ($V_{1/2}$) were 83mV and -38mV respectively, see Chapter 3) and so this simple model treats the channel as non-voltage sensitive. V_{TRPV5} was calculated by difference of whole-cell currents with and without 100µM gadolinium (see Chapter 3 for details), but for more general case, used solution of an adapted constant field equation (Lewis, 1979):

$$Vrev = \frac{RT}{F}\, ln\left(\frac{[Na^+]_o + \left([K^+]_o \frac{PK}{PNa}\right) + 4\ PCa'.[Ca^{2+}]_o}{[Na^+]_i + \left([K^+]_i \frac{PK}{PNa}\right) + 4\ PCa'.[Ca^{2+}]_i .e^{F.Vrev\,/\,RT}}\right) \qquad \text{Equation 30}$$

Where;

$$PCa' = \frac{PCa}{PNa}\left(\frac{1}{1+e^{F.Vrev/RT}}\right) \qquad \text{Equation 31}$$

Lewis (Lewis, 1979) showed that with 2mM extracellular Ca^{2+} and zero assumed surface charge, this equation satisfactorily describes the $Vrev$ of the K^+, Na^+ and Ca^{2+} permeant end-plate currents and variants of this are widely used in calculations of non-specific cation permeabilities including those of TRP (Kamouchi *et al.*, 1999; Vennekens *et al.*, 2000; Owsianik *et al.*, 2006). A further potentially important parameter is voltage dependent Mg^{2+} block of the TRP conductance. This is modelled as being equivalent to Mg^{2+} block of the TRP channel (Nilius *et al.*, 2000).

$$K_{D(Vm)} = K_{D(Vo)}exp\left(\frac{2\delta FVm}{RT}\right) \qquad \text{Equation 32}$$

Where;

$$G_{TRPV5} = \bar{G}_{TRPV5}\left(1 - \frac{[Mg^{2+}]}{[Mg^{2+}]+K_{D(Vm)}}\right) \qquad \text{Equation 33}$$

Parameter	Value	Source
a =	0.02	A
b =	28.2	A
c =	0.04	A
d =	0.01	A
G_{Kv}	1.67nS/cell	B
$BKEC_{50}$	3μM	C
$[Ca^{2+}]_i$	~0.2nM	D
$\bar{G}_{KATP}$	65nS/cell	E
Free-$[ATP]_i$	4.5mM	F

Parameter	Value	Source
Patch radius	1.5μm	G
Cell radius	7.5μm	H
G_{ENaC}	365pS/cell	I
G_{Cl}	1.65nS/cell	I
$\bar{G}_{TRPV5}$	8.15nS/cell	J
V_{TRPV5}	+32mV	K
P_K/P_{Na}	0.9	L
P_{Ca}/P_{Na}	80	L
$K_{D(Vm)}$	3.1mM	M

Table 6: Source of parameters used throughout the model. Source A) Fitted from the raw data shown in Mobasheri *et al* (2005a) as described in Chapter 6. B) From published maximum current densities of approximately 25pA/pF (Mobasheri *et al.*, 2005a). C) Estimated from Barrett *et al* (1982) at 10mV. D) Calculated as described in the text. E) From published maximum current densities of approximately 37pA/patch. F) Volume of chondrocytes; 1.77nL, total free ATP 8fmol/cell (Grishko *et al.*, 2010) G) Standard (estimated) value used for estimation of patch pipette tip opening (Sakmann & Neher, 1983). H) Measured by my group in May *et al* (2007). I) Where for each patch, $n.i.P_{open}$ are calculated as described in the text (see also Chapters 3 and 4 for Na^+ and Cl^- values, respectively). J) Value calculated in Chapter 3. L) Relative permeabilities are calculated as described in Chapter 3. M) Calculated previously (Nilius *et al.*, 2000). Note that whilst the absolute value of extracellular free $[Mg^{2+}]$ is difficult to estimate *in vivo, in vitro* studies suggest it is approximately 0.5mM (Gunther *et al.*, 1997).

7.2.3 Model predictions

Using the above model of the membrane potential (Equation 17) and including the above data a RMP of -8.1mV was computed, similar to the experimental RMP values. The TRPV4, V5 and ENaC channels identified in previous chapters all induced significant changes in membrane potential when inhibited (figure 7.2). Application of gadolinium moved the RMP of a whole-cell current clamped chondrocyte (in physiological saline) 30±4mV (n = 8) more negative (figure 7.2), suggesting that the gadolinium-sensitive TRP channels may be partly responsible for the positive RMP. Application of amiloride (10μM) moved the membrane potential 9.5±0.8mV (n = 5) more negative (figure 7.2), suggesting this conductance also contributed to the RMP. Block of these channels was simulated by the membrane potential model. Figure 7.2 shows a comparison of membrane potential changes computed by blocking gadolinium III and amiloride sensitive conductances in Equation 17 and the experimentally measured values upon gadolinium III, econazole and amiloride exposure.

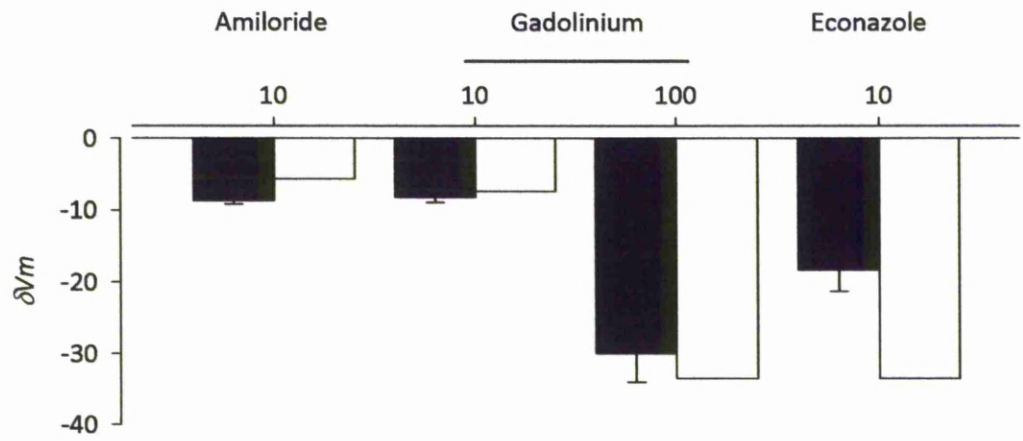

Figure 7.2 Comparison of predicted and experimentally measured changes in chondrocyte resting membrane potential. Simulated effect on membrane potential of blocking TRPV5 and ENaC channels in Equation 17 with 10 and 100μM gadolinium III, 100μM econazole or 10μM amiloride. Each of these conditions predicted a negative change in the membrane potential (empty bars). Membrane potentials were then measured by whole-cell current clamp in physiological solutions (described in Chapters 3 and 4; shown here by filled bars) Each of these conditions significantly shifted the membrane potential ($p<0.005$, $p<0.05$ and $p<0.00005$ respectively, ANOVA and Dunnett's multiple comparison).

7.3 Regulatory volume decrease

It seems likely that the unusual electrical properties of chondrocytes must confer a biological advantage to these cells. After measuring their RMP in a number of situations this chapter moved on to investigate this advantage and tested the hypothesis that it is the ability to withstand changes in osmotic potential. This follows because the rate and degree of cell swelling during osmotic shock is counteracted by the release of ions, particularly potassium, and concomitant reduction in osmotic drive for water entry, as discussed previously (Hoffmann & Dunham, 1995; Hoffmann *et al.*, 2009). One would expect that the predicted loss of potassium ions would be matched by an equal number of anions (chloride or HCO_3^-, for example), reducing the absolute loss of potassium ions (Nicholl *et al.*, 2002). Several different chondrocyte potassium channels have been proposed to open in response to membrane stretch and conduct these potassium ions (Hall *et al.*, 1996a; Martina *et al.*, 1997; Mobasheri *et al.*, 2010). From this, this chapter investigates the hypothesis that cell swelling would be much less at a positive RMP than it would be at substantially negative membrane potentials. This prediction follows from the fact that the driving force (*RMP-E_k*) for potassium ion efflux is much greater at more positive membrane potentials. The relationship is given by:

$$I_K = G_{kstretch}[RMP - E_k] \qquad \text{Equation 34}$$

where I_K is the potassium current, $G_{kstretch}$ the potassium conductance and E_k the equilibrium potential for potassium ions. This prediction was tested by experiment.

7.4 Role of the resting membrane potential

Chondrocytes were impaled with sharp electrodes and voltage-clamped under switch clamp mode (see Chapter 2 for details). Cells were held at +10mV and -80mV. Volume was calculated from 2D surface areas as the osmolarity of the bath (physiological solution, see Table 1) was decreased from 489mOsm to 309mOsm. One approach to this experimental design would be to decrease osmolarity from approximately 300mOsm to, for example 200mOsm, however, as discussed in Chapter 6, it is generally accepted that this is well outside the chondrocytes normal environmental range (Urban, 1994). Therefore, in order to make this experiment as physiologically relevant as possible, volume increases were measured when decreasing osmolarity from a relatively high (approx. 490mOsm), to a physiological minimum for cartilage (approx. 310mOsm (Urban, 1994)). This is the same approach as is used in Chapter 5 for the volume control experiments.

Chondrocytes clamped at +10mV and exposed to the reduced osmotic pressure increased in size by 29±3% at +10mV, (n = 10; figure 7.3a and b). This increase was reversible upon returning to the higher osmolarity solution (figure 7.3a and c). When this procedure was repeated with the membrane clamped to -80mV, cell volume increase was significantly greater. Cell volume increased by 57±4% (n = 12, $p<0.01$; figure 7.3a and b) and the chondrocytes were no longer able to recover their volume (figure 7.3a and c).

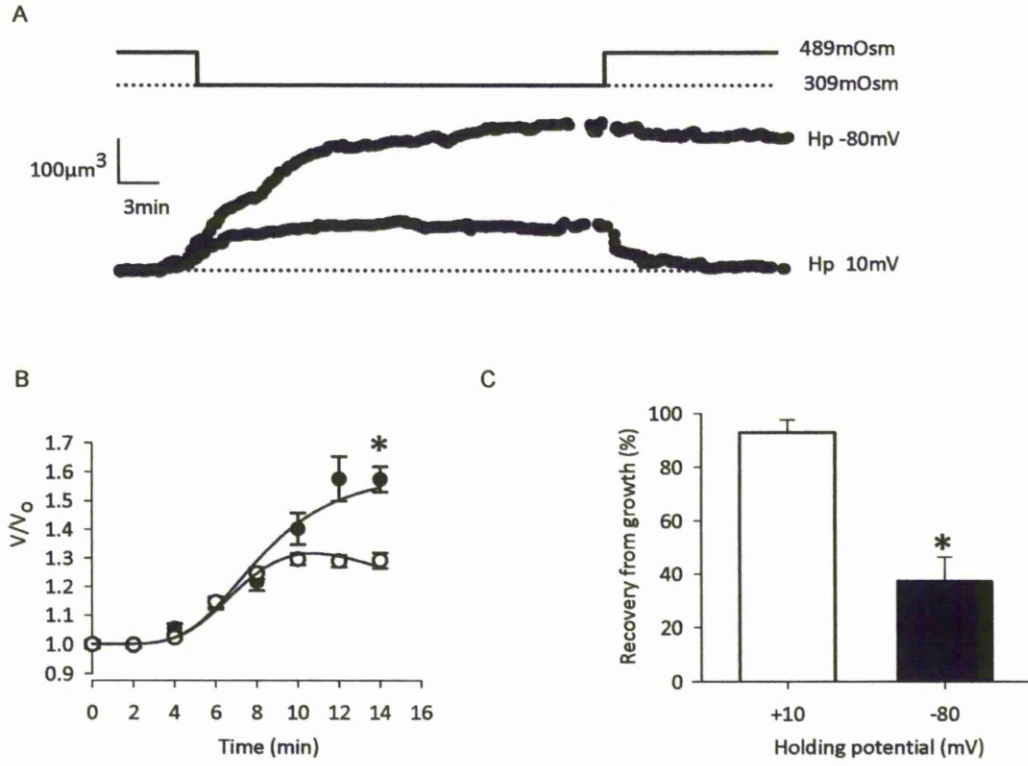

Figure 7.3 The positive resting membrane potential allows chondrocytes to more effectively regulate their volume. A) Change of cell volume with time during change of osmotic potential (where indicated). Cell volume was calculated at 30s intervals with cells voltage-clamped at either -80mV or +10mV with single sharp electrodes under switch clamp. B) Summary of a number of data such as that illustrated in A, but with data sampled at 120s intervals. Cell swelling measured at 14 minutes was significantly greater when cells were held at -80mV than +10mV ($p<0.0005$ $n = 7$ empty circles, 10 filled circles). The fitted line is one continuous fit to $\frac{dvol}{dt} = P_f . S_{(t)} . V_w (OsM_{in(t)} - OsM_{out(t)})$ as described in the text. The only difference between the two lines is the membrane potential. C) On returning cells from the 309mOsm to the 489mOsm solution the size of cells clamped at +10mV ($n = 10$) returned to near the pre-swell size whereas recovery at -80mV ($n = 12$) was significantly less ($p<0.0005$, $n = 10, 12$).

7.5 Model of dependence of resting membrane potential on osmotic swelling

To simulate the swelling of cells at different membrane potentials a variation of the equation from Zhang *et al* (Zhang *et al.*, 1990; Preston *et al.*, 1992) was used, with substitutions to allow for time variable osmolarities.

$$\frac{dvol}{dt} = P_f . SA_{(t)} . V_w (Osm_{in(t)} - Osm_{out}) \qquad \text{Equation 35}$$

Where; P_f is the water permeability of the cell (cms^{-1}), $SA_{(t)}$the surface area and the molar volume of water (V_w) is $18cm^3mol^{-1}$. The osmolarity inside the cell at time t ($Osm_{in(t)}$) is given by:

$$Osm_{in(t)} = \frac{Osmol_{in(t)}}{vol_{(t)}} \qquad \text{Equation 36}$$

Where $Osmol_{in}$ is the number of moles of intracellular solute. This changes as potassium ions efflux and so the rate of change in the moles of ions within the cell is equivalent to:

$$\frac{dOsmol_{in}}{dt} = \frac{G_{kstretch(t)}(RMP - E_{k(t)})}{e.N_A} \qquad \text{Equation 37}$$

Where e is the elementary charge and N_A is Avagadro's number. $G_{kstretch(t)}$ is the potassium conductance opened by stretch, this is likely to be composed of calcium-activated potassium channels as discussed in Chapter 6 (Wright *et al.*, 1992; Mobasheri *et al.*, 2010). A simple relationship for activation of this channel at time t is used. It is assumed that $G_{kstretch(t)}$ is simply proportional to percentage membrane *stretch* at time t.

$$G_{Kstretch(t)} = \bar{G}_{kstretch} \times \frac{stretch_{(t)}}{(\text{stretch}_{(t)} \times A)} \qquad \text{Equation 38}$$

Stretch was calculated simply as the fraction change in surface area. $G_{kstretch(t)}$ (the total stretch activated potassium conductance, 660pS) and A (a constant of proportionality, $10^{-4}s^{-1}$) were both obtained by fitting Equation 35 (by numerical integration) to the volume data by minimizing chi^2.

Additionally, for the cell to maintain electroneutrality the K^+ efflux is likely to be matched by an anionic efflux, although this is not modelled here.

This simulation also included a routine to account for the time dependent change of extracellular bath solution. This was relatively slow (approx 6 minutes) since sharp electrodes dislodge more readily than patch electrodes and cells were observed to be rather fragile when maintained at very hyperpolarised potentials. The only parameter changed between the simulations shown in figure 7.3 at -80mV and +10mV is the RMP parameter in Equation 37.

7.6 Changes in disease states

As chondrocytes of osteoarthritic cartilage are reported as being swollen (Stockwell, 1991), this study wanted to see whether the membrane potential of osteoarthritic chondrocytes differed to that of healthy chondrocytes. The volume control data suggested that cells with more negative membrane potentials were unable to successfully regulate their volume, therefore it would follow that cells from osteoarthritic cartilage may have more negative membrane potentials. The closer the membrane potential is to E_k (the potassium equilibrium potential) the less able the cell is to efflux potassium, meaning it becomes swollen as there is less of a drive for water to leave the cell. Osteoarthritic chondrocytes have been reported to have

up-regulated expression of BK channels. One might expect this could be due to the cell having to try to increase its ability to efflux potassium.

Membrane potentials from human healthy and osteoarthritic chondrocytes[4] were measured by current-clamp patch in the same physiological saline as the other RMPs. Healthy human chondrocytes were found to have a membrane potential of -14.3±2.7mV (n = 7), not significantly different to those of the other species described above (figure 7.4; $p>0.05$). Osteoarthritic chondrocytes had a significantly more negative membrane potential of -29±3.5mV (n = 6; $p<0.05$). The model predicts a change in membrane potential of -9mV in osteoarthritic chondrocytes compared to healthy and this appears to be the case. This change was predicted by increasing I_{BK} conductance in Equation 17.

[4] Human chondrocytes kindly provided by Dr S. Tew and Professor P. Clegg, Veterinary Sciences, University of Liverpool, Leahurst.

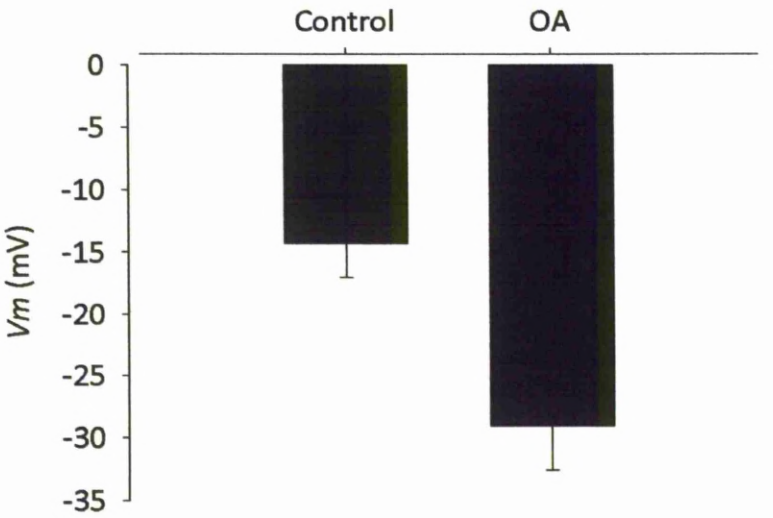

Figure 7.4 Resting membrane potential recordings from healthy and osteoarthritic human chondrocytes. "Control" chondrocytes were isolated from young, macroscopically intact cartilage and OA was osteoarthritic chondrocytes from a diagnosed patient. OA chondrocytes had significantly more negative membrane potentials than those from the healthy cartilage.

7.7 Discussion

This chapter found that positive RMPs significantly reduced the volume increase when cells were exposed to reduced osmotic pressure. At positive membrane potentials this increase in volume was very similar to that previously measured in unclamped chondrocytes in culture or *in situ* (Bush & Hall, 2001b).

The relatively positive RMPs reported here are similar to one of the earliest report of chondrocytes' RMP (Wright *et al.*, 1992) (sheep and human control chondrocytes; RMP: -10.6 and -12.4mV respectively). Since this time, a number of groups have observed more negative RMPs. These more negative RMPs include -46mV on mouse chondrocytes (Clark *et al.*, 2010) and -41mV on rabbit chondrocytes (Sugimoto *et al.*, 1996a). There are a number of possible explanations for this. The chondrocytes used throughout this thesis were prepared from larger animals using well-established protocols (Mobasheri *et al.*, 2005a; Mobasheri *et al.*, 2007b; Mobasheri *et al.*, 2010). It is entirely possible that these larger animals have more positive RMP, since their joints experience greater forces than those of rodents (Huberti & Hayes, 1984; Clarke *et al.*, 2001; Setterbo *et al.*, 2009). Direct experimental comparison is difficult, however, due to the problems inherent in isolating a pure chondrocyte preparation from rabbits and small rodents. The small cartilage depths in these smaller mammals will make isolating a pure chondrocyte population inherently more difficult (Stockwell, 1971; Frisbie *et al.*, 2006; Ahern *et al.*, 2009). In the joints of the larger animals used, cartilage depth was approximately 1mm or more (from larger dogs to horses) and so one can be confident of a pure chondrocyte preparation.

The model of chondrocyte membrane potential has been iteratively refined and tested using the data available from the single channel and whole-cell experiments presented throughout this thesis. This has resulted in a model which appears to accurately predict experimental changes in ionic conditions, pH and temperature. This model does have limitations; one such limitation is that it doesn't include ion pumps or co-transporters. These have been discovered in chondrocytes so the next step for the model could be trying to integrate the effects of these to determine changes in membrane potential upon their inhibition (Wilkins & Hall, 1992; Trujillo *et al.*, 1999a).

Several methods of measuring membrane potential were used in this Chapter. Whilst there was no significant difference between the values produced by any of the methods the oxonol dye method produced a relatively large standard error. The first reason for this could be because the dye is also a BK channel activator. It is difficult to find a fluorescent dye which does not affect ion channel function in some way. If BK channels are being activated by this dye, even by a small proportion, this could be enough to hyperpolarise the membrane potential of some of the cells, leading to greater variation in results. A second reason for this could be due to the inherent difficulty in using sharp electrodes on cells which exist with depolarised membrane potentials. One would usually confirm that a cell had been impaled by seeing a deflection in current once the cell had been struck by the electrode. Generally, cells such as neurons are measured by this method, which have significantly negative membrane potentials; therefore one knows that the cell is impaled simply by looking at the measured membrane potential. Chondrocytes do

not possess this negative membrane potential so it is difficult to determine that the cell has actually impaled.

The data described in this chapter shows for the first time a function for the chondrocytes depolarised membrane potential. The ability to regulate volume at positive membrane potentials was strikingly greater than at more negative potentials. Interestingly, these data also show that at very negative membrane potentials chondrocytes appeared unable to decrease their volume when exposed to the higher osmotic potential solution, i.e., cell shrinkage was slower, or non-existent. This could also be a consequence of the principle encapsulated by equation 24, or it could be that cells suffered damage from the osmotic challenge. The relationship between osmotic pressure and physical pressure is an important one for the chondrocyte, since it is believed that increasing compressive loads on joints leads to increases in osmotic pressure (Mow *et al.*, 1992; Urban, 1994). The ability of chondrocytes to withstand osmotic pressure changes is therefore coupled to their ability to withstand mechanical pressure. Indeed it has been shown that cells are more susceptible to physical damage at reduced osmolarities (Bush *et al.*, 2005). Furthermore, chondrocytes from osteoarthritic cartilage have been shown to exhibit poor recovery from cell volume increases (Jones *et al.*, 1999) and it has been suggested that inappropriate increases in chondrocyte volume may contribute to the progression of osteoarthritis (Bush & Hall, 2003). The membrane potential data recorded from human chondrocytes shows that osteoarthritic chondrocytes have more negative membrane potentials. This could potentially impact on their ability to regulate cell volume. As shown in this chapter and presented in Lewis *et al* (2011), the closer the membrane potential is to the potassium equilibrium potential

the less able the cell is to efflux potassium ions and decrease it's volume. This loss of volume regulation may be a contributory factor to the progression of arthritis. Maintaining a relatively positive membrane potential may therefore be important for the function and survival of healthy chondrocytes *in vivo.*

8

DISCUSSION

Investigations into the ion channels of chondrocytes were not started until the early 1990s. Potassium channels remained some of the most studied channels in chondrocytes until very recently. This thesis characterised other ion conductances within chondrocytes and uncovered possible functions for these channels. The development of a model of chondrocyte membrane function draws all this knowledge together and the predictions from this model enabled further analysis of, and insights into, the chondrocyte channelome.

Our group has been working on chondrocytes for a number of years now and has developed reliable cell isolation and culture methods. There have been several studies investigating the effect of culture on chondrocyte phenotype by examining the production of various matrix proteins (Martin *et al.*, 1999; Jakob *et al.*, 2001; Schulze-Tanzil *et al.*, 2004; Kang *et al.*, 2007). It has been shown that after four passages, chondrocytes fail to produce type II collagen and proteoglycans and start to undergo apoptosis (Schulze-Tanzil *et al.*, 2004; Kang *et al.*, 2007). For this reason experiments in this thesis were not performed on chondrocytes that had undergone more than four passages. The effect of passage on membrane potential was tested in Chapter 7 and it can be seen that there was no difference between the *Vm* measured from any of the passages. Chondrocyte *Vm* was also measured using sharp electrodes in cartilage slices and this produced remarkably similar results to the *Vm* data from isolated and cultured chondrocytes.

One will always question how similar cell types are across species. This thesis has examined chondrocytes from canine, bovine, ovine, equine and human cartilage and compared cell *Vm* across them, with no significantly different results (Lewis *et al.*, 2011). However, other studies have reported varying values for the chondrocyte *Vm* (see Chapters 1 and 7). There are two possible explanations for this. It is possible that the smaller animals (rat, mouse and rabbit) all have more negative *Vm*s than the larger mammals I have investigated. It is likely that the smaller mammals experience lesser forces on their joints compared to the larger mammals (Clarke *et al.*, 2001; Setterbo *et al.*, 2009). Therefore, the joints do not need to be able to cope with such huge fluxes in osmotic potential caused by joint loading so their *Vm* is not set as positively as the chondrocyte *Vm* of the heavier mammals. However, to determine whether this is the case one would ideally repeat the experiments presented in this thesis on chondrocytes isolated from these smaller mammals using my group's techniques. This brings us on to the second explanation for the difference in *Vm* between larger and smaller mammals. The methods used by my group to dissect cartilage from within the joint involve scraping the cartilage from the condyle in a manner similar to how one peels an apple. This method is easily applied to canine joints, and the other joints examined in this thesis, however, it remains to be seen whether it would be successful in producing a pure chondrocyte population from mice, for example. The depths of articular cartilage vary greatly between species although, generally, cartilage depth increases with increasing animal size. Small rodents and rabbits have cartilage depths of between 55 and 300μm (Stockwell, 1971; Frisbie *et al.*, 2006; Ahern *et al.*, 2009) whereas the larger mammals examined in this thesis all have cartilage depths greater than 1mm

(Stockwell, 1971). It is distinctly possible that when removing cartilage from smaller joints other cell types would be removed during the dissection. These would possibly include fibroblasts, osteoblasts, osteoclasts, stromal cells and even cells of blood vessel origin. These cells would inevitably have substantially more negative *Vm*s (Edelman *et al.*, 1986) and so would influence the mean *Vm* recorded from the "chondroycte" population. There may even be the possibility that the researchers would dismiss a *Vm* which was more positive than a certain threshold, as they may believe that the cell is "dead" if it has a *Vm* of around zero. This would also affect the mean *Vm*, effectively biasing the data to produce a negative value. This approach would be understandable if the researchers were looking at a neuron, for example, which typically exhibits a membrane potential of around -65mV. However, the *Vm* of a cell is set by its complement of ion channels whose activity within a cell membrane depends, in part, upon their reversal potential (V_{rev}), which is the point at which current flow through the membrane is in equilibrium. Neurons have substantially negative *Vm*s due to the activity of potassium channels, which have a V_{rev} of around -85mV, so assuming that a neuron that has a less negative *Vm* is "dead", or unable to propagate action potentials, could be accurate in that case. As shown in this thesis (Chapters 3 and 7 and also presented in Lewis *et al* (2011)) the chondrocyte *Vm* is maintained in part by the activity of TRPV5 channels. The cation selectivity of this channel contributes to the less negative *Vm* seen in chondrocytes.

Chapter 3 describes the detection of TRPV4 and TRPV5 cDNA in canine chondrocytes. This is the first identification of TRPV5 in chondrocytes, and the first reported identification of TRPV4 in canine chondrocytes. Our collaborators at the University of Nottingham have also detected the expression of TRPV6 by

immunohistochemistry (Ali Mobasheri, personal communication). PCR reactions shown in Chapter 3 did not detect the cDNA for this channel in canine chondrocytes. However, the expression of this channel in chondrocytes would go some way to explaining the differences in the effects of econazole and gadolinium on *Vm*. Gadolinium is a relatively non-selective inhibitor of most TRP channels, whereas econazole is selective for TRPV5. Gadolinium had a 12mV greater effect on *Vm* than econazole. This difference could be explained by gadolinium inhibiting TRPV5 and TRPV6, as they are both similarly calcium selective. The permeability experiments found that the gadolinium-sensitive current was heavily calcium selective (P_{Ca}/P_{Na} ~80). TRPV5 and TRPV6 have been reported to have higher permeability to calcium than this; however, the permeability measured in this thesis (Chapter 3) was obviously measured from cells containing a whole range of ion channels and in non-physiological solutions. The other reports of permeability come from expression systems containing just one type of channel (Nilius *et al.*, 2000; Vennekens *et al.*, 2000), where the permeability will be greater as there is only one method for calcium transport.

Distinguishing between members of the TRP family in electrophysiological experiments is difficult due to the lack of commercially available pharmacological agents. The only available agent for characterising TRPV4 is the agonist PDD. In Chapter 3 the effect of this on *Vm* was shown. In physiological solutions this substance caused an unexpected large hyperpolarisation of *Vm*. The chondrocyte *Vm* model predicted a depolarisation of the *Vm* when overall TRP conductance was increased, as it would be when PDD was added, due to the influx of cations that would occur. However, the model predicts that a 1000 fold increase in intra-cellular

calcium is necessary to see the hyperpolarisation measured in the PDD experiments. The *Vm* hyperpolarisation was remarkably absent when the same experiments were repeated with caesium, a non-permeant cation. This functional coupling of calcium-activated potassium channels and TRPV4 has been shown in other tissues and is suggested to be a response to hypotonicity induced cell swelling (Fernández-Fernández *et al.*, 2008). The activation of TRPV4 with PDD caused no increase in *Vm* when caesium was present, as may be expected upon activation of a cation channel. This, along with the membrane hyperpolarisation that happens upon both TRPV4 activation and membrane stretch, may suggest some sort of localisation of calcium-activated potassium channels and TRPV4. Calcium imaging and fluorescence experiments could be used to show possible local increases in intracellular Ca^{2+}.

As shown in Chapter 7, chondrocytes swell in response to decreased osmolarity, as they uptake water via aquaporins. This swelling is opposed by regulatory volume decrease (RVD), which was shown in Chapter 7 to be affected by the chondrocyte *Vm*. Cells clamped at very negative potentials were unable to regulate their volume, whereas those clamped at more positive potentials could effectively control the volume increase seen upon hypotonic challenge. The activity of TRPV5, and possibly TRPV6 channels, enables the chondrocyte to effectively regulate its volume due to the maintenance of *Vm* at a sufficient distance from the potassium equilibrium potential. This facilitates potassium efflux, allowing water to follow out of the cell and reducing cell volume. In Chapter 4 the epithelial sodium channel (ENaC) is also shown to have a small contribution to the depolarised *Vm*.

The ENaC data shown in Chapter 4 is the first electrophysiological data for this channel in chondrocytes. This is a very small channel and is difficult to detect using electrophysiology alone. The immunohistochemical identification of a number of ENaC subunits in cartilage prompted speculation about the channels possible function. Hypotheses included that ENaC was a stretch-sensitive channel involved in signalling pathways which regulate the ECM (Shakibaei & Mobasheri, 2003; Salter *et al.*, 2004). This thesis discovered that the ENaC is heavily involved in chondrocyte cell volume regulation, specifically regulatory volume increase (RVI; Chapter 4). Previous studies on chondrocytes have suggested a role for the sodium potassium chloride co-transporter (NKCC) in RVI (Kerrigan *et al.*, 2006; Bush *et al.*, 2010). These studies found that RVI could not be fully inhibited by significant concentrations of the NKCC inhibitor. The data presented in this thesis show that ENaC contributes to cell RVI. As mentioned previously, it can be difficult to obtain channel inhibitors which are specific to only one type of channel and it is recognised that benzamil can also inhibit the NKCC, although at higher concentrations than were used here (Kim *et al.*, 2001). However, the experiments with lithium, an ion which ENaC has a greater permeability for than sodium, showed that RVI still occurs even when no sodium is present, providing further evidence for ENaCs involvement in RVI. It is possible that both the NKCC and ENaC are responsible for the ionic influx that must occur for a cell to successfully increase its volume. ENaC may be the remaining conductance that was not inhibited in the previously mentioned studies on NKCC (Kerrigan *et al.*, 2006; Bush *et al.*, 2010). Indeed, early immunohistochemical studies showed co-localisation of ENaC with NKCC (Shakibaei & Mobasheri, 2003; Salter *et al.*, 2004) in chondrocytes. NKCC and ENaC may, therefore, have

complementary roles allowing for the influx of sodium following hypertonicity induced cell shrink.

The chloride channel data shown in Chapter 5 is the first example of a chloride conductance in canine chondrocytes. The data shown in Chapter 5 indicate that chondrocytes express a mixed population of chloride channels, not just the maxi-chloride/volume regulated channel that has previously been shown (Sugimoto *et al.*, 1996a; Tsuga *et al.*, 2002). The presence of a calcium-activated potassium channel that regulates volume by effluxing potassium brought about the hypothesis that there must be an anion channel matching the cation efflux to maintain electroneutrality across the membrane. As an influx of calcium was shown to occur upon hypotonic challenge it was hypothesised that this anion channel was the calcium-activated chloride channel (CaCC). However, inhibition of this channel appeared not to have an effect on cell volume regulation. It is possible that the maxi-chloride channel is involved in cell volume regulation. There is no selective inhibitor of this channel, however, so investigation of this hypothesis may prove difficult.

The chondrocyte model of membrane potential presented in Chapter 7 draws together all the data presented in the preceding chapters. The parameters within it are calculated from the data drawn from the numerous electrophysiological experiments. The model predicts the effect of changes in these parameters on *Vm*. These predictions are useful to compare to the experimental data to enable one to focus future studies. However, the model does have some limitations. The NKCC was discussed earlier in this chapter. Currently ion pumps and co-transporters are

not included within the model. This means it is not possible to determine the effect that these have on the *Vm*. More importantly, it is not possible to hypothesise about the pumps function using information from the model. Another limitation of the models presented in Chapter 7 is that they are not currently linked. It would seem sensible to combine these two models so that that the parameters for conductance of the stretch-activated channel, for example, were being provided by the osmolarity model for the *Vm* model. This would enable calculation of *Vm* at various degrees of membrane stretch. Hyperpolarisation of the membrane potential has been shown to occur upon hypotonic challenge (Mobasheri *et al.*, 2005a; Mobasheri *et al.*, 2007b; Mobasheri *et al.*, 2010); it would be interesting to see whether this is an effect which arises from the combined models.

8.1 Future studies

Considering the importance of *Vm* on cell volume regulation, numerous further studies could be instigated looking at various pharmacological modulators and their effect on channel activity. For example, the activity of PDD on OA chondrocytes may show that despite increasing the activation of TRPV4 channels, these cells are still unable to regulate their volume. This could possibly indicate a problem with BK function (Fernández-Fernández *et al.*, 2008).

One way to target these studies would be to continue testing the *Vm* model by determining the effect that differing degrees of channel activation or inhibition would have on *Vm*, and trying to find which increase or decreases in channel conductance produce the membrane potential hyperpolarisation seen in OA chondrocytes. The next goal for the models presented in Chapter 7 is to combine

them into one model, where the calculated *Vm* inputs into the cell volume model. One could then vary conditions directly in the *Vm* model and discover the effect this has on cell volume. A further advantage of continuing to develop and refine the model would mean that hypotheses could be tested within the model, creating less of a need for the use of cadavers for experiments. The cell volume model could also be adapted to mimic RVI conditions by changing the ion channel parameters it uses.

Further volume regulation experiments are necessary following the results in Chapter 5. These experiments showed that the calcium-activated chloride channel did not contribute to regulatory volume decrease. However, an anion efflux must exist to match the potassium efflux. Experiments using SITS would be useful in determining if chloride ions do provide this efflux, or if it is another ion, for example bicarbonate ions (Nicholl *et al.*, 2002). This effect of this anion could be examined by using bicarbonate solutions rather than HEPES buffered solutions as used here.

There are a number of other techniques, which were not utilised in this thesis that could be used to examine the chondrocyte channelome. For example, the siRNA knockout method is becoming increasingly utilised to examine the effect of channel knockdown on cell function (Gresch *et al.*, 2004). Unfortunately, there is no commercially available siRNA for the canine model, however there are versions available for human models. Comparing the knockout of channel proteins in both healthy and osteoarthritic chondrocytes could be an interesting step. Unfortunately, one drawback of using knockout techniques is that these techniques may indirectly alter other cell functions as the cell adapts in culture to the loss of certain proteins.

One emerging technique is the "NextGen" transcriptomics method (Roy *et al.*, 2011). This method is a relatively quick way of discovering all the proteins coded for within a cell. The results can then be sifted through to find proteins of interest, such as ion channel families, and the relative expressions of these can be examined. Performing this method on both healthy and osteoarthritic chondrocytes could uncover ion channels not yet discovered, the expression of which could then be investigated more fully using other techniques, for example electrophysiology or PCR. The transcriptomics method would also provide relative expression of the proteins between the two types of chondrocytes tested, enabling one to see which proteins were upregulated or downregulated in diseased compared to healthy tissue. These changes in channel expression could also be investigated using the methods presented in this thesis to determine their effects on membrane potential and control of cell volume.

8.2 Implications of this work

The data from individual channels combined with the RVI and RVD experiments presented in this thesis provide insights into healthy chondrocyte function. Understanding how healthy cells work is always important when comparing them to their diseased state. The progression of osteoarthritis (OA), a condition affecting over 60% of the adult population, is poorly understood (Goldring & Goldring, 2007). As described in Chapter 1, water volume changes within cartilage are believed to be contributory factors to cartilage degeneration with reports that chondrocytes from OA cartilage appear distended (Stockwell, 1991). It has been reported that loss of chondrocyte volume control leads to cell death and the progression of OA, but the

mechanisms behind this were not understood (Bush & Hall, 2003; Bush *et al.*, 2005). This thesis has presented novel work on the ion channels within chondrocytes and the influence these channels have on volume control. As shown here, the depolarised *Vm* of chondrocytes appears crucial for the maintenance of RVD when experiencing osmotic challenges. The model of chondrocyte volume also suggests that if the *Vm* is hyperpolarised then the cells will not be able to return their volume to its resting state, this will mean that the cells remain swollen. As described in Chapter 7, OA chondrocyte *Vm* was measured and found to be hyperpolarised compared to the healthy chondrocytes. This could suggest that OA chondrocytes have differences in expression of either TRPV4 or calcium-activated potassium channels. If pharmacological agents could be found which regulate the activity of these channels and thus influence cell volume control, these channels could be potential new targets for osteoarthritis treatments.

9

BIBLIOGRAPHY

Agre P, Preston GM, Smith BL, Jung JS, Raina S, Moon C, Guggino WB & Nielsen S. (1993). Aquaporin CHIP: the archetypal molecular water channel. *American Journal of Physiology - Renal Physiology* **265,** F463-F476.

Ahern BJ, Parvizi J, Boston R & Schaer TP. (2009). Preclinical animal models in single site cartilage defect testing: a systematic review. *Osteoarthr Cartilage* **17,** 705-713.

Alexander SPH, Mathie A & Peters JA. (2008). Guide to receptors and channels (GRAC), 3rd edition. *British Journal of Pharmacology* **153,** S1-S209.

Apell HJ & Bersch B. (1987). Oxonol VI as an optical indicator for membrane potentials in lipid vesicles. *Biochim Biophys Acta* **903,** 480-494.

Archer CW & Francis-West P. (2003). The chondrocyte. *Int J Biochem Cell Biol* **35,** 401-404.

Arniges M, Vazquez E, Fernandez-Fernandez JM & Valverde MA. (2004). Swelling-activated Ca2+ entry via TRPV4 channel is defective in cystic fibrosis airway epithelia. *J Biol Chem* **279,** 54062-54068.

Ashcroft FM & Gribble FM. (1998). Correlating structure and function in ATP-sensitive K+ channels. *Trends Neurosci* **21,** 288-294.

Babenko AP, Aguilar-Bryan L & Bryan J. (1998). A view of sur/KIR6.X, KATP channels. *Annu Rev Physiol* **60,** 667-687.

Barrett-Jolley R, Lewis R, Fallman R & Mobasheri A. (2010). The Emerging Chondrocyte Channelome. *Frontiers in Membrane Physiology and Biophysics* **1,** 10.

Barrett JN, Magleby KL & Pallotta BS. (1982). Properties of Single Calcium-Activated Potassium Channels in Cultured Rat Muscle. *J Physiol* **331,** 211-230.

Barry PH & Lynch JW. (1991). Liquid junction potentials and small cell effects in patch-clamp analysis. *J Membr Biol* **121,** 101-117.

Benya PD & Shaffer JD. (1982). Dedifferentiated chondrocytes reexpress the differentiated collagen phenotype when cultured in agarose gels. *Cell* **30,** 215-224.

Berridge MJ. (2005). Unlocking the secrets of cell signaling. *Annu Rev Physiol* **67,** 1-21.

Breittmayer JP, Pelassy C & Aussel C. (1996). Effect of membrane potential on phosphatidylserine synthesis and calcium movements in control and CD3-activated Jurkat T cells. *J Lipid Mediat Cell Signal* **13,** 151-161.

Brighton CT, Sugioka Y & Hunt RM. (1973). Cytoplasmic structures of epiphyseal plate chondrocytes. Quantitative evaluation using electron micrographs of rat costochondral junctions with special reference to the fate of hypertrophic cells. *J Bone Joint Surg Am* **55,** 771-784.

Broom ND & Marra DL. (1985). New structural concepts of articular cartilage demonstrated with a physical model. *Connect Tissue Res* **14,** 1-8.

Browning JA, Walker RE, Hall AC & Wilkins RJ. (1999). Modulation of Na+ x H+ exchange by hydrostatic pressure in isolated bovine articular chondrocytes. *Acta Physiol Scand* **166,** 39-45.

Bruckner P & Van der Rest M. (1994). Structure and function of cartilage collagens. *Microsc Res Tech* **28,** 378-384.

Buckwalter JA & Mankin HJ. (1998). Articular cartilage: tissue design and chondrocyte-matrix interactions. *Instr Course Lect* **47,** 477-486.

Bush PG & Hall AC. (2001a). The osmotic sensitivity of isolated and in situ bovine articular chondrocytes. *J Orthop Res* **19,** 768-778.

Bush PG & Hall AC. (2001b). Regulatory volume decrease (RVD) by isolated and in situ bovine articular chondrocytes. *J Cell Physiol* **187,** 304-314.

Bush PG & Hall AC. (2003). The volume and morphology of chondrocytes within non-degenerate and degenerate human articular cartilage. *Osteoarthr Cartilage* **11,** 242-251.

Bush PG & Hall AC. (2005). Passive osmotic properties of in situ human articular chondrocytes within non-degenerate and degenerate cartilage. *J Cell Physiol* **204,** 309-319.

Bush PG, Hodkinson PD, Hamilton GL & Hall AC. (2005). Viability and volume of in situ bovine articular chondrocytes--changes following a single impact and effects of medium osmolarity. *Osteoarthr Cartilage* **13,** 54-65.

Bush PG, Pritchard M, Loqman MY, Damron TA & Hall AC. (2010). A key role for membrane transporter NKCC1 in mediating chondrocyte volume increase in the mammalian growth plate. *Journal of Bone and Mineral Research* **25,** 1594-1603.

Canessa CM, Schild L, Buell G, Thorens B, Gautschi I, Horisberger JD & Rossier BC. (1994). Amiloride-Sensitive Epithelial Na+ Channel Is Made of 3 Homologous Subunits. *Nature* **367,** 463-467.

Carbrey JM, Gorelick-Feldman DA, Kozono D, Praetorius J, Nielsen S & Agre P. (2003). Aquaglyceroporin AQP9: Solute permeation and metabolic control of expression in liver. *Proceedings of the National Academy of Sciences of the United States of America* **100,** 2945-2950.

Carlton SM, Zhou S, Du J, Hargett GL, Ji G & Coggeshall RE. (2004). Somatostatin modulates the transient receptor potential vanilloid 1 (TRPV1) ion channel. *Pain* **110,** 616-627.

Catterall AW. (1995). Structure and Function of Voltage-Gated Ion Channels. *Annual Review of Biochemistry* **64,** 493-531.

Catterall WA. (1991). Functional subunit structure of voltage-gated calcium channels. *Science (New York, NY)* **253,** 1499-1500.

Chenna R, Sugawara H, Koike T, Lopez R, Gibson TJ, Higgins DG & Thompson JD. (2003). Multiple sequence alignment with the Clustal series of programs. *Nucleic Acids Research* **31,** 3497-3500.

Clapham DE, Runnels LW & Strubing C. (2001). The trp ion channel family. *Nat Rev Neurosci* **2,** 387-396.

Clark RB, Hatano N, Kondo C, Belke DD, Brown BS, Kumar S, Votta BJ & Giles WR. (2010). Voltage-gated K+ currents in mouse articular chondrocytes regulate membrane potential. *Channels* **4,** 179-191.

Clarke KA, Smart L & Still J. (2001). Ground reaction force and spatiotemporal measurements of the gait of the mouse. *Behavior Research Methods Instruments & Computers* **33,** 422-426.

Cox T. (1997). Amiloride analog stimulation of short-circuit current in larval frog skin epithelium. *Journal of Experimental Biology* **200,** 3055-3065.

Creamer P & Hochberg MC. (1997). Osteoarthritis. *Lancet* **350,** 503-508.

Cui J, Yang H & Lee US. (2009). Molecular mechanisms of BK channel activation. *Cellular and Molecular Life Sciences* **66,** 852-875.

Dart C & Standen NB. (1994). Hypoxia Induces a Potassium Current in Smooth-Muscle Cells Isolated from the Porcine Coronary-Artery. *J Physiol* **477P,** P85-P86.

DeCoursey TE. (1991). Hydrogen ion currents in rat alveolar epithelial cells. *Biophys J* **60,** 1243-1253.

Denker BM, Smith BL, Kuhajda FP & Agre P. (1988). Identification, purification, and partial characterization of a novel Mr 28,000 integral membrane protein from erythrocytes and renal tubules. *J Biol Chem* **263,** 15634-15642.

Eaton DC, Becchetti A, Ma HP & Ling BN. (1995). Renal Sodium-Channels - Regulation and Single-Channel Properties. *Kidney International* **48,** 941-949.

Eckstein F, Tieschky M, Faber S, Englmeier KH & Reiser M. (1999). Functional analysis of articular cartilage deformation, recovery, and fluid flow following dynamic exercise in vivo. *Anat Embryol (Berl)* **200,** 419-424.

Edelman A, Fritsch J & Balsan S. (1986). Short-term effects of PTH on cultured rat osteoblasts: changes in membrane potential. *American Journal of Physiology - Cell Physiology* **251,** C483-C490.

Erickson GR, Alexopoulos LG & Guilak F. (2001). Hyper-osmotic stress induces volume change and calcium transients in chondrocytes by transmembrane, phospholipid, and G-protein pathways. *Journal of biomechanics* **34,** 1527-1535.

Estévez R, Pusch M, Ferrer-Costa C, Orozco M & Jentsch TJ. (2004). Functional and structural conservation of CBS domains from CLC chloride channels. *The Journal of Physiology* **557,** 363-378.

Fassbender HG. (1987). Role of chondrocytes in the development of osteoarthritis. *Am J Med* **83,** 17-24.

Fernández-Fernández J, Andrade Y, Arniges M, Fernandes J, Plata C, Rubio-Moscardo F, Vázquez E & Valverde M. (2008). Functional coupling of TRPV4 cationic

channel and large conductance, calcium-dependent potassium channel in human bronchial epithelial cell lines. *Pflügers Archiv European Journal of Physiology* **457,** 149-159.

Fernandez MP, Selmin O, Martin GR, Yamada Y, Pfaffle M, Deutzmann R, Mollenhauer J & von der Mark K. (1990). The structure of anchorin CII, a collagen binding protein isolated from chondrocyte membrane. *J Biol Chem* **265,** 8344.

Frisbie DD, Cross MW & McIlwraith CW. (2006). A comparative study of articular cartilage thickness in the stifle of animal species used in human pre-clinical studies compared to articular cartilage thickness in the human knee. *Veterinary and Comparative Orthopaedics and Traumatology* **19,** 142-146.

Funabashi K, Ohya S, Yamamura H, Hatano N, Muraki K, Giles W & Imaizumi Y. (2010). Accelerated Ca2+ entry by membrane hyperpolarization due to Ca2+-activated K+ channel activation in response to histamine in chondrocytes. *Am J Physiol* **298,** C786-C797.

Garty H & Palmer LG. (1997). Epithelial sodium channels: Function, structure, and regulation. *Physiological Reviews* **77,** 359-396.

Gavenis K, Schumacher C, Schneider U, Eisfeld J, Mollenhauer J & Schmidt-Rohlfing B. (2009). Expression of ion channels of the TRP family in articular chondrocytes from osteoarthritic patients: changes between native and in vitro propagated chondrocytes. *Mol Cell Biochem* **321,** 135-143.

Gibson JS, Milner PI, White R, Fairfax TP & Wilkins RJ. (2008). Oxygen and reactive oxygen species in articular cartilage: modulators of ionic homeostasis. *Pflugers Arch* **455,** 563-573.

Gögelein H, Dahlem D, Englert HC & Lang HJ. (1990). Flufenamic acid, mefenamic acid and niflumic acid inhibit single nonselective cation channels in the rat exocrine pancreas. *Febs Letters* **268,** 79-82.

Goldman DE. (1943). Potential, Impedance, and Rectification in Membranes. *J Gen Physiol* **27,** 37-60.

Goldring MB & Goldring SR. (2007). Osteoarthritis. *J Cell Physiol* **213,** 626-634.

Grandolfo M, Calabrese A & D'Andrea P. (1998). Mechanism of mechanically induced intercellular calcium waves in rabbit articular chondrocytes and in HIG-82 synovial cells. *Journal of Bone and Mineral Research* **13,** 443-453.

Grandolfo M, Dandrea P, Martina M, Ruzzier F & Vittur F. (1992). Calcium-Activated Potassium Channels in Chondrocytes. *Biochem Biophys Res Commun* **182,** 1429-1434.

Grandolfo M, Martina M, Ruzzier F & Vittur F. (1990). A potassium channel in cultured chondrocytes. *CalcifTissue Int* **47,** 302-307.

Gresch O, Engel FB, Nesic D, Tran TT, England HM, Hickman ES, Körner I, Gan L, Chen S, Castro-Obregon S, Hammermann R, Wolf J, Müller-Hartmann H, Nix M, Siebenkotten G, Kraus G & Lun K. (2004). New non-viral method for gene transfer into primary cells. *Methods* **33,** 151-163.

Grishko V, Xu M, Wilson G & Pearsall AW, IV. (2010). Apoptosis and Mitochondrial Dysfunction in Human Chondrocytes Following Exposure to Lidocaine, Bupivacaine, and Ropivacaine. *J Bone Joint Surg Am* **92,** 609-618.

Grissmer S, Nguyen AN, Aiyar J, Hanson DC, Mather RJ, Gutman GA, Karmilowicz MJ, Auperin DD & Chandy KG. (1994). Pharmacological characterization of five cloned voltage-gated K+ channels, types Kv1.1, 1.2, 1.3, 1.5, and 3.1, stably expressed in mammalian cell lines. *MolPharmacol* **45,** 1227-1234.

Gronemeier M, Condie A, Prosser J, Steinmeyer K, Jentsch TJ & Jockusch H. (1994). Nonsense and missense mutations in the muscular chloride channel gene Clc-1 of myotonic mice. *J Biol Chem* **269,** 5963-5967.

Guilak F. (1994). Volume and Surface-Area Measurement of Viable Chondrocytes in-Situ Using Geometric Modeling of Serial Confocal Sections. *Journal of Microscopy-Oxford* **173,** 245-256.

Guilak F, Jones WR, Ting-Beall HP & Lee GM. (1999a). The deformation behavior and mechanical properties of chondrocytes in articular cartilage. *Osteoarthr Cartilage* **7,** 59-70.

Guilak F, Ratcliffe A & Mow VC. (1995). Chondrocyte deformation and local tissue strain in articular cartilage: a confocal microscopy study. *J Orthop Res* **13,** 410-421.

Guilak F, Zell RA, Erickson GR, Grande DA, Rubin CT, McLeod KJ & Donahue HJ. (1999b). Mechanically induced calcium waves in articular chondrocytes are inhibited by gadolinium and amiloride. *J Orthop Res* **17,** 421-429.

Gunther T, Rucker M, Forster C, Vormann J & Stahlmann R. (1997). In vitro evidence for a Donnan distribution of Mg2+ and Ca2+ by chondroitin sulphate in cartilage. *Archives of Toxicology* **71,** 471-475.

Hall AC, Starks I, Shoults CL & Rashidbigi S. (1996a). Pathways for K+ transport across the bovine articular chondrocyte membrane and their sensitivity to cell volume. *Am J Physiol* **270,** C1300-1310.

Hall AC, Starks I, Shoults CL & Rashidbigi S. (1996b). Pathways for K+ transport across the bovine articular chondrocyte membrane and their sensitivity to cell volume. *Am J Physiol* **270,** C1300-C1310.

Hodge WA, Fijan RS, Carlson KL, Burgess RG, Harris WH & Mann RW. (1986). Contact pressures in the human hip joint measured in vivo. *Proc Natl Acad Sci U S A* **83,** 2879-2883.

Hodgkin AL & Huxley AF. (1952a). The dual effect of membrane potential on sodium conductance in the giant axon of Loligo. *J Physiol* **116,** 497-506.

Hodgkin AL & Huxley AF. (1952b). A Quantitative Description of Membrane Current and Its Application to Conduction and Excitation in Nerve. *J Physiol* **117,** 500-544.

Hodgkin AL, Huxley AF & Katz B. (1949). Ionic Currents Underlying Activity in the Giant Axon of the Squid. *Archives Des Sciences Physiologiques* **3,** 129-150.

Hodgkin AL & Katz B. (1949a). The effect of sodium ions on the electrical activity of giant axon of the squid. *J Physiol* **108,** 37-77.

Hodgkin AL & Katz B. (1949b). The Effect of Sodium Ions on the Electrical Activity of the Giant Axon of the Squid. *J Physiol* **108,** 37-77.

Hoffmann E & Dunham P. (1995). Membrane mechanisms and intracellular signalling in cell volume regulation. *International review of cytology* **161,** 173-262.

Hoffmann EK, Lambert IH & Pedersen SF. (2009). Physiology of Cell Volume Regulation in Vertebrates. *Physiological Reviews* **89,** 193-277.

Huberti HH & Hayes WC. (1984). Patellofemoral contact pressures. The influence of q-angle and tendofemoral contact. *J Bone Joint Surg Am* **66,** 715-724.

Iannotti JP & Brighton CT. (1989). Cytosolic ionized calcium concentration in isolated chondrocytes from each zone of the growth plate. *Journal of Orthopaedic Research* **7,** 511-518.

Jakob M, Demarteau O, Schafer D, Hintermann B, Dick W, Heberer M & Martin I. (2001). Specific growth factors during the expansion and redifferentiation of adult human articular chondrocytes enhance chondrogenesis and cartilaginous tissue formation in vitro. *J Cell Biochem* **81,** 368-377.

Jones WR, Ting-Beall HP, Lee GM, Kelley SS, Hochmuth RM & Guilak F. (1999). Alterations in the Young's modulus and volumetric properties of chondrocytes isolated from normal and osteoarthritic human cartilage. *J Biomech* **32,** 119-127.

Kamouchi M, Mamin A, Droogmans G & Nilius B. (1999). Nonselective cation channels in endothelial cells derived from human umbilical vein. *J Mem Biol* **169,** 29-38.

Kang SW, Yoo SP & Kim BS. (2007). Effect of chondrocyte passage number on histological aspects of tissue-engineered cartilage. *Biomed Mater Eng* **17,** 269-276.

Katz B. (1949). *Les Constantes Electriques De La Membrane Du Muscle. *Archives Des Sciences Physiologiques* **3,** 285-300.

Kellenberger S & Schild L. (2002). Epithelial Sodium Channel/Degenerin Family of Ion Channels: A Variety of Functions for a Shared Structure. *Physiological Reviews* **82,** 735-767.

Kerr JF, Wyllie AH & Currie AR. (1972). Apoptosis: a basic biological phenomenon with wide-ranging implications in tissue kinetics. *Br J Cancer* **26,** 239-257.

Kerrigan MJP & Hall AC. (2008). Control of chondrocyte regulatory volume decrease (RVD) by [Ca2+](i) and cell shape. *Osteoarthr Cartilage* **16,** 312-322.

Kerrigan MJP, Hook CSV, Qusous A & Hall AC. (2006). Regulatory volume increase (RVI) by in situ and isolated bovine articular chondrocytes. *J Cell Physiol* **209,** 481-492.

Kim HA & Blanco FJ. (2007). Cell death and apoptosis in osteoarthritic cartilage. *Curr Drug Targets* **8,** 333-345.

Kim J-A, Kang YS & Lee YS. (2001). Activation of Na+, K+, Cl--Cotransport Mediates Intracellular Ca2+ Increase and Apoptosis Induced by Pinacidil in HepG2 Human Hepatoblastoma Cells. *Biochem Biophys Res Commun* **281,** 511-519.

Knight MM, Ghori SA, Lee DA & Bader DL. (1998). Measurement of the deformation of isolated chondrocytes in agarose subjected to cyclic compression. *Med Eng Phys* **20,** 684-688.

Knight MM, McGlashan SR, Garcia M, Jensen CG & Poole CA. (2009). Articular chondrocytes express connexin 43 hemichannels and P2 receptors - a putative mechanoreceptor complex involving the primary cilium? *J Anat* **214,** 275-283.

Kolker SJ, Walder RY, Usachev Y, Hillman J, Boyle DL, Firestein GS & Sluka KA. (2010). Acid-sensing ion channel 3 expressed in type B synoviocytes and chondrocytes modulates hyaluronan expression and release. *Ann Rheum Dis* **69,** 903-909.

Kunert-Keil C, Bisping F, Kruger J & Brinkmeier H. (2006). Tissue-specific expression of TRP channel genes in the mouse and its variation in three different mouse strains. *Bmc Genomics* **7,** 159.

Latorre R, Oberhauser A, Labarca P & Alvarez O. (1989). Varieties of Calcium-Activated Potassium Channels. *Annual Review of Physiology* **51,** 385-399.

Ledoux J, Werner ME, Brayden JE & Nelson MT. (2006). Calcium-Activated Potassium Channels and the Regulation of Vascular Tone. *Physiology* **21,** 69-78.

Lee HS, Millward-Sadler SJ, Wright MO, Nuki G & Salter DM. (2000). Integrin and mechanosensitive ion channel-dependent tyrosine phosphorylation of focal adhesion proteins and beta-catenin in human articular chondrocytes after mechanical stimulation. *Journal of Bone and Mineral Research* **15,** 1501-1509.

Lee RB & Urban JP. (1997). Evidence for a negative Pasteur effect in articular cartilage. *Biochem J* **321 (Pt 1),** 95-102.

Lewis CA. (1979). Ion-concentration dependence of the reversal potential and the single channel conductance of ion channels at the frog neuromuscular junction. *J Physiol* **286,** 417-445.

Lewis R, Asplin K, Bruce G, Dart C, Mobasheri A & Barrett-Jolley R. (2011). The role of the membrane potential in chondrocyte volume regulation. *J Cell Physiol.*

Lewis R, Purves G, Crossley J & Barrett-Jolley R. (2010). Modelling the Membrane Potential Dependence on Non-Specific Cation Channels in Canine Articular Chondrocytes. *Biophys J* **98.**

Li S, Wang X, Ye H, Gao W, Pu X & Yang Z. (2010). Distribution profiles of transient receptor potential melastatin- and vanilloid-related channels in rat spermatogenic cells and sperm. *Mol Biol Rep* **37,** 1287-1293.

Liang H, Yang L, Ma T & Zhao Y. (2010). Functional expression of cystic fibrosis transmembrane conductance regulator in mouse chondrocytes. *Clin Exp Pharmacol Physiol* **37,** 506-508.

Liang HT, Feng XC & Ma TH. (2008). Water channel activity of plasma membrane affects chondrocyte migration and adhesion. *Clin Exp Pharmacol Physiol* **35,** 7-10.

Liedtke W, Choe Y, Marti-Renom MA, Bell AM, Denis CS, Sali A, Hudspeth AJ, Friedman JM & Heller S. (2000). Vanilloid receptor-related osmotically activated channel (VR-OAC), a candidate vertebrate osmoreceptor. *Cell* **103,** 525-535.

Lindemann B. (2001). Receptors and transduction in taste. *Nature* **413,** 219-225.

Ling G & Gerard RW. (1949). The normal membrane potential of frog sartorius fibers. *J Cell Physiol* **34,** 383-396.

Long KJ & Walsh KB. (1994). A calcium-activated potassium channel in growth plate chondrocytes: regulation by protein kinase A. *Biochem Biophys Res Commun* **201,** 776-781.

Lytle C. (1997). Activation of the Avian Erythrocyte Na-K-Cl Cotransport Protein by Cell Shrinkage, cAMP, Fluoride, and Calyculin-A Involves Phosphorylation at Common Sites. *J Biol Chem* **272,** 15069-15077.

Mall M, Bleich M, Greger R, Schreiber R & Kunzelmann K. (1998). The amiloride-inhibitable Na+ conductance is reduced by the cystic fibrosis transmembrane conductance regulator in normal but not in cystic fibrosis airways. *Journal of Clinical Investigation* **102,** 15-21.

Mancilla EE, Galindo M, Fertilio B, Herrera M, Salas K, Gatica H & Goecke A. (2007). L-type calcium channels in growth plate chondrocytes participate in endochondral ossification. *Journal of Cellular Biochemistry* **101,** 389-398.

Mankin HJ. (1982). The response of articular cartilage to mechanical injury. *J Bone Joint Surg Am* **64,** 460-466.

Mano I & Driscoll M. (1999). DEG/ENaC channels: a touchy superfamily that watches its salt. *Bioessays* **21,** 568-578.

Maroudas A & Evans H. (1972). A study of ionic equilibria in cartilage. *Connective Tissue Research* **1,** 69-77.

Martel-Pelletier J, Boileau C, Pelletier JP & Roughley PJ. (2008). Cartilage in normal and osteoarthritis conditions. *Best Pract Res Clin Rheumatol* **22,** 351-384.

Martin I, Vunjak-Novakovic G, Yang J, Langer R & Freed LE. (1999). Mammalian chondrocytes expanded in the presence of fibroblast growth factor 2 maintain the ability to differentiate and regenerate three-dimensional cartilaginous tissue. *Exp Cell Res* **253,** 681-688.

Martin JA & Buckwalter JA. (2000). The role of chondrocyte-matrix interactions in maintaining and repairing articular cartilage. *Biorheology* **37,** 129-140.

Martina M, Mozrzymas JW & Vittur F. (1997). Membrane stretch activates a potassium channel in pig articular chondrocytes. *BBA-Biomembranes* **1329,** 205-210.

May H, Mobasheri A, Womack MD & Barrett-Jolley R. (2007). Functional expression of aquaporins in canine chondrocytes. *Biophys J* **92,** s543.

McCarty MF. (1999). Endothelial membrane potential regulates production of both nitric oxide and superoxide--a fundamental determinant of vascular health. *Med Hypotheses* **53,** 277-289.

McCutchen CW. (1962). The frictional properties of animal joints. *Wear* **5,** 1-17.

Minami K, Miki T, Kadowaki T & Seino S. (2004). Roles of ATP-sensitive K+ channels as metabolic sensors: studies of Kir6.x null mice. *Diabetes* **53 Suppl 3,** S176-180.

Mizoguchi F, Mizuno A, Hayata T, Nakashima K, Heller S, Ushida T, Sokabe M, Miyasaka N, Suzuki M, Ezura Y & Noda M. (2008). Transient receptor potential vanilloid 4 deficiency suppresses unloading-induced bone loss. *J Cell Physiol* **216,** 47-53.

Mobasheri A. (2002). Role of chondrocyte death and hypocellularity in ageing human articular cartilage and the pathogenesis of osteoarthritis. *Med Hypotheses* **58,** 193-197.

Mobasheri A, Carter SD, Martin-Vasallo P & Shakibaei M. (2002). Integrins and stretch activated ion channels; putative components of functional cell surface mechanoreceptors in articular chondrocytes. *Cell Biol Int* **26,** 1-18.

Mobasheri A, Dart C & Barrett-Jolley R. (2007a). Potassium Ion Channels in Articular Chondrocytes. *Mechanosensitive Ion Channels*, 157.

Mobasheri A, Gent TC, Nash AI, Womack MD, Moskaluk CA & Barrett-Jolley R. (2007b). Evidence for functional ATP-sensitive (K(ATP)) potassium channels in human and equine articular chondrocytes. *Osteoarthr Cartilage* **15,** 1-8.

Mobasheri A, Gent TC, Womack MD, Carter SD, Clegg PD & Barrett-Jolley R. (2005a). Quantitative analysis of voltage-gated potassium currents from primary equine (Equus caballus) and elephant (Loxodonta africana) articular chondrocytes. *Am J Physiol* **289,** R172-R180.

Mobasheri A, Lewis R, Maxwell JEJ, Hill C, Womack M & Barrett-Jolley R. (2010). Characterization of a Stretch-Activated Potassium Channel in Chondrocytes. *J Cell Physiol* **223,** 511-518.

Mobasheri A & Marples D. (2004). Expression of the AQP-1 water channel in normal human tissues: a semiquantitative study using tissue microarray technology. *Am J Physiol Cell Physiol* **286,** C529-537.

Mobasheri A, Mobasheri R, Francis MJ, Trujillo E, Alvarez de la Rosa D & Martin-Vasallo P. (1998). Ion transport in chondrocytes: membrane transporters involved in intracellular ion homeostasis and the regulation of cell volume, free [Ca2+] and pH. *Histol Histopathol* **13,** 893-910.

Mobasheri A, Richardson S, Mobasheri R, Shakibaei M & Hoyland JA. (2005b). Hypoxia inducible factor-1 and facilitative glucose transporters GLUT1 and GLUT3: putative molecular components of the oxygen and glucose sensing apparatus in articular chondrocytes. *Histol Histopathol* **20,** 1327-1338.

Mobasheri A, Shakibaei M & Marples D. (2004a). Immunohistochemical localization of aquaporin 10 in the apical membranes of the human ileum: a potential pathway for luminal water and small solute absorption. *Histochem Cell Biol* **121,** 463-471.

Mobasheri A, Trujillo E, Bell S, Carter SD, Clegg PD, Martin-Vasallo P & Marples D. (2004b). Aquaporin water channels AQP1 and AQP3, are expressed in equine articular chondrocytes. *Vet J* **168,** 143-150.

Morihata H, Nakamura F, Tsutada T & Kuno M. (2000). Potentiation of a Voltage-Gated Proton Current in Acidosis-Induced Swelling of Rat Microglia. *The Journal of Neuroscience* **20,** 7220-7227.

Morris CE & Homann U. (2001). Cell surface area regulation and membrane tension. *J Mem Biol* **179,** 79-102.

Mouw JK, Imler SM & Levenston ME. (2007). Ion-channel regulation of chondrocyte matrix synthesis in 3D culture under static and dynamic compression. *Biomechanics and Modeling in Mechanobiology* **6,** 33-41.

Mow VC, Ratcliffe A & Robin Poole A. (1992). Cartilage and diarthrodial joints as paradigms for hierarchical materials and structures. *Biomaterials* **13,** 67-97.

Mow VC, Wang CC & Hung CT. (1999). The extracellular matrix, interstitial fluid and ions as a mechanical signal transducer in articular cartilage. *Osteoarthr Cartilage* **7,** 41-58.

Mozrzymas JW, Martina M & Ruzzier F. (1997). A large-conductance voltage-dependent potassium channel in cultured pig articular chondrocytes. *Pflugers Archiv-European Journal of Physiology* **433,** 413-427.

Muramatsu S, Wakabayashi M, Ohno T, Amano K, Ooishi R, Sugahara T, Shiojiri S, Tashiro K, Suzuki Y, Nishimura R, Kuhara S, Sugano S, Yoneda T & Matsuda A. (2007). Functional gene screening system identified TRPV4 as a regulator of chondrogenic differentiation. *J Biol Chem* **282,** 32158-32167.

Nicholl, Killey, Leonard & Garner. (2002). The role of bicarbonate in regulatory volume decrease (RVD) in the epithelial-derived human breast cancer cell line ZR-75-1. *Pflügers Archiv European Journal of Physiology* **443,** 875-881.

Nilius B. (1998). *Ion Channels in nonexcitable cells. In; Cell Physiology Source Book, 2nd Edition, pp 436-455*. Academic Press, New York.

Nilius B & Droogmans G. (2003). Amazing chloride channels: an overview, pp. 119-147. Blackwell Science Ltd.

Nilius B, Prenen J, Vennekens R, Hoenderop JG, Bindels RJ & Droogmans G. (2001). Pharmacological modulation of monovalent cation currents through the epithelial Ca2+ channel ECaC1. *Br J Pharmacol* **134,** 453-462.

Nilius B, Vennekens R, Prenen J, Hoenderop JGJ, Bindels RJM & Droogmans G. (2000). Whole-cell and single channel monovalent cation currents through the novel rabbit epithelial Ca2+ channel ECaC. *J Physiol* **527,** 239-248.

Nilius B, Viana F & Droogmans G. (1997). Ion channels in vascular endothelium. *Annu Rev Physiol* **59,** 145-170.

Nilius B, Vriens J, Prenen J, Droogmans G & Voets T. (2004). TRPV4 calcium entry channel: a paradigm for gating diversity. *Am J Physiol* **286,** C195-C205.

Otte P. (1991). Basic cell metabolism of articular cartilage. Manometric studies. *Z Rheumatol* **50,** 304-312.

Owsianik G, Talavera K, Voets T & Nilius B. (2006). Permeation and selectivity of TRP channels. *Annual Review of Physiology* **68,** 685-717.

Patapoutian A, Tate S & Woolf CJ. (2009). Transient receptor potential channels: targeting pain at the source. *Nat Rev Drug Discov* **8,** 55-68.

Penyige A, Matko J, Deak E, Bodnar A & Barabas G. (2002). Depolarization of the membrane potential by beta-lactams as a signal to induce autolysis. *Biochem Biophys Res Commun* **290,** 1169-1175.

Phan MN, Leddy HA, Votta BJ, Kumar S, Levy DS, Lipshutz DB, Lee SH, Liedtke W & Guilak F. (2009). Functional Characterization of TRPV4 as an Osmotically Sensitive Ion Channel in Porcine Articular Chondrocytes. *Arthritis Rheum* **60,** 3028-3037.

Phillis JW. (2004). Adenosine and adenine nucleotides as regulators of cerebral blood flow: roles of acidosis, cell swelling, and KATP channels. *Crit Rev Neurobiol* **16,** 237-270.

Ponce A. (2006). Expression of voltage dependent potassium currents in freshly dissociated rat articular chondrocytes. *Cellular Physiology and Biochemistry* **18,** 35-46.

Preston GM, Carroll TP, Guggino WB & Agre P. (1992). Appearance of Water Channels in Xenopus Oocytes Expressing Red-Cell Chip28 Protein. *Science* **256,** 385-387.

Quayle JM, Nelson MT & Standen NB. (1997). ATP-sensitive and inwardly rectifying potassium channels in smooth muscle. *Physiol Rev* **77,** 1165-1232.

Ramage L, Martel MA, Hardingham GE & Salter DM. (2008). NMDA receptor expression and activity in osteoarthritic human articular chondrocytes. *Osteoarthr Cartilage* **16,** 1576-1584.

Redini F. (2001). [Structure and regulation of articular cartilage proteoglycan expression]. *Pathol Biol (Paris)* **49,** 364-375.

Rojek A, Praetorius J, Frøkiaer J, Nielsen S & Fenton RA. (2008). A Current View of the Mammalian Aquaglyceroporins. *Annual Review of Physiology* **70,** 301-327.

Rose RA, Hatano N, Ohya S, Imaizumi Y & Giles WR. (2007). C-type natriuretic peptide activates a non-selective cation current in acutely isolated rat cardiac fibroblasts via natriuretic peptide C receptor-mediated signalling. *J Physiol* **580,** 255-274.

Rossier BC, Pradervand S, Schild L & Hummler E. (2002). Epithelial sodium channel and the control of sodium balance: Interaction between genetic and environmental factors. *Annual Review of Physiology* **64,** 877-897.

Roy NC, Altermann E, Park ZA & McNabb WC. (2011). A comparison of analog and Next-Generation transcriptomic tools for mammalian studies. *Briefings in Functional Genomics* **10,** 135-150.

Rozen S & Skaletsky H. (2000). Primer3 on the WWW for general users and for biologist programmers. *Methods Mol Biol* **132,** 365-386.

Russell JM. (2000). Sodium-Potassium-Chloride Cotransport. *Physiological Reviews* **80,** 211-276.

Sachs F. (1991). Mechanical transduction by membrane ion channels: a mini review. *Molecular and Cellular Biochemistry* **104,** 57-60.

Sakmann B & Neher E. (1983). Geometric parameters of pipettes and membrane patches. *Single-channel recording*, 37-51.

Salter DM, Wright MO & Millward-Sadler SJ. (2004). NMDA receptor expression and roles in human articular chondrocyte mechanotransduction. *Biorheology* **41,** 273-281.

Sanchez JC, Danks TA & Wilkins RJ. (2003). Mechanisms involved in the increase in intracellular calcium following hypotonic shock in bovine articular chondrocytes. *Gen Physiol Biophys* **22,** 487-500.

Sanchez JC, Powell T, Staines HM & Wilkins RJ. (2006). Electrophysiological demonstration of voltage-activated H+ channels in bovine articular chondrocytes. *Cellular Physiology and Biochemistry* **18,** 85-90.

Sanchez JC & Wilkins RJ. (2004). Changes in intracellular calcium concentration in response to hypertonicity in bovine articular chondrocytes. *Comp Biochem Physiol A Mol Integr Physiol* **137,** 173-182.

Schulze-Tanzil G, Mobasheri A, de Souza P, John T & Shakibaei M. (2004). Loss of chondrogenic potential in dedifferentiated chondrocytes correlates with deficient Shc-Erk interaction and apoptosis. *Osteoarthr Cartilage* **12,** 448-458.

Setterbo JJ, Garcia TC, Campbell IP, Reese JL, Morgan JM, Kim SY, Hubbard M & Stover SM. (2009). Hoof accelerations and ground reaction forces of Thoroughbred racehorses measured on dirt, synthetic, and turf track surfaces. *American Journal of Veterinary Research* **70,** 1220-1229.

Shakibaei M & Mobasheri A. (2003). Beta1-integrins co-localize with Na, K-ATPase, epithelial sodium channels (ENaC) and voltage activated calcium channels (VACC) in mechanoreceptor complexes of mouse limb-bud chondrocytes. *Histol Histopathol* **18,** 343-351.

Shakibaei M, Schulze-Tanzil G, de Souza P, John T, Rahmanzadeh M, Rahmanzadeh R & Merker HJ. (2001). Inhibition of mitogen-activated protein kinase kinase induces apoptosis of human chondrocytes. *J Biol Chem* **276,** 13289-13294.

Simon WH & Green WT, Jr. (1971). Experimental production of cartilage necrosis by cold injury: failure to cause degenerative joint disease. *Am J Pathol* **64,** 145-154.

Sivan S, Neidlinger-Wilke C, Wurtz K, Maroudas A & Urban JP. (2006). Diurnal fluid expression and activity of intervertebral disc cells. *Biorheology* **43,** 283-291.

Smith PR & Benos DJ. (1991). Epithelial Na+ Channels. *Annual Review of Physiology* **53,** 509-530.

Stockwell RA. (1971). CELL DENSITY, CELL SIZE AND CARTILAGE THICKNESS IN ADULT MAMMALIAN ARTICULAR CARTILAGE. *J Anat* **108,** 584-&.

Stockwell RA. (1975). Structural and histochemical aspects of the pericellular environment in cartilage. *Philos Trans R Soc Lond B Biol Sci* **271,** 243-245.

Stockwell RA. (1991). Cartilage failure in osteoarthritis: Relevance of normal structure and function. A review. *Clinical Anatomy* **4,** 161-191.

Sudhof TC. (2004). The synaptic vesicle cycle. *Annu Rev Neurosci* **27,** 509-547.

Sugimoto T, Yoshino M, Nagao M, Ishii S & Yabu H. (1996a). Voltage-gated ionic channels in cultured rabbit articular chondrocytes. *Comp Biochem Physiol C Pharmacol Toxicol Endocrinol* **115,** 223-232.

Sugimoto T, Yoshino M, Nagao M, Ishii S & Yabu H. (1996b). Voltage-Gated Ionic Channels in Cultured Rabbit Articular Chondrocytes. *Comparative Biochemistry and Physiology Part C: Pharmacology, Toxicology and Endocrinology* **115,** 223-232.

Tabuchi K, Suzuki M, Mizuno A & Hara A. (2005). Hearing impairment in TRPV4 knockout mice. *Neurosci Lett* **382,** 304-308.

Tatari H. (2007). [The structure, physiology, and biomechanics of articular cartilage: injury and repair]. *Acta Orthop Traumatol Turc* **41 Suppl 2,** 1-5.

Teerapornpuntakit J, Dorkkam N, Wongdee K, Krishnamra N & Charoenphandhu N. (2009). Endurance swimming stimulates transepithelial calcium transport and alters the expression of genes related to calcium absorption in the intestine of rats. *American Journal of Physiology-Endocrinology and Metabolism* **296,** E775-E786.

Trujillo E, Alvarez de la Rosa D, Mobasheri A, Avila J, Gonzalez T & Martin-Vasallo P. (1999a). Sodium transport systems in human chondrocytes. I. Morphological and functional expression of the Na+,K(+)-ATPase alpha and beta subunit isoforms in healthy and arthritic chondrocytes. *Histol Histopathol* **14,** 1011-1022.

Trujillo E, Alvarez de la Rosa D, Mobasheri A, Gonzalez T, Canessa CM & Martin-Vasallo P. (1999b). Sodium transport systems in human chondrocytes. II. Expression of ENaC, Na+/K+/2Cl- cotransporter and Na+/H+ exchangers in healthy and arthritic chondrocytes. *Histol Histopathol* **14,** 1023-1031.

Tsuga K, Tohse N, Yoshino M, Sugimoto T, Yamashita T, Ishii S & Yabu H. (2002). Chloride conductance determining membrane potential of rabbit articular chondrocytes. *J Mem Biol* **185,** 75-81.

Unwin N. (1993). Neurotransmitter action: Opening of ligand-gated ion channels. *Cell* **72,** 31-41.

Urban JP. (1994). The chondrocyte: a cell under pressure. *Br J Rheumatol* **33,** 901-908.

Urban JPG, Hall AC & Gehl KA. (1993). Regulation of Matrix Synthesis Rates by the Ionic and Osmotic Environment of Articular Chondrocytes. *J Cell Physiol* **154,** 262-270.

Vennekens R, Hoenderop JGJ, Prenen J, Stuiver M, Willems PHGM, Droogmans G, Nilius B & Bindels RJM. (2000). Permeation and gating properties of the novel epithelial Ca2+ channel. *J Biol Chem* **275,** 3963-3969.

Villalonga N, David M, Bielanska J, Vicente R, Comes N, Valenzuela C & Felipe A. (2010). Immunomodulation of voltage-dependent K+ channels in macrophages: molecular and biophysical consequences. *Journal of General Physiology* **135,** 135-147.

Voets T, Prenen J, Vriens J, Watanabe H, Janssens A, Wissenbach U, Bodding M, Droogmans G & Nilius B. (2002). Molecular determinants of permeation through the cation channel TRPV4. *J Biol Chem* **277,** 33704-33710.

Walker RL, Hume JR & Horowitz B. (2001). Differential expression and alternative splicing of TRP channel genes in smooth muscles. *Am J Physiol Cell Physiol* **280,** C1184-1192.

Walsh KB, Cannon SD & Wuthier RE. (1992). Characterization of a delayed rectifier potassium current in chicken growth plate chondrocytes. *Am J Physiol* **262,** C1335-1340.

Weidmann S. (1951). Effect of current flow on the membrane potential of cardiac muscle. *J Physiol* **115,** 227-236.

Wemmie JA, Price MP & Welsh MJ. (2006). Acid-sensing ion channels: advances, questions and therapeutic opportunities. *Trends Neurosci* **29,** 578-586.

Wilkens MR, Kunert-Keil C, Brinkmeier H & Schroder B. (2009). Expression of calcium channel TRPV6 in ovine epithelial tissue. *Vet J* **182,** 294-300.

Wilkins RJ, Browning JA & Ellory JC. (2000). Surviving in a matrix: membrane transport in articular chondrocytes. *J Membr Biol* **177,** 95-108.

Wilkins RJ & Hall AC. (1992). Measurement of intracellular pH in isolated bovine articular chondrocytes. *Exp Physiol* **77,** 521-524.

Wilson JR, Duncan NA, Giles WR & Clark RB. (2004). A voltage-dependent K+ current contributes to membrane potential of acutely isolated canine articular chondrocytes. *J Physiol* **557,** 93-104.

Wohlrab D, Lebek S, Kruger T & Reichel H. (2002). Influence of ion channels on the proliferation of human chondrocytes. *Biorheology* **39,** 55-61.

Wohlrab D, Vocke M, Klapperstuck T & Hein W. (2004). Effects of potassium and anion channel blockers on the cellular response of human osteoarthritic chondrocytes. *Journal of Orthopaedic Science* **9,** 364-371.

Wohlrab D, Wohlrab J, Reichel H & Hein W. (2001). Is the proliferation of human chondrocytes regulated by ionic channels? *Journal of Orthopaedic Science* **6,** 155-159.

Wright M, Jobanputra P, Bavington C, Salter DM & Nuki G. (1996). Effects of intermittent pressure-induced strain on the electrophysiology of cultured human chondrocytes: Evidence for the presence of stretch-activated membrane ion channels. *Clinical Science* **90,** 61-71.

Wright MO, Stockwell RA & Nuki G. (1992). Response of plasma membrane to applied hydrostatic pressure in chondrocytes and fibroblasts. *Connective Tissue Research* **28,** 49-70.

Wu QQ & Chen Q. (2000a). Mechanoregulation of chondrocyte proliferation, maturation, and hypertrophy: Ion-channel dependent transduction of matrix deformation signals. *Experimental Cell Research* **256,** 383-391.

Wu QQ & Chen Q. (2000b). Mechanoregulation of chondrocyte proliferation, maturation, and hypertrophy: ion-channel dependent transduction of matrix deformation signals. *Exp Cell Res* **256,** 383-391.

Xu J, Wang W, Clark CC & Brighton CT. (2009). Signal transduction in electrically stimulated articular chondrocytes involves translocation of extracellular calcium through voltage-gated channels. *Osteoarthr Cartilage* **17,** 397-405.

Xu X, Urban JP, Tirlapur UK & Cui Z. (2010). Osmolarity effects on bovine articular chondrocytes during three-dimensional culture in alginate beads. *Osteoarthr Cartilage* **18,** 433-439.

Yellowley CE, Hancox JC & Donahue HJ. (2002). Effects of cell swelling on intracellular calcium and membrane currents in bovine articular chondrocytes. *J Cell Biochem* **86,** 290-301.

Yuan FL, Chen FH, Lu WG, Li X, Wu FR, Li JP, Li CW, Wang Y, Zhang TY & Hu W. (2010). Acid-sensing ion channel 1a mediates acid-induced increases in intracellular calcium in rat articular chondrocytes. *Mol Cell Biochem* **340,** 153-159.

Zhang R, Logee KA & Verkman AS. (1990). Expression of Messenger-Rna Coding for Kidney and Red-Cell Water Channels in Xenopus Oocytes. *J Biol Chem* **265,** 15375-15378.

Zuscik MJ, Gunter TE, Puzas JE & Rosier RN. (1997). Characterization of voltage-sensitive calcium channels in growth plate chondrocytes. *Biochem Biophys Res Commun* **234,** 432-438.

10

PUBLICATIONS AND PROCEEDINGS ARISING FROM THIS THESIS

Journal of Cellular Physiology

The Role of the Membrane Potential in Chondrocyte Volume Regulation

REBECCA LEWIS,[1] KATIE E. ASPLIN,[2] GARETH BRUCE,[3] CAROLINE DART,[4] ALI MOBASHERI,[2] AND RICHARD BARRETT-JOLLEY[1]*

[1]*Department of Musculoskeletal Biology, Institute of Aging and Chronic Disease, Faculty of Health and Life Sciences, University of Liverpool, Liverpool, UK*

[2]*Musculoskeletal Research Group, Division of Veterinary Medicine, Faculty of Medicine and Health Sciences, School of Veterinary Medicine and Science, University of Nottingham, Loughborough, UK*

[3]*Institute of Membrane and Systems Biology, University of Leeds, Leeds, UK*

[4]*Institute of Integrative Biology, Faculty of Health and Life Sciences, University of Liverpool, Liverpool, UK*

Many cell types have significant negative resting membrane potentials (RMPs) resulting from the activity of potassium-selective and chloride-selective ion channels. In excitable cells, such as neurones, rapid changes in membrane permeability underlie the generation of action potentials. Chondrocytes have less negative RMPs and the role of the RMP is not clear. Here we examine the basis of the chondrocyte RMP and possible physiological benefits. We demonstrate that maintenance of the chondrocyte RMP involves gadolinium-sensitive cation channels. Pharmacological inhibition of these channels causes the RMP to become more negative (100 μM gadolinium: $\Delta V_m = -30 \pm 4$ mV). Analysis of the gadolinium-sensitive conductance reveals a high permeability to calcium ions ($P_{Ca}/P_{Na} \approx 80$) with little selectivity between monovalent ions; similar to that reported elsewhere for TRPV5. Detection of TRPV5 by PCR and immunohistochemistry and the sensitivity of the RMP to the TRPV5 inhibitor econazole ($\Delta V_m = -18 \pm 3$ mV) suggests that the RMP may be, in part, controlled by TRPV5. We investigated the physiological advantage of the relatively positive RMP using a mathematical model in which membrane stretch activates potassium channels allowing potassium efflux to oppose osmotic water uptake. At very negative RMP potassium efflux is negligible, but at more positive RMP it is sufficient to limit volume increase. In support of our model, cells clamped at −80 mV and challenged with a reduced osmotic potential swelled approximately twice as much as cells at +10 mV. The positive RMP may be a protective adaptation that allows chondrocytes to respond to the dramatic osmotic changes, with minimal changes in cell volume.
J. Cell. Physiol. 226: 2979–2986, 2011.

Chondrocytes are the cells that produce, maintain, and degrade the extracellular matrix of articular cartilage in load-bearing joints (Huber et al., 2000; Archer and Francis-West, 2003). Their location, embedded in cartilage, means that these cells are subjected to significant dynamic loads during physical activity (Eckstein et al., 1999). The limb joints in a galloping horse, for example, will routinely experience compressive forces of 7,500 N (Setterbo et al., 2009). Contact pressures have been directly measured in human hip joints and are reported to be as high as 18 MPa (Hodge et al., 1986). Under pressure, cartilage exudes fluid (McCutchen, 1962) and thus decreases in volume. This involves changes in water content of the interstitial component of cartilage and consequent changes in extracellular osmotic potential (Mow et al., 1992, 1999; Sivan et al., 2006). Typical osmolarities for many mammalian cells are in the region of 300 mOsm. However, under load, the osmolarity of the extracellular matrix of cartilage is believed to be approximately 480 mOsm (Urban, 1994). More recently, osmolarities as high as 550 mOsm have been used to model the three-dimensional microenvironment of chondrocytes under load (Xu et al., 2010). This means that chondrocytes exist in a unique cellular environment. Changes in osmotic pressure are reversible upon relaxation (Mow et al., 1992; Urban, 1994) and so during normal usage chondrocytes will be cyclically exposed to both increasing and decreasing osmotic forces. Healthy chondrocytes are able to regulate their volume with remarkable resilience throughout these osmotic pressure cycles (Bush and Hall, 2001a). However, chondrocytes swell during the decreasing phases of the osmotic pressure cycle (Bush and Hall, 2001b) and are vulnerable to damage (Bush et al., 2005). Decrease in osmotic potential (increased water content) has been linked to the early onset of osteoarthritis (Stockwell, 1991) and loss of volume control has been specifically linked to chondrocyte death and the progression of osteoarthritis (Bush and Hall, 2003; Bush et al., 2005).

As a starting point to understanding how these specialized cells so effectively regulate their volume and the membrane ion fluxes involved, we decided to make a thorough examination of their resting membrane potential (RMP) properties in vitro. There have been a number of previous studies, which observe chondrocytes RMP in a range of species, but these have resulted in a very wide variety of values from −10.6 to −46 mV (Wright et al., 1992; Sugimoto et al., 1996; Clark et al., 2010; Funabashi et al., 2010b). We began by thoroughly examining the RMP of chondrocytes from larger mammals in vitro and found these to be much less negative than other cell types. Previous studies have investigated the role of potassium (Wilson et al., 2004) and chloride (Tsuga et al., 2002; Funabashi et al., 2010a) channels in

Abbreviations: RMP, resting membrane potential; TRP, transient receptor potential channel; TRPV, vanilloid type transient receptor potential channel; TRPV5, vanilloid type transient receptor potential channel

*Correspondence to: Richard Barrett-Jolley, Comparative Molecular Medicine, School of Veterinary Science, University of Liverpool, Veterinary Science Building, Brownlow Hill and Crown Street, Liverpool L69 7ZJ, UK. E-mail: RBJ@liv.ac.uk

Received 7 December 2010; Accepted 5 January 2011

Published online in Wiley Online Library (wileyonlinelibrary.com), 15 February 2011.
DOI: 10.1002/jcp.22646

the regulation of the RMP and so we examined the contribution of sodium and/or non-specific cation conductances. We then investigated what the physiological advantage of such positive RMPs is for chondrocytes.

Methods

Canine cartilage was removed from stifle and elbow condyles of large, skeletally mature, bull terrier types euthanatized for unrelated clinical reasons. Bovine, ovine, and equine cartilage were sourced from a local abattoir. Chondrocytes were isolated as described previously (Mobasheri et al., 2005, 2007, 2010) with type II collagenase. To ensure preservation of the chondrocyte phenotype we used only cartilage slices (collagenase treated), freshly dissociated, first expansion and first passage cells only. RT-PCR experiments used first expansion chondrocytes. When isolated, chondrocyte doubling time was within 24 h confirming that these cells are viable and vital. Other cell types were prepared by their respective standard methods: rat dorsal root ganglion neurones (Bruce et al., 2009), hypothalamic pre-autonomic neurones (Barrett-Jolley et al., 2000; Womack et al., 2007), and aortic smooth muscle (Sampson et al., 2007).

Electrophysiology

RMP were measured using whole-cell patch clamp in current clamp mode by three different amplifiers (Axon Axopatch 200a, 200b, Molecular Devices, Sunnyvale, CA Cairns Optoclamp, Faversham, UK). For RMP measurements we used a standard physiological saline for both intracellular and extracellular solutions of (in mM): 95 K-Gluconate, 26 KCl, 1 $MgCl_2$, 5 BAPTA and 10 HEPES (pH 7.2 with KOH), and 140 NaCl, 5 KCl, 2 $CaCl_2$, 1 $MgCl_2$ and 10 HEPES (pH 7.4 with NaOH), respectively. For sharp electrode recording (NPI SEC-05LX amplifier), electrodes were filled with 1 or 2 M KCl and the extracellular solutions were as above. For the cell-volume experiments, osmolarity was increased by addition of 180 mM sucrose.

Measurement of gadolinium III (Gd) difference currents was made with the Axon Axopatch 200a amplifier. A ramp protocol was applied consisting of a 50-msec voltage step at 0 mV followed by a 4.5 sec linear ramp from −60 to +80 mV. This was repeated every 50 sec. Whole-cell currents were recorded in "methanesulfonate solutions," containing: (in mM): 150 Na-methanesulfonate, 10 HEPES, 2 $CaCl_2$ (pH 7.4 with NaOH) in the bath and 150 Na-methanesulfonate, 10 HEPES, 5 mM BAPTA (pH 7.4 with NaOH) in the pipette solution. Difference currents were obtained by subtraction of a ramp in the presence of 100 μM Gd from that run in vehicle control.

To study the relative whole-cell permeability of monovalent cations and calcium ions, we used bath solutions containing (in mM) 2 $MgCl_2$, 10 HEPES and either 150 XCl (where X = Na, K, or Cs) or 30 mM $CaCl_2$ and 105 mM NaCl (all pH to 7.4 with the relevant monovalent hydroxide). In these experiments, the patch pipette (intracellular) solution contained (in mM): 135 CsCl, 1 $MgCl_2$, 10 Hepes, and 5 EGTA (pH 7.2 with NaOH). Permeability ratios were calculated using the equations of Voets et al. (2002), using the reversal potentials (V_{rev}) of the Gd sensitive current–voltage ramps.For monovalent cations:

$$P_x/P_{Na} = \exp\left(\Delta V_{rev}\frac{F}{RT}\right) \quad (1)$$

For calcium ions:

$$P_{Ca}/P_{Na} = \left(1+\exp\left(V_{rev}\frac{F}{RT}\right)\right)\frac{([Na]_i+\alpha[Cs]_i)\exp(V_{rev}(F/RT))-[Na]_e-\alpha[Cs]_e}{4[Ca]_e} \quad (2)$$

where

$$\alpha = P_{Cs}/P_{Na} \quad (3)$$

Video imaging and switch clamp

Cells were voltage clamped with single sharp electrodes, under switch clamp (SEC 05LX, NPI) and simultaneously videoed with a Hitachi (KP-M3E/K CCD) camera attached to a Nikon Eclipse microscope magnification ~1,000×.

Analysis

Electrophysiological data were digitized and analyzed using the WinEDR and WinWCP programs (John Dempster, University of Strathclyde). Visual data were analyzed with ImageJ (Abramoff et al., 2004) and ANOVA performed with SPSS (SPSS, Inc., Chicago, IL), multiple comparisons assessed with Dunnett tests. *t*-Tests were performed with Minitab (Minitab Ltd, Coventry, UK). All values are quoted as mean ± SEM, with sample size = n. All membrane potentials are corrected for liquid junction potentials estimated using JPCalc (Barry and Lynch, 1991).

Voltage-sensitive dye membrane potential measurements

To measure the membrane potential with optical dyes we used oxonol VI (Apell and Bersch, 1987; Wohlrab et al., 2001). Oxonol VI (100–300 nM) was added to the perfusion solution, for at least 15 min prior to commencement of recording. The optical system (Hitachi KP-M3E/K CCD camera attached to a Nikon Eclipse microscope, G-2A filter set, magnification ~1,000×) was calibrated by measuring the average intensity in a chondrocyte, under perforated patch clamp at a range of membrane potentials. Our perforated patch-clamp methods have been described elsewhere (Davies et al., 2010). This intensity versus voltage calibration curve was then used to extrapolate membrane potentials of surrounding un-clamped chondrocytes.

RT-PCR

Total RNA was extracted from canine chondrocytes by use of an RNeasy Mini Kit (Qiagen, Crawley, UK) according to manufacturer's instructions. Genomic DNA was eliminated using deoxyribonuclease I, Amplification Grade (Invitrogen, Paisley, UK). Isolated total RNA was then used as a template to create first-strand cDNA by Superscript II Reverse Transcriptase (Invitrogen). One microliter of this cDNA was used as a template for touchdown PCR using the primers in Table 1 (derived from murine transient receptor potential vanilloid channel subtype 5, TRPV5). PCR was performed with 35 cycles in total on a Techgene FTGene2D thermocycler (Techne, Stone, UK). The initial cycle consisted of a denaturation step at 92°C for 30 sec, an annealing step at 65°C for 30 sec, and an extension step of 72°C for 60 sec. The annealing step was decreased by 1°C with each cycle to a final temp of 56°C. PCR products (10 μl) were separated by electrophoresis on a 1.5% agarose gel (2 h at 80 mV) and the bands were visualized by Gel Red (Biotium, Cambridge, UK) staining using a UV transilluminator (BioRad, Hemel Hempstead, UK). Sequencing was performed by Beckman Coulter Genomics (Takeley, UK).

TABLE 1. Primer sequences for each of the proteins investigated

Protein	Primer pair sequences (5′–3′)	Size (bp)
TRPV5	Forward: GCCCCTAACATCTTCCCTCT Reverse: TGTCCATATTTCTTCCACTT	165
GAPDH	Forward: CATCAACGGGAAGTCCATCT Reverse: GTGGAAGCAGGGATGATGTT	429

GAPDH was used as a test for viable cDNA. Primers were purchased from Sigma-Aldrich, Poole, UK.

Ion channel immunohistochemistry

Sections of canine cartilage were probed for channel expression by immunohistochemistry essentially as described previously (Mobasheri et al., 2005). Slides were deparaffinized in xylene for 20 min to remove embedding medium, washed in absolute ethanol for 3 min, gradually rehydrated in a series of alcohol baths (96%, 85%, and 50%) and then placed water for 5 min. Endogenous peroxidase activity was blocked for 1 h in a solution of 97% methanol, 3% hydrogen peroxide, and 0.01% sodium azide. The slides were then incubated for 1 h at room temperature in tris-buffered saline (TBS) containing 1% bovine serum albumin (BSA, protease-free) and 0.01% sodium azide to block non-specific antibody binding. Slides were incubated overnight at 4°C with rabbit polyclonal antibodies to TRPV5 (Abcam plc., Cambridge, UK). Antibodies were diluted (various dilutions ranging from 1:200 to 1:1,500) in TBS containing 1% BSA. After 24 h at 4°C, the slides were washed three times for 5 min each in TBS containing 0.05% Tween-20 (TBS-T) before incubation with horseradish peroxidase-labeled polymer conjugated to affinity-purified goat anti-rabbit immunoglobulins (code no. K4010; Dako UK Ltd, Ely, UK) for 30 min at room temperature. The sections were washed a further three times for 5 min in TBS-T before application of liquid DAB+ chromogen (3,3′-diaminobenzidine solution; DakoCytomation). The development of the brown-colored reaction was stopped by rinsing in TBS-T. The stained slides were immersed for 5 min in a bath of aqueous hematoxylin (code no. S3309; DakoCytomation) to counterstain cell nuclei. Finally, the slides were washed for 5 min in running water and dehydrated in a series of graded ethanol baths before being rinsed in three xylene baths and mounted in 1,3-diethyl-8-phenylxanthine (BDH Laboratories, Atherstone, UK). Control experiments were performed by omitting the primary antibody from the immunohistochemical procedure. Immunostained tissue sections were examined with a Nikon Eclipse 80i microscope. Photomicrographs were digitally captured using Nikon Digital Sight DS-5M camera and Nikon Eclipsenet image capture software.

Results

Initial measurements of chondrocyte RMP

We measured the RMP of canine chondrocytes using both whole-cell patch clamp and sharp electrode recording. At temperatures of 24–25°C in physiological saline solution, we recorded values of -6.1 ± 0.5 mV, $n = 50$ with whole-cell patch clamp and -7.3 ± 1.8, $n = 19$ with sharp electrodes (Fig. 1A). The value measured by patch clamp was consistent across a range of large animal species (Fig. 1B). Studies have shown that these cells retain a substantially native chondrocyte phenotype for the first few passages in culture (Benya and Shaffer, 1982). We therefore compared RMP measured from chondrocytes in slices of cartilage (sharp electrodes -7.5 ± 0.7 mV, $n = 10$), freshly dissociated, first expansion and first passage chondrocytes (patch clamp). These were not significantly different to each other (Fig. 1C). As a control, we include RMP values recorded for other tissues on the same equipment; these all had RMP in the conventional significantly negative range (-48 to -64 mV) (Fig. 1D). To measure membrane potential from intact cells which had neither been impaled by a sharp electrode, or patch clamped, we also performed an optical dye study of the membrane potential (Fig. 1E,F). This gave a membrane potential value of -8.6 ± 8 mV, $n = 14$.

The identity of the principal cation conductance open at rest

Such a positive RMP in chondrocytes suggests that at rest the chondrocyte membrane is highly permeable to sodium and/or calcium ions (since these ions have equilibrium potentials above 0 mV). Having already investigated a number of potassium channels in the chondrocyte membrane (Mobasheri et al., 2005, 2007, 2010) we sought to identify cation channels with selectivity for sodium and/or calcium, at sufficient density to account for such a positive RMP. To investigate these conductances further, we switched to chloride and potassium-free "methanesulfonate solutions." We compared whole-cell voltage ramps in the presence and absence of gadolinium (Gd), a widely used cation channel blocker (Fig. 2A). We found that the whole-cell current was sensitive to 100 μM Gd (Fig. 2A). The calculated Gd difference current is shown in Figure 2B.

Since Gd is well known to be a blocker of transient receptor potential channels including TRPV channels (Vennekens et al., 2001; Clapham, 2007; Alexander et al., 2008), we investigated if these channels are constitutively active in chondrocytes. There are several subtypes, however, and a useful way of distinguishing between them is by analysis of the conductance's permeability ratio, since many of the subtypes have distinct permeability profiles. To calculate the permeability ratio of the Gd difference we adapted the methods of Voets et al. (2002), and measured changes in reversal potentials of the Gd sensitive difference currents in extracellular solutions with different cation compositions (Fig. 3A–E). The permeabilities of Cs^+ and K^+ were not significantly different to that of Na^+, but that of Ca^{2+} was significantly greater (P_K/P_{Na} 1.02 ± 0.06, $n = 10$, P_{Cs}/P_{Na} 1.2 ± 0.1, $n = 9$, P_{Ca}/P_{Na} 78 ± 9, $n = 5$, $P \leq 0.0001$). Since this permeability ratio is similar to that measured for TRPV5 (Vennekens et al., 2000; Owsianik et al., 2006) we investigated whether these cells contained TRPV5 mRNA by reverse-transcription PCR or expressed TRPV5 protein by immunohistochemistry. We clearly detected both TRPV5 mRNA and protein expression (Fig. 3F–H), confirming TRPV5 as a likely contributor to the Gd sensitive conductance. TRPV5 is known to be blocked by both Gd and econazole (Nilius et al., 2001) we investigated whether these compounds affected the RMP of chondrocytes (Fig. 4A,B). We found that both hyperpolarized the membrane, gadolinium by 30 ± 4 mV ($n = 8$, $P \leq 0.0005$) and econazole by 18 ± 3 mV ($n = 5$, $P \leq 0.005$; Fig. 4).

We hypothesized that the relatively positive RMP of chondrocytes would facilitate chondrocyte control of volume (see Appendix 1). In vivo chondrocytes are reported to experience osmolarities as high as 500 mOsm (Urban, 1994). On returning to lower osmolarity, chondrocytes swell (Bush and Hall, 2001a). To investigate the role of membrane potential in this process we used sharp-electrode voltage-clamp of chondrocytes with a switch-clamp amplifier. We controlled voltage and simultaneously calculated chondrocyte volume from measured 2D surface areas. Unlike conventional patch-clamp recording, which alters the intracellular environment of a cell, this method does not require alteration of the intracellular milieu. We measured cell volume continuously as the osmolarity of the extracellular bathing medium was reduced from 489 to 309 mOsm. Chondrocytes clamped at +10 mV and exposed to the reduced osmotic pressure increased in size by $129 \pm 3\%$, $n = 10$ (Fig. 5A,B). This increase was reversible upon returning to the higher osmolarity solution (Fig. 5A,C). Strikingly, when this procedure was repeated with the membrane clamped to −80 mV, cell volume increased by $157 \pm 4\%$, $n = 12$ (Fig. 5A,B) and the chondrocytes were no longer able to recover their volume (Fig. 5A,C).

Discussion

We propose that a diverse chondrocyte channelome, including TRPV5, contributes to a relatively positive RMP in chondrocytes. Since this potential is significantly more positive than the equilibrium potential for potassium ions, it will allow the cell to efflux potassium ions rapidly enough to limit cell-volume increase under conditions of reduced osmolarity. This suggests that a relatively positive RMP is a biological adaptation

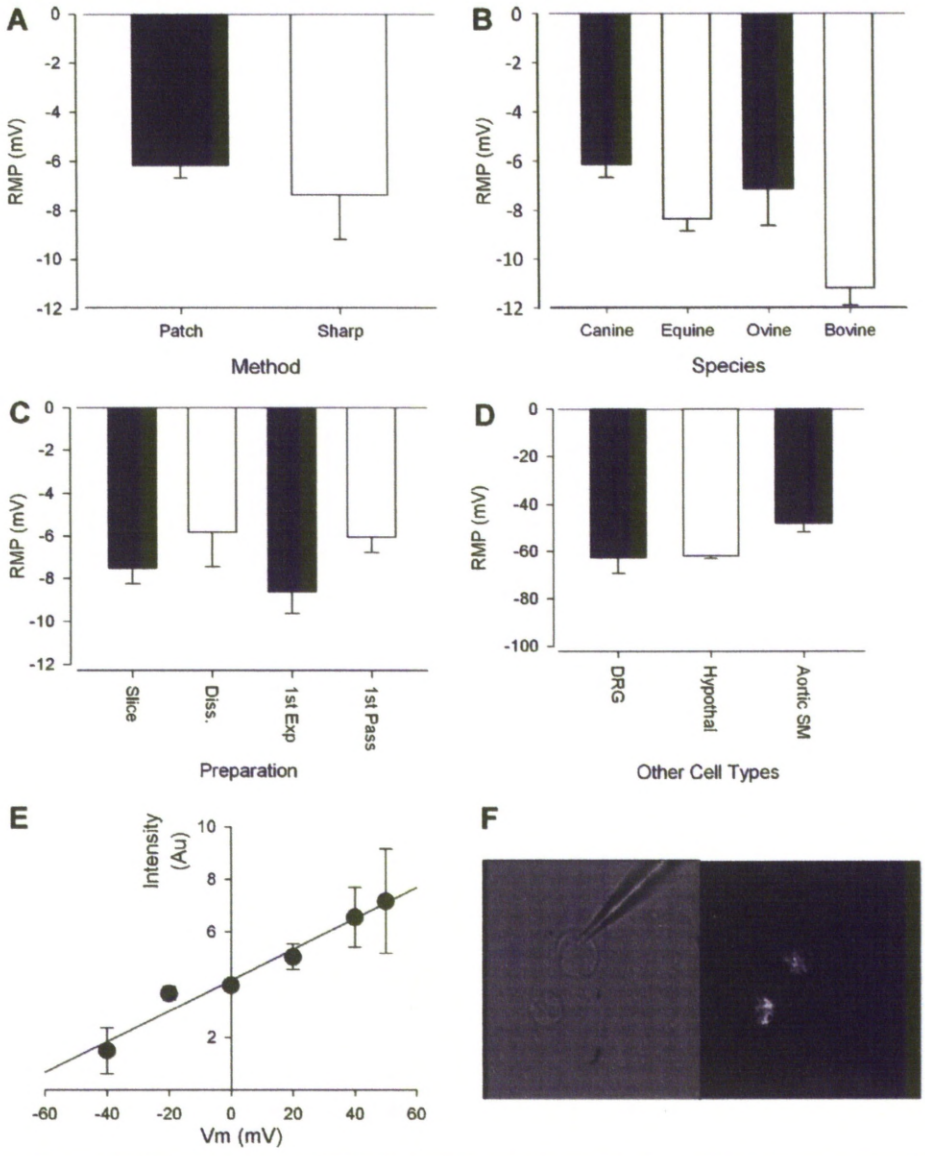

Fig. 1. Freshly dissociated and primary cultured chondrocytes from a range of species exhibit relatively positive resting membrane potentials (RMP). A: RMPs measured in canine chondrocytes using patch clamp and sharp electrodes (n = 50, 19). B: RMP measured by the whole-cell patch-clamp technique in canine (n = 50, as A), equine (n = 9), ovine (n = 8), and bovine (n = 5) chondrocytes. C: RMP measured by sharp electrodes in cartilage slices ("slice," n = 10) and whole-cell patch clamp from freshly dissociated canine chondrocytes ("diss.," n = 5), from first expansion chondrocytes ("1st Exp," n = 5) and canine chondrocytes following the first passage ("1st Pass," n = 22). D: Control cell type demonstrating conventionally negative RMP; DRG, dissociated rat dorsal root ganglion neurones; hypothalamic, paraventricular nucleus pre-autonomic neurones; aortic SM, isolated smooth muscle cells from rat aorta. All patch-clamp experiments in this figure were performed with standard physiological intracellular and extracellular solutions, except the sharp electrode recording experiment in (A) where the extracellular solution was the same standard physiological saline, but the electrode was filled with 1 or 2 M KCl. E: Calibration curve for the voltage sensitive dye measurements, "AU" is arbitrary units of relative intensity. F: Two chondrocytes, one patched, one not patched, under visible (left part) and epifluorescence (right part) with oxonol VI dye, bar indicates 10 μm.

to allow chondrocytes to survive the extreme osmotic challenges they routinely face.

The positive RMP in chondrocytes

The relatively positive RMPs we report in the current paper are similar to one of the earliest report of chondrocytes' RMP (Wright et al., 1992) (sheep and human control chondrocytes; RMP: −10.6 and −12.4 mV, respectively). Since this time, a number of groups have observed more negative RMPs. These more negative RMPs include −46 mV on mouse chondrocytes (Clark et al., 2010), −41 mV on rabbit chondrocytes (Sugimoto et al., 1996), and −20 mV on a human cell line, OUMS-27 (Funabashi et al., 2010b). We have a number of possible explanations for this. We have used, over several years now, chondrocytes prepared from larger animals (Mobasheri et al.,

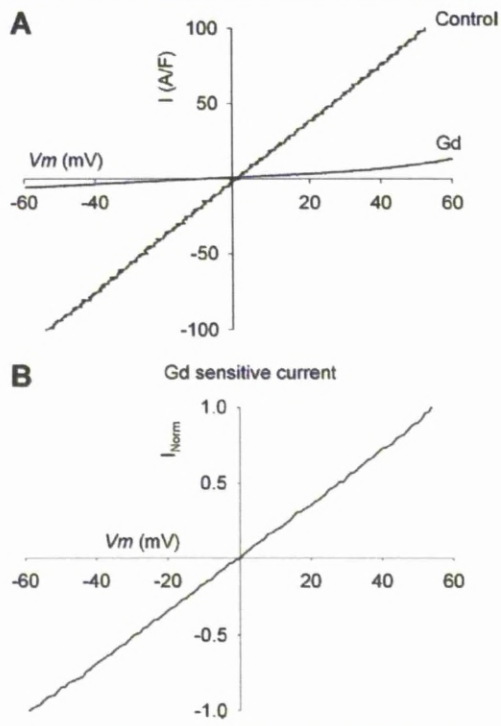

Fig. 2. Patch clamp electrophysiology demonstrates the presence of gadolinium III sensitive whole-cell conductances. A: Whole-cell current ramps in "methanesulfonate solutions." Command potential (V_m) on the x-axis, current on the y-axis (normalized for cell size). Mean inhibition of whole-cell current was 80 ± 9%, n = 5, $P \leq 0.001$. Control (vehicle) or in the presence of gadolinium III (Gd). B: The Gd sensitive current, normalized to that at −60 mV. The measured reversal potential of the difference current under these conditions was −1 ± 3 mV, n = 5.

2005, 2007, 2010). It is entirely possible that these larger animals have more positive RMP, since their joints experience greater forces than those of rodents (Huberti and Hayes, 1984; Clarke et al., 2001; Setterbo et al., 2009). Direct experimental comparison is difficult, however, due to the problems inherent in isolating a pure chondrocyte preparation from rabbits and small rodents. This is because these animals have cartilage depths as little as 55–300 μm (Stockwell, 1971; Frisbie et al., 2006; Ahern et al., 2009) and our isolation method involves manual shaving of cartilage from articular joints in a manner similar to the peeling of an apple. We feel we would, therefore, inevitably include other cell types in the extraction such as osteoclasts, osteoblasts, stromal cells, and cells of blood vessel origin. In the joints of the larger animals we used, cartilage depth was approximately 1 mm or more (from larger dogs to horses) and so we are confident of a pure chondrocyte preparation. Furthermore, our monolayer chondrocyte preparation reliably retains chondrocyte phenotype in terms of cells proliferation (Martin et al., 1999; Jakob et al., 2001; Schulze-Tanzil et al., 2004), secretion of collagen (type II) and chondrocyte specific proteoglycans for the first four passages in culture (Schulze-Tanzil et al., 2004). Isolated chondrocytes indeed exhibit similar volume regulating properties to in situ chondrocytes (Bush and Hall, 2001a,b), however, to ensure preservation of the chondrocyte phenotype, we used freshly dissociated, first expansion and first passage chondrocytes only. It is notable that we observe the relatively positive RMP even in slices of cartilage or in first passage chondrocytes.

The identity of the principal cation conductances open at rest

In previous reports we have focused on potassium conductances in chondrocytes (Mobasheri et al., 2005, 2007, 2010). In this study, however, we focused on non-potassium cation channels open at rest. Our whole-cell current–voltage ramp protocols clearly demonstrate that the majority of the total resting (non-potassium) current is generated by a Gd sensitive conductance. It is likely that the Gd sensitive conductance is comprised of more than one type of channel, however, our permeability data suggest that TRPV5 dominates. TRPV5 is one of the few ion channel conductances with little selectivity between Cs^+, Na^+, and K^+ ions, but high permeability to Ca^{2+} ions (Vennekens et al., 2000; Owsianik et al., 2006; Alexander et al., 2008). The presence of both TRPV5 mRNA and TRPV5 protein by RT-PCR and immunohistochemistry serve to further support the notion that these cells express TRPV5. In addition, econazole, a relatively selective inhibitor of TRPV5 (Nilius et al., 2001) hyperpolarized the membrane in a similar manner to Gd itself. That Gd hyperpolarizes the chondrocyte by more than the econazole implies that Gd may additionally inhibit other conductances in the cell, and these will be the subject of future investigations.

The physiological role of the RMP in chondrocytes

It seems likely that the unusual electrical properties of chondrocytes must confer a biological advantage to these cells. We propose that this advantage is the ability to withstand changes in osmotic potential. This follows because the rate and degree of cell swelling during osmotic shock is counteracted by the release of ions, particularly K^+ and concomitant reduction in osmotic drive for water entry (Hoffmann and Dunham, 1995; Hoffmann et al., 2009). One would expect that the predicted loss of potassium ions would be matched by an equal number of anions (e.g., chloride), reducing the absolute loss of potassium ions. Several different chondrocyte potassium channels have been proposed to open in response to membrane stretch and conduct these potassium ions (Hall et al., 1996; Martina et al., 1997; Mobasheri et al., 2010). From this, we predicted that cell swelling would be much less at a positive RMP than it would be at substantially negative membrane potentials. This prediction follows from the fact that the driving force ($RMP - E_k$) for potassium ion efflux is much greater at more positive membrane potentials. The relationship is given by:

$$I_k = G_{kstretch}[RMP - E_k] \quad (4)$$

where I_K is the potassium current, $G_{kstretch}$ is the potassium conductance, and E_K the equilibrium potential for potassium ions. We tested this prediction by experiment. One approach to this experimental design would be to decrease osmolarity from approximately 300 mOsm to, for example, 200 mOsm, however, it is generally accepted that this is well outside the chondrocyte's normal environmental range (Urban, 1994). Therefore, in order to make this experiment as physiologically relevant as possible, we measured volume increases when decreasing osmolarity from a relatively high (approximately 490 mOsm), to a physiological minimum for cartilage (approximately 320 mOsm, Urban, 1994). We found that positive RMPs significantly reduced the volume increase when cells were exposed to reduced osmotic pressure. At positive membrane potentials this increase in volume was very similar to that previously measured in unclamped chondrocytes in culture or in situ (Bush and Hall, 2001b).

Interestingly, our data show that at very negative membrane potentials, chondrocytes appeared unable to decrease their

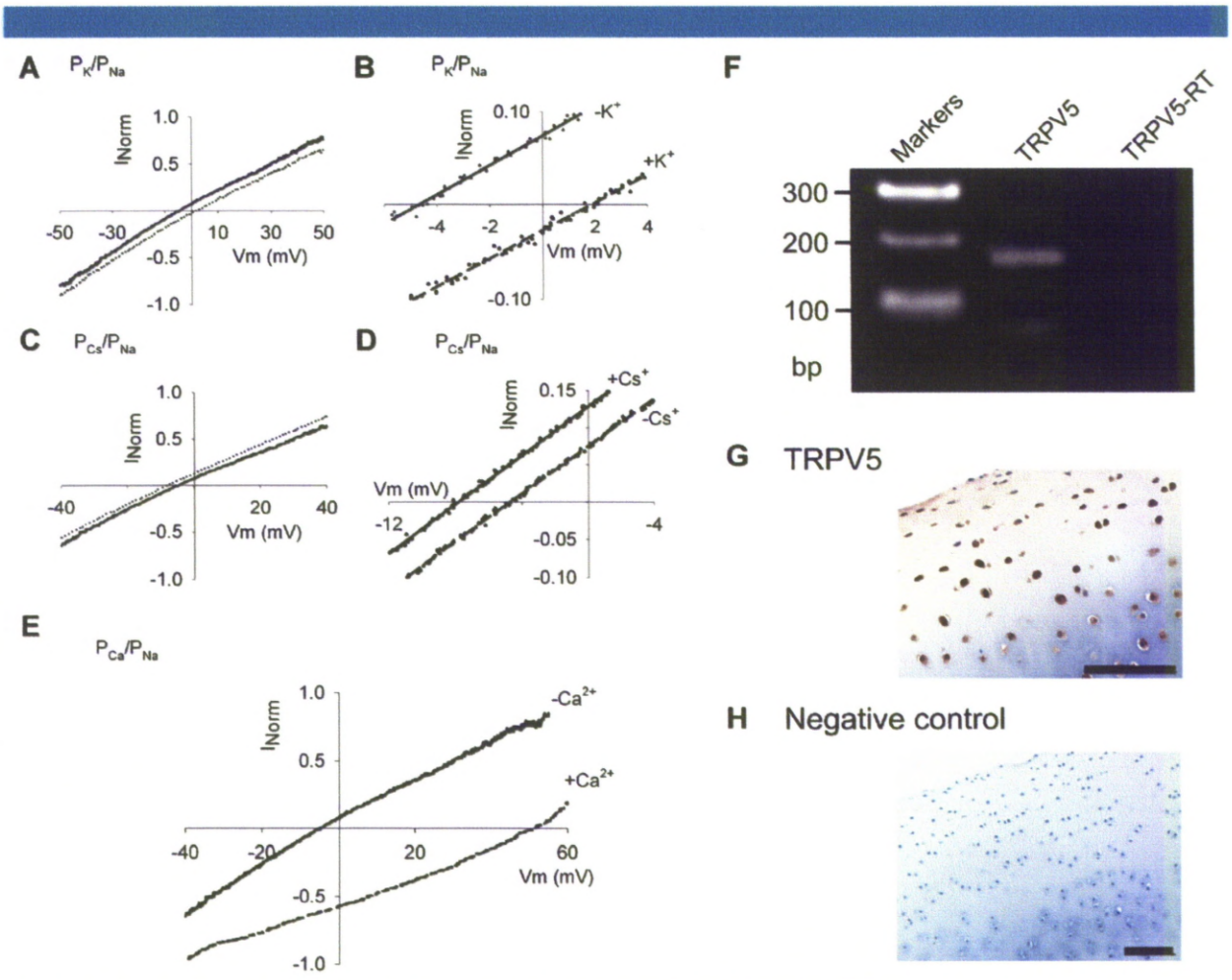

Fig. 3. Gadolinium III difference current has high permeability to calcium ions. A,B: Gd sensitive current–voltage ramp with 150 mM external NaCl (solid line) or 150 mM external KCl (broken line). (B) shows the same data as (A), but magnified to show ΔV_{rev} more clearly. The permeability ratio P_K/P_a (see text) was then calculated from Equation (1). C,D: Gd sensitive current–voltage ramp with 150 mM external NaCl (solid line) or 150 mM external CsCl (broken line). (D) shows the same data as (C), but magnified to show ΔV_{rev} more clearly. The permeability ratio P_{Cs}/P_{Na} (see text) was then calculated from Equation (1). E: Current–voltage ramp with 150 mM external NaCl (solid line) or 30 mM $CaCl_2$ and 105 mM NaCl (broken line). The permeability ratio P_{Ca}/P_{Na} (see text) was then calculated from Equation (2). The full solutions for (A) to (E) are described in the Methods Section. F: RT-PCR was performed as described in the Methods Section. Specific primers for TRPV5 were used and mRNA (164 bp) product encoding TRPV5 was detected in extracts of first expansion chondrocytes. Omission of reverse transcriptase served as a negative control G, sections of full-depth canine articular cartilage were probed for channel expression by immunohistochemistry using polyclonal antibodies raised against TRPV5. H: Omission of primary antibody from the immunohistochemical procedure served as a negative control. Sections of cartilage were otherwise treated in exactly the same way during the immunohistochemical procedure except that the primary antibody was omitted. Positive immunoreactivity (brown staining) was observed in chondrocytes throughout normal cartilage. Bars in the main parts represent 100 μm. [Color figure can be seen in the online version of this article, available at http://wileyonlinelibrary.com/journal/jcp]

volume when exposed to the higher osmotic potential solution, that is, cell shrinkage was slower, or non-existent. This could also be a consequence of the principle encapsulated by Equation (4), or it could be that cells suffered damage from the osmotic challenge. The relationship between osmotic pressure and physical pressure is an important one for the chondrocyte, since it is believed that increasing compressive loads on joints leads to increases in osmotic pressure (Mow et al., 1992; Urban, 1994). The ability of chondrocytes to withstand osmotic pressure changes is therefore coupled to their ability to withstand mechanical pressure. Indeed it has been shown that cells are more susceptible to physical damage at reduced osmolarities (Bush et al., 2005). Furthermore, chondrocytes from osteoarthritic cartilage have been shown to exhibit poor recovery from cell volume increases (Jones et al., 1999) and it has been suggested that inappropriate increases in chondrocyte volume may contribute to the progression of osteoarthritis (Bush and Hall, 2003). Maintenance of the relatively positive membrane potential may therefore be important for the function and survival of healthy chondrocytes in vivo.

Acknowledgments

The Authors would like to thank Prof. John Innes for their assistance. This work was funded by the Wellcome Trust and BBSRC.

Appendix 1

Dependence of Osmotic Swelling Upon Membrane Potential

To simulate the swelling of cells at different membrane potentials we used a variation of the equation from Zhang et al.

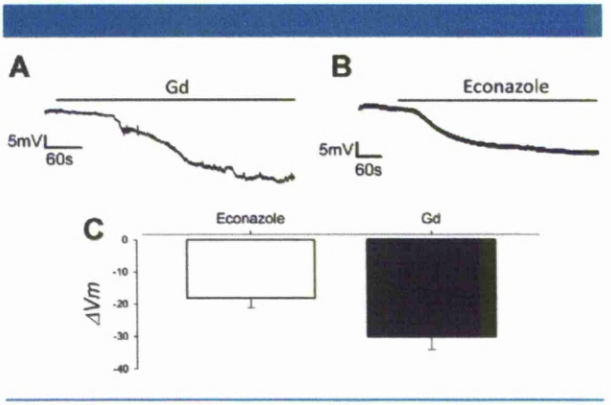

Fig. 4. Gadolinium and econazole sensitive ion channels contribute to the RMP. Block of channels by Gd (A,C) or econazole (B,C) drive the membrane potential in a negative direction. Membrane potential record during the application of (A) 100 μM Gd, and (B) 10 μM econazole. C: Summary data for; 100 μM Gd (n = 8) and 10 μM econazole (n = 5). Each of these conditions significantly shifted the membrane potential.

(1990; Preston et al., 1992), with substitutions to allow for time variable osmolarities

$$\frac{dvol}{dt} = P_f SA_{(t)} V_w (Osm_{in(t)} - Osm_{out}) \quad (5)$$

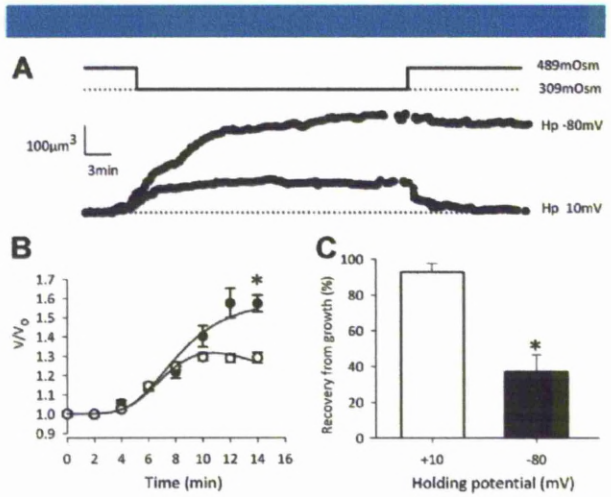

Fig. 5. The positive RMP allows chondrocytes to more effectively regulate their volume. A: Change of cell volume with time during change of osmotic potential (where indicated). Cell volume was calculated at 30 sec intervals with cells voltage-clamped at either −80 or +10 mV with single sharp electrodes under switch clamp. B: Summary of a number of data such as that illustrated in (A) but with data sampled at 120 sec intervals. Cell swelling measured at 14 min was significantly greater when cells were held at −80 than +10 mV ($P < 0.0005$, n = 7 empty circles, 10 filled circles). The fitted line is one continuous fit to $dvol/dt = P_f S_{(t)} V_w (OsM_{in(t)} - OsM_{out(t)})$ based on (Zhang et al., 1990; Preston et al., 1992), but including changes of intracellular osmolarity with time. The water permeability $P_f = 10.2 \times 10^{-4}$ cm sec^{-1}, $S_{(t)}$ the surface area and V_w the molar volume of water is 18 cm^3 mol^{-1}. Osmolarity inside and outside the cell at time t are $OsM_{in(t)}$ and $OsM_{out(t)}$, respectively. The only difference between the two fitted lines in (B) is the membrane potential. For a full explanation of the model see Appendix 1. C: On returning cells from the 309 mOsm to the 489 mOsm solution the size of cells clamped at +10 mV (n = 10) returned to near the pre-swell size whereas recovery at −80 mV (n = 12) was significantly less ($P < 0.0005$, n = 10, 12).

where P_f is the water permeability of the cell (cm sec^{-1}), $SA_{(t)}$ the surface area and the molar volume of water (V_w) is 18 cm^3 mol^{-1}. The extracellular osmolarity (Osm_{out}) is assumed to not change with time, but the osmolarity inside the cell at time t ($Osm_{in(t)}$) is given by:

$$Osm_{in(t)} = \frac{Osmol_{in(t)}}{vol_{(t)}} \quad (6)$$

where $Osmol_{in}$ is the number of moles of intracellular solute (osmol), not the osmolarity. This changes as potassium ions efflux and so the rate of change in the moles of ions within the cell is equivalent to:

$$\frac{dOsmol_{in}}{dt} = \frac{G_{Kstretch(t)}(RMP - E_{k(t)})}{eN_A} \quad (7)$$

where e is the elementary charge and N_A is the Avogadro's number. $G_{Kstretch}$ is the potassium conductance opened by stretch, this is likely to be composed of calcium activated potassium channels (Wright et al., 1992; Martina et al., 1997; Mobasheri et al., 2010). We then used the simplest relationship for activation of this conductance at time t; we assumed that:

$$G_{kstretch(t)} = \overline{G}_{Kstretch} \frac{stretch_{(t)}}{(stretch_{(t)} A)} \quad (8)$$

Stretch was calculated simply as the fractional change in surface area. $\overline{G}_{Kstretch}$ (the total stretch activated potassium conductance, 660 pS) and A (a constant of proportionality, 10^{-4} sec^{-1}) were both obtained by fitting Equation (5) (by numerical integration) to the volume data by minimizing χ^2. Additionally, for the cell to maintain electroneutrality the K^+ efflux is likely to be matched by an anionic efflux. All our simulations also included a routine to account for the time-dependent change of extracellular bath solution. This was relatively slow in some experiments (approximately 6 min), since sharp electrodes dislodge more readily than patch electrodes and we observed cells to be rather fragile when maintained at very hyperpolarized potentials. The only parameter changed between the simulations at −80 and +10 mV is the RMP parameter in Equation (7).

Literature Cited

Abramoff MD, Magelhaes PJ, Ram SJ. 2004. Image processing with imagej. Biophoton Int 11:36–42.

Ahern BJ, Parvizi J, Boston R, Schaer TP. 2009. Preclinical animal models in single site cartilage defect testing: A systematic review. Osteoarthritis Cartilage 17:705–713.

Alexander SPH, Mathie A, Peters JA. 2008. Guide to receptors and channels (grac), 3rd edition. Br J Pharmacol 153:S1–S209.

Apell HJ, Bersch B. 1987. Oxonol vi as an optical indicator for membrane potentials in lipid vesicles. Biochim Biophys Acta 903:480–494.

Archer CW, Francis-West P. 2003. The chondrocyte. Int J Biochem Cell Biol 35:401–404.

Barrett-Jolley R, Pyner S, Coote JH. 2000. Measurement of voltage-gated potassium currents in identified spinally-projecting sympathetic neurones of the paraventricular nucleus. J Neurosci Methods 102:25–33.

Barry PH, Lynch JW. 1991. Liquid junction potentials and small cell effects in patch-clamp analysis. J Membr Biol 121:101–117.

Benya PD, Shaffer JD. 1982. Dedifferentiated chondrocytes reexpress the differentiated collagen phenotype when cultured in agarose gels. Cell 30:215–224.

Bruce G, Barrett-Jolley R, Morris R. 2009. P2y activation affects the excitability of murine epidermal primary afferents through modulation of the kv7-mediated m-current. Proc Physiol Soc 15:C44.

Bush PG, Hall AC. 2001a. The osmotic sensitivity of isolated and in situ bovine articular chondrocytes. J Orthop Res 19:768–778.

Bush PG, Hall AC. 2001b. Regulatory volume decrease (rvd) by isolated and in situ bovine articular chondrocytes. J Cell Physiol 187:304–314.

Bush PG, Hall AC. 2003. The volume and morphology of chondrocytes within non-degenerate and degenerate human articular cartilage. Osteoarthritis Cartilage 11:242–251.

Bush PG, Hodkinson PD, Hamilton GL, Hall AC. 2005. Viability and volume of in situ bovine articular chondrocytes–changes following a single impact and effects of medium osmolarity. Osteoarthritis Cartilage 13:54–65.

Clapham DE. 2007. Snapshot: Mammalian trp channels. Cell 129:220–220.

Clark RB, Hatano N, Kondo C, Belke DD, Brown BS, Kumar S, Votta BJ, Giles WR. 2010. Voltage-gated K+ currents in mouse articular chondrocytes regulate membrane potential. Channels 4:179–191.

Clarke KA, Smart L, Still J. 2001. Ground reaction force and spatiotemporal measurements of the gait of the mouse. Behav Res Methods Instrum Comput 33:422–426.

Davies LM, Purves GI, Barrett-Jolley R, Dart C. 2010. Interaction with caveolin-1 modulates vascular atp-sensitive potassium (katp) channel activity. J Physiol 588:3255–3266.
Eckstein F, Tieschky M, Faber S, Englmeier KH, Reiser M. 1999. Functional analysis of articular cartilage deformation, recovery, and fluid flow following dynamic exercise in vivo. Anat Embryol (Berl) 200:419–424.
Frisbie DD, Cross MW, McIlwraith CW. 2006. A comparative study of articular cartilage thickness in the stifle of animal species used in human pre-clinical studies compared to articular cartilage thickness in the human knee. Vet Comp Orthop Traumatol 19:142–146.
Funabashi K, Fujii M, Yamamura H, Ohya S, Imaizumi Y. 2010a. Contribution of chloride channel conductance to the regulation of resting membrane potential in chondrocytes. J Pharmacol Sci 113:94–99.
Funabashi K, Ohya S, Yamamura H, Hatano N, Muraki K, Giles W, Imaizumi Y. 2010b. Accelerated Ca2+ entry by membrane hyperpolarization due to Ca2+-activated K+ channel activation in response to histamine in chondrocytes. Am J Physiol Cell Physiol 298:C786–C797.
Hall AC, Starks I, Shoults CL, Rashidbigi S. 1996. Pathways for K+ transport across the bovine articular chondrocyte membrane and their sensitivity to cell volume. Am J Physiol 270:C1300–C1310.
Hodge WA, Fijan RS, Carlson KL, Burgess RG, Harris WH, Mann RW. 1986. Contact pressures in the human hip joint measured in vivo. Proc Natl Acad Sci USA 83:2879–2883.
Hoffmann E, Dunham P. 1995. Membrane mechanisms and intracellular signalling in cell volume regulation. Int Rev Cytol 161:173–262.
Hoffmann EK, Lambert IH, Pedersen SF. 2009. Physiology of cell volume regulation in vertebrates. Physiol Rev 89:193–277.
Huber M, Trattnig S, Lintner F. 2000. Anatomy, biochemistry, and physiology of articular cartilage. Invest Radiol 35:573–580.
Huberti HH, Hayes WC. 1984. Patellofemoral contact pressures. The influence of q-angle and tendofemoral contact. J Bone Joint Surg Am 66:715–724.
Jakob M, Demarteau O, Schafer D, Hintermann B, Dick W, Heberer M, Martin I. 2001. Specific growth factors during the expansion and redifferentiation of adult human articular chondrocytes enhance chondrogenesis and cartilaginous tissue formation in vitro. J Cell Biochem 81:368–377.
Jones WR, Ting-Beall HP, Lee GM, Kelley SS, Hochmuth RM, Guilak F. 1999. Alterations in the young's modulus and volumetric properties of chondrocytes isolated from normal and osteoarthritic human cartilage. J Biomech 32:119–127.
Martin I, Vunjak-Novakovic G, Yang J, Langer R, Freed LE. 1999. Mammalian chondrocytes expanded in the presence of fibroblast growth factor 2 maintain the ability to differentiate and regenerate three-dimensional cartilaginous tissue. Exp Cell Res 253:681–688.
Martina M, Mozrzymas JW, Vittur F. 1997. Membrane stretch activates a potassium channel in pig articular chondrocytes. Biochim Biophys Acta 1329:205–210.
McCutchen CW. 1962. The frictional properties of animal joints. Wear 5:1–17.
Mobasheri A, Gent TC, Womack MD, Carter SD, Clegg PD, Barrett-Jolley R. 2005. Quantitative analysis of voltage-gated potassium currents from primary equine (*Equus caballus*) and elephant (*Loxodonta africana*) articular chondrocytes. Am J Physiol Regul Integr Comp Physiol 289:R172–R180.
Mobasheri A, Gent TC, Nash AI, Womack MD, Moskaluk CA, Barrett-Jolley R. 2007. Evidence for functional ATP-sensitive (K(ATP)) potassium channels in human and equine articular chondrocytes. Osteoarthritis Cartilage 15:1–8.
Mobasheri A, Lewis R, Maxwell JEJ, Hill C, Womack M, Barrett-Jolley R. 2010. Characterization of a stretch-activated potassium channel in chondrocytes. J Cell Physiol 223:511–518.
Mow VC, Ratcliffe A, Robin Poole A. 1992. Cartilage and diarthrodial joints as paradigms for hierarchical materials and structures. Biomaterials 13:67–97.
Mow VC, Wang CC, Hung CT. 1999. The extracellular matrix, interstitial fluid and ions as a mechanical signal transducer in articular cartilage. Osteoarthritis Cartilage 7:41–58.
Nilius B, Prenen J, Vennekens R, Hoenderop JG, Bindels RJ, Droogmans G. 2001. Pharmacological modulation of monovalent cation currents through the epithelial Ca2+ channel ecac1. Br J Pharmacol 134:453–462.
Owsianik G, Talavera K, Voets T, Nilius B. 2006. Permeation and selectivity of trp channels. Ann Rev Physiol 68:685–717.
Preston GM, Carroll TP, Guggino WB, Agre P. 1992. Appearance of water channels in xenopus oocytes expressing red-cell chip28 protein. Science 256:385–387.
Sampson LJ, Davies LM, Barrett-Jolley R, Standen NB, Dart C. 2007. Angiotensin ii-activated protein kinase c targets caveolae to inhibit aortic ATP-sensitive potassium channels. Cardiovasc Res 76:61–70.
Schulze-Tanzil G, Mobasheri A, de Souza P, John T, Shakibaei M. 2004. Loss of chondrogenic potential in dedifferentiated chondrocytes correlates with deficient shc-erk interaction and apoptosis. Osteoarthritis Cartilage 12:448–458.
Setterbo JJ, Garcia TC, Campbell IP, Reese JL, Morgan JM, Kim SY, Hubbard M, Stover SM. 2009. Hoof accelerations and ground reaction forces of thoroughbred racehorses measured on dirt, synthetic, and turf track surfaces. Am J Vet Res 70:1220–1229.
Sivan S, Neidlinger-Wilke C, Wurtz K, Maroudas A, Urban JP. 2006. Diurnal fluid expression and activity of intervertebral disc cells. Biorheology 43:283–291.
Stockwell RA. 1971. The interrelationship of cell density and cartilage thickness in adult mammalian articular cartilage. J Anat 109:411–421.
Stockwell RA. 1991. Cartilage failure in osteoarthritis: Relevance of normal structure and function. A review. Clin Anat 4:161–191.
Sugimoto T, Yoshino M, Nagao M, Ishii S, Yabu H. 1996. Voltage-gated ionic channels in cultured rabbit articular chondrocytes. Comp Biochem Physiol C Pharmacol Toxicol Endocrinol 115:223–232.
Tsuga K, Tohse N, Yoshino M, Sugimoto T, Yamashita T, Ishii S, Yabu H. 2002. Chloride conductance determining membrane potential of rabbit articular chondrocytes. J Membr Biol 185:75–81.
Urban JP. 1994. The chondrocyte: A cell under pressure. Br J Rheumatol 33:901–908.
Vennekens R, Hoenderop JGJ, Prenen J, Stuiver M, Willems PHGM, Droogmans G, Nilius B, Bindels RJM. 2000. Permeation and gating properties of the novel epithelial Ca2+ channel. J Biol Chem 275:3963–3969.
Vennekens R, Prenen J, Hoenderop JG, Bindels RJ, Droogmans G, Nilius B. 2001. Pore properties and ionic block of the rabbit epithelial calcium channel expressed in hek 293 cells. J Physiol 530:183–191.
Voets T, Prenen J, Vriens J, Watanabe H, Janssens A, Wissenbach U, Bodding M, Droogmans G, Nilius B. 2002. Molecular determinants of permeation through the cation channel trpv4. J Biol Chem 277:33704–33710.
Wilson JR, Duncan NA, Giles WR, Clark RB. 2004. A voltage-dependent K+ current contributes to membrane potential of acutely isolated canine articular chondrocytes. J Physiol (London) 557:93–104.
Wohlrab D, Wohlrab J, Reichel H, Hein W. 2001. Is the proliferation of human chondrocytes regulated by ionic channels? J Orthop Sci 6:155–159.
Womack MD, Morris R, Gent TC, Barrett-Jolley R. 2007. Substance p targets sympathetic control neurons in the paraventricular nucleus. Circ Res 100:1650–1658.
Wright MO, Stockwell RA, Nuki G. 1992. Response of plasma membrane to applied hydrostatic pressure in chondrocytes and fibroblasts. Connect Tissue Res 28:49–70.
Xu X, Urban JP, Tirlapur UK, Cui Z. 2010. Osmolarity effects on bovine articular chondrocytes during three-dimensional culture in alginate beads. Osteoarthritis Cartilage 18:433–439.
Zhang R, Logee KA, Verkman AS. 1990. Expression of messenger-RNA coding for kidney and red-cell water channels in xenopus oocytes. J Biol Chem 265:15375–15378.

frontiers in
PHYSIOLOGY

PERSPECTIVE ARTICLE
published: 14 October 2010
doi: 10.3389/fphys.2010.00135

The emerging chondrocyte channelome

Richard Barrett-Jolley[1], Rebecca Lewis[1], Rebecca Fallman[1] and Ali Mobasheri[2]*

[1] Musculoskeletal Research Group, Department of Comparative Molecular Medicine, School of Veterinary Science, University of Liverpool, Liverpool, UK
[2] Musculoskeletal Research Group, Division of Veterinary Medicine, School of Veterinary Medicine and Science, Faculty of Medicine and Health Sciences, University of Nottingham, Nottingham, Leicestershire, UK

Edited by:
Antonio Felipe, Universitat de Barcelona, Spain

Reviewed by:
Carmen Valenzuela, Instituto de Investigaciones Biomédicas CSIC-UAM, Spain
Peter Larsson, University of Miami School of Medicine, USA

***Correspondence:**
Ali Mobasheri, Faculty of Medicine and Health Sciences, School of Veterinary Medicine and Science, University of Nottingham, Sutton Bonington Campus, Sutton Bonington, Nottingham, Leicestershire LE12 5RD, UK.
e-mail: ali.mobasheri@nottingham.ac.uk

Chondrocytes are the resident cells of articular cartilage and are responsible for synthesizing a range of collagenous and non-collagenous extracellular matrix macromolecules. Whilst chondrocytes exist at low densities in the tissue (1–10% of the total tissue volume in mature cartilage) they are extremely active cells and are capable of responding to a range of mechanical and biochemical stimuli. These responses are necessary for the maintenance of viable cartilage and may be compromised in inflammatory diseases such as arthritis. Although chondrocytes are non-excitable cells their plasma membrane contains a rich complement of ion channels. This diverse channelome appears to be as complex as one might expect to find in excitable cells although, in the case of chondrocytes, their functions are far less well understood. The ion channels so far identified in chondrocytes include potassium channels (K_{ATP}, BK, K_v and SK), sodium channels (epithelial sodium channels, voltage activated sodium channels), transient receptor potential calcium or non-selective cation channels and chloride channels. In this review we describe this emerging channelome and discuss the possible functions of a range of chondrocyte ion channels.

Keywords: chondrocyte, K_v channel, K_{ATP} channel, BK (MaxiK) channel, ENaC

INTRODUCTION

Chondrocytes are metabolically active cells found in mature articular cartilage (Iannotti, 1990; Archer and Francis-West, 2003). The extracellular matrix (ECM) of cartilage is composed of elastic and collagen fibers (mainly type II collagen), which provide tensile strength with embedded proteoglycans forming a gel-like ground substance that provides elasticity and the ability to resist compressive forces (Buckwalter and Mankin, 1998). Chondrocytes occur singularly or in groups or clusters of three or more cells within spaces called lacunae in the ECM (Stockwell, 1975). Articular cartilage has a high matrix to cell ratio, with chondrocytes occupying only 10% of the total tissue in mammals (Carney and Muir, 1988). Articular cartilage is a type of hyaline cartilage that covers the surface of bones which meet at a synovial joint (Mankin, 1982). Synovial joints include a cavity between the bones within the articular capsule in order to allow free movement (Edwards et al., 1994). The synovial cavity contains synovial fluid, which acts as a lubricant to decrease friction between the bones meeting at the synovial joint and absorbs shock. Friction would be undesirable because it would damage the joint and also generate heat, thereby causing pain (Tatari, 2007). Articular cartilage is avascular without a perichondrium connective tissue surround. In human articular cartilage, chondrocytes may be as far away as 3 mm from the nearest artery. Therefore, synovial fluid supplies chondrocytes in adult articular cartilage with oxygen and nutrients, and removes carbon dioxide and metabolic waste products, by diffusion (Lee and Urban, 1997; Allan, 1998). Synovial fluid is periodically washed over the surface of the articular cartilage by the movement of the joint (Lee and Urban, 1997). Oxygen and substrate concentrations within cartilage reduce near to the cartilage-bone margin to almost zero (Otte, 1991). Therefore, chondrocytes generate ATP by substrate-level phosphorylation during anaerobic respiration, leading to the accumulation of lactate and lowering of the pH through the production of H^+ ions, which can continue in anoxic conditions (Lee and Urban, 1997). The extracellular pH affects the chondrocyte metabolism and its ability to synthesize matrix. Low pH reduces lactate production, but also slows down the synthesis of glycosaminoglycans. However, the rate of collagen synthesis appears to be independent of pH (Wu et al., 2007). Chondrocytes embedded within the ECM have an unusual ionic environment because they are surrounded by negatively charged proteoglycans, which attract large numbers of cations, such as Na^+ ions, creating a high extracellular osmolarity and contributing to the low pH (Urban et al., 1993).

Chondrocyte primary function is to synthesize and secrete proteoglycans, collagen and non-collagenous proteins to maintain the cartilage ECM (Fassbender, 1987). Chondrocytes maintain cartilage by establishing a balance between replacing degraded

Abbreviations: ASIC, acid sensing ion channel; BK, calcium-activated potassium channel, high conductance; CFTR, cystic fibrosis transmembrane conductance regulator; ClC, chloride channel; DEG, degenerin; ECM, extracellular matrix; ENaC, epithelial sodium channels; IC50, concentration causing 50% inhibition; K_{ATP}, ATP dependent potassium channel; $K_{(Ca)}$, calcium activated potassium channels; Kir, inwardly rectifying potassium channel; K_v, voltage-gated potassium channel; MIP, major intrinsic protein; NMDA, *N*-methyl D-aspartate; PCR, polymerase chain reaction; RMP, resting membrane potential; SERCA, sarco/endoplasmic reticulum Ca^{2+}-ATPase; SITS, 4-acetamido-4′-isothiocyanatostilbene-2,2-disulfonic acid; SK, calcium-activated potassium channel, low conductance; SUR, sulfonylurea receptor; TEA, tetraethylammonium; TRP, transient receptor potential channel; TTX, tetrodotoxin; VGCC, voltage-gated calcium channels; VGSC, voltage-gated sodium channel

macromolecules and increasing synthesis in response to injury (Martin and Buckwalter, 2000). Proteoglycans contribute to cartilage rigidity, stability and durability during compression (Redini, 2001). Types II, IX, and XI collagen form the tensile fibril networks within cartilage. Type VI collagens form adjacent to chondrocytes and may be involved in attachment of the chondrocyte to the ECM (Bruckner and van der Rest, 1994). Non-collagenous proteins, such as anchorin CII, are also involved in chondrocyte anchorage (Fernandez et al., 1990). The cartilage matrix protects chondrocytes from mechanical stress placed on the joint (Buckwalter and Mankin, 1998; Martin and Buckwalter, 2000). Chondrocyte metabolic activity is directly correlated with the weight of mechanical stress placed on the cartilage; increased activity when the cartilage is heavily loaded provides maximum proteoglycan content (Urban, 1994). The ability of articular cartilage to withstand and respond to pressure and shearing forces is vital for it to fulfill its function. Accumulating evidence suggests that the resting membrane potential (RMP) is vital for fulfilling this function. The RMP has been shown to be central to the secretion and synthesis of substances in a variety of other cell types (Breittmayer et al., 1996; McCarty, 1999; Penyige et al., 2002). It therefore seems likely that if the RMP of chondrocytes is changed by ion channel manipulation, their ability to produce ECM will be compromised. This conjecture is indeed supported by experiments where RMP modifying ion channel blockers reduced the production of matrix mRNAs (Wu and Chen, 2000), proteins and sulfated glycosaminoglycans (Mouw et al., 2007). Chondrocyte proliferation is also inhibited by channel blockers lidocaine and verapamil (Wohlrab et al., 2001, 2005) and apoptosis increased (Grishko et al., 2010). As with other cells, the chondrocyte RMP is determined by the balance of positive and negative ion permeabilities in the cell membrane (Hodgkin and Huxley, 1952a). These permeabilities are, in turn, controlled by the chondrocyte channelome (the complement of expressed ion channels and porins).

Ion channels are the essential components that control ion movement in and out of the cell (Hodgkin and Huxley, 1952a). They are embedded within the plasma membrane and usually consist of one or more proteins with a central aqueous pore, which opens by conformational change (Neher and Sakmann, 1992). The stimulus for opening (gating) is specific to each ion channel, and may be voltage, chemically or mechanically induced (Hille, 2001). A number of studies have now shown the presence of an ever-expanding list of ion channels in chondrocytes (**Figure 1**), and this review will summarize the data to date, both on the variety of expression and the proposed roles of these channels.

K_v CHANNELS

One of the first discovered ion conductances in biology was the potassium delayed rectifier (Hodgkin and Huxley, 1952b; Ramage et al., 2008). The ion channels underlying this are now known to be

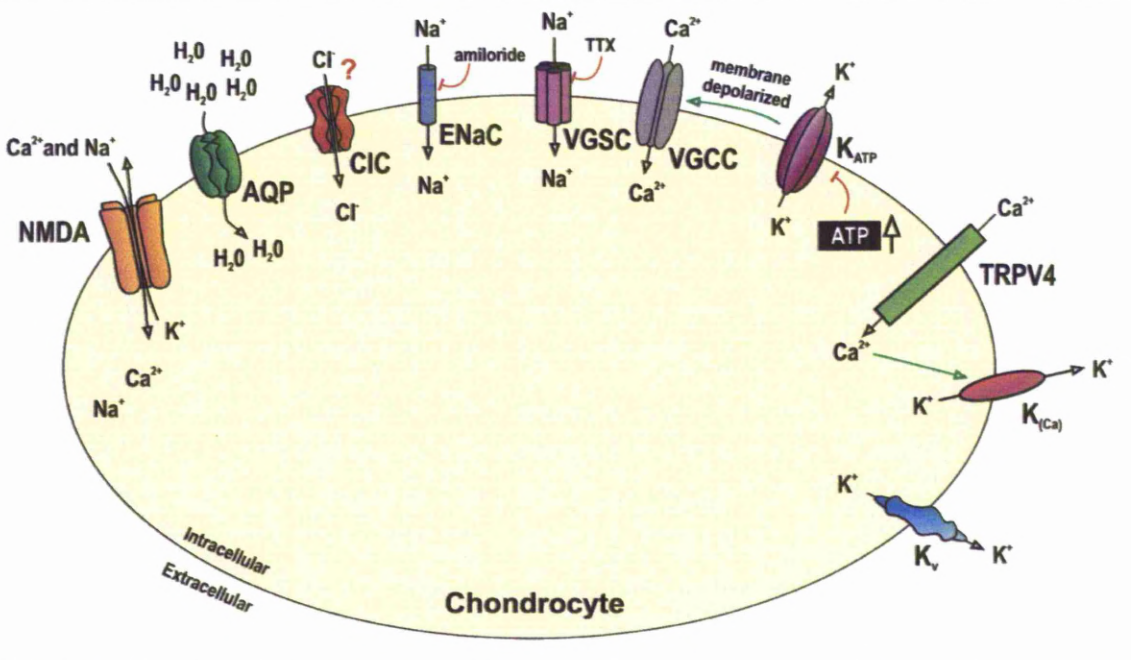

FIGURE 1 | Summary of the chondrocyte channelome. Many studies have now identified ion channels and porins in chondrocytes. Frequently the function of these channels is either unknown or controversial. This figure illustrates some of the major channel proteins identified to date, either by electrophysiological, immunological or molecular biological techniques. Note in this figure, $K_{(Ca)}$ is taken to be equivalent to any calcium activated potassium channel including BK and SK. AQP, aquaporin channel; BK, calcium-activated potassium cannel, high conductance; ClC, chloride channel; ENaC, epithelial sodium channels; K_{ATP}, ATP dependent potassium channel; Kv, voltage-gated potassium channel; NMDA, *N*-methyl D-aspartate; SK, calcium-activated potassium channel, low conductance; TRP, transient receptor potential channel; VGCC, voltage-gated calcium channels; VGSC, voltage-gated sodium channel; This data is summarized more fully in **Table 1**. For references please see text and or **Table 1**.

members of the K_v potassium channel family. This family is one of the largest ion channel families with at least 40 members (Gutman et al., 2005) of six transmembrane domains. Interestingly these were also one of the earliest ion channels discovered in chondrocytes (Walsh et al., 1992; Sugimoto et al., 1996). K_v channels have now been reported in chondrocytes by a number of authors and have been shown to be archetypal slowly inactivating ion channels (Walsh et al., 1992; Wilson et al., 2004; Mobasheri et al., 2005a; Ponce, 2006). In essence, these channels are very similar to those channels found in skeletal muscle (Pallotta and Wagoner, 1992) and in neurones (Barrett-Jolley et al., 2000) where, in those cell types, they are critical for repolarization of the membrane following an action potential. The role of a delayed rectifier channel in the chondrocyte plasma membrane is far less clear. Since the chondrocyte exists at far more depolarized levels than neurones or skeletal muscle (Wright et al., 1992; Wilson et al., 2004), logic would suggest that these channels would be constantly inactivated. Close study of the mathematical relationship between voltage, time and fractional inactivation (Hodgkin and Huxley, 1952b) reveals that a certain, albeit small, proportion of these channels will remain active even at the relatively depolarized RMP of a chondrocyte. This is supported by the observation by Wilson et al. (2004) and Clark et al. (2010b) that TEA inhibition of the potassium channels does have a significantly depolarizing effect on chondrocyte RMP, as it does with other non-excitable cells such as those of smooth muscle (Telezhkin et al., 2001; Park et al., 2007).

Relatively few studies have attempted to establish the molecular identity of the delayed rectifier in chondrocytes. However, reports suggest that these channels are similar between species (chicken, canine, equine, and elephant) in terms of their steady-state half-activation voltage and slope (Wilson et al., 2004; Mobasheri et al., 2005a; Ponce, 2006). Half activation parameters range from 12 to 25 mV; typical of K_v 1.x or K_v 4.x potassium channels (Coetzee et al., 1999). Activation time constants are, however, quite fast compared with many K_v channels (Mobasheri et al., 2005a). Such rapid kinetics have been reported for members of the K_v 1.x family and also homomeric K_v 3.4 (Coetzee et al., 1999). The inactivation time constant in the order of seconds (Mobasheri et al., 2005a) is typical of K_v 1.x, K_v 2.x and K_v 3.x channels (Coetzee et al., 1999). Together these data suggested that the potassium channel of chondrocytes is likely to be a member of the K_v 1.x. Pharmacological data are discussed in (Mobasheri et al., 2005a) and are not entirely consistent for K_v 1.x channels or one particular K_v channel. We therefore feel that the key, published data identifying the subunit identity of the chondrocyte K_v channels are the immunohistochemical and RT-PCR data. Such data have unequivocally revealed the presence of K_v 1.4 subunits in equine chondrocytes (Mobasheri et al., 2005a) and K_v 1.6 in the mouse (Clark et al., 2010b). Since K_v channels are known to exist as functional heteromultimers (Villalonga et al., 2010) we would tentatively suggest that articular chondrocytes may express K_v 1.x, probably as a heteromultimer including the K_v 1.4 or K_v 1.6 subunits and probably some other, as yet unidentified, K_v subunit(s).

INWARDLY RECTIFYING POTASSIUM CHANNELS

Study of inwardly rectifying potassium channels is greatly hampered by a lack of selective inhibitors. Barium and chloroethylclonidine are inhibitors of the strong inward rectifiers (Standen and Stanfield, 1978; Barrett-Jolley et al., 1999) and glibenclamide is an inhibitor of ATP dependent potassium channels (Tomai et al., 1994). So far only K_{ATP} channels have been observed in chondrocytes (Mobasheri et al., 2007). K_{ATP} channels are a widely expressed subfamily of inwardly rectifying potassium channels. These channels are closed by intracellular ATP and thus serve to couple metabolism to membrane excitability (Quayle et al., 1997; Ashcroft and Gribble, 1998; Minami et al., 2004). Structurally these channels exist as heteromultimers. Each functioning protein consists of four ATP binding cassette proteins (SUR) surrounding four inwardly rectifying potassium channel subunits (Kir 6.x) (Babenko et al., 1998). Of particular interest to investigators of chondrocyte function is the fact that, in addition to being opened by decreasing intracellular ATP (**Figure 2**), K_{ATP} channels are also frequently observed to be opened by low oxygen tension and hypoxia (Dart and Standen, 1994). This suggests that these channels are important in hypoxia-mediated cell signaling (Phillis, 2004). We showed recently that K_{ATP} channels were expressed in articular chondrocytes (Mobasheri et al., 2007). We used polyclonal antibodies raised against the K_{ATP} channel to show expression in both human and equine chondrocytes. Expression was largely restricted to the superficial and middle zones of normal cartilage and the superficial zone of fibrillated osteoarthritic cartilage in clusters (Mobasheri et al., 2007). In patch-clamp studies we found the biophysical properties of K_{ATP} channels to be broadly similar to K_{ATP} channels expressed elsewhere (Babenko et al., 1998; Mobasheri et al., 2007). Several K_{ATP} subtypes (i.e., Kir 6.1 and Kir 6.2) are each potentially coupled with one of the SUR subtypes; SUR1, 2A or 2B (Babenko et al., 1998). Pharmacological properties of K_{ATP} channels are thus very different between tissues. Glibenclamide is sometimes used as a functional discriminator between K_{ATP} subtypes. It is highly active in pancreatic β-cells (IC50 of <10 nM, Krause et al., 1995), but rather less potent in muscle (IC50 25–100 nM, Beech et al., 1993; Barrett-Jolley and Davies, 1997; Barrett-Jolley and McPherson, 1998). In pharmacological studies of chondrocytes, the K_{ATP} channel's IC50 is within the range seen in muscle (Mobasheri et al., 2007). It therefore seems highly likely that chondrocytes express at least one subtype of K_{ATP} channel and that these may be important for regulation of cartilage metabolism and sensing ATP levels within the cell (Mobasheri et al., 2005b).

LARGE CALCIUM-ACTIVATED POTASSIUM CHANNELS

Several studies have putatively identified BK channels in chondrocytes (Grandolfo et al., 1990, 1992; Long and Walsh, 1994; Martina et al., 1997; Mozrzymas et al., 1997; Mobasheri et al., 2010). In our own study (Mobasheri et al., 2010), the principal stretch-activated channel we identified had a slope conductance, reversal potential, and pharmacology consistent with it being a large calcium-activated potassium channel (BK) (Latorre et al., 1989; Cui et al., 2009). We found the sensitivity to iberiotoxin to be statistically significant but weak (Mobasheri et al., 2010). This is interesting because whilst the BK channel can exist as a standalone six trans-membrane α-subunit, complete with potassium conducting pore and Ca^{2+} sensor (Wang and Sigworth, 2009), the presence or absence of a β-subunit determines many of the channel's functional properties (Salkoff et al., 2006; Torres et al., 2007). In particular, low sensitivity to iberiotoxin is highly characteristic of the expression of

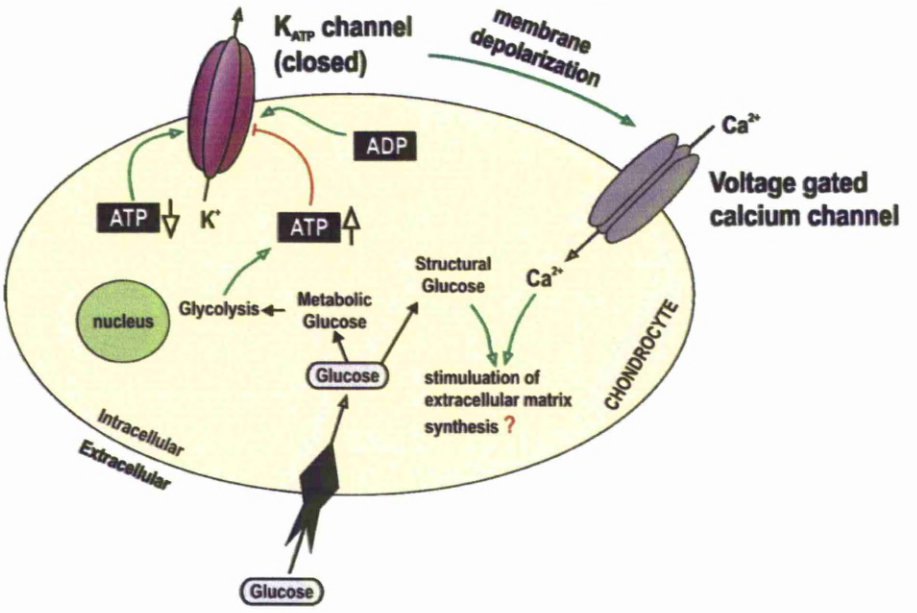

FIGURE 2 | K_{ATP} channels in chondrocytes. Chondrocytes have been shown to express K_{ATP} channels. The function of these is generally accepted to be coupling metabolic status with membrane potential and thus cell activity. In other cell types, endogenous triggers for activation of K_{ATP} include decrease of intracellular ATP (Babenko et al., 1998), increase in ADP (Dunne and Petersen, 1986), extracellular hypoxia (Dart and Standen, 1994) or other chemical signals such as adenosine (Dart and Standen, 1993; Barrett-Jolley et al., 1996), angiotensin (Sampson et al., 2007) etc., K_{ATP}, ATP dependent potassium channel.

BK channels consisting of both the α1 and β1-subunits (Lippiat et al., 2003). This correlated well with our identification of positive immunohistochemical staining of normal articular cartilage samples with antibodies to both α1 and β1-subunits.

In general terms, there appear to be two possibilities to explain the activation of BK channels by stretch. These could be termed either calcium dependent or calcium independent mechanisms. The calcium dependent hypothesis would require that stretch led to an increase in intracellular Ca^{2+} and that this activated the BK channel (**Figure 3**). Indeed a number of studies show changes in intracellular Ca^{2+} with osmotic or other mechanical challenge (Grandolfo et al., 1998; Guilak et al., 1999; Yellowley et al., 2002; Sanchez et al., 2003; Sanchez and Wilkins, 2004). The source of such Ca^{2+} is controversial, but potentially, dogma states that it must come from either influx (e.g., a channel or other transporter protein Sanchez et al., 2003; Sanchez and Wilkins, 2004; Phan et al., 2009) or from intracellular stores (e.g., Grandolfo et al., 1998). The calcium independent hypothesis would involve either direct sensing of stretch by the channel itself, or coupling of the channel to other mechanoreceptors such as integrins (Mobasheri et al., 2002). The function of BK activation by stretch is still unknown, but there are a few clear possibilities. Firstly, the BK channel could be acting as an "osmolyte" channel (Hall et al., 1996; Kerrigan and Hall, 2008), since activation of potassium conductances will allow potassium ions to leave, decrease intracellular osmotic potential and facilitate regulatory volume decrease. Secondly, it is possible that it is the influence of the BK channel on the membrane potential which is critical, as it is in vascular tissue (Ledoux et al., 2006).

SMALL CALCIUM-ACTIVATED POTASSIUM CHANNELS

In addition to the body of work showing the presence of BK channels, there have also been a few reports of SK activity in chondrocytes (Wright et al., 1996; Lee et al., 2000; Ramage et al., 2008; Funabashi et al., 2010b). In the study by Wright et al. (1996), osmotic shock led to a hyperpolarization, which was largely insensitive to iberiotoxin, but highly sensitive to the SK channel inhibitor, apamin. Interestingly, in our own study of stretch activated potassium channels in chondrocytes (Mobasheri et al., 2010), whilst single channel studies clearly identified BK channels, the hypo-osmotic hyperpolarization was resistant to the low concentrations of TEA which would be expected to block BK channels. The hyperpolarization was, however, inhibited by symmetrical 10 mM TEA. This was an observation consistent with the original observations of an SK component to the hyperpolarization shown by Wright et al. (1996), since both SK and BK are rather resistant to extracellular TEA (Latorre et al., 1989).

TRANSIENT RECEPTOR POTENTIAL CHANNELS

Transient receptor potential (TRP) channels are a family of loosely related ion channels that show relatively little selectivity between permeable cations such as sodium, calcium, and magnesium[1]. They were initially proposed to couple hypo-osmotic shock to intracellular Ca^{2+} mobilization in chondrocytes on the basis of gadolinium sensitivity (Sanchez et al., 2003), but since then several

[1] Transient receptor potential channels. Authors: David E. Clapham, Bernd Nilius, Grzegorz Owsianik. Last modified on 2010-04-07. Accessed on 2010-06-24. IUPHAR database (IUPHAR-DB), http://www.iuphar-db.org/DATABASE/FamilyMenuForward?familyId=78.

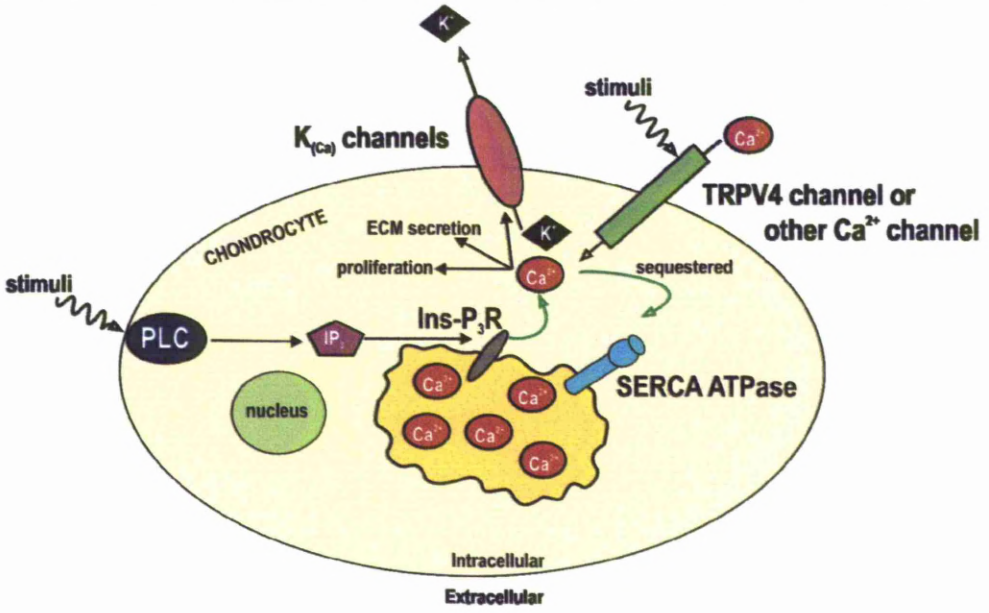

FIGURE 3 | Activation of BK by calcium ions. A number of studies have identified BK channels in chondrocytes (see text), but the function of these channels is not confirmed. Control of RMP or volume would are two theories. It is suggested that they are activated by calcium ions, which could be introduced to the cytoplasm by either release from stores, or by entry through divalent cation permeant ion channels. Both of these pathways could in turn, be activated by either mechanical or other (e.g., inflammatory) signals. ECM, extracellular matrix; Ins-P3-R, inositol trisphosphate receptor; IP3, inositol trisphosphate; $K_{(Ca)}$, calcium activated potassium channels; PLC, phospholipase C; SERCA, sarco/endoplasmic reticulum Ca 2+-ATPase; TRP, transient receptor potential channel.

TRP channels have been identified in osteoarthritic cartilage by PCR (Gavenis et al., 2009). TRPV4 has also been identified in both porcine and canine chondrocytes (Phan et al., 2009; Lewis et al., 2010) by PCR. TRPV4 is an established stretch activated channel and is widely regarded to be a conduit for stretch-activated entry of calcium ions (Nilius et al., 2004). TRPV4 has been shown to be a regulator of the chondrogenic SOX9 pathway (Muramatsu et al., 2007) and the deficiency of TRPV4 in knockout mice leads to a loss of Ca^{2+} response to hypo-osmotic challenge and the onset of osteoarthritic changes (Clark et al., 2010a). Thus, it may be that by linking chondrocyte membrane stretch to calcium mobilization TRPV4 is key to regulation of chondrogenesis, activation of calcium activated potassium channels and volume regulation.

VOLTAGE-GATED CALCIUM CHANNELS

Voltage-gated calcium channels (VGCC) are a group of calcium permeable voltage-gated ion channels found in excitable cells (e.g., muscle, glial cells, neurones, etc., Goldin, 2001; Dolphin, 2009). The presence of L-type VGCCs was suggested by Wright et al. (1996) on the basis of pharmacological inhibition of calcium dependent hyperpolarization by somatostatin and cadmium. It should be noted that whilst this is a plausible hypothesis, both somatostatin and cadmium affect a range of other ion channels including transient receptor potential channels (Carlton et al., 2004; Alexander et al., 2008), which may be present in chondrocytes. Ultrastructural studies have confirmed the presence of L-type VGCCs in mouse limb bud chondrocytes (Shakibaei and Mobasheri, 2003). These channels appear to be organized around β-1 integrin receptors with kinases and cytoskeletal complexes in close proximity. The presence of L-type (and T-type) calcium channels in chondrocytes was recently supported by Mancilla et al. (2007), however, (Sanchez and Wilkins, 2004) found that osmotically induced changes in intracellular calcium ions were *not* influenced by more selective L-type calcium channel blockers (including verapamil). In contrast aggrecan and collagen synthesis induced by electrical stimulation of cartilage is dependent upon the activity of VGCCs (Xu et al., 2009). Clearly, further evidence for the presence of this channel is needed to clarify these data.

VOLTAGE-GATED SODIUM CHANNELS (VGSC)

Voltage-gated sodium channels (VGSC) are integral membrane proteins that are activated in response to voltage-changes across the plasma membrane (Catterall, 1991, 1992, 1995, 2002). The presence of tetrodotoxin sensitive VGSC in rabbit chondrocytes has been reported by Sugimoto et al. (1996) and in chondrocytes from osteoarthritic cartilage by Ramage et al. (2008). It would be interesting to see how the expression of this channel fits into the control of the chondrocyte membrane potential, since current studies have failed to observe sufficient hyperpolarization of chondrocytes for a typical VGSC to be substantially reactivated. Under conditions of constant depolarization, for example, these channels would be permanently inactivated.

EPITHELIAL SODIUM CHANNELS

Epithelial sodium channels (ENaC) have been identified in chondrocytes both immunohistochemically (Trujillo et al., 1999) and functionally (Lewis et al., 2008). They are members of the

degenerin (DEG) and ENaC superfamily (Mano et al., 2009). ENaC is a heteromeric channel, formed of up to four subunits; α, β, δ, and γ (Canessa et al., 1994). Using immunohistochemistry, the α and β subunits have been shown to be present in chondrocytes (Trujillo et al., 1999). ENaCs are significantly more permeable to sodium than potassium (Eaton et al., 1995) and are sensitive to the channel inhibitor amiloride (IC50 100–200 nM; Alexander et al., 2008). The ENaCs main function in the kidney, bladder, and colon is control of sodium reabsorption (Rossier et al., 2002). They are found in lung tissue (Mall et al., 1998) and the taste buds (Lindemann, 2001) and are known to regulate blood volume and pressure through sodium balance in the cardiac system (Canessa et al., 1993). ENaC is known to have roles in various disease states, including cystic fibrosis and Liddle's Syndrome (Snyder et al., 1995; Stutts et al., 1995). Differential expression and up-regulation of the subunits between normal and disease states is thought to contribute to cellular changes in disease (Burch et al., 1995; Greig et al., 2004). In chondrocytes the role of ENaC is less clear; however, it is thought to be one of mechanotransduction, possibly where the channel contributes to the maintenance of the RMP. This, in turn, may regulate signaling pathways that allow chondrocytes to maintain their ECM and prevent chondrocyte apoptosis (Wright et al., 1996; Shakibaei et al., 2001; Shakibaei and Mobasheri, 2003). It is thought that the mechanotransduction pathways involving ENaC become progressively defective during osteoarthritis, leading to a loss of chondroprotective mechanisms (Salter et al., 2004). It is possible that ENaC subunits are differentially expressed in chondrocytes, potentially to cope with different mechanical stresses throughout the zones of articular cartilage, and changes in chondrocytic properties during disease (Trujillo et al., 1999; Shakibaei et al., 2001).

CHLORIDE CHANNELS

The chloride channel family (ClC) is widely expressed in many tissue types. It was first discovered by Jentsch et al. (1990) using *Xenopus* oocytes, who isolated and sequenced the channel primary structure using cDNA. Using the same cDNA, ClC-1 was identified in rat skeletal muscle. In skeletal muscle, ClC-1 is involved in stabilization of the RMP (Gronemeier et al., 1994). ClCs have been identified in rabbit articular cartilage (Sugimoto et al., 1996; Tsuga et al., 2002; Isoya et al., 2009) and in OUMS-27, the human chondrocyte-derived cell line (Funabashi et al., 2010a). A commonly used pharmacological inhibitor of ClCs is 4-acetamido-4′-isothiocyanatostilbene-2,2-disulfonic acid (SITS) (Pesente and Signorile, 1979; Lefevre et al., 1996; Vaca, 1999; Alexander et al., 2008). This and other ClC inhibitors were used by Sugimoto et al. (1996) and Tsuga et al. (2002) to show that ClCs are important for control of the RMP. Furthermore, exposure of chondrocytes to high concentrations of SITS leads to signs of necrotic damage (Wohlrab et al., 2004) suggesting that activity of ClCs may be critical to the survival of chondrocytes. Chondrocytes may express a number of ClCs. So far the only one successfully identified in molecular terms is the cystic fibrosis transmembrane conductance regulator (CFTR) (Liang et al., 2010). This is particularly interesting since CFTR is known to function both as a channel in its own right, and as a regulator of other ion channels known to be expressed in chondrocytes (Mall et al., 1998; Nilius and Droogmans, 2003; Arniges et al., 2004). As yet no studies have successfully identified other ClCs expressed by chondrocytes. Such identification will be a tricky task since the ClC family is large and the available pharmacological inhibitors are rather non-selective between each of the family members (Alexander et al., 2008). In our own laboratories we have attempted to locate ClC-1 mRNA using the primers based on the sequence already identified for canine skeletal muscle (Rhodes et al., 1999). These studies show a lack of ClC-1, but as yet there have been no positive studies on chondrocytes. The identity was suggested to be the maxi-ClC by Yabu and colleagues (Sugimoto et al., 1996; Tsuga et al., 2002), but further studies will be needed to clarify this. The ClC identified in rabbit articular cartilage by Isoya et al. (2009) proved to be swelling activated, but whilst its molecular identity is unknown, ClC-3 was suggested as a possibility on the basis of its biophysical and pharmacological properties. In terms of the function of ClCs in chondrocytes, at least two clear possibilities exist; the first would be that they are required for setting of the membrane potential as implied above, but the second would be that they could be important as anionic osmolyte channels. The latter hypothesis arises from the fact that any osmotic loss of K^+ ions as a part of volume regulation would need to be matched by an effective anion loss. ClCs would be an obvious candidate to fulfill such a role.

AQUAPORIN CHANNELS

Aquaporins (AQP) are a family of small integral membrane proteins related to the major intrinsic protein (MIP), sometimes called AQP0 (Agre et al., 1993). The first AQP discovered, AQP1, was identified during experiments investigating the identity of the rhesus blood group antigens (Agre et al., 1987; Denker et al., 1988; Smith and Agre, 1991). Oocytes from *Xenopus laevis* microinjected with *in vitro*-transcribed mRNA of AQP1 (previously known as CHIP28) exhibited increased osmotic water permeability compared to uninjected controls. This observation, combined with the reversible inhibition induced by mercuric chloride, provided the first molecular evidence for water channels (Preston et al., 1992). Since the identification of AQP1 the field has expanded to now include study of AQP in all types of organisms. In mammals, over a dozen AQP have been identified. The classical AQP transport water exclusively. However, a second class of AQP has now been identified (Rojek et al., 2008), these so-called aquaglyceroporins also transport small, uncharged molecules such as glycerol and urea; examples include AQP3, AQP7, and AQP9 (Carbrey and Agre, 2009). Many models of chondrocyte function involve changes in volume (Hall et al., 1996). For this to occur there must be pathways for the movement of water into and out of the cell. The discovery of AQP channels in chondrocytes would appear to provide an appropriate mechanism (Mobasheri and Marples, 2004; Mobasheri et al., 2004a,b; Trujillo et al., 2004; May et al., 2007). Whilst studies have already shown a loss of volume regulation with inhibition of AQP channels (May et al., 2007) and reductions in migration and adhesion (Liang et al., 2008), it would be interesting to investigate whether cell survival or progression of osteoarthritis are also affected by AQP block or by AQP knockouts.

NMDA CHANNELS

There have been a few reports of expression of excitatory neurotransmitter receptor (NMDA) channels in chondrocytes (Millward-Sadler et al., 2001; Salter et al., 2004; Ramage et al., 2008). These are

Table 1 | Ion channels that have been identified in the chondrocyte channelome.

Channel family	Identified in chondrocytes	Species	General phenotype	Proposed role in chondrocytes	References
POTASSIUM CHANNELS					
K_v	K_v1.4	Canine, chicken, elephant, equine, rat	Voltage activated	Regulation of membrane potential	Walsh et al. (1992), Wilson et al. (2004), Mobasheri et al. (2005a), Ponce (2006)
K_{ATP}	Kir6.x /SURx	Equine, human	Closed with normal intracellular [ATP]	Coupling cellular activity to metabolic state	Mobasheri et al. (2007)
BK	KCNMA1, KCNMNB1	Equine	Large Ca^{2+} activated	Coupling of membrane stretch to RVD	Long and Walsh (1994), Mobasheri et al. (2010)
SK	–	Human	Small Ca^{2+} activated	Intracellular Ca^{2+} regulation	Wright et al. (1996)
NON-SELECTIVE CATION CHANNELS					
TRPV4	–	Porcine, canine, equine	Mono and divalent cation conductor	Coupling membrane stretch and BK channel function; osmoregulation	Phan et al. (2009), Lewis et al. (2010), Lewis et al. (2010), Lewis et al. (2010), Gavenis et al. (2009)
TRPV5	–	Canine, equine	Highly calcium selective channel ($P_{Ca}/P_{Na} > 100$)	Not known	
TRPV6	–	Canine, equine	Highly calcium selective channel ($P_{Ca}/P_{Na} > 100$)	Not known	
TRPC1/3/6, TRPM5/7, TRPV1 /2	–	Human osteoarthritic cartilage	Cation channels	Not known	
SODIUM CHANNELS					
VGSC	–	Rabbit	TTX sensitive	Mechanotransduction	Sugimoto et al. (1996)
ENaC	α- and β-subunits	Canine, human	Low conductance, amiloride sensitive	Mechanotransduction	Trujillo et al. (1999), Shakibaei and Mobasheri (2003), Lewis et al. (2008)
OTHER CHANNELS					
Chloride	Maxi-Cl	Rabbit	Large conductance (~280 pS)	Control of membrane potential	Sugimoto et al. (1997), Tsuga et al. (2002)
VGCC	–	Rabbit, mouse	Voltage-activated	Calcium signaling	Poiraudeau et al. (1997), Shakibaei and Mobasheri (2003)
Aquaporins	AQP-1, AQP-3	Equine, porcine, bovine, cell lines, ovine	Water and small solute transport	Regulation of cell volume	Mobasheri and Marples (2004), Mobasheri et al. (2004a, b), Trujillo et al. (2004), May et al. (2007)
ASIC	–	Bovine	Voltage activated	Intracellular pH regulation	Sanchez et al. (2006)
NMDA	–	Human	Ligand-gated ion channel	Response to mechanical stimulation	Millward-Sadler et al. (2001), Salter et al. (2004), Ramage et al. (2008)
Connexins	Connexin 43	Bovine	Gap junction hemichannels	Mechanocoupling	Knight et al. (2009)

Ion channels either identified or proposed to exist in chondrocytes. AQP, aquaporin channel; ASIC, acid sensing ion channel; BK, calcium-activated potassium cannel, high conductance; ENaC, epithelial sodium channels; K_{ATP}, ATP-dependent potassium channel; Kir, inwardly rectifying potassium channel; K_v, voltage-gated potassium channel; MIP, major intrinsic protein; NMDA, N-methyl D-aspartate; SK, calcium-activated potassium channel, low conductance; SUR, sulfonylurea receptor; TRP, transient receptor potential channel; TTX, tetrodotoxin; VGCC, voltage-gated calcium channels; VGSC, voltage-gated sodium channel.

interesting observations however the role of these ligand-gated ion channels in chondrocyte function is not yet understood. It does not seem likely that they are involved with neurotransmission because, despite some similarities between neurone and chondrocyte phenotype, no "pre-synaptic" neurones project to the immediate vicinity of the chondrocytes. It again appears likely that NMDA channels are in someway involved in the mechanotransduction pathway, since mechanically induced hyperpolarizations are reduced by NMDA antagonists (Salter et al., 2004). Furthermore, glycine induces a number of changes on chondrocytes in cartilage explants (including accumulation of calcium) and these effects can be reduced with an NMDA antagonist as, presumably, glycine acts via the glycine binding site of the NMDA receptor (Takahata et al., 2008).

OTHER ION CHANNELS

Two further ion channels recently identified in chondrocytes are the acid sensing channel, ASIC1a and ASIC3 (Kolker et al., 2010; Yuan et al., 2010) and the connexin 43 hemichannel (Knight et al., 2009). ASIC are very small cation selective channels closely related to ENaC (reviewed by Wemmie et al., 2006). As their name implies, they are opened by extracellular protons. This is particularly relevant to chondrocyte biology since chondrocytes are routinely exposed to relatively acidic conditions, as low as pH 6.6 for example (Wilkins et al., 2000). *In vitro* studies show that these channels mediate an increase in intracellular calcium upon exposure of chondrocytes to acidic conditions. This intracellular Ca^{2+} is likely to be a signal for production of enzymes and for proliferation. Potentially, inappropriate increases in calcium could result in cell death from either necrosis or apoptosis (Kolker et al., 2010; Yuan et al., 2010). The role of the connexin 43 is possibly more complex. Knight et al. (2009) found it to be constitutively active in about 40% of chondrocytes, and as such it might be expected to profoundly depolarize the membrane. In summary, the suggested scheme of connexin 43 involvement was that mechanical stimulation of chondrocyte cilia activates the hemichannel which then acts as a conduit for ATP release. This released ATP then acts on chondrocyte membranes (via P2 purinoceptors) to increase intracellular Ca^{2+} (Knight et al., 2009).

CONCLUSIONS

There is growing interest in the expression and function of ion channels in chondrocytes. Part of this interest stems from the realization that many ion channels are involved in mechanotransduction, chemotransduction and osmoregulation. It is important to bear in mind that ion channels are also important drug targets because of their localization in the chondrocyte plasma membrane. A number of research groups, including ours, have used electrophysiology, molecular biology and immunohistochemistry to study ion channels in articular chondrocytes. **Table 1** contains a summary of the ion channels studied in the chondrocyte channelome so far. It is likely that some ion channels in chondrocytes are multifunctional, serving a number of different physiological purposes. The processes of mechanical and chemical sensing and metabolic regulation may well be intricately linked and make use of a number of ion channels as common denominators. In summary, ion channels are important for chondrocyte function and further investigations are required to explore the full complement of channels present in the chondrocyte channelome. This knowledge will help us understand the unique biology of chondrocytes and may lead to the development and formulation of therapeutic strategies to treat arthritis.

ACKNOWLEDGMENTS

The Biotechnology and Biological Sciences Research Council (BBSRC) and The Wellcome Trust have funded our research on the chondrocyte channelome. We thank Dr Madura Batuwangala for the illustrations in the figures.

REFERENCES

Agre, P., Preston, G. M., Smith, B. L., Jung, J. S., Raina, S., Moon, C., Guggino, W. B., and Nielsen, S. (1993). Aquaporin CHIP: the archetypal molecular water channel. *Am. J. Physiol.* 265, F463–F476.

Agre, P., Saboori, A. M., Asimos, A., and Smith, B. L. (1987). Purification and partial characterization of the Mr 30,000 integral membrane protein associated with the erythrocyte Rh(D) antigen. *J. Biol. Chem.* 262, 17497–17503.

Alexander, S. P. H., Mathie, A., and Peters, J. A. (2008). Guide to receptors and channels (GRAC), 3rd edition. *Br. J. Pharmacol.* 153(Suppl. 2), S1–S209.

Allan, D. A. (1998). Structure and physiology of joints and their relationship to repetitive strain injuries. *Clin. Orthop. Relat. Res.* 351, 32–38.

Archer, C. W., and Francis-West, P. (2003). The chondrocyte. *Int. J. Biochem. Cell Biol.* 35, 401–404.

Arniges, M., Vazquez, E., Fernandez-Fernandez, J. M., and Valverde, M. A. (2004). Swelling-activated Ca2+ entry via TRPV4 channel is defective in cystic fibrosis airway epithelia. *J. Biol. Chem.* 279, 54062–54068.

Ashcroft, F. M., and Gribble, F. M. (1998). Correlating structure and function in ATP-sensitive K+ channels. *Trends Neurosci.* 21, 288–294.

Babenko, A. P., Aguilar-Bryan, L., and Bryan, J. (1998). A view of sur/KIR6.X, KATP channels. *Annu. Rev. Physiol.* 60, 667–687.

Barrett-Jolley, R., Comtois, A., Davies, N. W., Stanfield, P. R., and Standen, N. B. (1996). Effect of adenosine and intracellular GTP on K-ATP channels of mammalian skeletal muscle. *J. Membr. Biol.* 152, 111–116.

Barrett-Jolley, R., Dart, C., and Standen, N. B. (1999). Direct block of native and cloned (Kir2.1) inward rectifier K+ channels by chloroethylclonidine. *Br. J. Pharmacol.* 128, 760–766.

Barrett-Jolley, R., and Davies, N. W. (1997). Kinetic analysis of the inhibitory effect of glibenclamide on KATP channels of mammalian skeletal muscle. *J. Membr. Biol.* 155, 257–262.

Barrett-Jolley, R., and McPherson, G. A. (1998). Characterization, of K(ATP) channels in intact mammalian skeletal muscle fibres. *Br. J. Pharmacol.* 123, 1103–1110.

Barrett-Jolley, R., Pyner, S., and Coote, J. H. (2000). Measurement of voltage-gated potassium currents in identified spinally-projecting sympathetic neurones of the paraventricular nucleus. *J. Neurosci. Methods* 102, 25–33.

Beech, D. J., Zhang, H., Nakao, K., and Bolton, T. B. (1993). K channel activation by nucleotide diphosphates and its inhibition by glibenclamide in vascular smooth muscle cells. *Br. J. Pharmacol.* 110, 573–582.

Breittmayer, J. P., Pelassy, C., and Aussel, C. (1996). Effect of membrane potential on phosphatidylserine synthesis and calcium movements in control and CD3-activated Jurkat T cells. *J. Lipid Mediat. Cell Signal.* 13, 151–161.

Bruckner, P., and van der Rest, M. (1994). Structure and function of cartilage collagens. *Microsc. Res. Tech.* 28, 378–384.

Buckwalter, J. A., and Mankin, H. J. (1998). Articular cartilage: tissue design and chondrocyte-matrix interactions. *Instr. Course Lect.* 47, 477–486.

Burch, L. H., Talbot, C. R., Knowles, M. R., Canessa, C. M., Rossier, B. C., and Boucher, R. C. (1995). Relative expression of the human epithelial Na+ channel subunits in normal and cystic fibrosis airways. *Am. J. Physiol.* 269, C511–518.

Canessa, C. M., Schild, L., Buell, G., Thorens, B., Gautschi, I., Horisberger, J. D., and Rossier, B. C. (1994). Amiloride-sensitive epithelial Na^+ channel is made of 3 homologous subunits. *Nature* 367, 463–467.

Carbrey, J. M., and Agre, P. (2009). Discovery of the aquaporins and development of the field. *Handb. Exp. Pharmacol.*, 190, 3–28.

Carlton, S. M., Zhou, S., Du, J., Hargett, G. L., Ji, G., and Coggeshall, R. E. (2004). Somatostatin modulates the transient receptor potential vanilloid

1 (TRPV1) ion channel. *Pain* 110, 616–627.

Carney, S. L., and Muir, H. (1988). The structure and function of cartilage proteoglycans. *Physiol. Rev.* 68, 858–910.

Catterall, W. A. (1991). Structure and function of voltage-gated sodium and calcium channels. *Curr. Opin. Neurobiol.* 1, 5–13.

Catterall, W. A. (1992). Cellular and molecular biology of voltage-gated sodium channels. *Physiol. Rev.* 72, S15–S48.

Catterall, W. A. (1995). Structure and function of voltage-gated ion channels. *Annu. Rev. Biochem.* 64, 493–531.

Catterall, W. A. (2002). Molecular mechanisms of gating and drug block of sodium channels. *Novartis Found Symp.* 241, 206–218; discussion 218–232.

Clark, A. L., Votta, B. J., Kumar, S., Liedtke, W., and Guilak, F. (2010a). chondroprotective role of the osmotically-sensitive ion channel TRPV4: age- and sex-dependent progression of osteoarthritis in Trpv4 deficient mice. *Arthritis Rheum.* doi: 10.1002/art.27624. [Epub ahead of print].

Clark, R. B., Hatano, N., Kondo, C., Belke, D. D., Brown, B. S., Kumar, S., Votta, B. J., and Giles, W. R. (2010b). Voltage-gated K^+ currents in mouse articular chondrocytes regulate membrane potential. *Channels* 4, 179–191.

Coetzee, W. A., Amarillo, Y., Chiu, J., Chow, A., Lau, D., McCormack, T., Moreno, H., Nadal, M. S., Ozaita, A., Pountney, D., Saganich, M., Vega-Saenz de Miera, E., and Rudy, B. (1999). Molecular diversity of K^+ channels. *Ann. N Y Acad. Sci.* 868, 233–285.

Cui, J., Yang, H., and Lee, U. S. (2009). Molecular mechanisms of BK channel activation. *Cell. Mol. Life Sci.* 66, 852–875.

Dart, C., and Standen, N. B. (1993). Adenosine-activated potassium current in smooth-muscle cells isolated from the pig coronary-artery. *J. Physiol. (Lond.)* 471, 767–786.

Dart, C., and Standen, N. B. (1994). Hypoxia induces a potassium current in smooth-muscle cells isolated from the porcine coronary-artery. *J. Physiol. (Lond.)* 477P, P85–P86.

Denker, B. M., Smith, B. L., Kuhajda, F. P., and Agre, P. (1988). Identification, purification, and partial characterization of a novel Mr 28,000 integral membrane protein from erythrocytes and renal tubules. *J. Biol. Chem.* 263, 15634–15642.

Dolphin, A. C. (2009). Calcium channel diversity: multiple roles of calcium channel subunits. *Curr. Opin. Neurobiol.* 19, 237–244.

Dunne, M. J., and Petersen, O. H. (1986). Intracellular ADP activates K^+ channels that are inhibited by ATP in an insulin-secreting cell-line. *FEBS Lett.* 208, 59–62.

Eaton, D. C., Becchetti, A., Ma, H. P., and Ling, B. N. (1995). Renal sodium-channels – regulation and single-channel properties. *Kidney Int.* 48, 941–949.

Edwards, J. C., Wilkinson, L. S., Jones, H. M., Soothill, P., Henderson, K. J., Worrall, J. G., and Pitsillides, A. A. (1994). The formation of human synovial joint cavities: a possible role for hyaluronan and CD44 in altered interzone cohesion. *J. Anat.* 185(Pt 2), 355–367.

Fassbender, H. G. (1987). Role of chondrocytes in the development of osteoarthritis. *Am. J. Med.* 83, 17–24.

Fernandez, M. P., Selmin, O., Martin, G. R., Yamada, Y., Pfaffle, M., Deutzmann, R., Mollenhauer, J., and von der Mark, K. (1990). The structure of anchorin CII, a collagen binding protein isolated from chondrocyte membrane. *J. Biol. Chem.* 265, 8344.

Funabashi, K., Fujii, M., Yamamura, H., Ohya, S., and Imaizumi, Y. (2010a). Contribution of chloride channel conductance to the regulation of resting membrane potential in chondrocytes. *J. Pharmacol. Sci.* 113, 94–99.

Funabashi, K., Ohya, S., Yamamura, H., Hatano, N., Muraki, K., Giles, W., and Imaizumi, Y. (2010b). Accelerated Ca2+ entry by membrane hyperpolarization due to Ca^{2+}-activated K^+ channel activation in response to histamine in chondrocytes. *Am. J. Physiol. Cell Physiol.* 298, C786–C797.

Gavenis, K., Schumacher, C., Schneider, U., Eisfeld, J., Mollenhauer, J., and Schmidt-Rohlfing, B. (2009). Expression of ion channels of the TRP family in articular chondrocytes from osteoarthritic patients: changes between native and *in vitro* propagated chondrocytes. *Mol. Cell. Biochem.* 321, 135–143.

Goldin, A. L. (2001). Resurgence of sodium channel research. *Annu. Rev. Physiol.* 63, 871–894.

Grandolfo, M., Calabrese, A., and D'Andrea, P. (1998). Mechanism of mechanically induced intercellular calcium waves in rabbit articular chondrocytes and in HIG-82 synovial cells. *J. Bone Miner. Res.* 13, 443–453.

Grandolfo, M., D'Andrea, P., Martina, M., Ruzzier, F., and Vittur, F. (1992). Calcium-activated potassium channels in chondrocytes. *Biochem. Biophys. Res. Commun.* 182, 1429–1434.

Grandolfo, M., Martina, M., Ruzzier, F., and Vittur, F. (1990). A potassium channel in cultured chondrocytes. *Calcif. Tissue Int.* 47, 302–307.

Greig, E. R., Boot-Handford, R. P., Mani, V., and Sandle, G. I. (2004). Decreased expression of apical Na+ channels and basolateral Na+, K+-ATPase in ulcerative colitis. *J. Pathol.* 204, 84–92.

Grishko, V., Xu, M., Wilson, G., and Pearsall, A. W. IV (2010). Apoptosis and mitochondrial dysfunction in human chondrocytes following exposure to lidocaine, bupivacaine, and ropivacaine. *J. Bone Joint Surg. Am.* 92, 609–618.

Gronemeier, M., Condie, A., Prosser, J., Steinmeyer, K., Jentsch, T. J., and Jockusch, H. (1994). Nonsense and missense mutations in the muscular chloride channel gene ClC-1 of myotonic mice. *J. Biol. Chem.* 269, 5963–5967.

Guilak, F., Zell, R. A., Erickson, G. R., Grande, D. A., Rubin, C. T., McLeod, K. J., and Donahue, H. J. (1999). Mechanically induced calcium waves in articular chondrocytes are inhibited by gadolinium and amiloride. *J. Orthop. Res.* 17, 421–429.

Gutman, G. A., Chandy, K. G., Grissmer, S., Lazdunski, M., McKinnon, D., Pardo, L. A., Robertson, G. A., Rudy, B., Sanguinetti, M. C., Stuhmer, W., and Wang, X. (2005). International union of pharmacology. LIII. Nomenclature and molecular relationships of voltage-gated potassium channels. *Pharmacol. Rev.* 57, 473–508.

Hall, A. C., Starks, I., Shoults, C. L., and Rashidbigi, S. (1996). Pathways for K+ transport across the bovine articular chondrocyte membrane and their sensitivity to cell volume. *Am. J. Physiol. Cell Physiol.* 270, C1300–C1310.

Hille, B. (2001). *Ion Channels of Excitable Membranes*. Sunderland, MA: Sinauer Associates.

Hodgkin, A. L., and Huxley, A. F. (1952a). The dual effect of membrane potential on sodium conductance in the giant axon of Loligo. *J. Physiol.* 116, 497–506.

Hodgkin, A. L., and Huxley, A. F. (1952b). A quantitative description of membrane current and its application to conduction and excitation in nerve. *J. Physiol. (Lond.)* 117, 500–544.

Iannotti, J. P. (1990). Growth plate physiology and pathology. *Orthop. Clin. North Am.* 21, 1–17.

Isoya, E., Toyoda, F., Imai, S., Okumura, N., Kumagai, K., Omatsu-Kanbe, M., Kubo, M., Matsuura, H., and Matsusue, Y. (2009). Swelling-activated Cl(-) current in isolated rabbit articular chondrocytes: inhibition by arachidonic acid. *J. Pharmacol. Sci.* 109, 293–304.

Jentsch, T. J., Steinmeyer, K., and Schwarz, G. (1990). Primary structure of Torpedo marmorata chloride channel isolated by expression cloning in Xenopus oocytes. *Nature* 348, 510–514.

Kerrigan, M. J. P., and Hall, A. C. (2008). Control of chondrocyte regulatory volume decrease (RVD) by [Ca2+] (i) and cell shape. *Osteoarthr. Cartil.* 16, 312–322.

Knight, M. M., McGlashan, S. R., Garcia, M., Jensen, C. G., and Poole, C. A. (2009). Articular chondrocytes express connexin 43 hemichannels and P2 receptors – a putative mechanoreceptor complex involving the primary cilium? *J. Anat.* 214, 275–283.

Kolker, S. J., Walder, R. Y., Usachev, Y., Hillman, J., Boyle, D. L., Firestein, G. S., and Sluka, K. A. (2010). Acid-sensing ion channel 3 expressed in type B synoviocytes and chondrocytes modulates hyaluronan expression and release. *Ann. Rheum. Dis.* 69, 903–909.

Krause, E., Englert, H., and Gogelein, H. (1995). Adenosine triphosphate-dependent K currents activated by metabolic inhibition in rat ventricular myocytes differ from those elicited by the channel opener rilmakalim. *Pflugers Arch.* 429, 625–635.

Latorre, R., Oberhauser, A., Labarca, P., and Alvarez, O. (1989). Varieties of calcium-activated potassium channels. *Annu. Rev. Physiol.* 51, 385–399.

Ledoux, J., Werner, M. E., Brayden, J. E., and Nelson, M. T. (2006). Calcium-activated potassium channels and the regulation of vascular tone. *Physiology* 21, 69–78.

Lee, H. S., Millward-Sadler, S. J., Wright, M. O., Nuki, G., and Salter, D. M. (2000). Integrin and mechanosensitive ion channel-dependent tyrosine phosphorylation of focal adhesion proteins and beta-catenin in human articular chondrocytes after mechanical stimulation. *J. Bone Miner. Res.* 15, 1501–1509.

Lee, R. B., and Urban, J. P. (1997). Evidence for a negative Pasteur effect in articular cartilage. *Biochem. J.* 321(Pt 1), 95–102.

Lefevre, T., Lefevre, I. A., Coulombe, A., and Coraboeuf, E. (1996). Effects of chloride ion substitutes and chloride channel blockers on the transient outward current in rat ventricular myocytes. *Biochim. Biophys. Acta.* 1273, 31–43.

Lewis, R., Mobasheri, A., and Barrett-Jolley, R. (2008). Electrophysiological identification of epithelial sodium channels in canine articular chondrocytes. *Proc. Physiol. Soc.* 11, C47.

Lewis, R., Purves, G., Crossley, J., and Barrett-Jolley, R. (2010). Modelling the Membrane potential dependence on non-specific cation channels in canine articular chondrocytes. *Biophys. J.* 98. (Suppl. 1), 340A

Liang, H., Yang, L., Ma, T., and Zhao, Y. (2010). Functional expression of cystic

fibrosis transmembrane conductance regulator in mouse chondrocytes. *Clin. Exp. Pharmacol. Physiol.* 37, 506–508.

Liang, H. T., Feng, X. C., and Ma, T. H. (2008). Water channel activity of plasma membrane affects chondrocyte migration and adhesion. *Clin. Exp. Pharmacol. Physiol.* 35, 7–10.

Lindemann, B. (2001). Receptors and transduction in taste. *Nature* 413, 219–225.

Lippiat, J. D., Standen, N. B., Harrow, I. D., Phillips, S. C., and Davies, N. W. (2003). Properties of BK(Ca) channels formed by bicistronic expression of hSloalpha and beta1-4 subunits in HEK293 cells. *J. Membr. Biol.* 192, 141–148.

Long, K. J., and Walsh, K. B. (1994). Calcium-activated potassium channel in growth-plate chondrocytes – regulation by protein-kinase-A. *Biochem. Biophys. Res. Commun.* 201, 776–781.

Mall, M., Bleich, M., Greger, R., Schreiber, R., and Kunzelmann, K. (1998). The amiloride-inhibitable Na+ conductance is reduced by the cystic fibrosis transmembrane conductance regulator in normal but not in cystic fibrosis airways. *J. Clin. Invest.* 102, 15–21.

Mancilla, E. E., Galindo, M., Fertilio, B., Herrera, M., Salas, K., Gatica, H., and Goecke, A. (2007). L-type calcium channels in growth plate chondrocytes participate in endochondral ossification. *J. Cell Biochem.* 101, 389–398.

Mankin, H. J. (1982). The response of articular cartilage to mechanical injury. *J. Bone Joint Surg. Am.* 64, 460–466.

Mano, I., and Driscoll, M. (1999). DEG/ENaC channels: a touchy superfamily that watches its salt. *Bioessays* 21, 568–578.

Martin, J. A., and Buckwalter, J. A. (2000). The role of chondrocyte-matrix interactions in maintaining and repairing articular cartilage. *Biorheology* 37, 129–140.

Martina, M., Mozrzymas, J. W., and Vittur, F. (1997). Membrane stretch activates a potassium channel in pig articular chondrocytes. *Biochim. Biophys. Acta Biomembr.* 1329, 205–210.

May, H., Mobasheri, A., Womack, M. D., and Barrett-Jolley, R. (2007). Functional expression of aquaporins in canine chondrocytes. *Biophys. J.* 92, S543.

McCarty, M. F. (1999). Endothelial membrane potential regulates production of both nitric oxide and superoxide – a fundamental determinant of vascular health. *Med. Hypotheses.* 53, 277–289.

Millward-Sadler, S. J., Wright, M. O., and Salter, D. M. (2001). The NMDA receptor is involved in the response of normal human articular chondrocytes to mechanical stimulation. *J. Pathol.* 193, 32a–32a.

Minami, K., Miki, T., Kadowaki, T., and Seino, S. (2004). Roles of ATP-sensitive K+ channels as metabolic sensors: studies of Kir6.x null mice. *Diabetes* 53(Suppl. 3), S176–S180.

Mobasheri, A., Carter, S. D., Martin-Vasallo, P., and Shakibaei, M. (2002). Integrins and stretch activated ion channels; putative components of functional cell surface mechanoreceptors in articular chondrocytes. *Cell. Biol. Int.* 26, 1–18.

Mobasheri, A., Gent, T. C., Nash, A. I., Womack, M. D., Moskaluk, C. A., and Barrett-Jolley, R. (2007). Evidence for functional ATP-sensitive (K(ATP)) potassium channels in human and equine articular chondrocytes. *Osteoarthr. Cartil.* 15, 1–8.

Mobasheri, A., Gent, T. C., Womack, M. D., Carter, S. D., Clegg, P. D., and Barrett-Jolley, R. (2005a). Quantitative analysis of voltage-gated potassium currents from primary equine (Equus caballus) and elephant (Loxodonta africana) articular chondrocytes. *Am. J. Physiol. Regul. Integr. Comp. Physiol.* 289, R172–R180.

Mobasheri, A., Richardson, S., Mobasheri, R., Shakibaei, M., and Hoyland, J. A. (2005b). Hypoxia inducible factor-1 and facilitative glucose transporters GLUT1 and GLUT3: putative molecular components of the oxygen and glucose sensing apparatus in articular chondrocytes. *Histol. Histopathol.* 20, 1327–1338.

Mobasheri, A., Lewis, R., Maxwell, J. E. J., Hill, C., Womack, M., and Barrett-Jolley, R. (2010). Characterization of a stretch-activated potassium channel in chondrocytes. *J. Cell. Physiol.* 223, 511–518.

Mobasheri, A., and Marples, D. (2004). Expression of the AQP-1 water channel in normal human tissues: a semiquantitative study using tissue microarray technology. *Am. J. Physiol. Cell Physiol.* 286, C529–C537.

Mobasheri, A., Shakibaei, M., and Marples, D. (2004a). Immunohistochemical localization of aquaporin 10 in the apical membranes of the human ileum: a potential pathway for luminal water and small solute absorption. *Histochem. Cell Biol.* 121, 463–471.

Mobasheri, A., Trujillo, E., Bell, S., Carter, S. D., Clegg, P. D., Martin-Vasallo, P., and Marples, D. (2004b). Aquaporin water channels AQP1 and AQP3, are expressed in equine articular chondrocytes. *Vet. J.* 168, 143–150.

Mouw, J. K., Imler, S. M., and Levenston, M. E. (2007). Ion-channel regulation of chondrocyte matrix synthesis in 3D culture under static and dynamic compression. *Biomech. Model. Mechanobiol.* 6, 33–41.

Mozrzymas, J. W., Martina, M., and Ruzzier, F. (1997). A large-conductance voltage-dependent potassium channel in cultured pig articular chondrocytes. *Pflugers Arch. Eur. J. Physiol.* 433, 413–427.

Muramatsu, S., Wakabayashi, M., Ohno, T., Amano, K., Ooishi, R., Sugahara, T., Shiojiri, S., Tashiro, K., Suzuki, Y., Nishimura, R., Kuhara, S., Sugano, S., Yoneda, T., and Matsuda, A. (2007). Functional gene screening system identified TRPV4 as a regulator of chondrogenic differentiation. *J. Biol. Chem.* 282, 32158–32167.

Neher, E., and Sakmann, B. (1992). The patch clamp technique. *Sci. Am.* 266, 44–51.

Nilius, B., and Droogmans, G. (2003). *Amazing Chloride Channels: An Overview*, Oxford, UK: Blackwell Science Ltd, 119–147.

Nilius, B., Vriens, J., Prenen, J., Droogmans, G., and Voets, T. (2004). TRPV4 calcium entry channel: a paradigm for gating diversity. *Am. J. Physiol. Cell Physiol.* 286, C195–C205.

Otte, P. (1991). Basic cell metabolism of articular cartilage. Manometric studies. *Z. Rheumatol.* 50, 304–312.

Pallotta, B. S., and Wagoner, P. K. (1992). Voltage-dependent potassium channels since Hodgkin and Huxley. *Physiol. Rev.* 72, S49–S67.

Park, J. K., Kim, Y. C., Sim, J. H., Choi, M. Y., Choi, W., Hwang, K. K., Cho, M. C., Kim, K. W., Lim, S. W., and Lee, S. J. (2007). Regulation of membrane excitability by intracellular pH (pH(i)) changers through Ca2+-activated K+ current (BK channel) in single smooth muscle cells from rabbit basilar artery. *Pflugers Arch. Eur. J. Physiol.* 454, 307–319.

Penyige, A., Matko, J., Deak, E., Bodnar, A., and Barabas, G. (2002). Depolarization of the membrane potential by beta-lactams as a signal to induce autolysis. *Biochem. Biophys. Res. Commun.* 290, 1169–1175.

Pesente, L., and Signorile, G. (1979). [Effect of SITS (4-acetamido-4'-isothiocyanatostilbene-2,2'-disulfonic acid) on the transport of chloride through the isolated skin of Rana esculenta]. *Ateneo Parmense Acta Biomed.* 50, 173–179.

Phan, M. N., Leddy, H. A., Votta, B. J., Kumar, S., Levy, D. S., Lipshutz, D. B., Lee, S. H., Liedtke, W., and Guilak, F. (2009). Functional characterization of TRPV4 as an osmotically sensitive ion channel in porcine articular chondrocytes. *Arthritis Rheum.* 60, 3028–3037.

Phillis, J. W. (2004). Adenosine and adenine nucleotides as regulators of cerebral blood flow: roles of acidosis, cell swelling, and KATP channels. *Crit. Rev. Neurobiol* 16, 237–270.

Poiraudeau, S., Lieberherr, M., Kergosie, N., and Corvol, M. T. (1997). Different mechanisms are involved in intracellular calcium increase by insulin-like growth factors 1 and 2 in articular chondrocytes: voltage-gated calcium channels, and/or phospholipase C coupled to a pertussis-sensitive G-protein. *J. Cell. Biochem.* 64, 414–422.

Ponce, A. (2006). Expression of voltage dependent potassium currents in freshly dissociated rat articular chondrocytes. *Cell. Physiol. Biochem.* 18, 35–46.

Preston, G. M., Carroll, T. P., Guggino, W. B., and Agre, P. (1992). Appearance of water channels in Xenopus oocytes expressing red cell CHIP28 protein. *Science* 256, 385–387.

Quayle, J. M., Nelson, M. T., and Standen, N. B. (1997). ATP-sensitive and inwardly rectifying potassium channels in smooth muscle. *Physiol. Rev.* 77, 1165–1232.

Ramage, L., Martel, M. A., Hardingham, G. E., and Salter, D. M. (2008). NMDA receptor expression and activity in osteoarthritic human articular chondrocytes. *Osteoarthr. Cartil.* 16, 1576–1584.

Redini, F. (2001). Structure and regulation of articular cartilage proteoglycan expression. *Pathol. Biol. (Paris)* 49, 364–375.

Rhodes, T. H., Vite, C. H., Giger, U., Patterson, D. F., Fahlke, C., and George, A. L. Jr (1999). A missense mutation in canine ClC-1 causes recessive myotonia congenita in the dog. *FEBS Lett.* 456, 54–58.

Rojek, A., Praetorius, J., Frokiaer, J., Nielsen, S., and Fenton, R. A. (2008). A current view of the mammalian aquaglyceroporins. *Annu. Rev. Physiol.* 70, 301–327.

Rossier, B. C., Pradervand, S., Schild, L., and Hummler, E. (2002). Epithelial sodium channel and the control of sodium balance: interaction between genetic and environmental factors. *Annu. Rev. Physiol.* 64, 877–897.

Salkoff, L., Butler, A., Ferreira, G., Santi, C., and Wei, A. (2006). High-conductance potassium channels of the SLO family. *Nat. Rev. Neurosci.* 7, 921–931.

Salter, D. M., Wright, M. O., and Millward-Sadler, S. J. (2004). NMDA receptor expression and roles in human articular chondrocyte mechanotransduction. *Biorheology* 41, 273–281.

Sampson, L. J., Davies, L. M., Barrett-Jolley, R., Standen, N. B., and Dart, C. (2007). Angiotensin II-activated

protein kinase C targets caveolae to inhibit aortic ATP-sensitive potassium channels. *Cardiovasc. Res.* 76, 61–70.

Sanchez, J. C., Danks, T. A., and Wilkins, R. J. (2003). Mechanisms involved in the increase in intracellular calcium following hypotonic shock in bovine articular chondrocytes. *Gen. Physiol. Biophys.* 22, 487–500.

Sanchez, J. C., Powell, T., Staines, H. M., and Wilkins, R. J. (2006). Electrophysiological demonstration of voltage-activated H+ channels in bovine articular chondrocytes. *Cell. Physiol. Biochem.* 18, 85–90.

Sanchez, J. C., and Wilkins, R. J. (2004). Changes in intracellular calcium concentration in response to hypertonicity in bovine articular chondrocytes. *Comp. Biochem. Physiol. A Mol. Integr. Physiol.* 137, 173–182.

Shakibaei, M., and Mobasheri, A. (2003). Beta1-integrins co-localize with Na, K-ATPase, epithelial sodium channels (ENaC) and voltage activated calcium channels (VACC) in mechanoreceptor complexes of mouse limb-bud chondrocytes. *Histol. Histopathol.* 18, 343–351.

Shakibaei, M., Schulze-Tanzil, G., de Souza, P., John, T., Rahmanzadeh, M., Rahmanzadeh, R., and Merker, H. J. (2001). Inhibition of mitogen-activated protein kinase kinase induces apoptosis of human chondrocytes. *J. Biol. Chem.* 276, 13289–13294.

Smith, B. L., and Agre, P. (1991). Erythrocyte Mr 28,000 transmembrane protein exists as a multisubunit oligomer similar to channel proteins. *J. Biol. Chem.* 266, 6407–6415.

Snyder, P. M., Price, M. P., McDonald, F. J., Adams, C. M, Volk, K. A., Zeiher, B. G., Stokes, J. B., and Welsh, M. J. (1995). Mechanism by which Liddle's syndrome mutations increase activity of a human epithelial Na+ channel. *Cell* 83, 969–978.

Standen, N. B., and Stanfield, P. R. (1978). A potential- and time-dependent blockade of inward rectification in frog skeletal muscle fibres by barium and strontium ions. *J. Physiol.* 280, 169–191.

Stockwell, R. A. (1975). Structural and histochemical aspects of the pericellular environment in cartilage. *Philos. Trans. R. Soc. Lond. B Biol. Sci.* 271, 243–245.

Stutts, M. J., Canessa, C. M., Olsen, J. C., Hamrick, M., Cohn, J. A., Rossier, B. C., and Boucher, R. C. (1995). CFTR as a cAMP-dependent regulator of sodium channels. *Science* 269, 847–850.

Sugimoto, T., Yoshino, M., Nagao, M., Ishii, S., and Yabu, H. (1996). Voltage-gated ionic channels in cultured rabbit articular chondrocytes. *Comp. Biochem. Physiol. C Pharmacol. Toxicol. Endocrinol.* 115, 223–232.

Takahata, Y., Takarada, T., Osawa, M., Hinoi, E., Nakamura, Y., and Yoneda, Y. (2008). Differential regulation of cellular maturation in chondrocytes and osteoblasts by glycine. *Cell Tissue Res.* 333, 91–103.

Tatari, H. (2007). The structure, physiology, and biomechanics of articular cartilage: injury and repair. *Acta. Orthop. Traumatol. Turc.* 41 (Suppl. 2), 1–5.

Telezhkin, V. S., Tsvilovskii, V. V., Dyskina, Y. B., Davydovskaya, N. V., and Shuba, M. F. (2001). Effects of K+ channel blockers and nitric oxide on the electrical and contractile activities of smooth muscles of the rabbit main pulmonary artery. *Neurophysiology* 33, 281–288.

Tomai, F., Crea, F., Gaspardone, A., Versaci, F., De Paulis, R., Penta de Peppo, A., Chiariello, L., and Gioffre, P. A. (1994). Ischemic preconditioning during coronary angioplasty is prevented by glibenclamide, a selective ATP-sensitive K+ channel blocker. *Circulation* 90, 700–705.

Torres, Y. P., Morera, F. J., Carvacho, I., and Latorre, R. (2007). A marriage of convenience: beta-subunits and voltage-dependent K+ channels. *J. Biol. Chem.* 282, 24485–24489.

Trujillo, E., Alvarez de la Rosa, D., Mobasheri, A., Gonzalez, T., Canessa, C. M., and Martin-Vasallo, P. (1999). Sodium transport systems in human chondrocytes. II. Expression of ENaC, Na+/K+/2Cl- cotransporter and Na+/H+ exchangers in healthy and arthritic chondrocytes. *Histol. Histopathol.* 14, 1023–1031.

Trujillo, E., Gonzalez, T., Marin, R., Martin-Vasallo, P., Marples, D., and Mobasheri, A. (2004). Human articular chondrocytes, synoviocytes and synovial microvessels express aquaporin water channels; upregulation of AQP1 in rheumatoid arthritis. *Histol. Histopathol.* 19, 435–444.

Tsuga, K., Tohse, N., Yoshino, M., Sugimoto, T., Yamashita, T., Ishii, S., and Yabu, H. (2002). Chloride conductance determining membrane potential of rabbit articular chondrocytes. *J. Membr. Biol.* 185, 75–81.

Urban, J. P. (1994). The chondrocyte: a cell under pressure. *Br. J. Rheumatol.* 33, 901–908.

Urban, J. P. G., Hall, A. C., and Gehl, K. A. (1993). Regulation of matrix synthesis rates by the ionic and osmotic environment of articular chondrocytes. *J. Cell. Physiol.* 154, 262–270.

Vaca, L. (1999). SITS blockade induces multiple subconductance states in a large conductance chloride channel. *J. Membr. Biol.* 169, 65–73.

Villalonga, N., David, M., Bielanska, J., Vicente, R., Comes, N., Valenzuela, C., and Felipe, A. (2010). Immunomodulation of voltage-dependent K+ channels in macrophages: molecular and biophysical consequences. *J. Gen. Physiol.* 135, 135–147.

Walsh, K. B., Cannon, S. D., and Wuthier, R. E. (1992). Characterization of a delayed rectifier potassium current in chicken growth plate chondrocytes. *Am. J. Physiol.* 262, C1335–C1340.

Wang, L. G., and Sigworth, F. J. (2009). Structure of the BK potassium channel in a lipid membrane from electron cryomicroscopy. *Nature* 461, 292–296.

Wemmie, J. A., Price, M. P., and Welsh, M. J. (2006). Acid-sensing ion channels: advances, questions and therapeutic opportunities. *Trends Neurosci.* 29, 578–586.

Wilkins, R. J., Browning, J. A., and Ellory, J. C. (2000). Surviving in a matrix: membrane transport in articular chondrocytes. *J. Membr. Biol.* 177, 95–108.

Wilson, J. R., Duncan, N. A., Giles, W. R., and Clark, R. B. (2004). A voltage-dependent K+ current contributes to membrane potential of acutely isolated canine articular chondrocytes. *J. Physiol. (Lond.)* 557, 93–104.

Wohlrab, D., Vocke, M., Klapperstuck, T., and Hein, W. (2004). Effects of potassium and anion channel blockers on the cellular response of human osteoarthritic chondrocytes. *J. Orthop. Sci.* 9, 364–371.

Wohlrab, D., Vocke, M., Klapperstuck, T., and Hein, W. (2005). The influence of lidocaine and verapamil on the proliferation, CD44 expression and apoptosis behavior of human chondrocytes. *Int. J. Mol. Med.* 16, 149–157.

Wohlrab, D., Wohlrab, J., Reichel, H., and Hein, W. (2001). Is the proliferation of human chondrocytes regulated by ionic channels? *J. Orthop. Sci.* 6, 155–159.

Wright, M., Jobanputra, P., Bavington, C., Salter, D. M., and Nuki, G. (1996). Effects of intermittent pressure-induced strain on the electrophysiology of cultured human chondrocytes: evidence for the presence of stretch-activated membrane ion channels. *Clin. Sci.* 90, 61–71.

Wright, M. O., Stockwell, R. A., and Nuki, G. (1992). Response of plasma membrane to pplied hydrostatic pressure in chondrocytes and fibroblasts. *Connect. Tissue Res.* 28, 49–70.

Wu, M. H., Urban, J. P., Cui, Z. F., Cui, Z., and Xu, X. (2007). Effect of extracellular ph on matrix synthesis by chondrocytes in 3D agarose gel. *Biotechnol. Prog.* 23, 430–434.

Wu, Q. Q., and Chen, Q. (2000). Mechanoregulation of chondrocyte proliferation, maturation, and hypertrophy: ion-channel dependent transduction of matrix deformation signals. *Exp. Cell. Res.* 256, 383–391.

Xu, J., Wang, W., Clark, C. C., and Brighton, C. T. (2009). Signal transduction in electrically stimulated articular chondrocytes involves translocation of extracellular calcium through voltage-gated channels. *Osteoarthr. Cartil.* 17, 397–405.

Yellowley, C. E., Hancox, J. C., and Donahue, H. J. (2002). Effects of cell swelling on intracellular calcium and membrane currents in bovine articular chondrocytes. *J. Cell. Biochem.* 86, 290–301.

Yuan, F. L., Chen, F. H., Lu, W. G., Li, X., Wu, F. R., Li, J. P., Li, C. W., Wang, Y., Zhang, T. Y., and Hu, W. (2010). Acid-sensing ion channel 1a mediates acid-induced increases in intracellular calcium in rat articular chondrocytes. *Mol. Cell. Biochem.* 340, 153–159.

Conflict of Interest Statement: The authors declare that the research was conducted in the absence of any commercial or financial relationships that could be construed as a potential conflict of interest.

Received: 07 July 2010; accepted: 09 September 2010; published online: 14 October 2010.

Citation: Barrett-Jolley R, Lewis R, Fallman R and Mobasheri A (2010) The emerging chondrocyte channelome. Front. Physio. 1:135. doi: 10.3389/fphys.2010.00135

This article was submitted to Frontiers in Membrane Physiology and Biophysics, a specialty of Frontiers in Physiology.

Journal of Cellular Physiology

Characterization of a Stretch-Activated Potassium Channel in Chondrocytes

ALI MOBASHERI,[1] REBECCA LEWIS,[2] JUDITH E.J. MAXWELL,[2] CLAIRE HILL,[2] MATTHEW WOMACK,[2] AND RICHARD BARRETT-JOLLEY[2]*

[1]*Musculoskeletal Research Group, Division of Veterinary Medicine, Faculty of Medicine and Health Sciences, University of Nottingham, Leicestershire, United Kingdom*

[2]*Ion Channel Research Group, Department of Comparative Molecular Medicine, Faculty of Health and Life Sciences, University of Liverpool, Liverpool, Merseyside, United Kingdom*

Chondrocytes possess the capacity to transduce load-induced mechanical stimuli into electrochemical signals. The aim of this study was to functionally characterize an ion channel activated in response to membrane stretch in isolated primary equine chondrocytes. We used patch-clamp electrophysiology to functionally characterize this channel and immunohistochemistry to examine its distribution in articular cartilage. In cell-attached patch experiments, the application of negative pressures to the patch pipette (in the range of 20–200 mmHg) activated ion channel currents in six of seven patches. The mean activated current was 45.9 ± 1.1 pA ($n = 4$) at a membrane potential of 33 mV (cell surface area approximately 240 μm^2). The mean slope conductance of the principal single channels resolved within the total stretch-activated current was 118 ± 19 pS ($n = 6$), and reversed near the theoretical potassium equilibrium potential, E_{K+}, suggesting it was a high-conductance potassium channel. Activation of these high-conductance potassium channels was inhibited by extracellular TEA (K_d approx. 900 μM) and iberiotoxin (K_d approx. 40 nM). This suggests that the current was largely carried by BK-like potassium (MaxiK) channels. To further characterize these BK-like channels, we used inside-out patches of chondrocyte membrane: we found these channels to be activated by elevation in bath calcium concentration. Immunohistochemical staining of equine cartilage samples with polyclonal antibodies to the α1- and β1-subunits of the BK channel revealed positive immunoreactivity for both subunits in superficial zone chondrocytes. These experiments support the hypothesis that functional BK channels are present in chondrocytes and may be involved in mechanotransduction and chemotransduction.

J. Cell. Physiol. 223: 511–518, 2010.

Chondrocytes play a critical role in the synthesis, maintenance, and degradation of extracellular matrix (ECM) macromolecules in load-bearing synovial joints (Archer and Francis-West, 2003; Huber et al., 2000). Recent studies suggest that these functions are modulated by ion channels (Mouw et al., 2007; Wohlrab et al., 2001, 2004). Furthermore, modulation of chondrocyte ion channels by inflammatory mediators may be important in the progression of disease (Sutton et al., 2009). Chondrocytes are exquisitely sensitive to mechanical load and their metabolism is acutely influenced by dynamic changes in the physicochemical environment of articular cartilage (Mobasheri et al., 1998; Lee et al., 2000). Although mechanical load is an important regulator of chondrocyte metabolic activity, the mechanisms of this electro-mechanical coupling are poorly understood (Urban, 1994, 2000). Cartilage responds to load-induced deformation with electrical changes in both the ECM and within the chondrocytes themselves (Lee et al., 2000; Lee and Knight, 2004). Recent studies have provided evidence for hydrostatic and mechanically induced changes in membrane potential of articular chondrocytes under load (Wright et al., 1996; Sanchez and Wilkins, 2004). The deformation of the chondrocyte membrane is thought to be one of several modes of mechanotransduction pathways involved in sensing and responding to changes in mechanical load (Guilak, 1995; Guilak et al., 1995; Knight et al., 1998). Thus, load-induced changes in the chondrocyte membrane, including membrane stretch, are likely to play a key role in the signal-transduction cascades associated with chondrocyte mechanotransduction. The open probability of stretch-activated ion channels generally increases in response to mechanical deformation of the plasma membrane (Sachs and Sokabe, 1990). Although very little is known about chondrocyte stretch-activated ion channels and the macromolecular complexes in which they function, it is thought that they may be linked to the cytoskeleton via β1-integrins (Mobasheri et al., 2002). This may be responsible for their gating by transmitting extracellular physical forces of stretch or pressure to the channels, causing them to undergo a conformational change (Mobasheri et al., 2002). Activation of these ion channels may lead to changes in cell activity via alteration of the resting membrane potential (Mobasheri et al., 2002). This is supported by studies using ion channel blockers that disrupt the process of mechanotransduction (Wu and Chen, 2000; Mouw et al., 2007). Other studies have suggested that the activation of ion channels may allow the efflux of sufficient ions to drive a decrease in cell volume (regulatory volume decrease) (Hall et al., 1996). The identity of these

Abbreviations: BK/MaxiK, large calcium-activated potassium channel; K_d, dissociation constant; TEA, tetraethylammonium; E_{K+}, equilibrium potential for potassium; ECM, extracellular matrix.

Contract grant sponsor: The Biotechnology and Biological Sciences Research Council (BBSRC), UK.
Contract grant sponsor: The Wellcome Trust, UK.

*Correspondence to: R. Barrett-Jolley, DPhil, Senior Lecturer, Ion Channel Research Group, Department of Comparative Molecular Medicine, Faculty of Health and Life Sciences, University of Liverpool, Brownlow Hill and Crown Street, Liverpool L69 7ZJ, United Kingdom. E-mail: RBJ@liverpool.ac.uk

Received 15 October 2009; Accepted 21 December 2009

Published online in Wiley InterScience (www.interscience.wiley.com.), 16 February 2010.
DOI: 10.1002/jcp.22075

channels has, however, remained unknown. Information available on the NCBI AceView database suggests that full-length cDNA clones encoding large-conductance (BK-like, MaxiK channels) calcium-activated potassium channels have been isolated from normal and osteoarthritic human articular cartilage and chondrosarcoma cells. There is also some published information about nonspecific mechanosensitive ion channels (Guilak et al., 1999) and transient receptor potential vanilloid 4 (TRPV4) channels in chondrocytes (Phan et al., 2009). However, thus far nothing is known about large-conductance BK-like channel expression and subunit composition in articular chondrocytes. Given the putative emerging role of potassium channels in a variety of cellular processes, we feel that establishing functional roles for these in mineralized tissues would be a welcome advance in the field. Accordingly, in this study, we propose the hypothesis that stretch-activated current is carried by large-conductance (BK-like, MaxiK channels) calcium-activated potassium channels. We used patch-clamp electrophysiology to functionally identify the principal stretch-activated ion channel in equine articular chondrocytes. We also explored the distribution of the stretch-activated channel in sections of equine articular cartilage using immunohistochemistry.

Materials and Methods

Chemicals

Unless otherwise stated, all chemicals used in this study were of molecular biology or ACS grade and supplied by Sigma-Aldrich (Poole, UK).

Cartilage source

Equine joints were obtained from a local abattoir (Nantwich, Cheshire). Articular cartilage was obtained from the femeropatellar, carpal, and metacarpophalangeal joints of skeletally mature male and female horses ($n = 6$). The study was conducted with local institutional ethical approval, in strict accordance with national guidelines. All the animals used were killed for unrelated clinical reasons.

Histology and tissue processing

Equine cartilage samples were fixed for 24 h in 10% neutral buffered formalin and decalcified in EDTA for a further 72 h. Full-depth samples were embedded in paraffin wax and processed for routine histological and immunohistochemical staining. Stained slide preparations were examined with a Nikon Eclipse 80i microscope. Normal equine sections were cut (7 μm paraffin sections) and mounted on 3-aminopropyltriethoxysilane (APES) treated slides for subsequent immunohistochemical studies.

Preparation of isolated chondrocytes

Equine cartilage shavings including both mid and superficial layers, but not full depth, were rinsed with phosphate-buffered saline (PBS) then cut into small slices. These were then incubated overnight with type I collagenase (EC 3.4.24.3 from *Clostridium histolyticum*, approximately 100 collagen digestion units ml^{-1}) in serum-free Dulbecco's modified Eagles medium (DMEM) supplemented with 1,000 $mg\,l^{-1}$ glucose and 1% penicillin/streptomycin solution. The filtered cell suspension was washed three times in fresh DMEM and the cells were grown in monolayer culture with 4% fetal calf serum (FCS) for up to two passages. Electrophysiological studies were carried out using freshly isolated chondrocytes, first expansion, first and second passage equine chondrocytes.

BK channel antibodies

Polyclonal rabbit antibodies developed against the α- and β-subunits of the BK channel (MaxiK) were obtained from Abcam Plc (Cambridge, UK). The immunizing peptide for the α1-subunit of the BK channel corresponds to amino acid residues 945–961 of the human α1-subunit of the human BK protein (KCNMA1 gene, encoding potassium large-conductance calcium-activated channel, subfamily M, alpha member 1): (945) ELVNDTNVQFLDQDDD (961). The immunizing peptide for the β1-subunit of the BK channel corresponds to amino acid residues 90–103 of the human β1-subunit of the human BK protein (KCNMB1 gene, encoding potassium large-conductance calcium-activated channel, subfamily M, beta member 1): (90) YHTEDTRDQNQQC (103). These two sequences are highly conserved across many mammalian species including mouse, rat, and human.

BK channel immunohistochemistry

Sections of equine cartilage were probed for BK channel expression by immunohistochemistry essentially as previously described (Mobasheri et al., 2005). Equine cartilage tissue microarrays (TMAs) were prepared as described in two recent studies (Mobasheri et al., 2005, 2007) using an Abcam Tissue Micro Array builder (ab1802; Cambridge, UK). Using this approach, equine cartilage samples were arranged in a 6 × 4 grid array on a single-charged microscope slide. This approach increases the throughput for screening equine cartilage samples for BK channel expression using the immunohistochemical technique (Mobasheri et al., 2004). TMA slides were deparaffinized in xylene for 20 min to remove embedding medium and washed in absolute ethanol for 3 min. The TMAs were gradually rehydrated in a series of alcohol baths (96%, 85%, and 50%) and placed in distilled water for 5 min. Endogenous peroxidase activity was blocked for 1 h in a solution of 97% methanol, 3% hydrogen peroxide, and 0.01% sodium azide. The TMAs were then incubated for 1 h at room temperature in Tris-buffered saline (TBS), containing 1% protease-free bovine serum albumin (BSA) and 0.01% sodium azide to block non-specific antibody binding. Slides were incubated overnight at 4°C with rabbit polyclonal antibodies to α (KCNMA1) and β (KCNMB1) subunits of the BK channel. Antibodies were diluted 1:200 in TBS containing 1% BSA. After 24 h at 4°C, the slides were washed three times for 5 min each in TBS containing 0.05% Tween 20 (TBS-T) before incubation with horseradish peroxidase-labelled polymer conjugated to affinity-purified goat anti-rabbit immunoglobulins (code no. K4010; Dako) for 30 min at room temperature. The sections were washed three times for 5 min in TBS-T before application of liquid DAB+ chromogen (3,3′-diaminobenzidine solution; Dako). The development of the brown-colored reaction was stopped by rinsing in TBS-T. The stained slides were immersed for 5 min in a bath of aqueous hematoxylin (code no. S3309; DakoCytomation) to counterstain cell nuclei. Finally, the slides were washed for 5 min in running water and dehydrated in a series of graded ethanol baths before being rinsed in three xylene baths and mounted in 1,3-diethyl-8-phenylxanthine (BDH Laboratories, Atherstone, UK). Control experiments were performed by omitting the primary antibody from the immunohistochemical procedure.

Microscopy and image acquisition

Immunostained tissue sections were examined with a Nikon Eclipse 80i microscope. Photomicrographs were digitally captured using a Nikon Digital Sight DS-5M camera and Nikon Eclipsenet image capture software.

Electrophysiological recording

Shards of coverslips with adherent chondrocytes were transferred to a custom tissue chamber and superfused with an extracellular solution (Table 1). Patch pipettes were fabricated from thick walled (Clarke 1.5 mm, filament borosilicate) capillary glass (Harvard Apparatus) on a Brown-Flaming MP P-80 horizontal puller (Sutter Instrument Co.). Pipette resistances were in the range of 5–12 MOhms. Voltage-clamp control was maintained with an Axon

200B Axopatch amplifier (Axon Instruments, Union City, CA), and data were filtered typically at 2 KHz (as appropriate) and digitized (10 kHz) with a DigiData 1200B interface attached to a PC running the AXGOX suit of Axobasic programs (Barrett-Jolley et al., 2000) and/or WinEDR PC software (Dr. John Dempster, University of Strathclyde).

Cell-attached patch experiments. Cell-attached patch was performed with high potassium extracellular solution in the bath and pipette (see Table 1), unless otherwise stated. The high extracellular potassium in the bath (Bath solution, Table 1) largely nullifies the resting membrane potential and allows the membrane potential (V_m) to be estimated directly from V_p (the pipette command potential or holding potential, H_p). For calculation unitary conductance using all-points amplitude histograms (Fig. 2), patches were chosen with low numbers of active channels. This allows characterization of unitary events.

Inside-out patch experiments. Inside-out patches of chondrocyte membranes were drawn from cells superfused with a 145 K^+ (pseudo-intracellular) bath solution, with either 200 μM Ca^{2+} or 0.5 mM EGTA added. The pipette solution, See Table 1. For cell-attached and inside-out patch figures, outward currents are shown as upward deflections. V_m is calculated as $-V_p + V_j$, where V_j is the junction potential (see Table 1).

Whole-cell membrane potential (V_m) measurement. Membrane potentials were recorded in whole-cell current clamp mode using an NPI SEC-05LX amplifier with relatively high resistance patch pipettes (approximately 15 MΩ), since the switch clamp electronics of this amplifier are not affected by series resistance. Patch pipettes were filled with a high KCl "intracellular" solution with 0.5 mM EGTA (see Table 1) and the bath was perfused with "extracellular" solutions of varying osmotic potentials (Table 1). Note that it was viewed important to not change the ionic compositions when exposing cells to changes in osmotic potential. To make this possible, NaCl was kept low at all times, and the only change that took place with changing osmolarity was the concentration of sucrose. In some experiments, 10 mM TEA was included; in these experiments TEA concentrations were also kept constant throughout the duration of the recording.

Electrophysiological data analysis. Analysis was performed with WinEDR PC software (John Dempster, University of Strathclyde). K_ds were calculated by solving the following equation

$$F = 1 - \frac{[c]}{[c] - 10^{K_d}} \qquad (1)$$

where F is the fractional current remaining and [c] is the concentration of ligand. K_d values are presented with 95% confidence intervals (95% CI) as described previously (Barrett-Jolley et al., 1999; Barrett-Jolley, 2001). Unless otherwise stated, statistical significance was assessed by ANOVA in StatsDirect (Altrincham, Cheshire, UK) with statistical significance defined as $P \leq 0.05$. Electrophysiological data were fitted in SigmaPlot (Systat Software, Inc. [SSI], San Jose, CA) and Microcal Origin (Northampton, MA). Figures were prepared using SigmaPlot. Values are expressed as mean ± SEM (n).

Predicted E_{K+} and E_{Cl-} values given in the text are calculated assuming 150 mM internal potassium and 10 mM internal chloride (Mobasheri et al., 1998). All membrane potentials have been corrected for junction potentials (see Table 1).

All experiments were performed at a slightly elevated room temperature (23–26°C).

Results

Cell-attached patch mode

We applied stretch to chondrocyte membranes by applying negative pressure directly to the patch pipette while recording ion channel activity with the cell-attached mode of the patch-clamp technique. This activated outward current in six of seven patches (Fig. 1). When activated, the mean total current activity was 45.9 ± 1.1 pA at a membrane potential of 33 mV. Under these conditions, the most conspicuous unitary activity was calculated to have a slope conductance of 118 ± 19 pS ($n = 6$, Fig. 2). Activation of current by stretch was significantly inhibited by TEA and by iberiotoxin (Fig. 1) Dissociation constants (K_d) calculated from Equation 1 were: TEA 0.9 mM (95% CI: 0.5–1.7 mM), $n = 4$. Iberiotoxin 40 nM (95% CI: 28.0–56.9), $n = 14$.

Current-voltage analysis revealed that these channels reversed near to predicted values for E_{K+} (Table 1 and Fig. 2), both with high (116 mM) and low (15 mM) extracellular (pipette solution) potassium concentrations. Slope conductance was 118 ± 19 pS ($n = 6$) with 116 mM extracellular potassium and nonlinear with 15 mM extracellular potassium (note that K^+ was replaced with Li^+ since Li^+ has a low permeability for BK channels (Latorre et al., 1989).

Isolated patch-clamp experiments

To confirm sensitivity of the channel to cytosolic Ca^{2+}, patches with stretch-activated channels were isolated (inside-out patches, Fig. 3) and Ca^{2+} applied to the intracellular face of the membrane (i.e., to the bath solution). In the presence of 200 μM bath Ca^{2+}, high levels of channel activity were maintained. In inside-out patch mode, unitary currents again reversed near to E_{K+} (Fig. 3D, and see Table 1); however, as predicted for calcium-activated potassium channels, channel activity ceased when cytosolic calcium was removed (addition of 0.5 mM EGTA).

Membrane potential (V_m) measurement experiments

Since we have shown the activation of a significant potassium current (above), one would expect the whole-cell V_m to be hyperpolarized by membrane stretch. To apply membrane

TABLE 1. All junction potentials (V_j) calculated with JPCalcW, by Prof. P. Barry, University of New South Wales, Australia

	K^+	Li^+	Na^+	Mg^{2+}	Ca^{2+}	Cl	Sucrose	Glucose	HEPES	EGTA	pH	E_{K+} (mV)	V_j (mV)
Cell-attached (bath solution)	115	0	0	1.6	2	123	0	10	10	0	7.4	—	—
Cell-attached (pipette; high K^+)	116	0	0	1.6	2	123	0	10	10	0	7.4	−7[2]	0[1]
Cell-attached (pipette; low K^+)	14	110	0	1.6	2	131	0	10	10	0	7.4	−57[1]	−6.1[1]
Inside-out (Bath)	145	0	0	1	—[2]	145	0	0	10	—[2]	7.2	—	
Inside-out (pipette)	50	0	90	1	0	142	0	0	10	0	7.4	−25[3]	−2.5[3]
Whole-Cell (pipette)	148	0	4	1	0	148	0	0	10	0.5	7.2	−85[4]	2.1[4]
Hypotonic 134 mOsm (bath solution)[5]	5	0	55[6]	1	2	61	0	0	10	0	7.4	—	
Hypotonic 224 mOsm (bath solution)[5]	5	0	55[6]	1	2	61	90	0	10	0	7.4	—	
Isontonic (bath solution)[5]	5	0	55[6]	1	2	61	180	0	10	0	7.4	—	

[1]When used with the standard cell attached "Bath" solution and assuming intracellular $K^+ = 150$ mM.
[2]Either 200 μM Ca was added or 0.5 mM EGTA as stated in the text.
[3]When combined with the standard inside-out "Bath" solution.
[4]When matched to either of the whole-cell bath solutions.
[5]For whole-cell TEA experiments: TEA was maintained at 10 mM both in the bath and the pipette.
[6]When changing the osmolarity of this system, it was essential not to disturb ionic concentrations, thus the only difference between the isotonic and hypotonic bath solutions is the concentration of sucrose. Thus, an initial low Na^+ concentration was required.

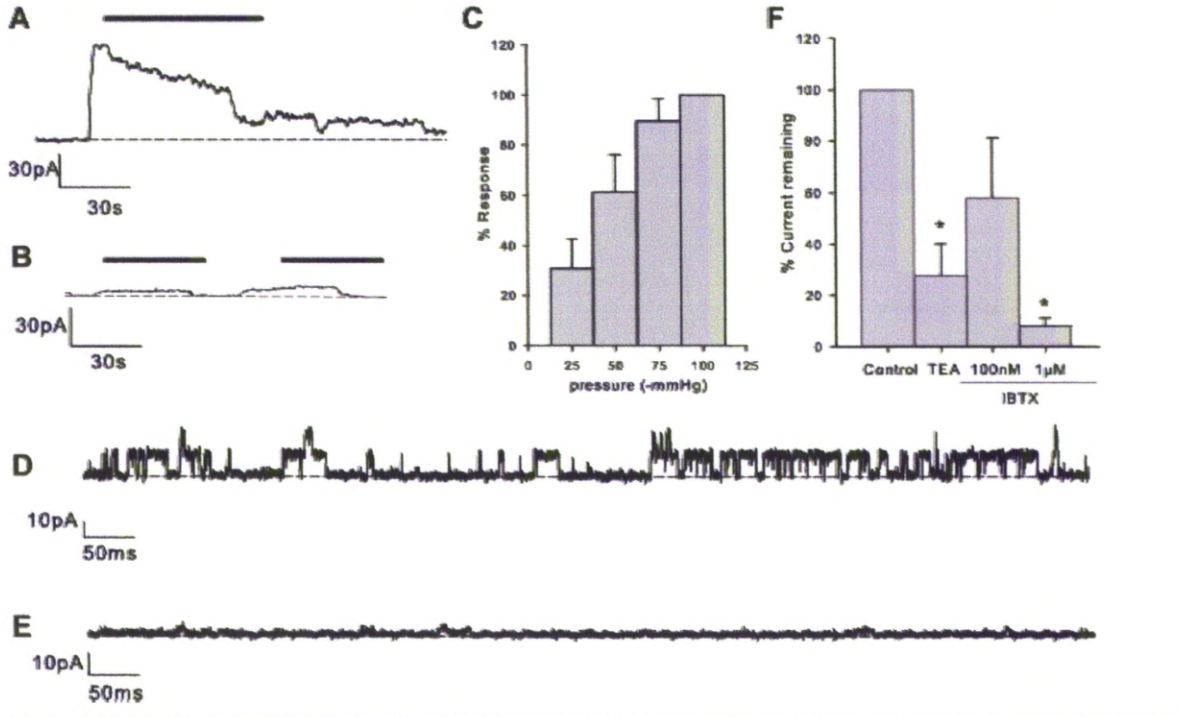

Fig. 1. Activation of ion channels by membrane stretch. A: Application of suction (as indicated by the solid bar) to the patch pipette of chondrocytes under cell-attached mode of recording increases membrane current. $V_m = 33$ mV. B: Similar experiment to "A," but with 3 mM TEA included in the patch pipette. The suction "response" is greatly reduced. C: Increasing negative pressures yield increasingly large activations of current. The y-axis is the percentage current activation of the maximum seen in each particular patch. Data from nine patches. D: Single channels ($V_m = 33$ mV) in the "tail" of the suction response for a control experiment similar to that in "A." E: Single channels ($V_m = 33$ mV) in the "tail" of the suction response for an experiment similar to that in "B," with 3 mM TEA in the patch pipette. F: Summary of experiments similar to that shown in A and B. *$P \leq 0.05$. IBTX, iberiotoxin.

stretch in this configuration, we applied solutions of decreased osmolarity (Fig. 4). This led to a hyperpolarization of 13.9 ± 3.1 mV ($n = 9$). This hyperpolarization was significantly inhibited by the presence of 10 mM TEA (5.2 ± 1.5 mV, $n = 6$; $P \leq 0.05$).

Immunohistochemical distribution of the BK channel

The results of the immunohistochemical experiments are summarized in Figure 5.

α1-subunit of the BK channel (KCNMNA1). The α1-subunit of the BK channel was mainly expressed in the superficial zone of macroscopically and microscopically normal articular cartilage from healthy joints (Fig. 5)[Q2]. The immunoreactivity observed for this subunit was much lower in the middle and deep zones of normal cartilage samples.

β1-subunit of the BK channel (KCNMNB1). We observed a similar pattern of immunoreactivity for the β1-subunit of the BK channel in articular cartilage. The β1-subunit was strongly expressed in the superficial zone of normal articular cartilage. As with the α1-subunit, immunoreactivity for the β1-subunit was much lower in the middle and deep zones of normal cartilage samples.

Discussion

In this study, we used the patch-clamp technique to functionally characterize an ion channel activated in response to mechanically applied membrane stretch in acutely isolated primary equine chondrocytes. These cells hyperpolarize when stretched using a hypotonic challenge applied to the whole cell. This hyperpolarization was greatly reduced by TEA. Having identified functional BK-like calcium-activated potassium channels electrophysiologically, we then employed immunohistochemistry to demonstrate the presence of the α1- and β1-subunits of the BK channel in sections of normal articular cartilage.

We chose the equine chondrocyte model since we have ready access to fresh equine joint tissues. Ideally, one would measure the electrical activity of chondrocytes in vivo or in fresh slices of articular cartilage. However, the presence of a tough ECM of collagens and aggregating proteoglycans makes this a technically impossible prospect. Consequently, most electrophysiological studies are performed with freshly isolated chondrocytes or with cell lines. Work from our own group has established that the primary isolated chondrocytes dedifferentiate to a fibroblastic phenotype after four or more passages in culture (Schulze-Tanzil et al., 2004) and cell lines themselves have the profound limitation that they have little phenotypic homology to primary chondrocytes (see, e.g., Benya and Shaffer, 1982; Gebauer et al., 2005; Schorle et al., 2005). For this reason, we used freshly dissociated chondrocytes and up to second passage cells for patch-clamp electrophysiological studies. This ensures that the cells being studied retain their unique phenotype, but still allows for the application of powerful patch-clamp techniques. Indeed, we have found a strong correlation between our immunohistochemical studies on native tissue and our patch-clamp studies on isolated cells. This has been the case both here and in previous studies (Mobasheri et al., 2005, 2007).

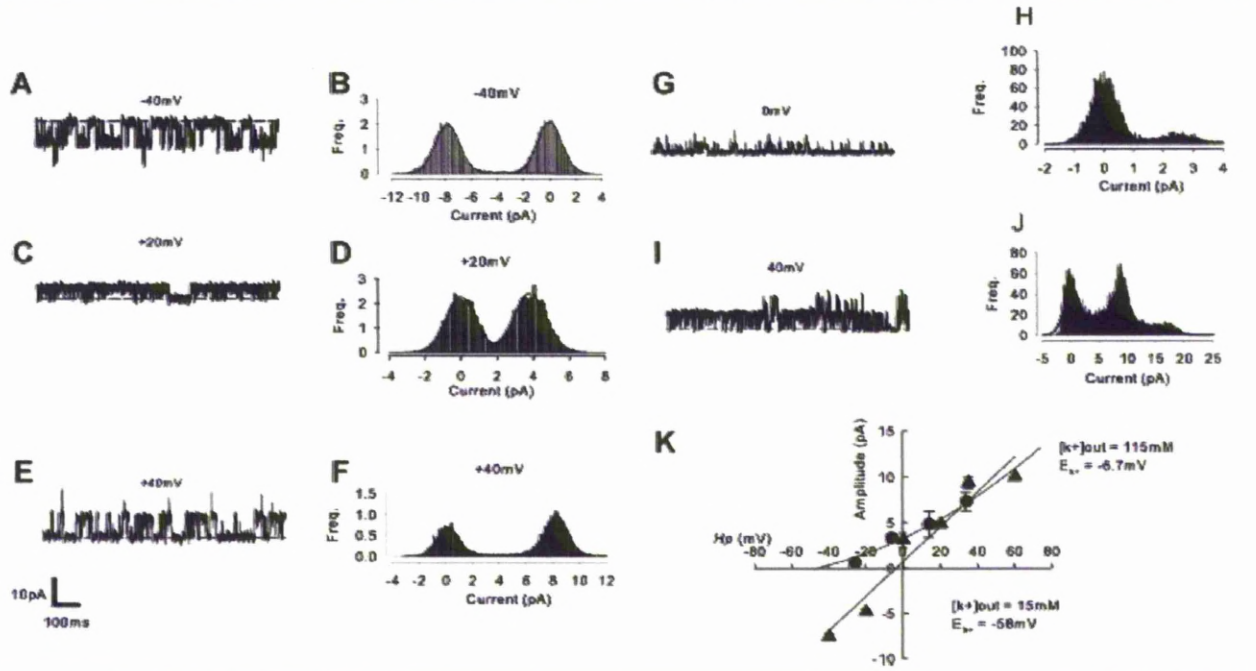

Fig. 2. Stretch activates a high-conductance potassium current. A–F: cell-attached patch recordings of stretch-activated channel activity with 115 mM pipette [K^+]. A,C,E: Raw traces at −40, +20, and +40 mV respectively. B,D,F: All-points amplitude histograms for the events shown in corresponding traces A, C, and E. Results from similar experiments are shown in G to J, but with 15 mM [K^+] in the pipette. K: Mean current-voltage curves from experiments similar to those illustrated in A to J. Triangles: pipette 115 mM ($n = 6$), circles: pipette 15 mM ($n = 5$). The straight line fitted through the 115 mM K^+ data has slope 192 pS. The 15 mM K^+ data are fit with the Hodgkin–Katz current equation (Hodgkin and Katz, 1949) assuming the presence of only potassium conductance with P_{K+} 0.4e $^{-12}$ m^3 s^{-1}. Complete solutions and calculated E_{K+} values are described in Table 1.

The principal stretch-activated channel we identified in these functional studies had a size (slope conductance), reversal potential, and pharmacology consistent with it being a large calcium-activated potassium channel (BK) (Latorre et al., 1989; Cui et al., 2009). We found the sensitivity to iberiotoxin to be statistically significant but weak. This is interesting because although the BK channel can exist as a standalone six transmembrane α-subunit, complete with potassium conducting pore and Ca^{2+} sensor (Wang and Sigworth, 2009), the presence of a β-subunit modifies many of the channel's functional properties (Salkoff et al., 2006). In particular, low sensitivity to iberiotoxin is highly characteristic of the expression of BK channels consisting of both the α_1 and β_1-subunits (Lippiat et al., 2003). This correlated well with our identification of positive immunohistochemical staining for BK channels in normal articular cartilage samples with antibodies both α1- and β1-subunits.

Membrane stretch is a realistic physiological challenge for the chondrocyte and directly linked to changes in matrix production (Urban et al., 1993). Stretch will occur in two contexts. First, when the chondrocyte is deformed by compressive force, the cell passes from a virtually spherical conformation to an approximate ellipsoid (Guilak, 1994; Urban, 1994). For a given volume, an ellipsoid has a greater surface area than a sphere and so membrane stretch is the result. Secondly hypo-osmotic conditions cause cell swelling (Urban et al., 1993), increase cell radius, and consequently increase its surface area. These increases in membrane surface area are likely to be met by stretch rather than the production of a new membrane. This membrane stretch will be limited to a theoretical maximum of approximately 3% at which point it may be expected to rupture (Morris and Homann, 2001). In our experiments, we used two different membrane stretch paradigms, but the results from both were consistent with the opening of potassium channels in response. Both of these approaches have their strengths and weaknesses. The direct membrane stretch (cell-attached patch) experiments allowed us to investigate the situation when neither intracellular or extracellular environments were altered, but this did not allow us to see the effects on the whole cell. Our osmotic challenge experiments required, by definition, alterations of extracellular environment and dialization of the cytosol with the patch-pipette solution. Nevertheless with the whole-cell experiments, we were able to measure the resultant hyperpolarization.

In general terms, there appear to be two possibilities to explain the activation of BK channels by stretch. These could be termed either calcium-dependent or calcium-independent mechanisms. The calcium-dependent hypothesis would require that stretch increases intracellular Ca^{2+} and that this activates the BK channel. Such Ca^{2+} ions could come either from stores (Grandolfo et al., 1998) or from TRP ion channels in the cell membrane (Phan et al., 2009). This is difficult to prove in patch-clamp experiments. In cell-attached patch mode, the intracellular milieu is controlled by the cell itself and, in our whole-cell experiments, Ca^{2+} is buffered partially, but not entirely by EGTA in the patch-pipette solution. More effective calcium buffers are available (BAPTA for example), but with these in the patch-pipette solution there may be brief local rises in Ca^{2+} as, for example, "sparks" (Cheng and Lederer, 2008) that are apparent in many cell types. The calcium-independent hypothesis could involve either direct sensing of stretch by the

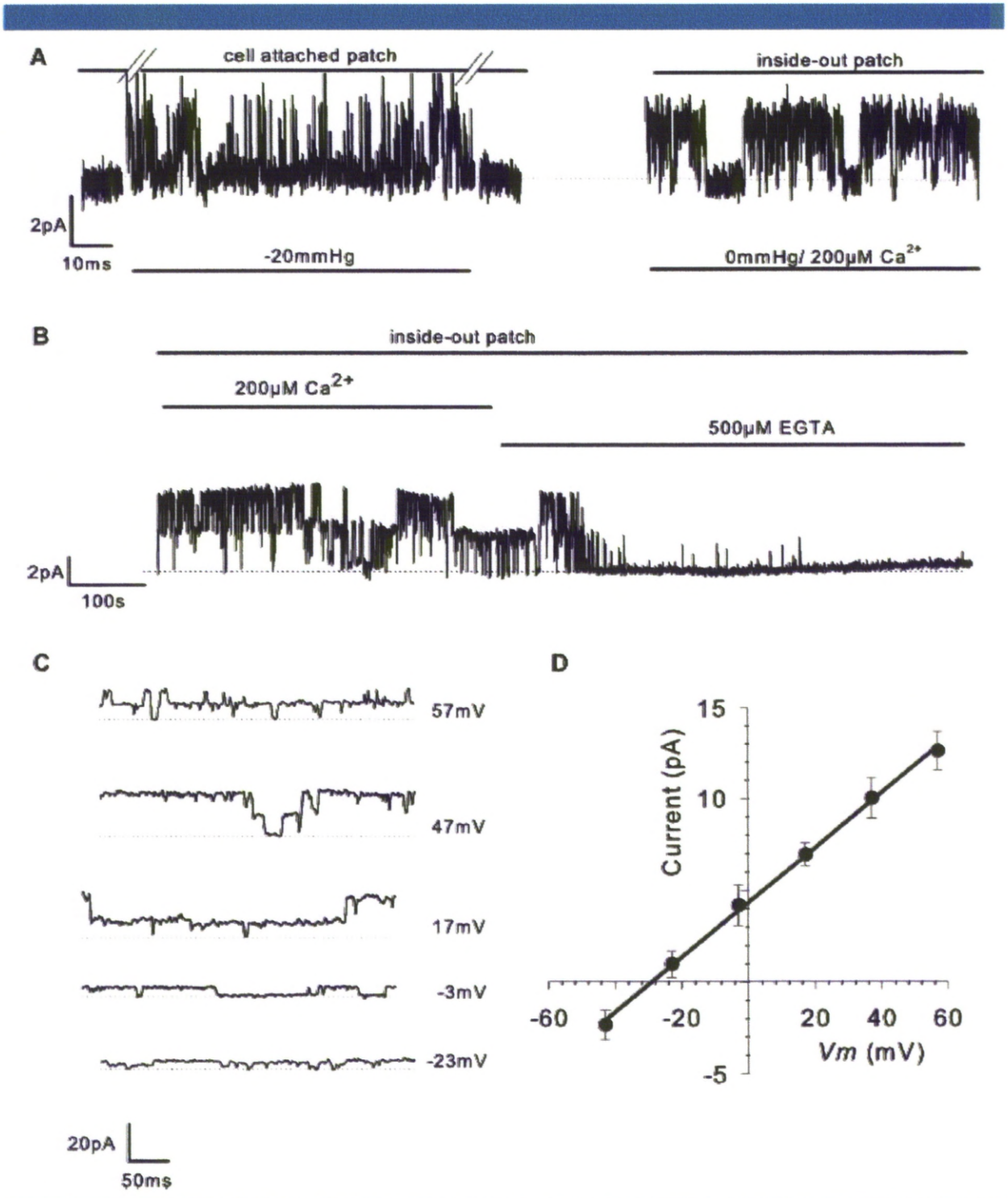

Fig. 3. Isolated patch recordings. A: Application of negative pressure to the side port of the pipette holder stretches the membrane beneath the patch pipette (cell-attached patch mode) and activates an ion channel current (−3 mV). B: Channel activity is still apparent following patch excision (inside-out patch) and is clearly sensitive to 200 μM cytoplasmic calcium or 500 μM EGTA (−3 mV). C: Ion channel activity activated as described in A and B (inside-out patch, 200 μM Ca^{2+}, but with 145/55 mM K^+ E_{K+} = 25 mV) at a range of holding potentials. D: Current-voltage curves from nine experiments such as that shown in C, in inside-out patch mode. The curve represents a straight line regression with slope 147 pS.

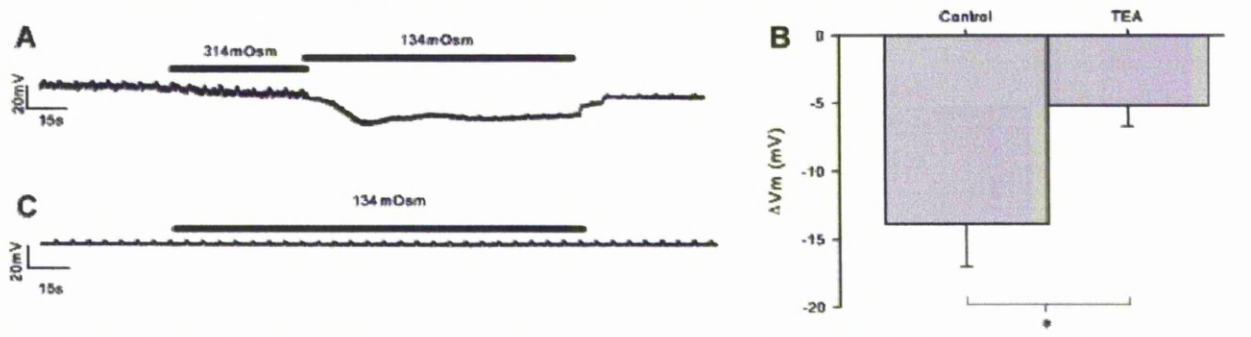

Fig. 4. Whole-cell stretch hyperpolarizes chondrocytes. A: Application of membrane stretch by means of hypotonic challenge (from 314 to 134 mOsm) hyperpolarizes the membrane. Membrane potential was measured continuously with periodic injections of current to monitor cell integrity. B: An equivalent experiment repeated (different cell) in the presence of 10 mM TEA. The hyperpolarization is significantly reduced by the presence of 10 mM TEA (B,C). *$P \leq 0.05$.

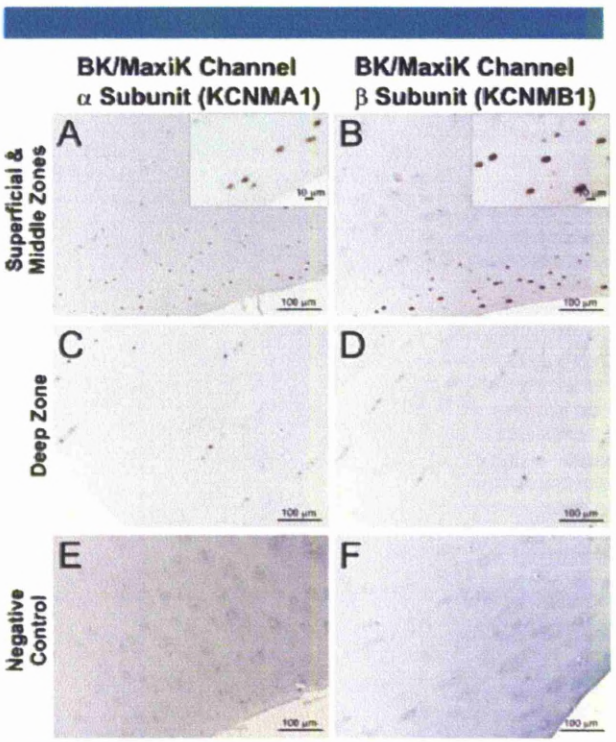

Fig. 5. Distribution of the α1- and β1-subunits of the BK channel (KCNMB1 and KCNMNB1) in equine articular cartilage. Immunohistochemical analysis of samples of full-depth equine articular cartilage was carried out using polyclonal antibodies raised against the α1- and β1-subunits of the BK channel. Sections of equine cartilage were immunostained with primary antibodies and horseradish peroxidase-labelled rabbit anti-goat secondary IgG (DakoCytomation). Positive immunoreactivity for both subunits was predominantly observed in superficial zone chondrocytes in normal cartilage. The magnified areas in the insets shown in panels A and B highlight the chondrocyte-specific immunostaining. Omission of primary antibody from the immunohistochemical procedure served as negative controls. Sections of equine articular cartilage were treated in exactly the same way during the immunohistochemical procedure except that the primary antibody was omitted. Original magnifications of the main panels: 200×. Bars in the main panels represent 100 μm. Bars in the magnified insets shown in panels A and B represent 10 μm.

channel itself or coupling of the channel to other mechanoreceptors such as β_1-integrins (Mobasheri et al., 2002).

The function of BK channels within the chondrocyte cell membrane is still unknown, but there are a few clear possibilities. First, the BK channel could be acting as an "osmolyte" channel (Hall et al., 1996; Kerrigan and Hall, 2008), since the activation of potassium conductances will allow potassium ion efflux, decreasing intracellular osmotic potential and facilitating regulatory volume decrease. Secondly, it is possible that it is the influence of the BK channel on the membrane potential that is critical, as it is in vascular tissue (Ledoux et al., 2006). In many cell types, BK channels also function as O_2 sensors (Kemp et al., 2006), and hypoxia is a condition important to the function of chondrocytes (Pfander and Gelse, 2007; Srinivas et al., 2009). BK channels could therefore be involved in coupling O_2 tension and mechanical pressure to membrane potential. The membrane potential in turn appears to be important for key chondrocyte functions. For example, ion channel blockers, such as SITS and 4-AP, depolarize the membrane potential (Tsuga et al., 2002; Ponce, 2006) and decrease cell proliferation and matrix secretion (Wohlrab et al., 2001, 2004; Mouw et al., 2007). These possibilities will be the subject of future investigations.

Acknowledgments

The authors thank their collaborator Professor John Innes. The work was supported, in part, by a BBSRC Doctoral Training Grant (R. Lewis) and a studentship from the Wellcome Trust (J.E.J. Maxwell).

Literature Cited

Archer CW, Francis-West P. 2003. The chondrocyte. Int J Biochem Cell Biol 35:401–404.
Barrett-Jolley R. 2001. Nipecotic acid directly activates GABA(A)-like ion channels. Br J Pharmacol 133:673–678.
Barrett-Jolley R, Dart C, Standen NB. 1999. Direct block of native and cloned (Kir2.1) inward rectifier K+ channels by chloroethylclonidine. Br J Pharmacol 128:760–766.
Barrett-Jolley R, Pyner S, Coote JH. 2000. Measurement of voltage-gated potassium currents in identified spinally-projecting sympathetic neurones of the paraventricular nucleus. J Neurosci Methods 102:25–33.
Benya PD, Shaffer JD. 1982. Dedifferentiated chondrocytes reexpress the differentiated collagen phenotype when cultured in agarose gels. Cell 30:215–224.
Cheng HP, Lederer WJ. 2008. Calcium sparks. Physiol Rev 88:1491–1545.
Cui J, Yang H, Lee US. 2009. Molecular mechanisms of BK channel activation. Cell Mol Life Sci 66:852–875.
Gebauer M, Saas J, Sohler F, Haag J, Soder S, Pieper M, Bartnik E, Beninga J, Zimmer R, Aigner T. 2005. Comparison of the chondrosarcoma cell line SW1353 with primary human adult articular chondrocytes with regard to their gene expression profile and reactivity to IL-1 beta. Osteoarthr Cartilage 13:697–708.
Grandolfo M, Calabrese A, D'Andrea P. 1998. Mechanism of mechanically induced intercellular calcium waves in rabbit articular chondrocytes and in HIG-82 synovial cells. J Bone Miner Res 13:443–453.

Guilak F. 1994. Volume and surface-area measurement of viable chondrocytes in-situ using geometric modeling of serial confocal sections. J Microsc Oxford 173:245–256.
Guilak F. 1995. Compression-induced changes in the shape and volume of the chondrocyte nucleus. J Biomech 28:1529–1541.
Guilak F, Ratcliffe A, Mow VC. 1995. Chondrocyte deformation and local tissue strain in articular cartilage: a confocal microscopy study. J Orthop Res 13:410–421.
Guilak F, Zell RA, Erickson GR, Grande DA, Rubin CT, McLeod KJ, Donahue HJ. 1999. Mechanically induced calcium waves in articular chondrocytes are inhibited by gadolinium and amiloride. J Orthop Res 17:421–429.
Hall AC, Starks I, Shoults CL, Rashidbigi S. 1996. Pathways for K+ transport across the bovine articular chondrocyte membrane and their sensitivity to cell volume. Am J Physiol-Cell Physiol 270:C1300–C1310.
Hodgkin AL, Katz B. 1949. The effect of sodium ions on the electrical activity of the giant axon of the Squid. J Physiol Lond 108:37–77.
Huber M, Trattnig S, Lintner F. 2000. Anatomy, biochemistry, and physiology of articular cartilage. Invest Radiol 35:573–580.
Kemp PJ, Williams SE, Mason HS, Wootton P, Iles DE, Riccardi D, Peers C. 2006. Functional proteomics of BK potassium channels: defining the acute oxygen sensor. Novartis Found Symp 272:141–151.
Kerrigan MJP, Hall AC. 2008. Control of chondrocyte regulatory volume decrease (RVD) by [Ca2+](i) and cell shape. Osteoarthr Cartilage 16:312–322.
Knight MM, Ghori SA, Lee DA, Bader DL. 1998. Measurement of the deformation of isolated chondrocytes in agarose subjected to cyclic compression. Med Eng Phys 20:684–688.
Latorre R, Oberhauser A, Labarca P, Alvarez O. 1989. Varieties of calcium-activated potassium channels. Annu Rev Physiol 51:385–399.
Ledoux J, Werner ME, Brayden JE, Nelson MT. 2006. Calcium-activated potassium channels and the regulation of vascular tone. Physiology 21:69–78.
Lee DA, Knight MM. 2004. Mechanical loading of chondrocytes embedded in 3D constructs: in vitro methods for assessment of morphological and metabolic response to compressive strain. Methods Mol Med 100:307–324.
Lee DA, Noguchi T, Frean SP, Lees P, Bader DL. 2000. The influence of mechanical loading on isolated chondrocytes seeded in agarose constructs. Biorheology 37:149–161.
Lippiat JD, Standen NB, Harrow ID, Phillips SC, Davies NW. 2003. Properties of BK(Ca) channels formed by bicistronic expression of hSloalpha and beta 1-4 subunits in HEK293 cells. J Membr Biol 192:141–148.
Mobasheri A, Mobasheri R, Francis MJ, Trujillo E, Alvarez de la Rosa D, Martin-Vasallo P. 1998. Ion transport in chondrocytes: membrane transporters involved in intracellular ion homeostasis and the regulation of cell volume, free [Ca2+] and pH. Histol Histopathol 13:893–910.
Mobasheri A, Carter SD, Martin-Vasallo P, Shakibaei M. 2002. Integrins and stretch activated ion channels; putative components of functional cell surface mechanoreceptors in articular chondrocytes. Cell Biol Int 26:1–18.
Mobasheri A, Airley R, Foster CS, Schulze-Tanzil G, Shakibaei M. 2004. Post-genomic applications of tissue microarrays: basic research, prognostic oncology, clinical genomics and drug discovery. Histol Histopathol 19:325–335.
Mobasheri A, Gent TC, Womack MD, Carter SD, Clegg PD, Barrett-Jolley R. 2005. Quantitative analysis of voltage-gated potassium currents from primary equine (*Equus caballus*) and elephant (*Loxodonta africana*) articular chondrocytes. Am J Physiol Regul Integr Comp Physiol 289:R172–R180.
Mobasheri A, Gent TC, Nash AI, Womack MD, Moskaluk CA, Barrett-Jolley R. 2007. Evidence for functional ATP-sensitive (K(ATP)) potassium channels in human and equine articular chondrocytes. Osteoarthr Cartilage 15:1–8.
Morris CE, Homann U. 2001. Cell surface area regulation and membrane tension. J Membr Biol 179:79–102.
Mouw JK, Imler SM, Levenston ME. 2007. Ion-channel regulation of chondrocyte matrix synthesis in 3D culture under static and dynamic compression. Biomech Model Mechanobiol 6:33–41.
Pfander D, Gelse K. 2007. Hypoxia and osteoarthritis: how chondrocytes survive hypoxic environments. Curr Opin Rheumatol 19:457–462.
Phan MN, Leddy HA, Votta BJ, Kumar S, Levy DS, Lipshutz DB, Lee SH, Liedtke W, Guilak F. 2009. Functional characterization of TRPV4 as an osmotically sensitive ion channel in porcine articular chondrocytes. Arthritis Rheum 60:3028–3037.
Ponce A. 2006. Expression of voltage dependent potassium currents in freshly dissociated rat articular chondrocytes. Cell Physiol Biochem 18:35–46.
Sachs F, Sokabe M. 1990. Stretch-activated ion channels and membrane mechanics. Neurosci Res Suppl 12:S1–S4.
Salkoff L, Butler A, Ferreira G, Santi C, Wei A. 2006. High-conductance potassium channels of the SLO family. Nat Rev Neurosci 7:921–931.
Sanchez JC, Wilkins RJ. 2004. Changes in intracellular calcium concentration in response to hypertonicity in bovine articular chondrocytes. Comp Biochem Physiol A Mol Integr Physiol 137:173–182.
Schorle CM, Finger F, Zien A, Block JA, Gebhard PM, Aigner T. 2005. Phenotypic characterization of chondrosarcoma-derived cell lines. Cancer Lett 226:143–154.
Schulze-Tanzil G, Mobasheri A, de Souza P, John T, Shakibaei M. 2004. Loss of chondrogenic potential in dedifferentiated chondrocytes correlates with deficient Shc-Erk interaction and apoptosis. Osteoarthr Cartilage 12:448–458.
Srinivas V, Bohensky J, Zahm AM, Shapiro IM. 2009. Autophagy in mineralizing tissues microenvironmental perspectives. Cell Cycle 8:391–393.
Sutton S, Clutterbuck A, Harris P, Gent T, Freeman S, Foster N, Barrett-Jolley R, Mobasheri A. 2009. The contribution of the synovium, synovial derived inflammatory cytokines and neuropeptides to the pathogenesis of osteoarthritis. Vet J 179:10–24.
Tsuga K, Tohse N, Yoshino M, Sugimoto T, Yamashita T, Ishii S, Yabu H. 2002. Chloride conductance determining membrane potential of rabbit articular chondrocytes. J Membr Biol 185:75–81.
Urban JP. 1994. The chondrocyte: a cell under pressure. Br J Rheumatol 33:901–908.
Urban JP. 2000. Present perspectives on cartilage and chondrocyte mechanobiology. Biorheology 37:185–190.
Urban JPG, Hall AC, Gehl KA. 1993. Regulation of matrix synthesis rates by the ionic and osmotic environment of articular chondrocytes. J Cell Physiol 154:262–270.
Wang LG, Sigworth FJ. 2009. Structure of the BK potassium channel in a lipid membrane from electron cryomicroscopy. Nature 461:U177–U292.
Wohlrab D, Wohlrab J, Reichel H, Hein W. 2001. Is the proliferation of human chondrocytes regulated by ionic channels? J Orthop Sci 6:155–159.
Wohlrab D, Vocke M, Klapperstuck T, Hein W. 2004. Effects of potassium and anion channel blockers on the cellular response of human osteoarthritic chondrocytes. J Orthop Sci 9:364–371.
Wright M, Jobanputra P, Bavington C, Salter DM, Nuki G. 1996. Effects of intermittent pressure-induced strain on the electrophysiology of cultured human chondrocytes: evidence for the presence of stretch-activated membrane ion channels. Clin Sci (Lond) 90:61–74.
Wu QQ, Chen Q. 2000. Mechanoregulation of chondrocyte proliferation, maturation, and hypertrophy: ion-channel dependent transduction of matrix deformation signals. Exp Cell Res 256:383–391.

CHARACTERISATION OF A CHLORIDE CONDUCTANCE IN CANINE CHONDROCYTES

Rebecca Lewis, William Wilkinson, Rebecca Fallman, Robert Whiffin and Richard Barrett-Jolley

Healthy chondrocytes can exist with strikingly depolarised resting membrane potentials (RMP) (Wright *et al.*, 1992; Wright *et al.*, 1996). Several papers have investigated the role of potassium conductances in control of RMP (including Wilson *et al.*, 2004) and we showed that the RMP was also dependent upon TRPV5 (Lewis *et al.*, 2011). In the same study we showed that this depolarised RMP was crucial to the control of chondrocyte volume. A number of studies have also suggested that chloride channels are important for control of the RMP (reviewed by Barrett-Jolley *et al.*, 2010) so in this study we investigated the functional expression of these channels in chondrocytes, using both inside-out patch clamp and whole-cell electrophysiology.

Chondrocytes were isolated from canine articular cartilage by standard methods (Lewis *et al.*, 2011). Cells were used up to and including the third passage. For inside-out patch experiments, membrane potential (*Vm*) was calculated as *Vm=-Hp-Vj* where *Hp* was the holding potential and *Vj* the calculated junction potential. Data are expressed as mean±standard error, p-values are from unpaired t-tests.

We identified a population of ion channels with a mean slope unitary conductance of 183±3pS (n=5) using inside-out patch experiments. These channels reversed at a membrane potential of -34±6mV (n=5) in the presence of 40mM internal and 158mM external Cl^- solutions, indicative of a chloride current (calculated equilibrium potential, E_{Cl}~-35mV). This channel activity was inhibited by the chloride-channel blocker 4-Acetamido-4'-isothiocyanato-stilbene-2,2'-disulfonic acid (SITS) at a concentration of 100μM and seen in approximately 30% of patches with a mean open probability (P_o) of 0.7±0.1 (n=3). Application of 100μM SITS decreased channel P_o by 83±6% (n = 3; $p<0.05$). In whole-cell voltage clamp mode, 100μM SITS inhibited voltage ramps by 52±6% (n = 4; $p<0.05$) at 20mV. We investigated the effect of SITS on the RMP with whole cell current-clamp experiments and found 100μM induced a significant change of +12±3mV (n=5; $p<0.01$).

SITS is a relatively non-selective inhibitor of anionic currents so to further characterise this chloride current, we used a more specific channel inhibitor; niflumic acid (NFA). NFA inhibits the calcium-activated chloride channel (CaCC), which is also believed to be a volume-sensitive chloride channel. 100μM NFA inhibited whole-cell current by 18±2% (n = 15; $p<0.01$) at 20mV.

Our combined single channel and whole-cell data are consistent with the expression of a mixed population of chloride channels in chondrocytes, including both high conductance maxi-chloride and CaCC-like channels.

Barrett-Jolley R, Lewis R, Fallman R & Mobasheri A. (2010). The Emerging Chondrocyte Channelome. *Frontiers in Membrane Physiology and Biophysics* **1,** 10.

Lewis R, Asplin K, Bruce G, Dart C, Mobasheri A & Barrett-Jolley R. (2011). The role of the membrane potential in chondrocyte volume regulation. *J Cell Physiol.*

Wilson JR, Duncan NA, Giles WR & Clark RB. (2004). A voltage-dependent K+ current contributes to membrane potential of acutely isolated canine articular chondrocytes. *J Physiol* **557,** 93-104.

Wright M, Jobanputra P, Bavington C, Salter DM & Nuki G. (1996). Effects of intermittent pressure-induced strain on the electrophysiology of cultured human chondrocytes: Evidence for the presence of stretch-activated membrane ion channels. *Clinical Science* **90,** 61-71.

Wright MO, Stockwell RA & Nuki G. (1992). Response of plasma membrane to applied hydrostatic pressure in chondrocytes and fibroblasts. *Connective Tissue Research* **28,** 49-70.

Characterisation of a chloride conductance in canine chondrocytes

Rebecca Lewis, William Wilkinson, Rebecca Fallman, Robert Whiffin and Richard Barrett-Jolley

Institute of Ageing and Chronic Disease, University of Liverpool, UK

Introduction

Chondrocytes are the cells of articular cartilage, responsible for the production and maintenance of their extracellular milieu. Healthy chondrocytes can exist with strikingly depolarised resting membrane potentials (RMP) (Wright et al., 1992; Wright et al., 1996). Several papers have investigated the role of potassium conductances in control of RMP (including Wilson et al., 2004) and we showed that the RMP was also dependent upon TRPV5 (Lewis et al., 2011). In the same study we showed that this depolarised RMP was crucial to the control of chondrocyte volume. A number of studies have also suggested that chloride channels are important for control of the RMP (reviewed by Barrett-Jolley et al., 2010) so in this study we investigated the functional expression of these channels in chondrocytes, using both inside-out patch clamp and whole-cell electrophysiology.

Single channel physiology

Fig. 1

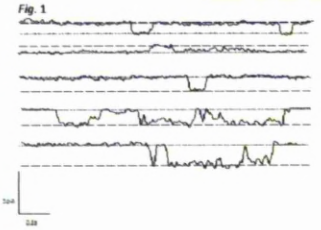

We identified a population of ion channels with a mean slope unitary conductance of 183±3pS (n = 5) using inside-out patch experiments. These channels reversed at a membrane potential of -34±6mV (n = 5) in the presence of 40mM internal and 158mM external Cl- solutions, indicative of a chloride current (calculated equilibrium

Fig. 2

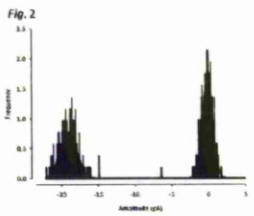

Fig. 3

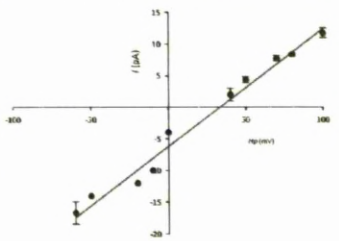

This channel activity was inhibited by the chloride-channel blocker, SITS, at a concentration of 100μM and seen in approximately 30% of patches with a mean open probability (Po) of 0.7±0.1 (n = 3). For inside-out channel data, membrane potential (*Vm*) was calculated as *Vm* = -*Hp*-*Vj* where *Hp* was the holding potential and *Vj* the calculated junction potential. Data are expressed as mean ± standard error.

Contribution to the *Vm*

Fig. 4

Fig. 5

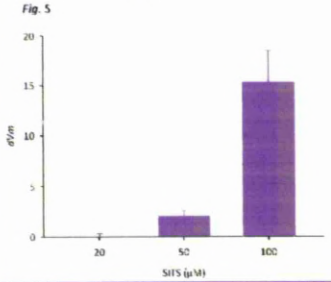

As SITS had a significant inhibitory effect on the single channel activity (application of 100μM decreased channel P_o by 83±6% (n = 3; p<0.05)), we investigated the effect of SITS on the RMP with whole cell current-clamp experiments and found 100μM induced a significant change of +15±3mV (n=5; p<0.01).

Methods

Single channel data was obtained using inside-out patch clamp. Whole-cell currents were obtained using a voltage ramp protocol. Voltage ramp protocols consisted of a 50ms voltage step at 0mV followed by a 4.5s linear ramp from -60mV to +80mV. This was repeated every 50s. Difference currents were obtained by subtraction of a ramp in the presence of 4-Acetamido-4'-isothiocyanato-stilbene-2,2'-disulfonic acid (SITS) or niflumic acid (NFA) from that run in vehicle control. Whole-cell current clamp was used to obtain RMP measurements.

Whole cell current

Fig. 6

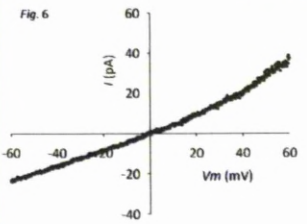

In whole-cell voltage clamp mode, 100μM SITS inhibited voltage ramps by 52±6% (n = 4; p<0.05) at 20mV (*Fig. 6*). SITS is a relatively non-

NFA inhibits the calcium-activated chloride channel (CaCC), which is also believed to be a volume-sensitive chloride channel. 100μM NFA inhibited whole-cell current by 18±2% (n = 15; p<0.01) at 20mV.

Fig. 7

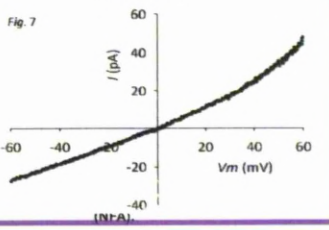

(NFA).

Regulatory Volume Decrease

Fig. 8

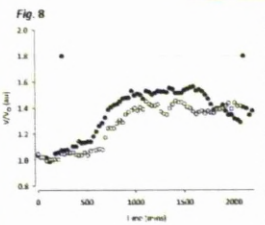

It is thought that a potassium efflux allows a cell to return to its original volume after cell swelling following a hypotonic challenge. We hypothesised that there must be an equivalent anionic efflux. Cell volume was measured continuously throughout a hypotonic challenge in control solutions (filled circles) and in the presence of 100μM NFA (white circles). No significant difference in cell volume recovery was seen between the two conditions.

Summary

Our combined single channel and whole-cell data are consistent with the expression of a mixed population of chloride channels in chondrocytes, including both high conductance maxi-chloride and CaCC-like channels. Inhibition of the NFA sensitive conductance did not have a significant effect on volume regulation.

Future work could include the effect of NFA on single channel conductance and on the Vm. Further investigation of the combined effect of SITS and NFA is necessary. The contribution of an anionic current to control of chondrocyte volume regulation also requires additional research.

References

Barrett-Jolley R, Lewis R, Fallman R & Mobasheri A. (2010). The Emerging Chondrocyte Channelome. *Frontiers in Membrane Physiology and Biophysics* **1**, 10.

Lewis R, Asplin K, Bruce G, Dart C, Mobasheri A & Barrett-Jolley R. (2011). The role of the membrane potential in chondrocyte volume regulation. *J Cell Physiol*.

Wilson JR, Duncan NA, Giles WR & Clark RB. (2004). A voltage-dependent K+ current contributes to membrane potential of acutely isolated canine articular chondrocytes. *J Physiol* **557**, 93-104.

Wright M, Jobanputra P, Bavington C, Salter DM & Nuki G. (1996). Effects of intermittent pressure-induced strain on the electrophysiology of cultured human chondrocytes: Evidence for the presence of stretch-activated membrane ion channels. *Clinical Science* **90**, 61-71.

Wright MO, Stockwell RA & Nuki G. (1992). Response of plasma membrane to applied hydrostatic pressure in chondrocytes and fibroblasts. *Connective Tissue Research* **28**, 49-70.

MODELLING ION CHANNEL BEHAVIOUR IN CHONDROCYTES

Rebecca Lewis and Richard Barrett-Jolley

Several reports of chondrocyte membrane potential (*Vm*) have shown that these cells have significantly depolarised *Vm* compared to other cell types, such as neurones and muscle cells.

Here, we measured the *Vm* of canine chondrocytes embedded in cartilage using sharp electrode electrophysiology (*Vm* = -7±1mV; *n* = 10) and of isolated chondrocytes in physiological saline using the whole-cell current-clamp technique (*Vm* = -6±1mV; *n* = 53). This depolarised value was consistent across a range of species (Bovine = -12±1mV; *n* = 5, Equine = -9±1mV; *n* = 9, Ovine = -8±1mV; *n* = 8).

We developed a mathematical model to simulate *Vm* and describe the behaviour of ion channels in the chondrocyte membrane. The model was developed combining data from our own experiments with the approach of Hodgkin and Huxley[1]. It allows manipulation of extracellular and intracellular conditions and simulates the time dependent effects of these changes on *Vm*. We incorporated the effects of pH, temperature and several channel blockers (magnesium, gadolinium III and amiloride) into the model and tested its predictions using the whole-cell current-clamp technique.

Previously, large-conductance chloride and voltage-sensitive potassium channels have been reported to be important in the maintenance of chondrocyte *Vm*. This model of *Vm*, combined with data from our previous studies, indicates that a number of non-selective cation channels also contribute to the maintenance of *Vm* in the chondrocyte.

1 Hodgkin, A. L. & Huxley, A. F. A Quantitative Description of Membrane Current and Its Application to Conduction and Excitation in Nerve. *Journal of Physiology-London* **117**, 500-544 (1952).

Modelling ion channel behaviour in chondrocytes

Rebecca Lewis and Richard Barrett-Jolley

Musculoskeletal Biology, Institute of Ageing and Chronic Disease, University of Liverpool, UK

Introduction

Several reports of chondrocyte membrane potential (*Vm*) have shown that these cells have significantly depolarised *Vm* compared to other cell types, such as neurones and muscle cells. It has been shown that chondrocyte *Vm* is important for control of volume regulation. Here we set out to characterise the main ion conductances in the chondrocyte and create a testable model of *Vm*.

Indentifying the principal ion conductances

Single channel and whole cell electrophysiological experiments were carried out to characterise the main channel conductances in chondrocytes.

Potassium

BK

Fig. 1a We characterised a calcium-activated potassium channel (Mobasheri *et al* 2010) and used these parameters in the model.

Kv

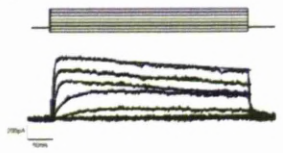

Fig. 1b Kv parameters were calculated from the raw data shown in Mobasheri *et al* 2005.

K_{ATP}

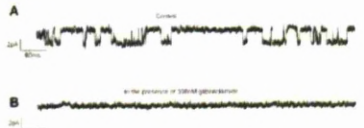

Fig. 1c K_{ATP} parameters were taken from Mobasheri *et al* 2007.

Chloride

Maxi-Cl

Fig. 4 Chloride conductance (186±3pS) suggestive of a Maxi-Cl channel and P_o decreased by 83±6% (n=3) upon application of 100M SITS.

Non-specific

Transient Receptor Potential (TRP)

Fig. 2a Single channel trace of a non-specific cation channel. 100μM Gadolinium III (Gd^{3+}) inhibited channel P_o by 85±7% (n=5). Immunohistochemistry and PCR revealed TRPV4 and TRPV5 channels.

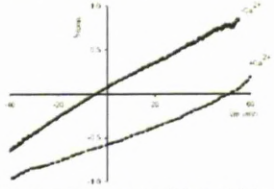

Fig. 2b Difference I/V curves of the gadolinium-sensitive current. Calculated P_{Ca}/P_{Na} of ~ 80, similar to TRPV5.

Sodium

Epithelial Sodium Channel (ENaC)

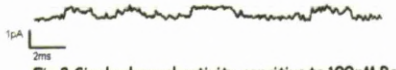

Fig. 3 Single channel activity sensitive to 100nM Benzamil and 10μM amiloride, suggestive of ENaC. Immunohistochemistry revealed α, β and γ ENaC subunits.

The chondrocyte *Vm*

Since the chondrocyte is a small spherical cell and, assuming that the principal ion channel conductances have now been identified, we calculated the RMP as the equilibrium *Vm* obtained by solving:

$$Cm\frac{dV_m}{dt} = -(I_{BK} + I_{Kv} + I_{KATP} + I_{ENaC} + I_{Cl} + I_{TRPV5})$$

Our model combines the approach of Hodgkin and Huxley (Hodgkin & Huxley, 1952), our current data and data from our previous studies of chondrocyte ion channels (Mobasheri *et al.*, 2005; 2007; 2010, Lewis *et al.*, 2011).

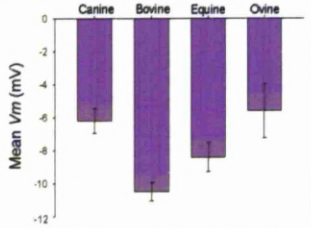

Fig 5 Chondrocyte *Vm* measured in current-clamp mode in a range of species. Model prediction = -8.1mV

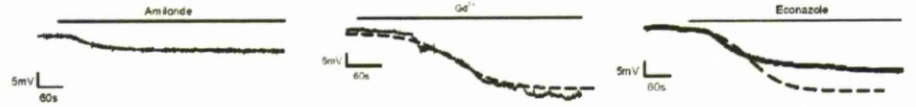

Fig. 6 Simulated block of all non-specific cation (TRP) channels leads to a predicted -27mV change in *Vm* (dashed line). Current-clamp experiments with 100μM Gd^{3+} induced a -32±1mV change (*Fig.* 6b), the TRPV5 inhibitor econazole a -18±3mV change (10μM: *fig.* 6c), with 10μM amiloride a -9.5±0.8 change in *Vm* (*Fig* 6a).

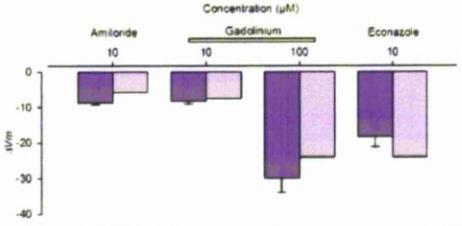

Fig. 7 Δ*Vm* values measured in current-clamp mode (dark purple) compared to values predicted by simulated block of these conductances (light purple).

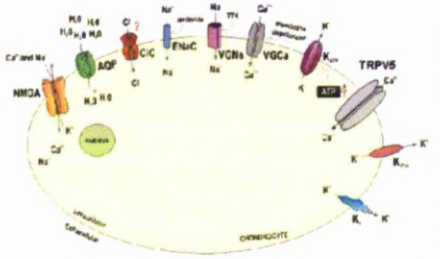

Fig. 8 Schematic showing identified ion channels in the chondrocyte membrane.

Conclusions and future work

The model is able to predict membrane potential changes with a significant degree of accuracy. Future work will involve combining this model of membrane potential with another we are working on which simulates the role of ion channels in cell volume control. Once these are combined we will have a complex model of chondrocyte function.

References

Hodgkin A and Huxley A. 1952. J. Physiol. 117 p500-544

Lewis *et al.*, 2011 J. Cell. Physiol. DOI: 10.1002

Mobasheri *et al* 2005 Am. J. Physiol. Regul. Integr. Comp. Physiol. 289(1):172-180

Mobasheri *et al* 2007 Osteoarthritis and Cartilage 15(1):1-8

Mobasheri *et al* 2010 J. Cell. Physiol. 223(2):511-8

MODELLING THE MEMBRANE POTENTIAL DEPENDENCE ON NON-SPECIFIC CATION CHANNELS

Rebecca Lewis, Gregor Purves, Julia Crossley and Richard Barrett-Jolley

In a previous report, we showed that the predominant ion channel in potassium-free solutions was a gadolinium III (Gd^{3+}) sensitive non-specific cation channel, with functional characteristics similar to that expected for transient receptor potential (TRP) type channels.

In this study reverse transcription-PCR (RT-PCR) was used to investigate the expression of TRP channels in canine articular chondrocytes. Both a mathematical model based on the Goldman-Hodgkin-Katz voltage equation and current clamp whole-cell electrophysiology were then used to investigate the effect of these channels on membrane potential (*Vm*).

Chondrocytes isolated from canine articular cartilage were cultured for 5 days in Dulbeccos Modified Eagles Medium with 10% Foetal Calf Serum. For RT-PCR analysis, total RNA was extracted from first passage cells. Electrophysiological recording was carried out on first to third passage cells.

RT-PCR analysis of chondrocyte mRNA, and subsequent sequencing of products, showed a member of the TRP vanilloid group of channels (TRPV4) to be present; sequence homology to the human TRPV4 was 94%. We have so far failed to find mRNA for the functionally similar TRPC3 and TRPC6 channels.

Using whole-cell and single-channel data from our own experiments and the literature, our model predicts the membrane to be heavily dependent on the activity of TRPV4. Simulated block of all non-specific cation channels in the chondrocyte membrane leads to a predicted -27mV change in *Vm*. This prediction closely matches our current clamp experiments with 100μM Gd^{3+} inducing a -32 ± 1mV (n = 6) change of *Vm*.

Previously, large-conductance chloride and voltage-sensitive potassium channels have been reported to be important in the maintenance of chondrocyte *Vm*. The data presented here shows that the TRPV4 channel also has a significant contribution to maintenance of the chondrocyte *Vm*.

Modelling the membrane potential dependence on non-specific cation channels

Ms R. Lewis, Mr G. Purves, Ms J. Crossley and Dr R. Barrett-Jolley

School of Veterinary Science, University of Liverpool, UK

Introduction

Articular chondrocytes are the cells of articular cartilage and are responsible for the balance between synthesis and breakdown of their extra-cellular matrix (ECM) (Stockwell, 1979). The ECM is made up of a collagen fibre meshwork and negatively charged proteoglycans, which attract positive cations (Broom and Marra, 1985). A number of ion channels have been shown to be present within the chondrocyte membrane, including several types of potassium, sodium, chloride and calcium channels. Here we identify and characterise a type of non-specific cation channel in canine articular chondrocytes using patch-clamp electrophysiology and RT-PCR.

Whole cell current

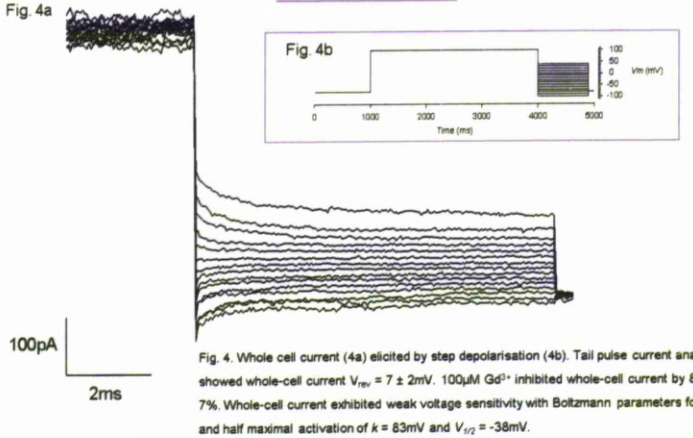

Fig. 4. Whole cell current (4a) elicited by step depolarisation (4b). Tail pulse current analysis showed whole-cell current V_{rev} = 7 ± 2mV. 100μM Gd^{3+} inhibited whole-cell current by 85 ± 7%. Whole-cell current exhibited weak voltage sensitivity with Boltzmann parameters for slope and half maximal activation of k = 83mV and $V_{1/2}$ = -38mV.

RT-PCR

Reverse transcription-PCR analysis of chondrocyte mRNA showed a member of the TRP vanilloid group of channels (TRPV4) to be present; sequence homology to the human TRPV4 was 94%.

Fig. 5. 1.5% Agarose gel showing TRPV4 at 621bp. Total RNA was extracted from 1st passage chondrocytes. Primers were designed from the canine TRPV4 mRNA sequence. GAPDH was run as a test for viable cDNA and a negative control using water was run alongside (not shown here).

Single channel physiology

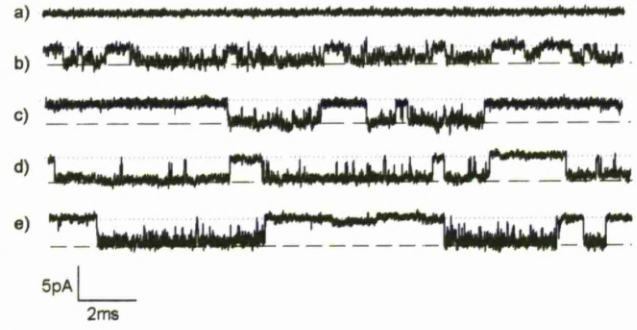

Channel amplitudes (*fig.* 1; recorded on WinEDR; a) 0, b) -20, c) -30, d) -40, e) -50mV) were measured at different holding potentials by creation of an amplitude histogram (*fig.* 2; *Hp* of -50mV) and used to create an *IV* Curve (*fig.* 3). For inside-out channel data, membrane potential (*Vm*) was calculated as $Vm = -Hp - Vj$ (*Hp* is holding potential; *Vj* is the calculated junction potential).

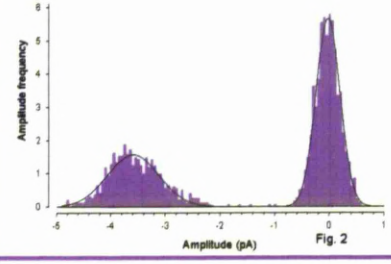

Fig. 2

Fig. 2 and 3. Single channel V_{rev} = 3 ± 2mV (n = 5) with 196mM internal and 155mM external Na^+. Mean slope conductance = 67 ± 5pS (*fig.* 3). Gadolinium III (Gd^{3+}) K_D = 57 ± 1μM. Note: whole cell data *I* is multiplied by a factor of 10.

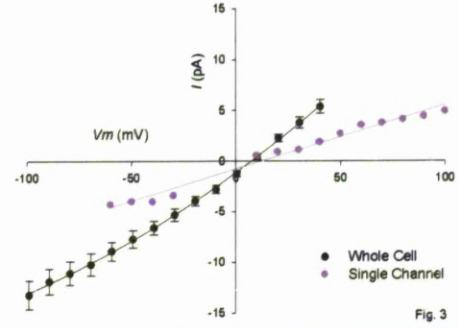

Fig. 3

Vm change

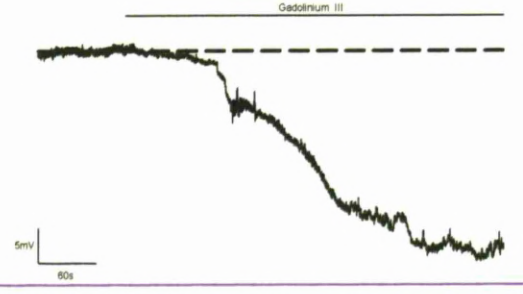

Our model (based on the Hodgkin and Huxley equations; Hodgkin and Huxley, 1952) predicts the membrane to be heavily dependent on the activity of TRP cation channels. Simulated block of all non-specific cation channels leads to a predicted -27mV change in Vm. This closely matches our current clamp experiments with 100μM Gd^{3+} inducing a -32 ± 1mV change (*fig.* 6; dashed line at 0mV).

Conclusion and future work

Previously, large-conductance chloride and voltage-sensitive potassium channels have been reported to be important in the maintenance of chondrocyte Vm. The data presented here shows that the TRPV4 channel also has a significant contribution to maintenance of the chondrocyte Vm. We aim to continue the identification of TRP channels in chondrocytes through use of RT-PCR.

References

Broom N and Marra D. 1985. New Structural Concepts of Articular Cartilage Demonstrated with A Physical Model. Conn. Tiss. Res. 14;1 p1-8

Hodgkin A and Huxley A. 1952. A quantitative description of membrane current and its application to conductation and excitation in nerve. J. Physiol. 117 p500-544

Stockwell, R. A. 1979. Biology of Cartilage Cells. Cambridge University Press

A GADOLINIUM-SENSITIVE NON-SPECIFIC CATION CHANNEL IN CANINE ARTICULAR CHONDROCYTES

Rebecca Lewis and Richard Barrett-Jolley

Non-specific cation channels are present in a number of cell membranes and can be activated by diverse cellular stimuli, allowing mono- and divalent cations to cross the cell membrane (Sanchez & Wilkins 2003).

In the present study we used both inside-out and whole-cell patch clamp electrophysiology to characterise the predominant ion channel in potassium free solutions.

Isolated chondrocytes were cultured for 7 to 9 days in Dulbeccos Modified Eagles Medium with 10% Foetal Calf Serum. Recording was carried out on first to third passage cells. For single channel data, membrane potential (*Vm*) was calculated as $Vm = -Hp-Vj$ where *Hp* was the holding potential and *Vj* the calculated junction potential. Data are expressed as mean ± standard error.

Single-channel activity reversed at a membrane potential of 3 ± 2mV (n = 5) in the presence of 196mM internal and 155mM external Na^+, indicative of a non-specific cation channel. Mean slope conductance of the channel was calculated to be 67 ± 5pS (n = 5). This channel activity was seen in 53% of patches (32/61), with mean open probability of 0.6 at -40mV. 100µM gadolinium III reduced this open probability by 75 ± 9%.

In identical solutions the predominant whole-cell current showed a reversal potential of 1 ± 5mV. 100µM gadolinium III inhibited whole-cell current by 85 ± 7%. The whole-cell current exhibited weak voltage sensitivity with Boltzmann parameters for slope and half maximal activation of $k = 83$mV and $V_{1/2} = -38$mV.

The ion channels identified in these electrophysiological experiments may underlie the gadolinium-sensitive stretch-activated increases in calcium observed by Guilak *et al* (1999) in bovine tissue.

A Gadolinium-Sensitive Non-Specific Cation Channel in Canine Articular Chondrocytes

Ms R. Lewis and Dr R. Barrett-Jolley

Faculty of Veterinary Science, University of Liverpool, UK

Introduction

Articular chondrocytes are the cells of articular cartilage and are responsible for the balance between synthesis and breakdown of their extra-cellular matrix (ECM) (Stockwell, 1979). The ECM is made up of a collagen fibre meshwork and negatively charged proteoglycans, which attract positive cations (Broom and Marra, 1985). A number of ion channels have been shown to be present within the chondrocyte membrane, including several types of potassium, sodium, chloride and calcium channels.

Non-specific cation channels

Non-specific cation channels are present in a number of cell membranes and can be activated by diverse cellular stimuli, allowing mono- and divalent cations to cross the cell membrane (Sanchez & Wilkins, 2003). An example of this channel type is the transient receptor protein (TRP) channels.

In this work we characterise a newly identified channel in canine chondrocytes.

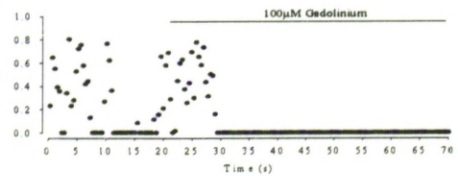

Figure 4. Graph showing a representative sample of P_o. This inside-out channel activity was seen in 53% of patches (32/61), with mean open probability (P_o) of 0.6 at -40mV. 100μM gadolinium III reduced this P_o by 75 ± 9% (*Figure* 4).

Whole cell current

Figure 5a

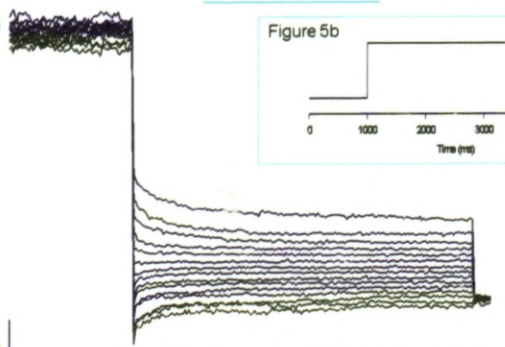

Figure 5b

100pA

2ms

Figure 5. Whole cell current (5a) elicited by step depolarisation as shown in schematic (5b). Tail pulse current analysis showed whole-cell current V_{rev} = 1 ± 5mV. 100μM gadolinium III inhibited whole-cell current by 85 ± 7%. Whole-cell current exhibited weak voltage sensitivity with Boltzmann parameters for slope and half maximal activation of k = 83mV and $V_{1/2}$ = -38mV.

Single channel physiology

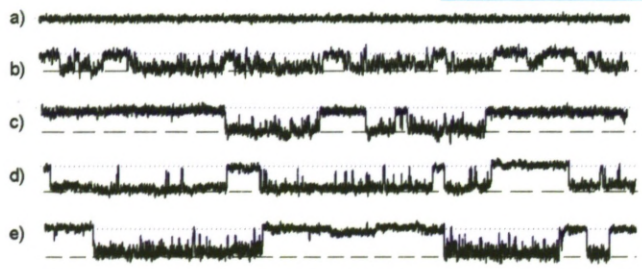

5pA

2ms

Figure 1. Traces of inside-out single channel activity at a) 0, b) -20, c) -30, d) -40, e) -50mV.

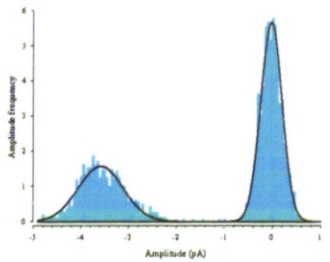

Figures 2 and 3. Single channel V_{rev} = 3 ± 2mV (n = 5) in the presence of 196mM internal and 155mM external Na^+.

Mean slope conductance = 67 ± 5pS (n = 5) (*figure* 3).

K_D was calculated to be 57± 1μM.

Using recordings taken on WinEDR software (Dempster, Strathclyde, UK) (*figure* 1), channel amplitudes were measured at different holding potentials by creation of an amplitude histogram (*figure* 2, taken at *Hp* of -50mV) and used to create an *IV* Curve (*figure* 3). For inside-out channel data, membrane potential (*Vm*) was calculated as *Vm* = *-Hp-Vj* where *Hp* was the holding potential and *Vj* the calculated junction potential. Data are expressed as mean ± standard error.

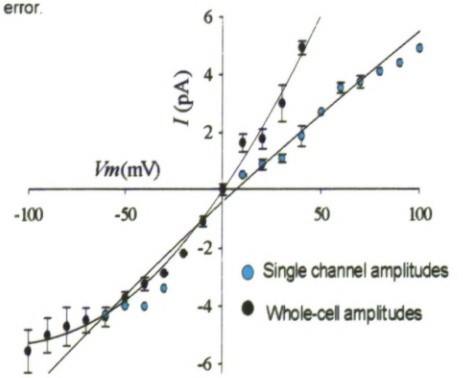

RMP and non-specific cation channels

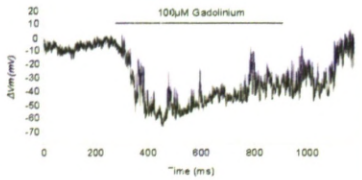

Figure 6. Cell-attached recordings in current clamp mode showing the affect of gadolinium III on membrane potential (*figure* 6). Mean change in membrane potential during application of gadolinium III = -36 ± 9 mV.

Conclusion and future work

Whole cell and single channel evidence for a type of TRP channel has been identified. This data will be input into a predictive computer model, based on the Hodgkin and Huxley equations (Hodgkin and Huxley, 1952). This model will take into account physiological conditions then use differential equations to determine the change in membrane potential facilitated by different ion channels. RT-PCR will also be used to fully identify the channel type.

References

Broom N, and Marra D. 1985. New Structural Concepts of Articular Cartilage Demonstrated with A Physical Model. Conn. Tissue Res. 14,1 p 1-8

Hodgkin A and Huxley A. 1952. A quantitative description of membrane current and its application to conductation and excitation in nerve. J. Physiol. 117 p500-544

Sanchez J and Wilkins R. 2003. Effects of hypotonic shock on intracellular Ca2+ concentration on bovine articular chondrocytes. J. Physiol. 547 p. PC60.

Stockwell, R. A. 1979. Biology of Cartilage Cells. Cambridge University Press

ELECTROPHYSIOLOGICAL IDENTIFICATION OF EPITHELIAL SODIUM CHANNELS IN CANINE ARTICULAR CHONDROCYTES

Rebecca Lewis, Ali Mobasheri and Richard Barrett-Jolley

Amiloride-sensitive epithelial Na^+ channels (ENaC) play a key role in Na^+ transport and fluid homeostasis across the epithelia of the kidney, lung, and colon. ENaC is also known to be present in skin (Mauro *et al.*, 2002, Charles *et al.*, 2008) and articular cartilage (Trujillo *et al.*, 1999) although functional evidence for ENaC in articular cartilage is still lacking.

In the present study, inside-out patch clamp electrophysiology was used to identify ENaC-like unitary currents in isolated canine articular chondrocytes. Isolated chondrocytes were cultured for 7 to 9 days in Dulbeccos Modified Eagles Medium with 10% Foetal Calf Serum. Recording was carried out on first to third passage cells. Membrane potential (*Vm*) was calculated as *Vm = -Hp-Vj* where *Hp* was the holding potential and *Vj* the calculated Junction potential. Data is expressed as mean±standard error.

Single-channel activity reversed at a membrane potential of -1±5mV (n = 5) in the presence of 196mM internal and 155mM external Na^+ solutions, indicative of a sodium current (calculated equilibrium potential, E_{Na} = -6mV). Mean slope conductance of the channel was calculated to be 9±0.4pS (n = 5). The ENaC-like channel activity was inhibited by the sodium-channel blocker amiloride at a concentration of 10μM. ENaC-like unitary currents were seen in approximately 60% of patches and had a mean open probability (P_o) of 0.3±0.06 (n = 3). After application of amiloride, channel P_o decreased by 97±2% (n = 3).

This study provides the first single channel electrophysiological

evidence of functional ENaC expression in canine articular chondrocytes and supports previously published molecular evidence for the presence of ENaC in chondrocytes (Trujillo *et al., 1999).*

Charles, R.P., Guitard, M., Leyvraz, C., Breiden, B., Haftek, M., Haftek-Terreau, Z., Stehle, J.C., Sandhoff, K., Hummler, E. (2008) Postnatal requirement of the epithelial sodium channel for maintenance of epidermal barrier function. J Biol Chem **283**, 2622-2630

Mauro, T., Guitard, M., Behne, M., Oda, Y., Crumrine, D., Komuves, L., Rassner, U., Elias, P.M., Hummler, E. (2002) The ENaC channel is required for normal epidermal differentiation. J Invest Dermatol **118**, 589-594

Trujillo, E., Alvarez de la Rosa, D., Mobasheri, A., Gonzalez, T., Canessa, C.M., Martin-Vasallo, P. (1999) Sodium transport systems in human chondrocytes. II. Expression of ENaC, Na+/K+/2Cl- cotransporter and Na+/H+ exchangers in healthy and arthritic chondrocytes. Histol Histopathol **14**, 1023-1031